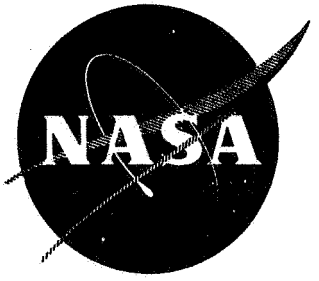
N 70 11947

NASA CR 72621



CASE FILE
COPY

FINAL REPORT

260-IN.-DIA MOTOR PROPELLANT IMPROVEMENT PROGRAM

by:

Dr. B. A. Simmons, Manager, Space Booster Department

and

Dr. C. L. Rogers, Chemistry Supervisor, Propellant Development

AEROJET-GENERAL CORPORATION

NATIONAL AERONAUTICS AND SPACE ADMINISTRATION

NASA Lewis Research Center
Contract NAS3-12002
H. Bankaitis, Project Manager



AEROJET-GENERAL CORPORATION

SACRAMENTO, CALIFORNIA

NOTICE

This report was prepared as an account of Government-sponsored work. Neither the United States, nor the National Aeronautics and Space Administration (NASA), nor any person acting on behalf of NASA:

A.) Makes any warranty or representation, expressed or implied, with respect to the accuracy, completeness, or usefulness of the information contained in this report, or that the use of any information, apparatus, method, or process disclosed in this report may not infringe privately-owned rights; or

B.) Assumes any liabilities with respect to the use of, or for damages resulting from the use of, any information, apparatus, method or process disclosed in this report.

As used above, "person acting on behalf of NASA" includes any employee or contractor of NASA, or employee of such contractor, to the extent that such employee or contractor of NASA or employee of such contractor prepares, disseminates, or provides access to any information pursuant to his employment or contract with NASA, or his employment with such contractor.

FINAL REPORT

260-IN.-DIA MOTOR PROPELLANT IMPROVEMENT PROGRAM

by:

Dr. B. A. Simmons, Manager, Space Booster Department
and
Dr. C. L. Rogers, Chemistry Supervisor, Propellant Development

Prepared for:

National Aeronautics and Space Administration

November 1969

Contract NAS3-12002

NASA-Lewis Research Center
Cleveland, Ohio
H. Bankaitis, Project Manager
Chemical Propulsion Office

AEROJET-GENERAL CORPORATION
A SUBSIDIARY OF THE GENERAL TIRE & RUBBER COMPANY

ABSTRACT

This program was directed toward the development of process controls and propellant formulations which will assure sound propellant grains for very large motors. Experiments included the casting of ten 42-in. (1.07 m) dia subscale molds and two full-scale molds simulating a segment of a 260-in. (6.6 m)-dia motor grain. Investigations included formulation, mixing, and casting variables. Grain defects were related to propellant flow behavior. Primary contributors to poor flow behavior were propellant ingredients and inadequate deaeration during mixing. Improved processes, an improved formulation, and process guidelines were developed and demonstrated to provide assurance of the capability for producing sound, high-quality grains.

TABLE OF CONTENTS

		Page
I.	Introduction	1
II.	Summary	3
III.	Technical Discussion	4
	A. Program Objectives	4
	B. Technical Approach	4
	C. Discussion of Results	11
IV.	Conclusions	76

FIGURE LIST

	Figure
Effect of Applied Shear on the Viscosity of Different Fluids	1
Propellant Casting Rate as a Function of Bayonet Length	2
Schematic Diagram of Subscale Mold Showing Locations of Specimens Taken for Property Testing	3
Summary of ANB-3254 Propellant Formulation Variables and Casting Parameters for Subscale Mold No. 1	4
Summary of Uncured Propellant Data for ANB-3254 Propellant Cast into the First Subscale Mold	5
Viscosity Characteristics for Batch 68-232, Subscale Mold No. 1	6
Sections of First Subscale Mold	7
Mechanical Properties of Carton Samples from Propellant Cast into Subscale Mold No. 1	8
Properties of Propellant Taken from First Subscale Mold	9
Bond Strength of Liner-Propellant Specimens from First Mold	10
Summary of ANB-3254 Propellant Formulation Variables and Casting Parameters for Subscale Mold No. 2	11
Summary of Uncured Propellant Data for ANB-3254 Propellant Cast into Subscale Mold No. 2	12
Mechanical Properties of Carton Samples of Propellant Cast into Mold No. 2	13
Properties of Specimens from Second Subscale Mold (Section A)	14
Properties of Specimens from Second Subscale Mold (Section B)	15

FIGURE LIST (cont)

	Figure
Properties of Specimens from Second Subscale Mold (Section C)	16
Bond Strength of Liner-Propellant Specimens, Second Subscale Mold	17
Summary of ANB-3254 Propellant Mixing Variables and Casting Parameter for Subscale Mold 3	18
Viscosity Characteristics, Batch 68-264, Subscale Mold 3	19
Viscosity Characteristics, Batch 68-268, Subscale Mold 3	20
Comparison of Viscosity Build-Up Characteristics of Batches 68-264 and 68-268	21
Summary of Uncured Propellant Data, Subscale Mold 3	22
Mechanical Properties of Carton Samples from Propellant Cast into Third Subscale Mold	23
Mechanical and Bonding Properties, Third Subscale Mold	24
Summary of ANB-3265 Propellant Mixing Variables and Casting Parameter for Subscale Mold No. 4	25
Summary of Uncured Propellant Data, Subscale Mold 4	26
Grain Defect Map for the Fourth Subscale Mold Interior View (ID)	27
Grain Defect Map for the Fourth Subscale Mold Exterior View (OD)	28
Mechanical Properties of Carton Samples from Propellant Cast into Subscale Mold 4	29
Properties of Specimens from Fourth Subscale Mold	30
Viscosity as a Function of Shear Stress and Time from Curing Agent Addition for First Batch (68-290) Cast into Fifth Subscale Mold	31
Summary of Uncured Propellant Data, Fifth Subscale Mold	32
Summary of ANB-3254 Propellant Casting Parameters for Subscale Mold No. 5	33
Grain Defect Map for the Fifth Subscale Mold Interior View (ID)	34
Grain Defect Map for the Fifth Subscale Mold Exterior View (OD)	35
Mechanical Properties of Carton Samples from Propellant Cast into Fifth Subscale Mold	36
Properties of Specimens from Fifth Subscale Mold	37
Summary of ANB-3254 Propellant and Casting Parameters for Subscale Mold 6	38
Summary of Uncured Propellant Data, Sixth Subscale Mold	39
Grain Defect Map for the Sixth Subscale Mold Interior View (ID)	40
Grain Defect Map for the Sixth Subscale Mold Exterior View (OD)	41
View of Sixth Subscale Mold	42

FIGURE LIST (cont)

	Figure
Mechanical and Bond Properties and Solid Strand Burning Rate of Propellant Specimens Taken from the Sixth Subscale Mold	43
Summary of Propellant Variables Cast into Subscale Mold 7	44
Propellant Viscosity as a Function of Shear Stress and Time from Curing Agent Addition	45
Summary of Uncured Propellant Data, Seventh Subscale Motor	46
Mechanical Properties of Carton Samples of Propellant Cast into the Seventh Subscale Mold	47
Properties of Specimens from Seventh Subscale Mold	48
Summary of Results, Subscale Molds 1 through 7	49
Viscosity Buildup Characteristics of ANB-3254 Propellant Prepared in a 5500-lb (2500 Kg) Vertical Batch Mix	50
Viscosity Buildup Characteristics of ANB-3254 Propellant Prepared in a 5500-lb (2500 Kg) Vertical Batch Mix	51
Comparison of Viscosity Buildup Measurements - Continuous Use of One Sample vs New Sample/Test	52
Viscosity Buildup Characteristics in a 5500-lb (2495 Kg) Batch after 20 Minutes Final Mix	53
Viscosity Buildup Characteristics in a 5500-lb (2495 Kg) Batch after 30 Minutes Final Mix	54
Viscosity Buildup Characteristics in a 5500-lb (2495 Kg) Batch after 60 Minutes Final Mix	55
Effect of Final Vacuum Mix Time on the Viscosity Buildup of ANB-3254 Propellant	56
Effect of Vacuum Mix Time on the Mechanical Properties of ANB-3254 Propellant, 5500 lb (2500 Kg) Batch	57
Full-Scale Casting Form	58
View of Casting Bay	59
Casting Sequence, First Full-Scale Mold	60
Propellant Flow Characteristics First Full-Scale Mold	61
Submix and Premix Analyses for Propellant Cast into First Full-Scale Mold	62
Uncured Propellant Data for First Full-Scale Mold	63
Summary of Process Times for First Full-Scale Mold Casting	64
Cast Propellant Surface, Batch 22D-172-A	65
Cast Propellant Surface, Batch 22D-172-B	66
Cast Propellant Surface, Batch 22D-172-D	67
Cast Propellant Surface, Batch 22D-172-E	68

FIGURE LIST (cont)

	Figure
Cast Propellant Surface, Batch 22D-172-F	69
Cast Propellant Surface, Batch 22D-172-G	70
Cast Propellant Surface, Batch 22D-172-I	71
Cast Propellant Surface, Batch 22D-172-J	72
Batch-to-Batch Surface Contours, Inside Wall, First Full-Scale Mold	73
Batch-to-Batch Surface Contours, Midpoints, First Full-Scale Mold	74
Batch-to-Batch Depth Contours	75
Overhead View, First Full-Scale Mold	76
Outside Diameter of Cured Mold, Overall View	77
Outside Diameter of Cured Mold, Left Hand View	78
Outside Diameter of Cured Mold, Central View	79
Inside Diameter of Cured Mold, Left Hand View	80
Inside Diameter of Cured Mold, Central View	81
Inside Diameter of Cured Mold, Right Hand View	82
Northeast End of Cured Mold, Upper View	83
West End of Cured Mold, Lower View	84
Surface Defects Map, First Full-Scale Mold	85
Mechanical Properties from Carton Samples of Propellant Cast into the First Full-Scale Mold	86
Sample Locations for the First Full-Scale Mold	87
Properties of Specimens from First Full-Scale Mold	88
Mechanical Properties and Burning Rates of Propellant Specimens Taken from the First Full-Scale Mold (Section A)	89
Mechanical Properties and Burning Rates of Propellant Specimens Taken from the First Full-Scale Mold (Section A)	90
Properties of Specimens from First Full-Scale Mold	91
Mechanical Properties and Burning Rates of Propellant Specimens Taken from the First Full-Scale Mold (Section B)	92
Mechanical Properties and Burning Rates of Propellant Specimens Taken from the First Full-Scale Mold (Section B)	93
Properties of Specimens from First Full-Scale Mold	94
Mechanical Properties of Propellant Specimens from First Full-Scale Mold Containing Bipropellant Interfaces	95

FIGURE LIST (cont)

	Figure
Effect of Final Mix Vacuum Level on Propellant Flow and Mechanical Properties in 10-lb (4.5 Kg) Vertical Mixer Batches, Using a Large Vacuum Pump	96
Effect of Final Vacuum Mix Level and Time on Propellant Flow and Mechanical Properties in 10-lb (4.5 Kg) Vertical Mixer Batches Using a Small Vacuum Pump	97
Effect of Final Mix Time at High Temperature on Propellant Flow and Mechanical Properties	98
Effect of Final Mix Time at Low Temperature on Propellant Flow and Mechanical Properties	99
Effect of Mixer Speed on Propellant Flow and Mechanical Properties	100
Sections of Laboratory Scale Casting	101
Sections of Laboratory Scale Casting	102
Effects of Oxidizer Blend and Burning Rate Additive on Properties of ANB-3254 Propellant	103
Effect of Plasticizer Type on Flow Behavior and Cure of ANB-3254 Type Propellant	104
Effect of Surface Active Agents on Flow Behavior and Cure of ANB-3254 Type* Propellants	105
Effect of Curing Agent and Cure Catalyst Concentration on Flow Behavior of ANB-3254 Propellant	106
Viscosity as a Function of Shear Stress and Time from Curing Agent Addition	107
Viscosity as a Function of Shear Stress and Time from Curing Agent Addition	108
Effect of FC-167 Wetting Agent on Viscosity Buildup	109
Storage Stability at 180°F(82°C) of PBAN Propellant Containing PBNA Antioxidant	110
Propellant Viscosity as a Function of Shear Stress and Time from Curing Agent Addition	111
Effect of Cure Catalyst Type and Concentration on Mechanical Properties of PBAN Propellant*	112
Improved Formulation ANB-3350	113
Effect of Premix Storage on Mechanical Properties of ANB-3350 Propellant	114
Comparison of Viscosity Tests	115

FIGURE LIST (cont)

	Figure
Summary of Propellant Formulation and Casting Parameters for Eighth Subscale Mold	116
Summary of Uncured Propellant Data, Eighth Subscale Mold	117
View of Eighth Subscale Mold	118
Mechanical Properties of Carton Samples of Propellant Cast into Eighth Subscale Mold	119
Mechanical and Bond Properties of Solid Strand Burning Rate of Propellant Specimens Taken from the Eighth Subscale Mold	120
Summary of Propellant Formulation and Casting Parameters for Ninth Subscale Mold	121
Uncured Propellant Data, Ninth Subscale Mold	122
Mechanical Properties Carton Samples of Propellant Cast into the Ninth Subscale Mold	123
Mechanical and Bond Properties and Solid Strand Burning Rate of Propellant Specimens Taken from the Ninth Subscale Mold	124
Summary of Propellant Formulation and Casting Parameters for Tenth Subscale Mold	125
Uncured Propellant Data, Tenth Subscale Mole	126
Mechanical Properties Carton Samples of Propellant Cast into the Tenth Subscale Mold	127
Mechanical and Bond Properties and Solid Strand Burning Rate of Propellant Specimens Taken from the Tenth Subscale Mold	128
Safety Classification Testing for ANB-3350 Type Propellant	129
ANB-3350 Propellant Formulation Selection for Task III Process Demonstration	130
Casting Sequence for Task III	131
Submix and Premix Analyses for Propellant Cast into Second Full-Scale Mold	132
Uncured Propellant Data, Second Full-Scale Mold	133
Correlation of Falling Ball Test with Rotovisko Data	134
Process Time for Second Full-Scale Mold Casting	135
Batch-to-Batch Depth Contours for Inside Wall, Second Full-Scale Mold	136
Batch-to-Batch Depth Contours for Midpoints, Second Full-Scale Mold	137
Batch-to-Batch Depth Contours for Outside Wall, Second Full-Scale Mold	138

FIGURE LIST (cont)

	Figure
Outside Diameter of Cured Mold, Overall View	139
Inside Diameter of Cured Mold, Left Hand View	140
Inside Diameter of Cured Mold, Central View	141
Inside Diameter of Cured Mold, Right Hand View	142
Northeast End of Cured Mold	143
West End of Cured Mold	144
Surface Defects in Outside Diameter of Cured Mold	145
Surface Defects in Northeast End of Cured Mold	146
Map of Surface Defects in the Second Full-Scale Mold	147
Mechanical Properties from Carton Samples of Propellant Cast into the Second Full-Scale Mold	148
Sample Locations for the Second Full-Scale Mold	149
Mechanical and Bonding Properties and Burning Rate of Propellant Specimens Taken from the Second Full-Scale Mold (Section A)	150
Mechanical and Bonding Properties and Burning Rate of Propellant Specimens Taken from the Second Full-Scale Mold (Section A)	151
Specimen Properties, Second Full-Scale Mold	152
Mechanical and Bonding Properties and Burning Rate of Propellant Specimens Taken from the Second Full-Scale Mold (Section B)	153
Mechanical and Bonding Properties and Burning Rate of Propellant Specimens Taken from the Second Full-Scale Mold (Section B)	154
Specimen Properties, Second Full-Scale Mold	155
Specimen Properties, Second Full-Scale Mold	156
Comparison of Propellant Viscosities at Different Levels with Surface Height in Mold (Right Half of Mold)	157
Comparison of Propellant Viscosities at Different Levels with Surface Height in Mold (Left Half of Mold)	158
Comparison of Propellant Viscosities at Different Levels with Incidence of Surface Irregularities in Second Full-Scale Mold	159
Comparison of Height Differentials with Area of Surface Irregularities	160

APPENDIX

260-in.-dia Motor Processing Guidelines

I. INTRODUCTION

This report presents the results of the 260-in.-Dia Motor Propellant Improvement Program. The work was conducted by the Aerojet-General Corporation for the National Aeronautics and Space Administration, Lewis Research Center, under Contract NAS3-12002. The 12-month program was initiated in June 1968 to investigate the critical factors that must be controlled to cast high-quality propellant grains for large solid rocket motors.

The need for this program was demonstrated by the abnormal ballistic performance of Motor 260-SL-3. Large chamber pressure increases during the static test firing were attributed to unscheduled grain surface area exposure, caused by defects within the grain and in the propellant-to-liner bond. These defects indicated the casting process and uncured propellant flow characteristics were inadequate. The work described in this report was directed toward solution of this problem and development of processing criteria that would assure the capability for processing sound propellant grains.

The primary technical emphasis in this work is on flow behavior of propellant at low shear stresses, and on the processes and formulation ingredients necessary to minimize viscosity at those conditions.

II. SUMMARY

The 260-In.-Dia Motor Propellant Improvement Program was initiated in June 1968 under Contract NAS3-12002 for the purpose of investigating factors contributing to propellant grain defects in Motor 260-SL-3, and to establish process and formulation improvements that would assure sound, high-quality grains. The major technical emphasis was placed on the non-Newtonian pseudoplastic flow behavior of the uncured propellant during casting. The critical parameter was the apparent viscosity at a low applied shear stress, 5,000 dynes/cm^2 (500 N/m^2).

Program effort was organized into three tasks. Task I encompassed casting studies that included the casting of ten subscale 42-in. (1.07 m)-dia molds and one full-scale segment of a 260-in. (6.6 m)-dia grain. In Task II process and formulation variables were studied and an improved formulation was developed. The optimized processes and formulation were demonstrated in Task III with the successful casting of a full-scale mold.

The first seven subscale molds were used to define critical process variables in the casting of the 260-SL-3 propellant formulation ANB-3254, with emphasis on simulating the types of defects observed in the grain of Motor 260-SL-3. For this propellant, the most critical factor affecting flow behavior was the vacuum mix cycle. This factor was used in propellant preparation for the first full-scale mold, which successfully simulated the 260-SL-3 processes and resultant defects. The defects consistently occurred at propellant batch interfaces and were clearly the result of flow behavior. The most significant deficiencies in the full-scale mold were in the bonding-to-liner samples. Anisotropy in ballistic and mechanical properties prevailed in this and all other molds cast.

II. Summary (cont)

In the propellant modification studies, mixing variables studies included vacuum level, final mix time, mix temperature, and mixer speed. Combinations of low vacuum level and short mix time were found to increase propellant pseudoplasticity through inadequate deaeration. The most significant ingredient contributing to highly pseudoplastic flow behavior was the BRA-101 burning-rate additive.

An improved formulation, designated ANB-3350, was developed containing iron oxide and Iron Blue as burning rate additives, a cure catalyst which was not subject to hydrolysis, a wetting agent, and an antioxidant. The flow properties of this formulation were significantly improved over the 260-SL-3 formulation and were slightly superior to those of ANB-3105, the formulation successfully demonstrated in Motors 260-SL-1 and 260-SL-2. The mechanical and ballistic properties of ANB-3350 are equivalent to those of ANB-3254. Additionally, a simplified in-process test for measuring viscosity at low shear stress was demonstrated. Storage stability of the ANB-3350 premix for up to 11 days was also demonstrated.

The last three subscale molds were used to verify the adequacy of flow properties, evaluate formulation variables, and demonstrate above-surface casting using the improved formulation. The specific formulation to be used in the Task III Processing Demonstration was selected. Above-surface bayonet casting was shown to be promising as an improved casting technique.

A second full-scale mold was processed, demonstrating the improved formulation using an extended vacuum mix cycle and new limitations on casting bayonet submergence. The improvements were found to reduce significantly surface defects, to promote adequate propellant-to-liner bonding, and to assure the capability of processing sound high-quality propellant grains. In culmination of Task III, motor processing guidelines were prepared and are included as an appendix to this report.

III. TECHNICAL DISCUSSION

A. PROGRAM OBJECTIVES

The purpose of this program was to resolve the causes of defects in the propellant grain of Motor 260-SL-3 by pursuing the following objectives:

1. Determine propellant casting parameters that insure high quality grains.
2. Determine propellant characteristics compatible with the selected casting parameters.
3. Modify the propellant formulation used in Motor 260-SL-3 to achieve acceptable processing characteristics while maintaining the required mechanical and ballistic properties.
4. Demonstrate the optimum processing procedures and propellant formulation for producing sound grains with a simulated propellant grain casting.

B. TECHNICAL APPROACH

1. Definition of Problem

a. Processing of Motor 260-SL-3

Some of the ANB-3254 propellant batches prepared for the casting of Motor 260-SL-3 exhibited abnormal flow behavior. Visual inspection of the propellant in the mix bowl revealed a highly irregular surface and an impression of the mixer blades. The ANB-3105 propellant cast into Motors 260-SL-1 and -2 in contrast exhibited a smooth glossy surface in the mix bowls. Application of a light force on the surface of the abnormal ANB-3254 propellant batches resulted in propellant flow and a smooth surface in the bowl. These batches were then bayonet cast without difficulty, and required about the same amount of cast time as other batches which did not

III.B. Technical Approach (cont)

exhibit the irregular surface. As a result of cumulative visual evidence it was determined that the length of the final vacuum mix cycle should be increased from 20 to 30 minutes for the final two-thirds of the run. This change resulted in a decrease in the incidence of the abnormal appearing batches.

Visual observations of the propellant surface in Motor 260-SL-3 during casting showed that the surface was smooth. Subsequent examination of the inner bore after the grain had been cured and the core stripped revealed numerous defects, apparently caused by propellant folding against the core in such a way as to entrap air and produce elongated surface defects. There were significantly fewer defects in that portion of the grain corresponding to propellant mixed with the longer (30 minute) final vacuum mix cycle. During static test firing of the motor, ballistic abnormalities, which could only be related to exposure of unplanned burning area, and localized failure of liner-propellant bond occurred. In retrospect, it was evident that the grain bore surface defects, while not serious in themselves, were symptomatic of both within-grain and propellant-to-liner bond defects.

Because propellant flow behavior was the most likely cause of the observed grain bore defects and the subsequent ballistic abnormalities, NASA-LeRC awarded Contract NAS3-12002 to Aerojet to investigate the mechanism of defect formation, relate this mechanism to the propellant formulation variables that were responsible for the observed flow behavior, and develop and demonstrate an improved propellant formulation with the same ballistic properties as ANB-3254.

III.B. Technical Approach (cont)

b. Rheology of Uncured Solid Propellants

Accomplishment of the objectives of the program required an understanding of the rheology of uncured solid propellants. The rheology of highly filled liquid polymers such as uncured solid propellants is extremely complex from a theoretical point of view, and determination of the flow behavior of such a system from a knowledge of the properties of its component parts is generally not possible. Even empirical treatments (sparsely available in the literature) of the flow properties of systems with volume loadings comparable with current solid propellant formulations are so complicated by factors such as particle size distribution, particle shape, and other physical and chemical interactions that they quickly lose their generality. Clearly any attempt to advance the state-of-the-art in this difficult field was beyond the scope of this program. Rather, the approach to development of an understanding of the problems encountered during the processing of Motor 260-SL-3 was to examine the individual components of the propellant system used in this motor and to determine how these components affected the ultimate flow properties of the propellant.

Most uncured solid propellants exhibit non-Newtonian flow behavior, i.e., the viscosity of the material is a function of the applied shear stress. On the current program it was found that the degree of departure from Newtonian behavior is a good measure of the incidence and size of grain defects which could be expected in a large motor such as the 260-in.-dia (6.6-m-dia) motors. The filled systems represented by uncured solid propellants depart from Newtonian behavior in that the viscosity increases as the applied shear stress decreases as shown in Figure 1. A material such as an uncured propellant whose viscosity increases steadily as the shear stress is reduced

III.B. Technical Approach (cont)

to zero is termed a "pseudoplastic" material. In an extreme instance, the propellant viscosity may actually become infinite at some finite value of shear stress. Materials that exhibit a "yield point" such as this are termed "Bingham plastic".

The viscosity characteristics of uncured solid propellants can be measured in many ways with a variety of commercially available instruments including rotational viscometers, extrusion rheometers, parallel plate plastometers, or falling ball devices. Of the instruments available, the Rotoviski viscometer is the most versatile and accurate.

The Rotovisko viscometer is basically a rotational type of viscometer which measures the resistance (torque) to the rotation of a small star-shaped rotor submerged in the propellant sample (sample size is about 50 gm). Measurements are made at many fixed rates of rotation to provide viscosity as a function of shear rate (or shear stress) over a wide range of shear rates. The data may be plotted in various ways which show the interrelationships between shear rate, shear stress and time after curing agent addition. Viscosity as a function of shear stress was selected as the form for the data portrayal on this program.

Most uncured solid propellants also exhibit a type of flow behavior known as thixotropy. A thixotropic material subjected to a constant rate of shear shows a decrease in viscosity as a function of time of shearing. From the standpoint of propellant processing characteristics and processability, this thixotropic effect has not been found to be of major importance.

III.B. Technical Approach (cont)

Another unique property of uncured solid propellants is that their flow characteristics change with time as the cure reaction proceeds. Thus an uncured propellant may exhibit nearly Newtonian flow behavior shortly after curing agent addition, but then the flow characteristics will show progressively increasing pseudoplastic behavior (with increasing values of yield stress), and finally visco-elastic behavior when the cure is complete. Consequently, a realistic assessment of the flow properties of a propellant must include measurements of viscosity as a function of shear stress and time after curing agent addition.

c. Considerations of Propellant Flow Behavior in the Motor Casting Process

Since the viscosity or flow characteristics of uncured solid propellants are dependant on shear stress (or shear rate) and time, the establishment of meaningful processing criteria requires an examination of the motor casting process in terms of these critical parameters. This examination reveals three distinctly differing zones of applied stress and flow: (1) plug flow through the casting bayonet under relatively high shear stress, (2) mixing of the propellant stream emerging from the bayonet with stagnant propellant in the motor, and (3) flow under low shear stress around the core and to the motor wall.

Propellant flow characteristics through the casting bayonet during the processing of Motor 260-SL-3 were acceptable and not a significant contributor to grain defect formation. Casting rate is a direct measure of the viscosity in this process step. In fact, the casting pot bayonet assembly is a form of an extrusion rheometer. As shown in Figure 2, comparison of the casting rates of the ANB-3254 propellant with the ANB-3105 propellant (260-SL-1 and -2) indicated that the propellant viscosities under these conditions (high applied shear stress) were similar and acceptable.

III.B. Technical Approach (cont)

The result is not surprising because the viscosity of a pseudoplastic material is lowest under high shear stress conditions. At the start of this program knowledge of the flow processes or patterns occurring in the "mixing" zone was very limited. Because propellant viscosity characteristics are both stress and time dependent and material under a high applied stress is emerging from the bayonet and "mixing" with stagnant propellant, it is evident that this is a critical region. The characteristics of the stagnant propellant are dependent on its age (time after curing agent addition), which in turn is dependent on production rate and bayonet submergence depth.

After the propellant leaves the mixing zone, the flow toward the wall and around the core occurs under a low applied stress, viz, hydrostatic head; under these stress conditions the apparent viscosity of a pseudoplastic material will be very high. The characteristics of the propellant in this zone are directly dependent on the flow processes occurring in the mixing zones. If old propellant (long elapsed time after curing agent addition) is being forced into the zone, a high probability of defect formation exists. It is clear from a defect formation standpoint that flow in this zone is the most critical element in the motor casting process.

2. Technical Plan

Program effort was organized into three tasks. Task I, Propellant Casting Studies, and Task II, Propellant Modification Studies, were conducted concurrently, resulting in the development of optimized processes and an optimized formulation which then were demonstrated in Task III. The following is a description of the three work tasks:

III.B. Technical Approach (cont)

a. Task I - Propellant Casting Studies

Initial effort in this task consisted of the design and fabrication of two types of casting forms to be used in subsequent evaluations. A small subscale form of 42-in. (1.07 m) dia were designed to enable casting of about 2000 lb (900 Kg) of propellant in a 240-degree (4.19 rad) segment. A large full-scale form approximating a 120-degree (2.09 rad) segment of the 260-in. (6.6 m) dia motor was designed to contain more than 60,000 lb (27,000 Kg) of propellant. A plan for conduct of propellant mixing and casting experiments was prepared. The experimental program included mixing, casting, and curing of propellant in one full-scale and ten subscale forms. Data obtained included viscosity, flow patterns, and mechanical, ballistic and bonding properties of the cast propellant. The task was concluded with the compilation and analysis of all experimental data, and the selection of a formulation and mixing and casting procedures to be used in the subsequent Task III casting demonstration.

b. Task II - Propellant Modification Studies

In this task, the significant propellant formulation and process variables were identified, and the effects evaluated in the selection of a reliable propellant and casting process. Effects of variables in the propellant composition, the mixing process, and the casting process on propellant flow and bonding characteristics were evaluated in laboratory-scale batches. Optimum values selected were verified and used in the final subscale mold castings of Task I. A significant element of this task was to define process control limits for the critical factors influencing propellant flow characteristics.

III.B. Technical Approach (cont)

c. Task III - Processing Demonstration

The capability to produce sound propellant grains, using the optimized propellant formulation and process procedures as determined in Tasks I and II, was demonstrated by casting a mold simulating a section of a 260-in. (6.6 m) dia motor. The same full-scale mold employed in Task I was used. The cured grain was sectioned and specimens were tested to verify mechanical and ballistic properties of the propellant, and adequacy of propellant bonding. This task effort was concluded with the preparation of motor process guidelines implementing the optimum formulation characteristics and process procedures.

C. DISCUSSION OF RESULTS

1. Subscale Molds 1 through 7

The propellant cast into the first seven 42-in.-dia by 48-in.-high (1.07 by 1.22 m) subscale molds was ANB-3254, the propellant formulation cast into Motor 260-SL-3. The plans used for casting these molds were designed to evaluate the casting rate, bayonet submergence, propellant age, and propellant flow characteristics. Critical mixing variables affecting propellant flow characteristics were defined during the processing of the propellant used for casting these molds.

a. Subscale Mold 1

The basic ANB-3254 propellant formulation was modified to produce five distinct propellant colors for each of the five 450 lb. (200 Kg) batches to obtain data of the flow patterns and inter-mixing of individual propellant batches within the motor.

III.C. Discussion of Results (cont)

On the basis of laboratory scale propellant batches, dyes and pigments were selected that could be substituted for Iron Blue and provide different propellant colors without causing significant changes in the viscosity of the propellant. These multi-colored batches were cast into a mold, designed to provide a 240-degree (4.19 rad) cloverleaf-shaped grain segment shown schematically in Figure 3. Formulation and casting parameters are summarized in Figure 4 and the laboratory test data for the propellant and components are presented in Figure 5.

While casting the first batch of propellant, which was the nominal ANB-3254 formulation, defects of small irregular waves of built-up propellant that flowed out around the core and into the lobes were observed. Subsequent batches did not reveal the formation of any additional defects. Viscosity measurements as a function of applied shear stress and time from curing agent addition were made on samples of propellant from each batch cast using the Rotovisko viscometer. As described previously, data are presented as a graph of viscosity-vs-applied shear stress for different time intervals after curing agent addition. A typical graph is shown in Figure 6 that shows the viscosity characteristics of Batch 68-232, the first batch of propellant cast into this mold. To simplify the presentation of viscosity data obtained on the many batches of propellant prepared on this program, measured viscosities will generally be reported at two time intervals from curing agent addition (6 and 10 hr) and at a fixed value of shear stress. The shear stress value selected for this purpose is 5,000 dynes/cm^2 (500 Newtons/m^2), which, although arbitrary, is sufficiently low to ensure that any significant pseudoplasticity will be revealed. It is a convenient value of shear stress to visualize as it corresponds to about 1 in. (2.54 cm) of propellant hydrostatic head.

The viscosity data (Figure 5), from the batches cast into this first subscale mold, as well as visual observation, indicated that all batches were significantly more fluid than corresponding 10-lb (4.5 Kg) batches of the same formulations.

III.C. Discussion of Results (cont)

When the mold was sectioned, the flow patterns were readily apparent because of the different color of each batch cast, as shown in Figure 7. Immediately it was obvious that early batches cast into the mold were sequentially displaced by subsequent batches to the extent that the last batch was completely encased within the previously cast batches. There was a negligible amount of mixing of the batches within the mold; the lines of demarcation between batches were clear. Significantly, the second batch cast was displaced outward and upward to the top of the mold and over a considerable part of the circumferential bonding area. Thus, the age of propellant contacting the liner became progressively more as the mold was filled.

Mechanical properties from carton samples taken from each batch (Figure 8) show that the state of cure had become constant within 30 days at 135°F (57°C). Properties of specimens taken from the cured grain (Figure 9) indicate some anisotropic behavior with respect to both mechanical properties and burning rate. This is considered normal and was observed also with the ANB-3105 propellant cast into Motors 260-SL-1 and -2. Bond data (Figure 10) show no effect of circumferential or vertical location on the outer periphery of the grain. Although the numerical values appear to be lower for specimens taken from the A position (web of the grain), all samples randomly failed within the propellant or at the propellant-to-plate bond line, so that no conclusions can be drawn with respect to propellant-liner bond strength.

The apparent state of cure, as measured by initial modulus (E_o), is indicated to be greater in the cured grain than in the carton samples. This relationship is frequently observed in solid propellants and is attributed to the orientation resulting from flow during casting. In the grain the propellant has passed through a long tube before flowing into the mold. The sample cartons are drawn directly from the mix bowl. This program presented an unusually extensive opportunity to document this relationship.

III.C. Discussion of Results (cont)

b. Subscale Mold 2

A summary of propellant variables and casting parameters for the second subscale mold is given in Figure 11. With the exception of the fourth batch, this mold was cast with the standard ANB-3254 propellant. The fourth batch cast into this mold contained 0.1% benzidine yellow added to the standard formulation to impart a green color to the propellant. The casting rate used for the second mold was the same as for the first mold with the bayonet submergence limited to a maximum of 12 in. (30 cm). The propellant was processed normally. Laboratory test data for the propellant components and uncured propellant are shown in Figure 12.

No significant defects were formed in this mold, apparently because the propellant did not exhibit extreme pseudoplasticity Because definition of the 450-lb (200 Kg) batch mix cycle required for producing propellant with the desired flow characteristics was a program requisite, mix cycle variations were evaluated during the processing of propellant for this mold. The variations evaluated included reducing the efficiency of deaeration during final vacuum mix. One batch was mixed with the vacuum pump off during the final mix cycle and another batch was mixed with the final vacuum mix cycle shortened from 20 to 10 min, with the vacuum pump off. Visual examination of these batches and subsequent viscosity measurements indicated that these mixing variations did not have a major effect on propellant flow characteristics. Observations during casting indicated the surface of the propellant in the mold remained relatively level and smooth with no waves of the type that could have caused defects in the first batch of the first subscale mold.

III.C. Discussion of Results (cont)

Sectioning of the cured mold revealed no internal defects or flaws. Since the color of the fourth batch cast into this mold was green, the flow patterns of this batch were clearly defined and generally conformed to what would be expected from examination of the sections of the first sub-scale mold.

Mechanical properties from carton samples of each batch cast into the second mold show the effect of the changed mix procedure used for the third and fifth batches as shown in Figure 13. With the vacuum pump off during the final mix cycle of the third batch and shortening the final mix cycle of the fifth batch evidently removed less moisture from the batch, which in turn caused more degradation of the FeAA cure catalyst by hydrolysis. Consequently, the initial modulus for these two batches was 330 to 387 psi (228 to 267 N/cm^2) compared with 433 to 538 psi (299 to 371 N/cm^2) for the other batches after a 25-day cure.

The results of the mechanical properties and burning rate tests on specimens from the second propellant grain are summarized in Figures 14 through 16. These data indicate that the propellant initial modulus is higher in the area of the grain where the propellant from the two bayonet streams converge. As in the first mold, some anisotropy in both mechanical properties and burning rate is apparent in all three specimen locations, and the initial modulus is significantly greater than in the carton samples.

Bond specimens were taken from the grain in three circumferential and five vertical locations, shown schematically in Figure 2 and tested at 77°F (25°C) in both tensile and shear. The data given in Figure 17, do not show any effect of location on the grain periphery on liner-propellant bond strength.

III.C. Discussion of Results (cont)

c. Subscale Mold 3

In processing propellant for the third mold, the evaluation of mixing parameters affecting the flow properties of propellant mixed in the 450-lb (200 Kg) mixer was continued. Parameters evaluated were a lengthened final vacuum mix cycle, increased from 20 to 60 min, increased FeAA level and elimination of a vacuum mix step after oxidizer addition. The first factors were selected for evaluation on the basis of 10-lb (4.5 Kg) mix data that indicated that the amount of active FeAA in the propellant influenced flow properties. Increasing the efficiency of the final vacuum mix would result in a higher concentration of active FeAA through more effective removal of water that hydrolyzes FeAA. The active FeAA concentration was increased with higher initial concentrations. As shown in Figure 18, the first three batches were standard ANB-3254, with 0.032 wt% FeAA, processed with a 60 min final vacuum mix cycle. The fourth batch also was mixed for 60 min but was formulated with 0.045 wt% FeAA. All batches were cast into the mold at the maximum rate.

Visual examination of these propellant batches in the mixer gave no evidence of the extreme pseudoplastic flow behavior that had been observed in the A-DD mixers during the casting of Motor 260-SL-3. The viscosity data were found to be consistent with these observations. Typical is the data for the first batch, shown in Figure 19. On the basis of these observations, it was concluded that less efficient vacuum mixing would probably yield the highly pseudoplastic flow characteristics. Therefore, the fifth batch, which had the same formulation as the fourth batch, was prepared by a procedure that eliminated all vacuum mixing during the batch preparation, except for a 10-min final vacuum mix. This procedure was expected to more closely duplicate the A-DD mix conditions. The flow characteristics of this batch were very similar to those observed during the Motor 260-SL-3 casting. Subsequent viscosity data, shown in Figure 20, confirmed that the propellant from this

III.C. Discussion of Results (cont)

batch showed much higher viscosity at low shear stress than all previous batches made in the 450-lb (200 Kg) vertical batch mixer. Viscosity build-up at 10,000 dynes/cm^2 (1,000 N/m^2) shear stress for the fourth and fifth batches is compared in Figure 21.

Laboratory analyses of the propellant components and uncured propellant were normal and are presented in Figure 22.

During casting of all batches the propellant surface was smooth and no defect formations were observed. On the basis of its location and the flow patterns found in the first mold, the fifth batch would not be expected to cause defects.

Stripping and sectioning of the cured mold revealed no visible defects. The location of the fifth batch could be seen in the sectioned pieces, because the altered mix procedure apparently caused a difference in shading of the blue pigment in the propellant. Its location was as expected on the basis of flow patterns observed in the first mold casting.

Mechanical properties data from carton samples of propellant taken from each batch cast into this mold are shown in Figure 23 and show the changes in formulation and mix cycle in the fourth and fifth batches. The fourth batch with the long final mix and increased FeAA content shows the highest state of cure, while the fifth batch with the short final mix cycle, and increased FeAA content, did not cure as rapidly as the preceding batch, but more rapidly than the first three batches.

The mechanical properties specimens taken from the sectioned grain show the typical anisotropy observed previously, with the lowest propellant initial modulus generally occurring in the vertical orientation, as shown in Figure 24. The bond strength between the propellant and the

III.C. Discussion of Results (cont)

SD-850-2 liner is not affected by the vertical location on the grain periphery. All bond specimens failed at random within the propellant, indicating bond strength in excess of the cohesive strength of the propellant.

d. Subscale Mold 4

All of the 450-lb (200 Kg) batches cast into this mold were prepared using the mix procedure used in the last batch of the third mold. The mixing variables and casting parameters are summarized in Figure 25. Laboratory test data of the propellant components and the uncured propellant are shown in Figure 26. All batches exhibited the type of flow behavior which caused the defects observed in Motor 260-SL-3.

During the casting of the mold using the maximum casting rate, the formation of many defects was observed. The mechanism of the defect formation was apparent. Resistance of the propellant to flow at low shear stress caused mounds or waves to form around the bayonet; the waves were as high as 10 in. (25 cm). When the mound had reached a height where the hydrostatic head exceeded the yield strength of the propellant, each wave began to flow, relatively rapidly because of shear thinning of the propellant, away from the bayonet. As the "wave front" passed along the core and the outer periphery of the mold, air was entrapped between the moving and static propellant with the resulting creation of a void or a fold. The first 5500-lb (2500 Kg) scale-up batch of this propellant formulation was prepared during the casting of the fourth mold and a portion of the batch used to cast the mold along with four 450-lb (200 Kg) batches. The preparation of this batch is described in Section III.C.1.i.

III.C. Discussion of Results (cont)

The cured mold was stripped and the core removed to reveal the observed defects. Several elongated defects up to 14 in. (36 cm) long and up to 2 in. (5 cm) wide were found. Maps of the defects found on the grain exterior and core surfaces are presented in Figures 27 and 28, respectively. There were also many voids beneath the surface of the propellant. Cutting into these voids indicated that some were as deep as 2 in. (5 cm). These defects were such that there was little doubt the defects were formed by the same mechanism as observed on the bore of Motor 260-SL-3. Partial sectioning of the cured grain has also revealed many internal defects, including both voids and what might be described as "fault lines."

Carton samples cast from the batches cast into the fourth mold confirm the observations from the last batch cast into the third mold that the abbreviated vacuum mix cycle reduced the propellant initial modulus. Carton data are shown in Figure 29.

The mechanical properties and solid-strand burning rates of propellant specimens compiled from the fourth mold are summarized in Figure 30. As in the first three molds, there is anisotropy apparent in the mechanical properties, with the lowest propellant initial modulus being observed in vertically oriented specimens. There was some anisotropy evident in the solid-strand burning rate, but with no apparent correlation with orientation or mechanical properties. Similarly, the apparent state of cure, as indicated by initial modulus data, is greater in the mold than in the sample cartons. A trend in propellant bond strength is indicated from the samples tested from this mold with a significant decrease in tensile and shear strength occurring in the upper half of the mold. However, this trend is attributable largely to batch differences, as seen in the modulus and tensile strength data.

III.C. Discussion of Results (cont)

e. Subscale Mold 5

The objective of this mold casting was to evaluate the effect of propellant viscosity characteristics on grain quality. This was accomplished by using the same casting plan as for the third mold, but using a mix procedure that accentuated pseudoplastic flow behavior. All batches prepared for this mold were processed by the same mix procedure used for the fourth mold, i.e., mix after oxidizer addition shortened to 5 min without vacuum, and final vacuum mix cycle shortened to 10 min. As with the propellant prepared for mold 4, all batches exhibited the pseudoplastic flow behavior similar to that observed with some of the propellant batches prepared for Motor 260-SL-3. Viscosity build-up as a function of shear stress and time from curing agent addition for the first propellant batch cast into mold 5 is shown in Figure 31, and is typical of all batches. Laboratory test data for these batches are shown in Figure 32.

The casting parameters for the fifth mold, shown in Figure 33, were similar to those used to cast the third mold, which was essentially defect-free. Significant differences between the sets of casting parameters for the fourth and fifth molds were the single bayonet and cylindrical core configuration for the former, and two bayonets with cloverleaf core for the latter. The average casting rate into the fifth mold also was slower than into the fourth mold. The shorter flow path length with two bayonets and casting in smaller increments were observed to cause less of the "mounding" of propellant in the fifth mold, with consequent formation of fewer defects. Figures 34 and 35 show maps of the location of defects found in the cured grain.

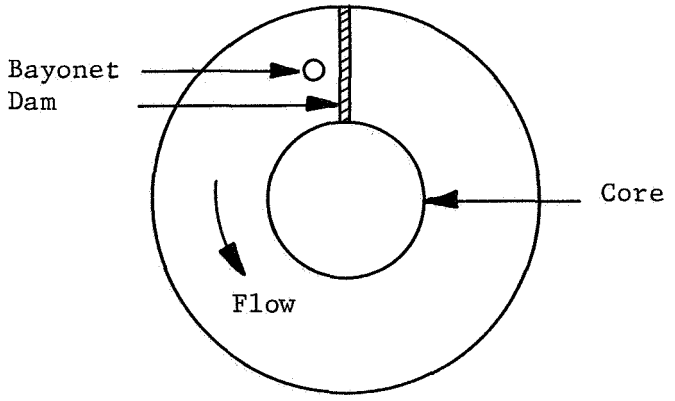
Mechanical properties tests from carton samples from propellant batches cast into the fifth mold, Figure 36, show the same low initial moduli observed in the two previous molds that were processed with a short vacuum mix cycle.

III.C. Discussion of Results (cont)

No apparent trends are evident in the mechanical and bonding properties or the solid-strand burning rates of samples removed from the cured grain presented in Figure 37. This may be because of the proximity of the sample location to the bayonet and the very shallow submergence used in casting the grain. As with the previous molds, the initial modulus data of specimens from the grain are higher than the comparable data for the carton samples.

f. Subscale Mold 6

The propellant mixing and casting parameters for processing of this mold were selected to provide an assessment of the effects of shallow bayonet submergence and long flow path length on the formation of defects in the grain. A summary of the formulation and casting parameters is given in Figure 38. All batches cast into the mold were ANB-3254 propellant processed to yield extreme pseudoplasticity. In-process data for the batches processed for this mold are shown in Figure 39. The flow path length in this mold was increased by using a 16-in. (41 cm) dia cylindrical core configuration and casting a 360 degree (6.28 rad) grain as shown below:



The location of the bayonet next to the vertical dam forced the propellant to flow completely around the annulus, thus increasing the flow path length by a factor of about 3 compared with the previous subscale mold castings.

III.C. Discussion of Results (cont)

The effect of this increased flow path length was readily apparent during the casting. Large defects were formed inside the grain as well as on the inner and outer periphery. Shear planes were formed that were very similar to those observed during the casting of the first full-scale mold. Maps of the observed grain defects, presented in Figures 40 and 41, show an increase in defect size and frequency as compared with mold 4. The difference in grain height at the bayonet location and various circumferential positions provides a direct and vivid measurement of propellant flow behavior under low shear stress, as shown in Figure 42. The difference in grain height at the bayonet location and opposite side of the dam, at the maximum flow path length, was 18 in (41 cm) for this extreme pseudoplastic propellant.

Mechanical and bond property and solid-strand burning rate test data on specimens taken from the sixth subscale grain are shown in Figure 43. As in all previous subscale grains, anisotropy in both mechanical properties and burning rate were found. In spite of the increased flow path length and the resultant increased frequency and severity of defects, there was no effect of location on the grain periphery on the measured bond strength to SD-850-2 liner.

g. Subscale Mold 7

The propellant mixing and casting parameters for processing the seventh mold were selected to provide further assessment, along with molds 6 and 8, of the effects of shallow bayonet submergence and long flow path lengths on the formation of defects in the grain, as summarized in Figure 44. As with the sixth mold, the flow patch length in this mold was increased by using a 16-in (41 cm) dia cylindrical core configuration and casting a 360 degree (6.28 rad) grain. The bayonet was placed adjacent to the vertical dam that forced the propellant to flow all the way around the annulus formed by

the core and the mold. The propellant formulation used for the first four batches cast into this mold was ANB-3254. The processing methods selected for these batches were designed to achieve the optimum flow characteristics for this formulation. Long mix times at maximum vacuum resulted in a propellant that exhibited a lesser amount of mounding and thus, less visible defect formation. The difference in propellant height on opposite sides of the dam was about 10 in. (25 cm) after the four batches were cast compared with 18 in. (46 cm) after five batches cast into the sixth mold.

The fifth batch cast into this mold was ANB-3350, the improved propellant formulation developed under the Task II efforts and described later in this report. Flow characteristics of this batch were so significantly improved, as indicated by viscosity data (Figure 45), over even the best ANB-3254 batch, that the height differential across the dam was virtually eliminated. The batch flowed to the lowest area of the mold, at the maximum flow path length, and filled the mold to the point of no height difference.

Figure 46 shows the laboratory test data for the propellant components and uncured propellant used in the casting of the seventh mold. All batches processed normally. The 0.744 in./sec (1.89 cm/s) liquid-strand burning rate of the improved formulation ANB-3350 exceeds the 0.68 in./sec (1.73 cm/s) target. It was therefore concluded that the burning-rate additive content of the formulation (0.5% Iron Blue, 2.0% iron oxide) could be reduced.

The mechanical properties from carton samples of each batch of propellant cast into the seventh mold are shown in Figure 47. Batch 69-11 is the improved propellant formulation ANB-3350. The data indicate that the cure of this batch stabilized in about 17 days at 135°F (57°C) and the modulus of 480 to 490 psi (331 to 338 N/cm^2) is very close to the target value of 500 $\pm$ 100 psi (345 $\pm$ 69 N/cm^2).

III.C. Discussion of Results (cont)

No difference is apparent between the mechanical and bond properties and solid-strand burning rate of specimens obtained from the seventh mold and the properties obtained on previous molds. These data for the seventh mold are shown in Figure 48. The initial modulus data from the grain specimens are typically higher than the carton sample data.

h. Interpretation of Results

Analysis of the data obtained for the first seven subscale molds cast with ANB-3254 provided an indication of many critical factors governing the size and frequency of grain and bond defects. These critical variables include:

(1) Propellant viscosity characteristics
(2) Flow path length
(3) Propellant cast rate
(4) Bayonet submergence
(5) Vacuum mix cycle

Propellant viscosity characteristics largely govern the size and frequency of defect formation. The extent of defect formation is dependent on the extent of pseudoplasticity. This is illustrated by a comparison in Figure 49 of the results of subscale castings 1, 2, 3, and 7, that demonstrated little pseudoplasticity, with castings 4, 5, and 6, that displayed a high degree of pseudoplasticity. It appears from the viscosity data in Figure 49 that propellant viscosities of 40,000 poise (4,000 Ns/m^2) or less, at three hours from curing agent addition, at 5 K dynes/cm^2 (500 N/m^2) shear stress result in essentially defect-free castings over a range of processing variables. When the propellant viscosities cast into the subscale molds are in the range of 50,000 to 150,000 poise (5,000 to 15,000 Ns/m^2), as cast into molds 4, 5, and 6, frequent and large defects are produced.

III.C. Discussion of Results (cont)

The effects of flow path length on defect formation are most clearly shown by a comparison of subscale molds 4 and 6. Both molds 4 and 6 were cast with propellant exhibiting a high degree of pseudoplasticity. The configuration of mold 4 was a 240 degree (4.19 rad) cylindrical segment with one centrally located bayonet while mold 6 was a 360 degree (6.28 rad) cylinder with one bayonet located adjacent to the vertical separator. This difference in configuration resulted in a flow path length for mold 6 of approximately three times that for mold 4. The defects produced in mold 6, shown in Figure 49 were both more numerous, 28-vs-13, and larger, 4 by 20 in. vs 3 by 12 in. (10 by 51 cm-vs-8 by 30 cm) than those in mold 4. These data suggest that the 360 degree (6.28 rad) configuration in the subscale mold provides a more severe, and probably more realistic, evaluation of the adequacy of the propellant flow properties. Duplication of 260-in. (6.6 m) motor flow conditions apparently requires enough flow path length to allow development of surface level differences and flow planes. The potential then exists for defects anywhere along the flow path at the case wall and core surface.

Propellant cast rate appears to be an important factor based on a comparison of results of molds 4 and 5, only when casting a propellant with extreme pseudoplastic characteristics. On the basis of visual observations, it can be concluded that the casting rate governs the propellant head height that builds up around the bayonet. This head height determines the size of the wave front that follows the mold wall. Intersection of the wave front with the wall produces a defect. This flow occurs when the hydrostatic head force exceeds the yield strength of the pseudoplastic propellant. When slow cast rates are used, the head height does not build up, apparently due to the stress relaxation properties of the propellant.

III.C. Discussion of Results (cont)

Cast rate does not appear to be critical with propellants that do not exhibit high pseudoplasticity. With these propellants, the head height around the bayonet does not vary significantly with cast rate and therefore, defect formation did not occur.

Bayonet submergence may be concluded to be a factor in defect formation since the age of the propellant at the bayonet tip is governed by the submergence depth. The flow patterns in mold 1 show that the propellant batch at the bayonet tip is moved outward and upward against the mold wall. As the degree of pseudoplasticity increased with propellant age, deep submergence is obviously deleterious to propellant liner bonding. Movement of a pseudoplastic material favors defect formation. To avoid movement of such material, the extent of bayonet submergence should be minimized.

For ANB-3254 propellant, the vacuum mix cycle was shown to be a critical element in governing flow characteristics. Slight pseudoplastic flow behavior was achieved in the ANB-3254 type batches processed for molds 1 through 3, when vacuum was applied to the mix after oxidizer addition. After vacuum mixing for 10 min, the DER-332 curing agent was added and then a final vacuum mix was used. When the vacuum mix cycle was altered to eliminate the vacuum mix interval after oxidizer addition prior to DER-332 addition, a propellant with extreme pseudoplastic behavior resulted. Casting of this type of propellant in molds 4, 5, and 6 resulted in a high incidence of grain defects.

i. Scale-Up Batch

Prior to the casting of the first full-scale mold, a 5500-lb (2500 Kg) vertical batch mix was prepared to evaluate the effect of final mix time on propellant flow behavior. Observations of the last 450-lb

III.C. Discussion of Results (cont)

(200 Kg) batch used to cast the third subscale mold indicated that a short vacuum mix cycle would produce the extreme pseudoplastic effect in ANB-3254 propellant. To evaluate this in the large VBM batch the final mix was stopped at intervals of 10, 20, and 30 min and terminated at 60 min. At each mix interval samples were taken for viscosity build-up and mechanical properties testing.

Viscosity build-up measurements on this batch were determined by two methods. Previously, all measurements at fixed intervals after curing agent addition were done using the same propellant sample. A cup containing about 50 gm is normally used. In addition to testing the samples using this procedure, each batch also was tested in accordance with a method which used a different sample of propellant for each measurement. A series of cups was prepared and placed in 135°F (57°C) conditioning and allowed to remain undisturbed until testing. This technique invariably indicated a more rapid viscosity build-up for a given sample, most probably because the continual shearing of the single sample did not allow sufficient time for the propellant to recover between tests. Typical of the results obtained on this VBM scale-up batch are the two viscosity build-up curves for the 10 min final mix time shown in Figures 50 and 51, and compared at a low shear stress in Figure 52. The viscosity data presented for the 20, 30, and 60 min final mix intervals in Figures 53 through 55 use the second (individual cups) procedure. Visual observation of the propellant in the mix bowl at the various final mix intervals indicated the extreme pseudoplastic effect definitely prevailed at 10 min, was less evident at 20 min and disappeared at 30 and 30 min. Although this is not clearly shown in the initial viscosity indications, there appears to be a correlation with the viscosity build-up at later time periods. For example the viscosity at 10 hr after curing agent addition and an applied shear stress of 20 K dynes/cm^2 (2,000 N/m^2) ranges from off-scale at 10 min of mixing to 26,000 poise (2,600 Ns/m^2) at 60 min of mixing. The effect of final vacuum mix time on viscosity build-up at a low shear stress level is shown in Figure 56.

III.C. Discussion of Results (cont)

There appears to be a correlation between final mix time and mechanical properties also. The mechanical properties data given in Figure 57 show a definite increase in the state of cure with increased final mix time, with a plateau occurring at 30 min, the same interval that the observed extreme pseudoplastic effect disappeared. This is undoubtedly because less moisture is removed during the shorter vacuum mix times, and moisture remaining in the propellant caused partial degradation of the FeAA polymerization catalyst during cure.

2. Full-Scale Mold Casting

a. Description of Casting Form

The objective of this casting was to duplicate the conditions of propellant flow, bayonet location, casting rate, and propellant age that resulted in the grain defects observed in Motor 260-SL-3. A full-scale grain segment was simulated by casting 12 5500-lb (2500 Kg) batches of ANB-3254 propellant into a 120-degree (2.09 rad) sector casting form to yield a propellant mold of the configuration shown in Figure 58. This arrangement represented one of three casting positions used to cast the 260-SL motors.

The casting form was of steel-framed, sheet metal construction and was fastened to the floor of the casting bay. Three 24 by 80-in. (0.60 by 2.0 m) panels of V44 insulation were prepared with SD-850-2 liner and attached to the inside of the 130-in.-radius (3.3 m) wall to provide propellant-to-liner bond samples. The 135°F (57°C) cast-and-cure temperature was maintained by passing heated air through an oven assembled around the casting form and through flexible tubing which shrouded the casting bayonet (Figure 59). For casting, the propellant pots were placed on a stand at the top of the bay, allowing an initial bayonet length of about 40 ft (12 m).

III.C. Discussion of Results (cont)

The bayonet tip was centrally positioned in the mold. The bayonet tubing, valves, plugs, and related tooling, as well as all applicable procedures, were identical to those employed in the casting of Motor 260-SL-3. The only variance was that the propellant pot discharge valves used at the Sacramento facility are smaller than those used at the Aerojet-Dade facility, requiring the addition of a short adapter section.

b. Casting Plan

In the simulation of the conditions prevailing during the casting of Motor 260-SL-3, typical batch times were established to represent the propellant manufacturing facility characteristics for each cast position:

(1) Time between batches: 3 to 4 hr plus 16- to 20-hr delay.

(2) Time from the end of final mix to the start of casting: 1 hr, 40 min to 2 hr, 30 min.

The planned casting sequence shown in Figure 60 was designed to evaluate the effects on grain defect formation of bayonet submergence and propellant age at the bayonet efflux as follows:

(1) Cast the first three batches with a fixed bayonet location 5 in (13 cm) from the bottom of the mold, resulting in bayonet submergence of 0 to 13 in (33 cm). Allow 3 to 4 hr between batches.

(2) Clean and remove bayonet. Shorten bayonet by 7 in (18 cm).

III.C. Discussion of Results (cont)

(3) After a 16 to 20-hr delay, insert the bayonet to a depth of 6 in. (15 cm) and cast the fourth and fifth batches, resulting in a bayonet submergence of 6 to 18 in. (15 to 46 cm). For batches 4 through 12, maintain the casting interval at 3 to 4 hr.

(4) Clean, remove, shorten, and insert the bayonet to a submergence of 6 in. Cast the remaining batches without moving the bayonet, thereby varying the submergence from 6 to 48 in. (15 to 122 cm) and the propellant age at bayonet efflux from about 4 to 28 hr.

c. Propellant Mixing

The 12 batches of ANB-3254 propellant were prepared in accordance with the procedures used for Motor 260-SL-3, with selected controls on the final 20 min. vacuum mix cycle. The procedures used for 260-SL-3 required a minimum vacuum level of 27 in. (690 mm) Hg for the final mix cycle of 20 min (later changed to 30 min). The vacuum level for the first three batches was 29, 25, and 29 (740, 640, and 740 mm) in. Hg, respectively, to evaluate the process sensitivity of ANB-3254 in large batches. The batch mixed at 25 in. (640 mm) Hg exhibited the extreme pseudoplastic flow appearance observed on some of the 260-SL-3 batches, i.e., stiff, irregular surface, while the batches mixed at the higher vacuum displayed a normal "fluid" surface. Because the vacuum in the mixers at A-DD is not measured directly, it was concluded that this factor was the most significant mixing process variable affecting flow behavior. As a major objective of this program is to simulate the Motor 260-SL-3 propellant grain defects, the remaining nine batches were mixed at reduced vacuum levels. Batches 4 through 7 were mixed at 25 in. (640 mm) Hg., while Batches 8 through 12 were mixed at 26.5 in. (670 mm) Hg to demonstrate an intermediate level. All of the batches mixed at reduced vacuum displayed the extreme pseudoplastic appearance. Figure 61 summarizes the flow characteristics of the 12 batches.

III.C. Discussion of Results (cont)

Acceptance data for the propellant liquid components and uncured propellant (Figures 62 and 62) were normal and within acceptance limits, with the exception of liquid strand burning rate (LSBR). The LSBR data are consistently high, with seven batches exceeding the upper limit of 0.71 in./sec. (1.80 cm/sec). This characteristic is attributed to slight differences in oxidizer particle size distribution produced by the Raymond mill for the MA fraction. (The Mikro Atomizer mill capacity at Aerojet was inadequate for this program). The differences in burn rate were not considered to be detrimental to the casting objectives.

d. Propellant Casting

The casting of the 12 propellant batches was accomplished according to plan. The time between batches tended to exceed the target range because of the unpredictability of oxidizer addition times during mixing. The batch casting times were more than the nominal range for the bayonet length, due to higher pressure drop through the pot valves discussed previously (Paragraph III.C.2.a.). The casting span times are summarized in Figure 64.

The propellant surface during casting was monitored visually, with time-lapse photography, and with surface level measurements. The following is a summary of visual observations.

Batch 172A, (first batch) was mixed at 29-in. (740 mm) Hg vacuum and displayed normal flow characteristics. The flow in the mold covered the entire base, except for two corners (Figure 65).

III.C. Discussion of Results (cont)

Batch 172B (second batch) was mixed at 25-in. (640 mm) Hg vacuum and had a stiff, irregular surface in the mix bowl. Casting was stopped with about 1200 to 1400 lb (540 to 640 Kg) of propellant remaining in the mix bowl when several large bubbles appeared. This apparently resulted from pot diaphragm leakage. Propellant flow in the mold was uniform, with about a 6-in. (15 cm) level gradient from the center to the ends. The surface of the propellant developed small wrinkles and shear planes (Figure 66).

Batch 172C, like the first, was mixed at the high vacuum level and had a normal surface appearance. Flow in the mold was uniform. The bayonet was pigged and removed after the cast and was shortened by 7 in. (18 cm).

Batch 172D (fourth batch) was mixed at 25-in. (640 mm) Hg vacuum and included the addition of 0.1% of benzidine yellow dye, resulting in green propellant, for color contrast in the mold with the normally blue propellant. The bayonet was inserted to 6 in. (15 cm) submergence. Casting was initiated 16 hr, 40 min after the casting of the third batch and covered the entire surface of the west end of the mold. Figure 67 shows the central area of the mold, with the bayonet at the left and the small portion of the batch that flowed northeast.

The flow of batch 172E (fifth batch) was to the northeast end of the mold. Initial flow at the surface was green, which later blended to blue-green. Following the casting of this batch, the bayonet was pigged, removed, cut and inserted to a submergence of a minimum of 6 in. (15 cm). The propellant surface height around the bayonet varied by several in. Figure 68 shows the propellant surface at the end of the casting of the fifth batch.

III.C. Discussion of Results (cont)

Batch 172F (sixth batch) flowed toward the west uniformly, with a small amount of flow to the northeast, the latter portion being shown in Figure 69. Part of the green propellant of the fourth batch remained at the surface near the center of the mold as an "island."

Batch 172G flow during the seventh batch casting was in both directions, but the surface became increasingly irregular, displaying folds, mounds, lumps, and shear planes (Figure 70). This trend continued throughout the mold casting.

Starting with the eighth batch (Batch 172H), the propellant final mix cycle was performed at an intermediate vacuum level of 26.5 in. (670 mm) Hg. Flow during this cast was toward the northwest end.

Flow of the ninth batch (Batch 172I) was again in the northeast direction. This batch included 0.1% benzidine yellow to produce green propellant. The color surfaced intermittently, resulting in a churned, but not mixed, appearance. In Figure 71, the light-colored propellant at the top is green. The small lumps visible on the surface were entirely homogeneous. These were apparently higher viscosity, older propellant picked up by the moving stream, and are not indicative of formulation variance.

Batch 172J (tenth batch) again flowed to the northeast. The ninth batch propellant (green) flowed over a large portion of the surface. In Figure 72 (looking toward the center of the mold), the propellant in the foreground is green. The maximum surface height was 6 in. (15 cm) above the top of the mold.

flow of Batch 172K (eleventh batch) initially caused the large mound to rise vertically, about 2 ft (60 cm) above the mold. The cast was stopped momentarily on two occasions to allow horizontal flow to be established in the westerly direction to avoid spillage. Once a channel was established, the propellant flowed rapidly to the end of the mold, and continued for several minutes after cessation of bayonet flow.

Batch 172L (final batch) was cast without incident, flowing through the same channel as the previous batch and toward the west end of the mold. The bayonet was pigged and removed.

Analysis of the time-lapse films and surface height measurements acquired during casting of the full-scale mold confirmed a visual observation that no significant movement occurred during the time spans between batches. This is consistent with the highly pseudoplastic, nature of the cast propellant, characterized by extreme viscosity at low shear stress levels. Between-batch movement was recorded by surface height measurements within the first hour after casting each of the first three batches. Movement occurred where a distinct height differentail or "wave" formed near an end of the mold and subsequently leveled. Figure 73 through 75 summarize graphically the surface height measurements recorded at the cessation of flow of each batch cast.

e. Cured Propellant Analysis

At two weeks after the completion of casting, Shore A hardness measurements on propellant samples indicated the state of cure of the mold was sufficient to interrupt the cure and initiate sectioning of the propellant. Following 3 days of cooldown, the environmental enclosure was removed and the casting form was disassembled. Figure 76 is an overhead view of the mold.

III.C. Discussion of Results (cont)

When the mold had been stripped, numerous defects were observed on all sides (Figures 77 through 84). The vertical lines on the mold surface result from wires installed in the casting form for cutting of the cured propellant; thermocouple wires; depth scales; and the tape used to hold the wires against the casting form. Other vertical and horizontal stripes which are evident resulted from a color transfer from rubber strips used to seal the casting form. Propellant from the fourth and ninth batches, which were green, appears darker in the photograph. A map of surface defects is shown in Figure 85. These defects were not as severe as the worst of those observed in the grain of Motor 260-SL-3, but were more frequent and generally of the same character. Excluding porous type defects, the 260-SL-3 grain inner bore had 166 defects, or 0.56 defects/m^2, while the mold had approximately 168 defects, or 7.8 defects/m^2. The surface defects ranged in size up to 91 in. (2.3 m) long, 4.0 in. (10 cm) wide, and 1.0 in. (2.5 cm) deep. Virtually without exception, the defects were associated with batch interfaces and conversely, except for the first three batches, every batch interface produced extensive defects. Consequently, the defects were largely horizontal, although the severe surface irregularity observed during the mold casting created unusual batch interfaces and defects. It is evident that, while the flow characteristics of the propellant used in the mold casting were more consistently undesirable than Motor 260-SL-3 propellant characteristics, the mechanism of defect formation at the cured grain surface clearly was demonstrated.

The mold half which included the liner bond panels was cut into eight 7.5 degree (0.13 rad) sections. Sectioning was accomplished with music wire and a dead-weight tension arrangement. Only a few small defects were exposed by the cuts. These 1- to 2-in. (2.5 to 5 cm) dia voids were more frequently near the end of the mold. The maximum quantity observed in any of the 5.5 by 6 ft cuts was six, at the cut nearest the end, and the cut at the center of the mold exposed no voids. Some of the batch interfaces

III.C. Discussion of Results (cont)

appeared to be slightly torn or partially separated as a result of the cutting process, apparently indicating low-strength propellant-to-propellant bonds. However, this condition was not verified by tensile testing of batch interfaces.

In the cutting of the remaining half of the mold for disposal, the largest internal defect was exposed. This 12 by 18 by 1 in. (30 by 46 by 2.5 cm) defect was associated with the batch interface created during the casting of the eleventh batch. The location of the defect was such that it was nearly connected to the large surface defects shown in the upper-left portion of Figure 82.

Carton samples of the batches cast into the mold were tested at intervals through a 40-day cure at 135°F (57°C). The data (Figure 86) indicate that cure had stabilized between 20 and 25 days. The propellant initial modulus ranged from 300 to 575 psi (207 to 397 N/cm^2) for the 12 batches.

A schematic of the full-scale grain showing the locations from which test specimens were prepared, as well as the code used to designate these locations, is given in Figure 87. A summary of the data obtained to date from these tests is presented in Figures 88 through 94. The mechanical properties and solid-strand burning rate data show the same type of anisotropic behavior observed in all of the subscale molds. In addition, the apparent state of cure, as indicated by initial modulus of elasticity (E_o), is higher in the mold specimens than in the carton samples, similar to the effect noted in the subscale molds. However, the liner-propellant bond strength (Figures 88, 91, and 94) shows a definite trend toward lower values as the location from which the test specimens were taken gets closer to the top of the mold, with some upper locations showing no measurable bond strength. This decrease in bond strength near the top of the mold is believed to be related to the age of the propellant being forced into contact with the liner.

III.C. Discussion of Results (cont)

With the bayonet at a relatively deep submergence, up to 4 ft (1.2 m), the casting of each batch forces progressively older propellant to the surface and into contact with the liner eventually resulting in poor "wetting" of the liner by the old propellant and subsequent poor bonds. This behavior could easily explain some of the ballistic abnormalities observed during the latter part of the firing of Motor 260-SL-3.

Additional propellant-liner bond tests were conducted to determine if the lack of liner-bond found near the top of the first large mold was attributable to contamination, overcure of the liner, or the propellant flow behavior in the mold. Samples of the unbonded SD-850-2 liner/V-44 insulation were removed from the mold for these bond tests. Fresh ANB-3254 propellant from a 10-lb (4.5 Kg) batch was cast against the liner. Double-plate sandwich bond specimens were then prepared and tested. These specimens gave average bond tensile strengths of 86 psi (59 N/cm^2) with normal cohesive breaks in the propellant. On the basis of these tests it can be concluded that the SD-850-2 liner in the mold was normal and that the lack of bond in the mold was due to the propellant flow process.

Mechanical properties specimens were taken randomly from interfacial locations that were found during the sectioning of the grain. In general, the test results, shown in Figure 95, were similar to properties obtained from propellant specimens which showed no interface.

f. Interpretation of Results

The conditions of the casting of Motor 260-SL-3 grain were successfully simulated. The slightly reduced vacuum level in the 5500-lb (2500 Kg) vertical batch mixer represented the probable conditions in the mixers at A-DD and produced the type of flow behavior and resultant grain defects observed in the grain of Motor 260-SL-3.

III.C. Discussion of Results (cont)

The types of defects produced were primarily propellant-to-propellant voids at the walls of the casting form, similar to the defects of Motor 260-SL-3. The defects occurred at the interface between stationary, previously cast propellant and propellant which flowed during the casting of batches. In most instances, the flowing propellant creating the defects was not from the batch actually being cast, but from an earlier-cast batch being displaced and pushed ahead in a wave over the surface. The defects were formed because of non-uniform surface conditions in both the stationary propellant and the flowing propellant. These surface conditions were indicative of pseudoplastic viscosity characteristics.

The effect of time between batches was to increase the viscosity of the propellant being displaced. However, this effect apparently was mitigated partially by the tendency of flow through aged propellant to displace less aged propellant and to create a smaller channel from the bayonet tip to the surface, resulting in a higher proportion of fresh propellant in the flow.

The effect of bayonet submergence was to create more flow distance between the bayonet tip and the surface of the cast propellant, thereby disturbing more propellant of greater age with greater submergence. The tendency to create flow channels was greater with increased bayonet submergence, resulting in mounding around the bayonet and non-uniform distribution of flowing propellant over the surface. Each batch cast tended to follow the channel of the previous batch, because of the lower resistance to flow by the more recently cast propellant, until the hydrostatic head in channel became greater than the resistance of the aged propellant at some lower level in the mound, thereby resulting in the formation of a new channel. This behavior had the effect of increasing the batch intervals. For example, the

III.C. Discussion of Results (cont)

casting of the eleventh batch resulted in flow over a surface that had been stationary for 24 hr, as derived from the surface contours (Figures 73 through 75) and the processing times of Figure 64. The largest internal defect and some of the most severe surface defects were observed at this interface.

The flow paths within the full-scale mold were similar to those documented in the first subscale mold, except that most of the vertical flow was within a radius of about 2 ft (60 cm) of the bayonet and did not occur immediately adjacent to the walls of the casting form. The pattern was for the propellant to emerge from the bayonet tip and flow upward, without flowing more than about 6 to 8 in. (15 to 20 cm) below the bayonet tip. In the flow upward the propellant would either spread outward around the bayonet at low submergence, or channel to one side of the bayonet, at high submergence, causing the surface mount to rise initially, and then to flow horizontally. Contact of the propellant with the walls resulted from horizontal flow.

The poor bonding of the propellant to the liner can be attributed to high viscosity and subsequent inadequate wetting of the liner, rather than to a low potential for chemical bonding, or to disturbance of gelled propellant at the bond interface. This propellant will normally bond to liner for periods up to 3 days after curing agent addition. The adequacy of the liner was proved by bonding fresh propellant to a sample of the liner panels at a later date. The flow patterns do not indicate subsurface flow along the walls of the casting form that might disturb gelled propellant at the liner surface.

III.C. Discussion of Results (cont)

3. Propellant Modification Studies (Task II)

a. Evaluation of Mixing Variables

Visual observations of the propellant batches mixed for Motor 260-SL-3 indicated that the flow behavior of the ANB-3254 propellant was influenced by the mixing procedure used in the 300-gal (1.14 m^3) vertical mixers at A-DD. Small scale 10 lb (4.5 Kg) propellant batches were prepared to evaluate the effect of mixing variables on propellant flow characteristics, cure, and mechanical properties. The variables investigated and the levels of each variable are shown below:

(1) Vacuum level: 10, 15, 20, 25, and 29 (max) in. (250, 380, 510, 640, and 740 mm) hg.

(2) Final mix time: 5, 10, 20, 40, and 60 min.

(3) Mix temperature: 130, 135, and 145°F (54, 57, and 63°C).

(4) Mixer speed: 31, 67, and 104 ft/min (16, 34, and 53 cm/s) planetary blade tip speed.

The results of these studies are summarized in Figures 96 through 100. Mixer vacuum level, Figure 96, had a definite effect on propellant density and viscosity. Vacuum levels below 25 in. (640 mm) Hg caused significant reductions in measured propellant liquid density indicating that this acceptance test could detect a failure of the mixer vacuum system which produced a vacuum below 25 in. (640 mm) Hg. High propellant viscosity at low shear stress also was a characteristic of propellant mixed at reduced vacuum levels indicating that this is a critical parameter in the processing of ANB-3254 propellant.

III.C. Discussion of Results (cont)

Propellant final mix time has no apparent effect on liquid density, liquid-strand burning rate or mechanical properties (Figures 98 and 99). There is, however, an influence of length of final mix time on propellant viscosity. At both maximum vacuum and reduced vacuum levels the propellant viscosity after only 5 min of final mix is significantly higher than comparable batches with longer final mixes. This may be interrelated to vacuum level in that total vacuum exposure or mixer vacuum efficiency is probably the true critical parameter.

Another indication of the importance of deaeration on the propellant properties is shown by comparison of the mechanical properties data in Figures 96 and 97. Figure 96 shows that decreasing the vacuum level from the maximum level of approximately 27 to 29 in. (690 to 740 mm) Hg state of cure, i.e., the propellant initial modulus decreases from 625 to 507 psi (431 to 350 N/cm^2), respectively. These propellant batches were made using the relatively large high-capacity mix station vacuum pump with the lower vacuum levels being obtained by bleeding air into the line between the mixer and the pump. This procedure eventually caused damage to the pump and a small inexpensive laboratory vacuum pump was installed in the mix bay for subsequent batch mixes at below-maximum vacuum level. The major difference between the two setups was that with the small pump the vacuum line to the mixer was much smaller, about one-tenth of the area of the line to the mixer from the large pump. As shown in Figure 97, this difference in line size apparently resulted in significantly lower states of cure for batches mixed at the same vacuum level. This difference is attributed to the fact that even though the vacuum levels were comparable, less water was removed from the propellant through the small line, and more extensive degradation of the FeAA cure catalyst, through hydrolysis, occurred, which in turn resulted in a lower state of cure.

Variation in mix temperature, as shown in Figures 98 and 99, from 130 to 145°F (54 to 63°C) showed no significant effect on viscosity,

III.C. Discussion of Results (cont)

density, burning rate or mechanical properties. Propellant batch mix temperature when controlled within normal limits should therefore not be a critical processing parameter.

Mixer blade speed (Figure 100) appears to have an effect on propellant properties. A significantly lower viscosity was obtained from mixing the propellant at a fast mixer blade speed. This also may be related to mixer vacuum efficiency in that the higher blade speed would allow a more rapid deaeration of the propellant mix. Mechanical properties were affected by the fast blade speed. Initial modulus of this batch was about one-half to two-thirds the modulus obtained in mixes using lower blade speeds.

b. Laboratory Scale Casting

To determine if the propellant flow patterns observed in the subscale molds could be duplicated in molds of still smaller size requiring less propellant, and consequently at lower cost, laboratory scale molds approximately 12-in. (30 cm) in dia with a 6 in. (15 cm) cylindrical core were cast using 10-lb (4.5 Kg) propellant batches. The propellant was transferred from the mixer to a pressure vessel and bayonet cast through 1-in. (2.5 cm) dia tube into the mold. The first laboratory scale mold was cast in exactly the same way as the first 42-in. (1.07 m) subscale mold casting, using the multi-colored propellant formulations in five 10-lb (4.5 Kg) batches. When cured, the mold was sectioned and the flow patterns were examined (Figure 101). The flow patterns are almost identical to those observed in subscale mold 1.

A second laboratory scale mold was cast on the basis of this encouraging similarity to determine what the effect on flow patterns would be if the bayonet tip was positioned above the surface of the propellant during the entire casting. The same five multi-colored propellant formulations were used, and the casting of each batch was started with the bayonet tip sufficiently

III.C. Discussion of Results (cont)

above the surface about 1.5 in. (3.8 cm) so that when the casting of the batch was complete, the level of the propellant in the mold had risen just to the end of the bayonet. As shown in Figure 102 of the cured and sectioned grain, a high degree of layering of each batch occurred. This is, of course, highly desirable from the standpoint of ensuring the contact of both propellant and liner bond interfaces with fresh propellant. A comparison of the flow patterns of these two laboratory scale molds strongly suggest that shallow bayonet submergence or even above-surface casting is the most favorable condition from the standpoint of preventing grain and bond defects.

c. Evaluation of Propellant Compositional Factors

The objectives of the propellant compositional studies were to determine the compositional factors in ANB-3254 propellant responsible for its undesirable flow behavior and, through the use of alternative ingredients, to develop a new formulation exhibiting improved processing and viscosity characteristics and the same ballistic and mechanical properties as ANB-3254. In accomplishing these objectives, the burning rate additive type, oxidizer blend, plasticizer type, surface active agents, and cure catalyst type were evaluated.

A summary of the results from 10-lb (4.5 Kg) propellant batches made to evaluate the effects of burning rate additives and oxidizer blends are summarized in Figure 103. As shown, the burning rate additive system of the control formulation ANB-3254 (1.2 wt% Iron Blue/BRA-101) gave a burning rate of 0.691 in./sec (1.76 cm/s) at 600 psi (414 N/cm^2) with an oxidizer blend composed of 60/40 SSMP/MA. This batch, 7200-17, exhibited flow behavior typical of ANB-3254, i.e., undesirable pseudoplasticity. Decreasing the amount of fine ground oxidizer in the blend to 65/35 or 70/30 produced the expected decrease in burning rate to 0.666 and 0.629 in./sec (1.69 and 1.60 cm/s), respectively, but did not significantly affect the flow characteristics. Thus, changes in oxidizer blend do not appear to be a critical factor.

III.C. Discussion of Results (cont)

The next two batches shown in Figure 103 (Batches 7245 and 7246) were formulated with 1.2 wt% Iron Blue and 1.2 wt% BRA-101, respectively, to determine which of these burning rate additives had the greatest effect on processability of the propellant. As the viscosity data show, the batch made with BRA-101 as the sole burning rate additive exhibited extremely poor flow behavior while the batch made with Iron Blue only showed better processability than the control ANB-3254. Based on these results, it is apparent that BRA-101 is a major contributor to the undesirable flow characteristics of ANB-3254 propellant. Therefore, its use was precluded from consideration as an improved formulation ingredient. Iron Blue does not adversely affect processing properties and received further consideration.

However, the burning rate achieved with only Iron Blue (with a 65/35 SSMP/MA blend) was 0.645 in./sec (1.64 cm/s), which is below the target of 0.68 in./sec (1.73 cm/s). Additional work was performed (discussed below) that indicated that the burning rate of this propellant could be increased to meet the target requirement though the use of a finer oxidizer blend at some sacrifice of the desirable processing characteristics.

A very desirable burning rate additive from the standpoint of its effect on propellant flow behavior is iron oxide. Two batches (7288 and 7312) were prepared to determine if the target burning rate could be achieved with iron oxide as the only burning rate additive and with oxidizer blends containing large amount of MA-ground oxidizer. With 1.5 wt% iron oxide and a 55/45 SSMP/MA blend, the processability of the propellant was excellent, but the burning rate was only 0.595 in./sec (1.51 cm/s). Increasing the concentration of iron oxide to 2.0 wt% and the fineness of the oxidizer grind to 50/50 SSMP/MA increased the burning rate to 0.663 in./sec (1.68 cm/s) but the processability with this fine blend was no better than the control. From this data, it appears that iron oxide by itself cannot provide sufficient burning rate catalysis to meet the target rate.

III.C. Discussion of Results (cont)

Alternative burning rate additives investigated included CuO202 and a mixture of Iron Blue with a modified Silon S (Batches 7289 and 7314, respectively). The batch mixed with CuO202 was very difficult to process and did not cure while the Iron Blue/Silon batch showed excellent processability, but the burning rate was only 0.610 in./sec (1.55 cm/s) at 600 psig (414 N/cm^2). These materials were eliminated from further consideration.

Because the binder ingredient with the greatest effects on processability is the plasticizer, 10-lb (4.5 Kg) laboratory batches were prepared to evaluate plasticizers other than the DOA used in ANB-3254. The results of this investigation (Figure 104) indicate that none of these materials offered any advantage over DOA. One of the lowest cost plasticizers commercially available is a low molecular weight polybutene (M.W. = 600).

However, in the PBAN binder, this plasticizer does not appear to be compatible and the resulting propellant (Batch 7290) exhibited very poor processability. Another plasticizer investigated because of its potential as an aging stabilizer as well as a plasticizer was the thio-ester TTIA. This material was evaluated in two batches (7334 and 7289) with the burning rate additives CuO202 and Iron Blue, both of which are known to cause postcure in polybutadiene propellants. The processability of both batches was poor; neither cured. Two other plasticizers which had been used previously in solid propellants, oleyl nitrile and an ester of ricinoleic acid, also were investigated in this study. The oleyl nitrile provide low viscosities, comparable to DOA, but retarded the cure. The batch prepared with ricinoleate plasticizer processed poorly. On this basis of these data, it can be concluded that none of the plasticizers investigated showed any advantage over DOA.

Surface active agents have been shown to enhance the processing characteristics of many solid propellants. Three commercially available materials, sorbitan oleate, a polydimethylisiloxane, and FC-167 (an Aerojet

III.C. Discussion of Results (cont)

proprietary propellant wetting agent) were evaluated. The results of this evaluation (Figure 105) show that all three compounds reduced the apparent viscosity at 6 hr after curing agent addition from 50,000 poise (5,000 Ns/m^2) to 30,000 to 31,000 poise (3,000 to 3,100 Ns/m^2) at a shear stress of 5,000 dynes/cm^2 (500 N/m^2). At 10 hr after curing agent addition, only the batch containing FC-167 still exhibited a lower viscosity than the control. Based on this and on other work described in a subsequent section, FC-167 was selected for further evaluation in the improved formulation.

The initial scale-up batches of ANB-3254 propellant made at A-DD revealed that higher concentrations of FeAA cure catalyst and DER-332 curing agent were required to achieve the same target modulus than in the smaller laboratory scale mixers used at SRD. For example, in the 10-lb (4.5 Kg) SRD mixers, 113 equivalents of curing agent and 0.02 wt% FeAA were required to yield a modulus of about 500 $\pm$ 100 psi (345 $\pm$ 69 N/cm^2), while at A-DD, the same modulus could be achieved only with 125 to 130 equivalents of DER-332 and 0.035 wt% FeAA. As shown in Figure 106, this change in formulation had a large effect on flow behavior and mechanical properties of propellant prepared at Aerojet. At the lower curing agent and cure catalyst levels the propellant exhibited pseudoplastic viscosity characteristics and cured to a modulus of 625 psi (432 N/cm^2), but at the higher levels, the propellant pseudoplastic characteristics became more pronounced and the propellant initial modulus was nearly doubled. A probable explanation for this lies in the large difference in surface-to-volume ratio between the 10-lb (4.5 Kg) and 5500-lb (2500 Kg) mixers, with the larger mixer being less efficient in removing volatiles such as moisture from the propellant. The resulting higher moisture present in the large batch caused degradation of the FeAA through hydrolysis, leading to a lower state of propellant cure. Tentative confirmation of this effect was obtained from actual moisture measurements on propellant taken from both mixers:

Mixer Size, lb (Kg)	10 (4.5)	5500 (2500)
Propellant Moisture Content, wt%	0.017	0.048

III.C. Discussion of Results (cont)

The moisture content of the propellant mixed in the laboratory mixer was only about one-fourth that of the propellant from the production mixer. Additional confirmation of the proposed mechanism was obtained from experiments whereby samples of the volatiles removed from the propellant during mixing were trapped and analyzed. These analyses showed conclusively that the degradation product of FeAA by hydrolysis, acetyl acetone, was present, indicating that hydrolysis was taking place even during the propellant mixing. It was concluded that a propellant cure catalyst more stable than FeAA was required in the improved formulation.

d. Improved Propellant Formulation

The formulation ingredients selected to provide a propellant exhibiting the same ballistic and mechanical properties as ANB-3254, but with improved processing characteristics, are summarized below:

Burning rate additives	Iron oxide/Iron Blue
Wetting agent	FC-167
Cure catalyst	FC-151
Antioxidant	PBNA

The basis for these selections are discussed in the following paragraphs.

The use of Iron Blue as the sole burning rate additive was considered for the improved propellant formulation. Although less active ballistically than the combination of Iron Blue and BRA-101, it does not appear to have adverse effects on propellant flow behavior. As described earlier, the viscosity characteristics of a propellant with 1.2 wt% Iron Blue and a 65/35 SSMP/MA oxidizer blend are excellent with a viscosity of only 18,000 poise (1,800 Ns/m^2) at 5 kdynes/cm^2 (500 N/m^2) shear stress, 6 hr after curing agent

III.C. Discussion of Results (cont)

addition. However, because of its lower ballistic activity, the burning rate of this propellant was below the target requirement. The burning rate was increased by increasing the amount of fine ground oxidizer, and with a 60/40 SSMP/MA oxidizer blend, the target burning rate of 0.68 in./sec (1.73 cm/s) at 600 psig (414 N/cm^2) was achieved. However, the viscosity characteristics of this formulation (Figure 107) were not substantially better than ANB-3254 with the mixed burning rate additives.

A considerable improvement in the flow behavior of the propellant with 1.2 wt% Iron Blue and a 60/40 SSMP/MA oxidizer blend was made possible by the development on an Aerojet IR&D program of a new wetting agent designated FC-167. This material, which also enters into the cure reaction, has been shown to provide substantial reductions in the viscosity of PBAN propellants. When 20 equivalents of FC-167, less than 0.10 wt% on the propellant, are incorporated into the binder of the above formulation, the viscosity is significantly reduced, as presented in Figure 108 and compared to a batch with standard binder components in Figure 109. This batch cured in 20 days to the following 77°F (25°C) mechanical properties.

σ_m	77 psi (53 N/cm^2)
ε_m	25%
ε_b	29%
E_o	387 psi (267 N/cm^2)

This improvement on processing characteristics warranted the selection of FC-167 for incorporation into the improved formulation.

Relatively large amounts of Iron Blue are known to cause cure inhibition in polybutadiene propellants and require the use of excessive curing agent to achieve the desired rate and state of cure of the propellant. On long term storage this excess curing agent could conceivably cause postcure.

III.C. Discussion of Results (cont)

The use of conventional antioxidants such as PBNA (phenyl β-naphthylamine) could stabilize the propellant state of cure, even at a temperature of 180°F (82°C) for up to 2 weeks (Figure 110).

Iron oxide possesses many advantages over other available burning rate additives, including stability, low moisture content, chemical inertness, and little effect on propellant processing or cure. Therefore, the most promising approach to achieving the target burning rate appeared to be a combination of relatively large amounts of iron oxide, about 2.0 wt%, with the minimum quantity of Iron Blue necessary to meet the burning rate requirement. In a laboratory scale batch, a burning rate of 0.685 in./sec (1.74 cm/s) at 600 psig (414 N/cm^2) could be achieved with a mixture of 2.0 wt% iron oxide and 0.5 wt% Iron Blue. The viscosity characteristics of this formulation were excellent (Figure 111). Based on the storage stability data given above for a formulation containing 1.2 wt% Iron Blue, the smaller amount contained in this formulation should minimize the problem of stabilization. When this formulation subsequently was processed in larger batch sizes, the burning rate scaled up sufficiently to enable a further reduction in Iron Blue content to only 0.1 wt%.

Evidence of the relative insensitivity of propellant cure, mechanical properties, and storage stability to this small amount of Iron Blue is the significant reduction of epoxy curing agent required to achieve the same propellant initial modulus compared with the formulation containing 1.2 wt% Iron Blue. The latter formulation required 113 equivalents of DER-332 to achieve a modulus of 387 psi (267 N/cm^2) while the propellant with 2.0 wt% iron oxide and 0.5 wt% Iron Blue cured to a modulus of 418 psi (288 N/cm^2) with only 83 equivialents of DER-332.

As discussed previously, the use of FeAA as the polymerization catalyst is undesirable because of its lack of hydrolytic stability.

III.C. Discussion of Results (cont)

Aerojet's cure catalyst, designated FC-151, has been selected for use in the improved propellant formulation. As shown in Figure 107, FC-151 is about equal to FeAA in catalytic activity. However, because of its chemical structure it is much more stable and has been shown to exert no influence on the storage stability of the propellant.

A laboratory scale batch of the improved formulation incorporating all of the above ingredients (2.0 wt% iron oxide, 0.5 wt% Iron Blue, 20 equivalents of FC-167, 0.1 wt% PBNA, and 0.05 wt% FC-151) cured to the following mechanical properties:

σ_m	76 psi (52 N/cm^2)
ε_m	22%
ε_b	23%
E_o	418 psi (288 N/cm^2)

Although the general composition of ANB-3350 can thus be derived from work accomplished under the Task II effort (Figure 113), selection of the specific formulation to be cast into the second full-scale mold for the Task III processing demonstration was deferred, pending intermediate scale-up to 450-lb (200 Kg) vertical batch mixes used in casting the final three sub-scale molds, minor formulation variables were also investigated to enable selection of an optimized formulation for the Task III processing demonstration.

e. ANB-3350 Premix Storage Stability

To gain a preliminary evaluation of the stability of the ANB-3350 premix, which includes all propellant ingredients except oxidizer and curing agent, a series of 10-lb (4.5 Kg) propellant batches were prepared using premix stored up to 14 days prior to propellant mixing. The formulation selected for evaluation was based on 2.0 wt% iron oxide and 0.5 wt% Iron Blue as the

III.C. Discussion of Results (cont)

burning rate additives, 30% DOA plasticizer, and 83 equivalents of DER-332 curing agent. The test was conducted by preparing a single batch of premix sufficient for seven 10-lb (4.5 Kg) batches of propellant and by mixing batches using aliquots from the master batch at intervals of 0 (control), 1, 2, 3, 4, 11, and 14 days. The viscosity and mechanical properties data (Figure 114) indicate no significant effect of premix storage through the 11-day storage period. The initial modulus of the batch mixed with premix stored for 14 days appears to be low, but it is possible that this difference represents normal batch-to-batch variability. Based on these data, and confirmed subsequently in the casting of the tenth subscale mold, the premix appears to have good stability.

f. Rapid Evaluation of Propellant Flow Behavior

Although the Rotovisko viscometer is the most accurate and sensitive instrument available for measuring propellant viscosity, the data accuracy deteriorates at the low shear stress levels, which are of the greatest interest in this application. Furthermore, the reduction of the data is laborious, normally requiring a computer, and the results are subject to interpretation differences. For these reasons, experimentation has been conducted to devise a simple representative test to estimate rapidly the flow behavior of a batch of propellant. Such a test is required for use as batch qualification or acceptance test. Several methods were considered and evaluated: one of which is a test of the flow of the propellant under its own hydrostatic head. The results were obtained by filling a rectangular 2 by 2 by 6-in. (5 by 5 by 15 cm) box with propellant and turning the box on end to observe the propellant flow from the box. Differences in flow behavior can be directly observed by this simple test.

Box flow tests were made on propellant samples from a batch used to cast the first full-scale mold, batches used to cast the seventh subscale mold, and batches of the improved formulation (see following section)

III.C. Discussion of Results (cont)

used to cast the eighth subscale mold. The data, summarized in Figure 115, show a good correlation between measured viscosity at low shear stress, 5 kdynes/cm^2 (500 N/m^2), and the size of the pool of propellant flowing from the box. For example, the propellant from the batch used to cast the full scale mold showed a viscosity of 55,000 poise (5,500 Ns/m^2) and the pool of propellant formed was only about 2 by 4 in. (5 by 10 cm), i.e., the propellant barely flowed from the box. In contrast, a sample of the improved formulation showed a viscosity of 15,000 poise (1,500 Ns/m^2) and the flow from the box formed a pool 8.5 by 15 in. (22 by 38 cm).

Although the box test has advantages of simplicity and good apparent correlation with propellant viscosity characteristics, it also has the disadvantages of requiring relatively stringent temperature control and a considerable oven space when conducting many tests simultaneously. The most promising method developed to overcome these disadvantages and to provide as good, or better, correlation with propellant flow behavior involved the use of a falling-ball type of viscometer adapted for use directly in the mix bowl. In this test a steel ball of about 1.312 in. (3.34 cm) dia is allowed to fall through the uncured propellant. The time required to fall a specific distance, 3 in. (7.62 ccm), is measured. A thin steel rod is attached to the ball to enable retrieval and to indicate when the ball has fallen the required distance. The simplicity of this test is particularly valuable: it can be conducted in the mix station by quality control personnel as part of the normal inspection routine. The capability of this test to distinguish between "good" and "bad" propellant is indicated in Figure 115 which compares the times required for the ball to fall 3 in. (7.62 cm) in the five 450-lb (200 Kg) batches of the improved formulation cast into subscale mold 8 with the rate of fall in a smaller batch of ANB-3254. In the improved formulation, the ball fell 3 in. (7.62 cm) in 21 to 34 sec, while in ANB-3254 the rate of fall was only 1 in. (2.54 cm) in 20 min (1200 sec).

III.C. Discussion of Results (cont)

Falling-ball measurements were made on all subsequent batches of propellant prepared for the ninth and tenth subscale molds as well as all of the 5500-lb (2500 Kg) batches prepared to cast the second full-scale mold. As noted in the following section describing the casting of this second full-scale mold, the falling-ball test provided the first indication of a processing anomoly on one of the 5500-lb (2500 Kg) batches. From all of the data available and considering the relative accuracy and simplicity of the test, the falling ball appears to be very promising as a propellant acceptance test. Complete characterization of the test, including determination of limits, corrections for temperature, etc., were not within the scope of this program.

III.C. Discussion of Results (cont)

4. Subscale Molds 8 through 10

Subscale molds 8 through 10 were cast with ANB-3350, the improved propellant formulations. The effects of casting process variables on grain quality were determined. ANB-3350 formulation variables were evaluated in the 450-lb (200 Kg) batches prepared for these molds to define the exact formulation composition for processing the final full-scale mold cast under Task III.

a. Subscale Mold 8

The casting process and propellant formulation variables evaluated in the enghth mold are summarized in Figure 116. Variations in Iron Blue, DER-332, FC-167, antioxidant, and plasticizer concentrations were evaluated. The Iron Blue burning rate additive was varied from 0 to 0.5% to establish the burning rate sensitivity of the improved formulation with an oxidizer blend of 60/40 SSMP/MA. Two levels of DER-332 curing agent and two levels of plasticizer, 25 and 30%, were evaluated. The relative effects of 10 and 20 equivalents of FC-167 and of 0.10 and 0.20% antioxidant were also assessed.

A summary of the uncured propellant data is shown in Figure 117. The data show that the target burning rate of 0.68 in./sec (1.74 cm/s) at 600 psi (414 N/cm^2) was bracketed by Iron Blue levels of 0.10 and 0.25 wt% using 60/40 SSMP MA oxidizer blend.

The propellant batches were cast into a mold with a 360-degree (6.28 rad) configuration and a minimum bayonet submergence. All batches cast into this mold exhibited excellent flow characteristics as evidenced by the viscosity data listed in Figure 117. The appearance of the mold also testified to the excellent flow properties of the propellant. The surface

III.C. Discussion of Results (cont)

of the mold was smooth with no height differential across the vertical dam (Figure 118). The formulation variable evaluated in the fifth batch was the reduction of DOA plasticizer from 30 to 25 wt% of the binder. In comparison with the other batches mixed for casting the eighth mold, no significant change in flow characteristics was noted with the reduced plasticizer level.

The effects of the formulation modifications on cure and mechanical properties based on carton samples data are presented in Figure 119. Conclusions based on evaluation of the Mold 8 data are presented below:

Addition of the antioxidant PBNA appears to increase both the cure rate and the final state of cure based on a comparison of the first two batches containing 0.1 and 0.2 wt%, respectively. After 22 days cure, the batch with the lower level of PBNA had reached an initial propellant modulus of 564 psi (389 N/cm^2) compared with 651 psi (449 N/cm^2) for the batch with increased PBNA. These data might also be compared with the properties of Batch 69-11, the fifth batch cast into the seventh mold. This batch had no PBNA and after 24 days cure, the modulus was 483 psi (333 N/cm^2). This effect of PBNA content on cure is undoubtedly because it is an amine. Amines exert a catalytic influence on the reaction between epoxides and carboxyls such as DER-332 and PBAN.

Reduction of the level of FC-167 from 20 to 10 equivalents results in a lower state of cure, as shown by the initial modulus of 424 psi (292 N/cm^2) after 22 days cure. This is due partly to the fact that FC-167 exhibits some catalytic activity, as it is also an amine. Reduction of the FC-167 concentration may also reduce the cross link density of the propellant binder, since it is a functional material that can enter into the cure reaction. However, the extent to which this actually occurs is not completely known at the present time.

III.C. Discussion of Results (cont)

Reduction of the DER-332 curing agent level from 85 to 32 equivalents apparently did not produce the expected reduction in cure level as shown by comparison of Batches 69-24 and 69-21 in Figure 119. However, the batch with the lower DER-332 level was prepared without any Iron Blue burning rate additive compared with 0.5 wt% Iron Blue used in Batch 60-21. It has been previously shown that Iron Blue causes some retardation of the cure of these propellants, and this is probably the reason that the propellant initial moduli of these two batches is essentially the same, even though the curing agent level was reduced.

The fifth batch cast into this subscale mold was prepared with the DOA plasticizer content reduced from 30 to 25% by weight from 85 to 82 equivalents in this batch, the propellant initial modulus increased to 708 psi (488 N/cm^2) after 22 days cure at 135°F (57°C). Achieving the target modulus with a 25% plasticized formulation will require still further reduction in the curing agent concentration.

The mechanical and bond properties and solid strand burning rate data from the eighth subscale mold are shown in Figure 120. It is difficult to assess anisotropy in this mold because of the wide variation in mechanical properties and burning rates of individual batches, due to formulation variations, cast into this mold. The modulus and strength data exhibit the usual trend toward higher values in the grain than in the cartons. The comparatively low bond strength data for the eighth subscale mold do not reflect the bond between the improved formulation propellant and SD-850-2 lined Gen-Gard V44 rubber. An adhesive used to bond steel plates to the cured propellant surface resulted in a bond failure at the adhesive-propellant interface. Tensile testing specimens prepared by casting propellant from this mold between two plates, each lined with SD-850-2 on Gen-Gard V44 rubber, gave random breaks in the propellant at a stress of 105 psi (72 N/cm^2).

III.C. Discussion of Results (cont)

b. Subscale Mold 9

This mold was also cast with the improved propellant formulation and the 360-degree (6.28 rad) grain configuration. The bayonet location was controlled to assess the feasibility of casting with the bayonet tip above the surface of the propellant. The first four batches were cast with the bayonet tip about 1, 3, 6, and 9 in. (2.5, 8, 15, and 23 cm) above the surface, respectively. The stream of propellant effluxing from the bayonet flowed smoothly onto the propellant mass at the 1 and 3-in. (2.5 and 8 cm) locations above the surface; at 6 in. (15 cm) the stream began to oscillate slowly, but the propellant flowed into the mass without entrapping any air. However, with the bayonet tip 9 in. (23 cm) above the surface, the propellant stream from the bayonet began to curl into the resident propellant in such a way as to entrap small amounts of air at practically every turn of the stream. Numerous air bubbles could be seen at the surface away from the bayonet. As this was unacceptable from a grain homogeneity standpoint, the fifth and final batch was cast with the bayonet tip 6 in. (15 cm) from the surface.

An additional objective of the fifth batch of propellant was to assess the sensitivity of the improved formulation to changes in the batch mix cycle. The fifth batch was mixed using the same procedure employed to produce the extreme pseudophastic characteristics in ANB-3254, i.e., no vacuum mix before curing agent addition and a shortened final vacuum mix cycle. This had no observable effect on the flow behavior of the improved formulation. The appearance of the propellant in the mix bowl, in the mold, and in the effluent from the bayonet was identical to the other batches. These observations indicate a very desirable lack of sensitivity of flow behavior to mixing conditions.

III.C. Discussion of Results (cont)

As with the eighth mold, all batches cast into this mold were of the improved propellant formulation with minor compositional variations including cure catalyst level and Iron Blue burning rate additive concentration as summarized in Figure 121. A summary of the uncured propellant data for these batches is given in Figure 122. The first batch was prepared with 0.1 wt% Iron Blue burning rate additive to confirm the data obtained from the last batch of the eighth mold. However, the burning rate proved to be considerably below the expected value, i.e., 0.64 vs 0.68 in./sec (1.62 vs 1.73 cm/S) at 600 psig (414 N/cm^2). The second batch was mixed with 0.25 wt% Iron Blue which yielded the target burning rate of 0.68 in./sec (1.73 cm/s). It was determined subsequently that the low burning rates of these batches compared with those cast into the eighth mold were related to the lot of ammonium perchlorate used. All batches for the eighth mold were made with newly purchased oxidizer from American Potash while the batches cast into the ninth mold which exhibit the lower burning rates were made from residual PEPCON oxidizer from Motor 260-SL-3 casting.

The third batch cast into the ninth mold was made with the new AMPOT oxidizer to confirm this effect of oxidizer lot burning rate. At 0.25 wt% Iron Blue the burning rate was 0.72 in./sec (1.83 cm/s) at 600 psig (414 N/cm^2), comparable to the results obtained in the eighth mold. The fourth and fifth batches were made with the residual PEPCON oxidizer at the 0.25 wt% Iron Blue level and exhibited burning rates of 0.69 and 0.68 in./sec (1.75 and 1.73 cm/s), respectively. Since both lots of oxidizer used in the eighth and ninth molds were ground at the same time, these differences in burning rate appear to be due to oxidizer lot differences rather than grind differences. However, as shown by data in Figures 117 and 122, the target burning rate can be achieved readily with either lot of oxidizer by a minor adjustment of the Iron Blue level.

III.C. Discussion of Results (cont)

There also appears to be an effect of oxidizer lot on propellant cure, as indicated by the modulus of elasticity data (E_o). By comparing mechanical property data from carton samples (Figure 123), Batches 69-32, 69-35, and 69-36 display significantly lower moduli than Batch 69-21 from the eighth mold (Figure 119) even though the formulations are essentially identical. A similar effect can be seen by comparing Batches 69-33 and 69-34. This behavior probably is due not to an actual difference in state of cure, but to a difference in oxidizer particle size distribution between the blends ground from the two lots of raw material. The greater amount of fines contained in the oxidizer ground from the new lot of material apparently increased the moduli as well as the burning rate in Batches 69-21 and 69-34.

Cure characteristics of propellant cast into the ninth mold were similar to the previously cast batches of ANB-3350 in that carton samples indicated steady state cure had been achieved within 18 days. The stripped propellant grain showed no evidence of external defects and, when sectioned, no internal voids were found. Mechanical property data obtained from the propellant grain exhibited the same anisotropic behavior observed in previous molds cast with ANB-3254 propellant. The data show typically higher values for initial modulus and tensile strength than indicated by the carton samples. These data along with bond data and solid strand burning rate data are presented in Figure 124. For the same reason discussed in connection with subscale Mold 8, the bond strength of samples prepared for this mold appeared low due to failure of the specimen at the propellant-steel interface.

c. Subscale Mold 10

The processing parameters evaluated in the casting of the tenth subscale mold were selected to provide a simulation of the casting of the second full-scale mold. The grain configuration was a two-thirds segment with a cylindrical core and a single centrally located bayonet.

III.C. Discussion of Results (cont)

All of the five propellant batches were of the improved formulation (ANB-3350) with minor composition variables. Figure 125 summarizes these variables. All batches were prepared with 25% DOA plasticizer (by weight of binder), and varying amounts of DER-332 curing agent and FC-151 cure catalyst. The propellant premixes for Batches 69-43, -44 and -45 were prepared in such a way as to evaluate the effects of premix storage for up to 3 days prior to propellant preparation.

The first batch was cast with the bayonet tip fixed at 3 in. (8 cm) from the bottom of the mold. For subsequent batches casting was started with the bayonet tip 6 in. (15 cm) below the surface, resulting in a range of 6 to 13 in. (15 to 33 cm) submergence for each batch. As with molds eight and nine, the propellant flow behavior was such that propellant surface remained level and smooth throughout with no evidence of defect formation.

The flow characteristics of these propellant batches showed no significant effect of any of the formulation variables investigated or of the premix storage time on propellant flow behavior. Viscosity and uncured propellant data are summarized in Figure 126. Similarly, no effect of premix storage was evident from sample carton mechanical property data as shown in Figure 127. These data indicate that even with the lower cure catalyst level of 0.03 wt% for Batches 69-41 and -42, steady state cure is achieved in a relatively short time. Comparing mechanical properties from these batches with Batches 69-43, -44, and -45 used to investigate premix storage time, the effect of curing agent level can be determined. Batches 69-41, and -42 were prepared with 84 equivalents of DER-332 while Batches 69-43, -44 and -45 were prepared with 78 equivalents of DER-332. Interpolation indicates that 81 equivalents would be required to achieve the target modulus

III.C. Discussion of Results (cont)

of elasticity, 500 ± 100 psi (345 ± 69 N/cm^2) for propellants prepared with a plasticizer level of 25 wt% of binder.

No voids or defects were observed during stripping or sectioning of the propellant grain. Mechanical properties and bond data for this grain were similar to the previous grains of the improved formulation. These data, along with solid strand burning rate data, are shown in Figure 128.

Safety classification tests were conducted on samples of propellant from one of the batches cast into the tenth mold. The results of these tests (Figure 129) indicate that ANB-3350 propellant would probably receive a DOT classification of B.

d. Interpretation of Results

As with the casting of the first seven subscale molds, it appears that propellant viscosity characteristics are of paramount importance in determining if grain or bond defects occur in the casting. Subscale Mold 8, which had propellant viscosities of 16,000 to 23,000 poise (1,600 to 2,300 Ns/m^2) 3 hr from curing agent addition at a shear stress of 5 $kdynes/cm^2$ (500 N/m^2), was cast in exactly the same manner as subscale Mold 6 with respect to core configuration, bayonet location, etc., but Mold 8 was free of any kind of defect and exhibited a smooth, glossy propellant surface both during and after casting. Mold 6, however, which had propellant viscosities of 47,000 to 150,000 poise (4,700 to 15,000 Ns/m^2) at the same condition, showed the highest incidence of defects of any of the subscale molds cast.

Casting of the ninth subscale mold showed conclusively the feasibility of casting with the bayonet tip located above the surface of the propellant. The process appears particularly desirable from the standpoint

III.C. Discussion of Results (cont)

of ensuring that a minimum amount of movement of old propellant within the motor occurs which, because of the increase in viscosity due to age, could contribute to grain or bond defects. Comparison of the types of flow patterns to be expected with above-surface casting with the flow patterns actually observed in subscale Mold 1 provide increased confidence that fresh propellant will always be contacting the liner on the chamber wall with consequent assurance of liner-propellant bond integrity.

The tenth subscale mold, cast using the same processing parameters planned for the Task III process demonstration, was probably a less severe test of the propellant capability than the two previous molds since the flow path length was reduced. However, the results of this casting indicated that no problems would be encountered in casting the second full scale mold.

Based on carton mechanical property data from the 15 450-lb (200 Kg) batches of ANB-3350 propellant cast into these subscale molds, the formulation selected for processing in the Task III demonstration was based on 82 equivalents of curing agent, 30% DOA plasticizer, and utilizing 2.00 wt% iron oxide and 0.10 wt% Iron Blue as the burning rate additive system. A more detailed summary of the formulation parameters selected are shown in Figure 130.

5. Processing Demonstration

a. Demonstration Plan

The objective of the second full-scale mold casting was to demonstrate the propellant processes and formulation optimized in Tasks I and II. The demonstration plan featured an extended vacuum mix cycle, a propellant formulation with improved casting characteristics, and restrictions on casting bayonet submergence. The casting plan was otherwise similar to

III.C. Discussion of Results (cont)

the plan for the first full-scale mold (Task I), simulating batch intervals typical of the Motor 260-SL-3 casting, including an 18-hr delay.

(1) Propellant Formulation

ANB-3350 propellant was selected for the processing demonstration, the formulation developed under Task II and demonstrated in subscale mold castings in Task I. The specific formulation was discussed previously in this report.

(2) Propellant Mixing

Twelve 5500-lb (2500 Kg) propellant batches were to be mixed in a vertical batch mixer for casting in the mold. The mixing procedure was to be the same as that used for the Task I, except as follows:

(a) Following oxidizer addition, close the oxidizer valve and mix for 10 min at a vacuum of 27 in. (690 mm) Hg minimum.

(b) Final mix for 30 min at a vacuum of 27 in. (690 mm) Hg minimum. Interrupt the final mix after 5 min to visually verify completion of oxidizer and final fuel addition.

(3) Propellant Casting

The planned casting sequence for this mold is shown in Figure 131. The target between-batch intervals are the same as those used in the Task I mold to simulate a propellant production rate typical of the Motor 260-SL-3 casting. Each batch was to be cast in approximately 25 min with 3 to 4 hr between batches, except for one 18-hr delay. The casting

III.C. Discussion of Results (cont)

process was improved by limiting bayonet submergence to a maximum of 18 in. (46 cm). To limit bayonet cutting and cleaning operations, cast stand and bayonet support spacers were available to allow bayonet tip height adjustment up to 12 in. (30 cm). The casting sequence is described as follows:

(a) Cast the first three batches with a fixed bayonet location 5 in. (13 cm) from the bottom of the mold. Then raise the bayonet to 12 in. from the bottom, cast the fourth batch, and remove the bayonet.

(b) Cut the bayonet and, after an 18-hr delay, insert to a depth of 6 in. (15 cm).

(c) Cast the fifth and sixth batches, followed by 6-in. (15 cm) increases in bayonet tip height.

(d) At the completion of the casting of the eighth batch, the bayonet submergence would be about 18 in. (46 cm). Cut the bayonet and insert to a depth of 6 in. (15 cm).

(e) Cast the ninth and tenth batches, followed by 6-in. (15 cm) increases in bayonet tip height. Cast the eleventh and twelfth batches with the same bayonet position, resulting in a maximum submergence of 18 in. (46 cm) at the completion of the mold casting. Clean and remove the bayonet. (Referring to Figure 131, it should be noted that the twelfth batch was not cast due to scrappage of an earlier batch, No. 22D-181-010.)

b. Casting Demonstration

(1) Propellant Processing

Propellant processing proceeded essentially as planned. However, acceptance test results on liquid strand burning rate (LSBR)

III.C. Discussion of Results (cont)

indicated that the upper limit of the target range of 0.68 ± 0.03 in./sec (1.727 ± 0.076 cm/sec) at 600 psig (414 N/cm^2) was being consistently exceeded. The effect of oxidizer lot and grind characteristics were checked previously by the preparation of a 10 lb (4.5 Kg) batch using a sample of the blended oxidizer. The liquid strands indicated that the nominal burning rate would be achieved. Since the oxidizer has been blended for the first six propellant batches and the first premix master batch containing the burning rate additives was of sufficient quantity for six propellant batches, a formulation modification was directed for the last six batches. This modification consisted of a change in oxidizer blend ratio from 60/40 SSMP/MA to 65/35 SSMP/MA, as used in ANB-3254. This reduction in MA fraction could not be detrimental and could only improve processing characteristics.

The LSBR reduction was achieved as expected. To rule out any difference in premix batches, propellant Batch 22D-181-006 was mixed using the 60/40 oxidizer blend ratio and the second premix batch, while propellant Batch 22D-181-008, the seventh batch cast, was mixed using the 65/35 oxidizer blend ratio and the first premix batch. A summary of submix and premix analyses is given in Figure 132. The uncured propellant data are summarized in Figure 133.

Visual observations during casting indicated that the apparent fluidity of the cast propellant surface was increasing more rapidly than anticipated. It was suspected, therefore, that the viscosity build-up rate was higher than that experienced previously with 450-lb (200 kg) batches. Because the cure catalyst level selected for this formulation was intentionally conservative, the formulation for the last two batches was altered by reducing the FC-151 cure catalyst from 0.05 to 0.03 wt%, allowing an opportunity for evaluation of the sensitivity of the rate of cure to catalyst level. However, viscosity results from Rotovisko tests, as summarized in Figure 133, indicate

III.C. Discussion of Results (cont)

that there was no significant effect from the change in catalyst level, and that the range of viscosities of all accepted batches at the low shear stress level was the same as that documented in the subscale mold batches.

The LSBR for the tenth propellant batch was well below the target acceptance limits. The liquid density was near the lower limit, indicating a possible oxidizer shortage in the batch. This was confirmed by tests for oxidizer content and total solids content, and was also indicated by an unusually low drop time from the falling-ball viscometer test (Figure 133). Since the casting of this batch might have interfered with the process demonstration objectives, the batch was scrapped, resulting in only eleven batches cast into the mold.

The falling ball viscosity test was performed on each batch as it was received at the casting building, and on carton samples at selected time intervals. The as-received test data are included in the uncured propellant data summary (Figure 133), and were plotted against Rotovisko viscosity data at approximately comparable conditions in Figure 134. A calibration line was fitted to these points to show linear correlation. The data scatter can be attributed to lack of precision in both the falling-ball and Rotovisko data and to differences in time at which the two tests were performed. However, the slope of the line suggests the conservatism of the test, in that large increases in drop time would be noticed before the development of extreme pseudoplasticity.

The low oxidizer content of the tenth batch has been attributed to hangup in the mixer dispensing chute. This conclusion was given credence by the relatively high density and LSBR of the subseqent batch, indicating above-normal oxidizer content.

(2) Propellant Casting

Casting of the mold was accomplished in accordance with the process demonstration plan. Casting intervals summarized in Figure 135 were similar to the first full-scale mold. The intervals between batches and the

III.C. Discussion of Results (cont)

intervals from curing agent to end of casting averaged nearly an hour longer than the comparable intervals for the first full-scale mold, making a more severe condition for the demonstration. The batch casting times were essentially identical to those for the first mold. The appearance of the cast propellant was dramatically improved over the first full-scale mold, as evidenced by relatively smooth and level propellant surface, contrasting with the stiff, mounded surface documented previously. The characteristic mounds, lumps, and shear planes of the first casting were essentially non-existent. The propellant surface contours measured at the cessation of flow of each batch cast are shown graphically in Figures 136 through 142. These may be compared with Figures 72 through 74, showing the contours of the first full-scale mold.

In the casting of nearly every batch, the propellant surface rose uniformly in all areas of the mold. The fifth batch, cast after the 18-hr delay, formed small 2 in. (5 cm) waves in the older propellant ahead of the new batch, progressing to the end of the mold, eventually leveling everywhere except in three of the four corners. At the start of the sixth batch, propellant level adjacent to the bayonet rose initially to create waves up to 6-in. (15 cm) high, but the surface ultimately flowed to a level condition. One of the corners developed a pocket during the casting of the seventh through tenth batches, as indicated by surface contours in Figure 138, which filled during the casting of the eleventh batch. In all other areas, the propellant was smooth and level. The propellant appeared to wet the casting form in a satisfactory manner, indicating a low probability of folding or void formation.

One of the differences between ANB-3254 and ANB-3350 in casting characteristics is that with ANB-3254 the flowing propellant generally flowed in waves over the surface of the previously-cast propellant without forcing waves in the older propellant, while with ANB-3350, the fresh propellant tends to displace the older propellant horizontally. This results in the desired layered effect, with fresh propellant on top, except at the extremities, where propellant from the previous batch has accumulated. This would help to explain the occasional resistance to surface leveling in the corners.

III.C. Discussion of Results (cont)

The occasional failure of the propellant to fill the corners of the mold is indicative of a peculiar situation where the driving force behind the moving propellant is extremely small, resulting in maximum pseudoplastic behavior, while the resistance to flow created by the converging walls effectively increases as the corner is penetrated. This does not represent a real situation in the casting experience of the 260-in.-dia (6.6 m) short-length motors, because the flow does not encounter that type of resistance at that distance from the bayonet, but it could indicate a problem with more complex core configurations. Perhaps significantly, the frequency of defects in Motors 260-SL-1 and -2 was greatest in the lobes of the grain, where the core is similar to a corner, even though this area is relatively close to the bayonet.

c. Analysis of Cured Mold

The 135°F (57°C) cure of the second full-scale mold was terminated when Shore A hardness measurements of propellant batch samples indicated that the state of cure had stabilized throughout the mold. When the mold had cooled to ambient temperature, the casting bay and casting form were disassembled and removed.

Visual inspection of the propellant mold (Figure 139 through 144) indicated that the casting objective was achieved. The improved formulation and processes resulted in a simulated full-scale grain of high quality and low frequency of defects. Of the defects that were observed, most were seams, less than 0.03-in. (0.8 mm) deep, associated with batch interfaces which showed fuel-rich layers and occasional 0.25 to 0.50 in. (6 to 13 mm) voids. Examples of these are shown in Figure 145. There were a few instances of folds of up to 7 in. (18 cm) long. One of these, shown in Figure 146, was located at one end of the mold near the corner where a pocket had developed during casting. The quantity and severity of surface defects were much less than those observed in the first full-scale mold.

The number of surface defects was reduced from 168 to 34. A comparison of the two full-scale molds is roughly the same as a comparison of

III.C. Discussion of Results (cont)

the observed defects in Motors 260-SL-2 and -3. Motor 260-SL-2 grain bore had 99 defects, only three of which were more than 6 in. (15 cm) long, while the comparable quantities in the 260-SL-3 grain were 171 and 84, respectively. A map of surface defects in the second full-scale mold is given in Figure 147.

One-half of the mold was sectioned at approximately 7.5-degree (0.13 radian) increments for acquisition of samples and disposal of the remaining propellant. With one exception, no internal defects were observed.

Carton samples from batches cast into the second full-scale mold were tested for mechanical properties at various intervals through 21 days cure at 135°F (57°C). The carton samples were cured with the full-scale mold until cure on the mold was terminated and then placed into a 135°F (57°C) oven to test additional cure intervals. The data shown in Figure 148 indicate that steady state of cure was reached within 14 days. Initial modulus for the eleven batches cast in the mold ranged from 335 to 485 psi at 14 days cure, approximately one-half the range observed with the ANB-3254 propellant cast into the first full-scale mold. The effect of the reduction in cure catalyst in the last two batches is inconclusive, based on the modulus data from the carton samples. Whereas both batches are at the low end of the range at 14 days cure time, Batch 011 continues to increase in modulus through 21 days indicating a reduction in the rate of cure, while Batch 012 appears to have reached a steady state of cure at 14 days, similar to the batches with the higher cure catalyst level.

Samples were prepared from this mold in a manner similar to those taken from the first full-scale mold cast with ANB-3254 propellant. A sketch of the sample location within the mold is shown in Figure 149. Propellant mechanical properties and solid strand burning rates were determined at each vertical elevation (1 through 8) and at the ID, mid and OD locations

III.C. Discussion of Results (cont)

for Sections A and B. Only the midpoint of Section C was tested for mechanical properties and solid strand burning rate. At each test location both vertically and horizontally oriented specimens were tested. The bond strength of SD-850-2 lined Gen-Gard V44 rubber was tested ay each vertical elevation in the OD location of Sections A, B, and C.

The test data are tabulated in Figures 150 through 156. In general, the following conclusions may be reached concerning the mechanical properties of this mold. The propellant cast into the mold reached an apparent higher state of cure than the sample cartons cast from individual batches as experienced with all previous molds. This phenomenon may be the result of anisotropy in the sample cartons. The propellant initial modulus ranged from 335 to 485 psi (231 to 335 N/cm^2) for the sample cartons and 378 to 760 psi (261 to 524 N/cm^2) for the propellant cut from the full-scale mold segment. The propellant from the mold showed typical anisotropic behavior with the vertically oriented specimens being higher in modulus in 27% of the test locations and the horizontally oriented specimens being higher in only 7% of the test locations. For this comparison, only modulus values differing by more than 100 psi (69 N/cm^2), approximately two standard deviations, were considered to be significantly different. The data obtained from the first full-scale mold, cast with ANB-3254 propellant, indicated a slightly higher degree of anisotropic behavior with the vertically oriented specimens being higher in 27% of the test locations compared with horizontal specimens being higher in 17% of the locations. These differences between the two molds are probably the result of the more uniform flow conditions which existed during the casting of the second mold.

Analysis of the burning rate data in a similar manner indicates an anisotropic effect with the higher burning rate occurring in the horizontal plane. Certain burning rate anomalies appear at one elevation

III.C. Discussion of Results (cont)

within the second mold. The burning rates for the vertical specimens, Level 3, middle of Sections A and B, are unusually high, 0.950 in./sec (2.41 cm/s) and 0.896 in./sec (2.28 cm/s), as seen in Figures 151 and 154. It is entirely possible that some irregularity occurred during the processing of these strands. These anomalies are perpendicular to the plane of the propellant surface exposed during the planned 18-hr delay.

Bond strength values obtained from samples prepared at the OD position of each section showed consistently good values throughout, demonstrating the most significant improvement over the first full-scale mold. The failure mode of all samples occurred as a fracturing of the propellant within the sample.

Anisotropic behavior in mechanical and ballistic properties is observed in essentially all composite solid propellants. The degree to which this behavior exists in the propellant samples described in this report is typical, but this type of data is not commonly reported. The data acquisition plans for this program specifically were established to document anisotropy, since it is an unusual opportunity for large grains to be available for samples. Anisotropy in ANB-3105 propellant has been reported previously for carton samples and structural test slabs. Ballistic curve shape distortion experienced in all motors of the 260-in. (6.6 m)-dia motor program and in other large motors is possibly the result of burning rate anisotropy.

The cause of this behavior cannot be confidently identified, and an investigation was not within the scope of this program. Additional studies would be needed to determine how to assess the data in terms of reliability and performance prediction. However, experience has shown that the performance of the resultant propellant grains has been reliable and reproducible, and that the magnitude of the effect is within acceptable limits.

III.C. Discussion of Results (cont)

d. Interpretation of Results

Based on the analysis of the grain defects found in the second large mold, and contour measurements and observations of flow during casting of the mold, it can be concluded that the flow characteristics of the improved propellant formulation ANB-3350 are adequate. In addition, propellant viscosity at the low shear stress of 5000 dynes/cm^2 (500 N/m^2) can be concluded to provide a realistic assessment of the compatibility of the flow characteristics with the 260-in. (6.6 m)-dia motor casting process. Whereas ANB-3254 propellant cast into the first large mold gave viscosities at 5000 dynes/cm^2 (500 N/m^2) of greater than 100,000 poise (10,000 Ns/m^2) at about 6 hr after curing agent addition, the improved ANB-3350 formulation exhibits viscosities of less than 30,000 poise (3,000 Ns/m^2).

Further substantiation of the adequacy of the ANB-3350 flow characteristics is provided by a comparison with the viscosity data for ANB-3105. The compatibility of the flow characteristics of ANB-3105 with the 260-in. (6.6 m)-dia. motor process, has been adequately demonstrated in the processing and successful firing of Motors 260-SL-1 and -2. The following tabulation compares the viscosity characteristics of ANB-3105 and ANB-3350 (Batch 22D-181-012) formulated with the optimum 0.03 wt% cure catalyst.

III.C. Discussion of Results (cont)

Propellant	Time After Curing Agent Addition, hr	Viscosity at 5000 dynes/cm^2, (500 N/m^2) poise (Ns/m^2)
ANB-3105	3.35	12,000 (1,200)
	7.35	21,000 (2,100)
	11.35	26,000 (2,600)
ANB-3350	3.0	12,000 (1,200)
	7.0	16,000 (1,600)
	11.0	22,000 (2,200)

As shown, the viscosity characteristics of ANB-3350 are equivalent to or slightly superior to the well demonstrated ANB-3105 propellant.

The significance of the propellant mixing processing improvement is indicated perhaps only indirectly by the results of the processing demonstration. The extended vacuum mix cycle was used on the basis that it was necessary when processing ANB-3254 propellant and would be a conservative feature. The viscosity characteristics of ANB-3350 propellant in the large mixer were similar to those measured in propellant processing in small mixers, suggesting that the objective of adequate deaeration was achieved.

Observations of defect formation during casting of both the 42-in. (1.07 m)-dia and full scale molds, showed that the mechanism involved formation of a wave, followed by movement of the wave front against the case wall or core surface. The flow characteristics of the propellant govern the wave height which in turn governs the size of the defect formed when the wave traps air against the wall surface. Thus defect formation involves movement of the propellant surface. The more uneven the surface, the greater the probability of defect formation.

Data supporting this mechanism of defect formation and showing the influence of bayonet submergence was obtained during the casting

III.C. Discussion of Results (cont)

of the second large scale mold with ANB-3350. Because of the complex patterns occurring around the bayonet tip, it is not possible to ascertain the location of any given batch. To evaluate the flow patterns, the interrelationships among propellant viscosity, surface level differentials and grain surface irregularities were studied. The results of this study are summarized in Figures 157 and 160. First, the viscosity of the propellant at various vertical locations, when each batch was cast, was determined from cast time, viscosity buildup and bayonet depth data. Not surprisingly, increasing viscosities are noted at increasing submergence levels. A viscosity peak occurred after the fourth batch due to a scheduled 18-hour casting delay. A second viscosity peak occurred at the eighth batch because submergence was permitted to increase to 18-in. (46 cm) from the 6 to 12 inches (15 to 30 cm) used for all other batches.

An overlay of the surface level differentials measured on the right and left halves of the mold (Figures 157 and 158) over the viscosity plot, shows a large height differential occurred at Batch 8 (right half of the mold). A peak in the viscosity plot (bayonet tip + 12-in. level) also occurred at this level. For the left half of the mold, peaks in both height differential and viscosity occur at Batches 5 and 8. A comparison of viscosity at the different levels with the estimated area of surface irregularities (Figure 159) shows corresponding peaks at Batches 5 and 8. The peak at Batch 11 does not appear to relate directly to viscosity.

A cross plot of the height differential with the estimated area of observed surface irregularities in Figure 160, reveals corresponding peaks and indicates that height differentials and defects are probably related.

On the basis of this analysis and related observations it is apparent that bayonet submergence depth is an important factor even when casting an optimized propellant such as ANB-3350. With greater bayonet tip

III.C. Discussion of Results (cont)

submergence, the bayonet efflux displaces propellant of greater age which moves to the surface. The older propellant becomes part of the moving surface which ultimately forms the cured propellant at the core or the chamber wall. Thus, increased bayonet submergence contributes to the age factor in increasing propellant surface viscosity, thereby increasing the probability of defect formation.

The limitations placed on bayonet submergence generally achieved the desired effect of allowing fresh propellant to flow on the surface, thereby minimizing movement of older, more viscous propellant. Further limitations to near-surface or above-surface could be expected to provide a slightly improved situation.

The success in achieving adequate bonding of the propellant to the liner is probably the largest contribution to assurance of successful grain performance.

The flow behavior of the cast propellant, after the 18-hour delay, and the subsequent surface defects emphasize that long delays are to be avoided in processing large motors.

The results of this demonstration have been used in compilation of processing guidelines for 260-in. (6.6 m)-dia motors. These guidelines are presented in detail in the appendix to this report.

IV. CONCLUSIONS

An improved propellant formulation, designated ANB-3350, has been developed and the adequacy of its processing characteristics demonstrated by casting a 120-degree (2.09 rad) segment of a 260-in.(6.6 m)-dia mold using full-scale motor processing methods. Examination of the cured mold showed a very low and acceptable level of grain defects. ANB-3350 meets the ballistic and mechanical property requirements of the program.

Propellant viscosity under a low, applied shear stress was found to be a critical parameter. Viscosity measurements at 5000 dynes/cm^2 (500 N/m^2) applied stress correlate with the frequency of grain defect formation. Comparison of the viscosity of ANB-3350 with that of ANB-3105 propellant, which has been successfully demonstrated in Motors 260-SL-1 and -2, shows the ANB-3350 formulation viscosity to be slightly lower at this stress level. A five- to ten-fold improvement over the viscosity characteristics of the ANB-3254 propellant cast into the first large mold and Motor 260-SL-3 has been achieved.

The greatly improved flow characteristics of ANB-3350 formulation are primarily due to the use of iron oxide as the primary burning rate additive. This material is chemically inert, dense, has no effect on propellant flow, and has a low moisture content. Additional improvement in viscosity characteristics resulted from the use of an Aerojet wetting agent designated FC-167. The viscosity of the improved formulation was found to be insensitive to mix procedure variations including low vacuum levels and short vacuum mix times.

An understanding of the interrelationships between propellant viscosity characteristics and grain defect formation during casting has been developed. The grain defects observed in Motor 260-SL-3 were duplicated in the first large scale mold. The defects are attributable to the undesirable pseudoplastic flow behavior of the ANB-3254 propellant formulation. Under the

IV. Conclusions (cont)

conditions of low, applied shear stress in the motor the propellant viscosity is high and causes the propellant to mound around the bayonet. When the hydrostatic head of the mound exceeds the propellant yield stress, the propellant flows out in waves that entrap air next to the core surfaces.

The poor flow behavior of the ANB-3254 propellant at low shear stress is caused largely by the use of the burning-rate additive BRA-101, and the inadequate vacuum mixing cycle. Under ideal conditions of mixing (high vacuum, long mix cycles) the BRA-101 does not appear to influence the flow behavior of the propellant to an unacceptable degree. In the production vertical batch mixers that have a low (compared to the development scale mixers) surface-to-volume ratio and generally less efficient deaeration, the BRA-101 causes the propellant to exhibit highly pseudoplastic flow characteristics.

As the propellant cure reaction proceeds, all propellant formulations will eventually show extreme pseudoplastic behavior. The major difference between formulations is the rate at which they develop pseudoplastic behavior. For this reason the bayonet submergence must be controlled so as to minimize the movement of the older, more viscous propellant within the motor. Observations of propellant flow patterns in the subscale and full-scale molds cast indicate that the best location of the bayonet tip is at or just below the surface of the propellant (i.e., minimum submergence). Preliminary data indicate that above-surface casting may provide even more assurance of freedom from grain and bond defects, but additional work is required to confirm this.

The development of pseudoplastic flow behavior in even the optimized ANB-3350 formulation indicates that casting delays are a significant factor to be considered. Because the propellant which contacts the core or bond surface frequently is not part of the batch being cast, even with near-surface bayonet casting, between-batch intervals should be minimized.

IV. Conclusions (cont)

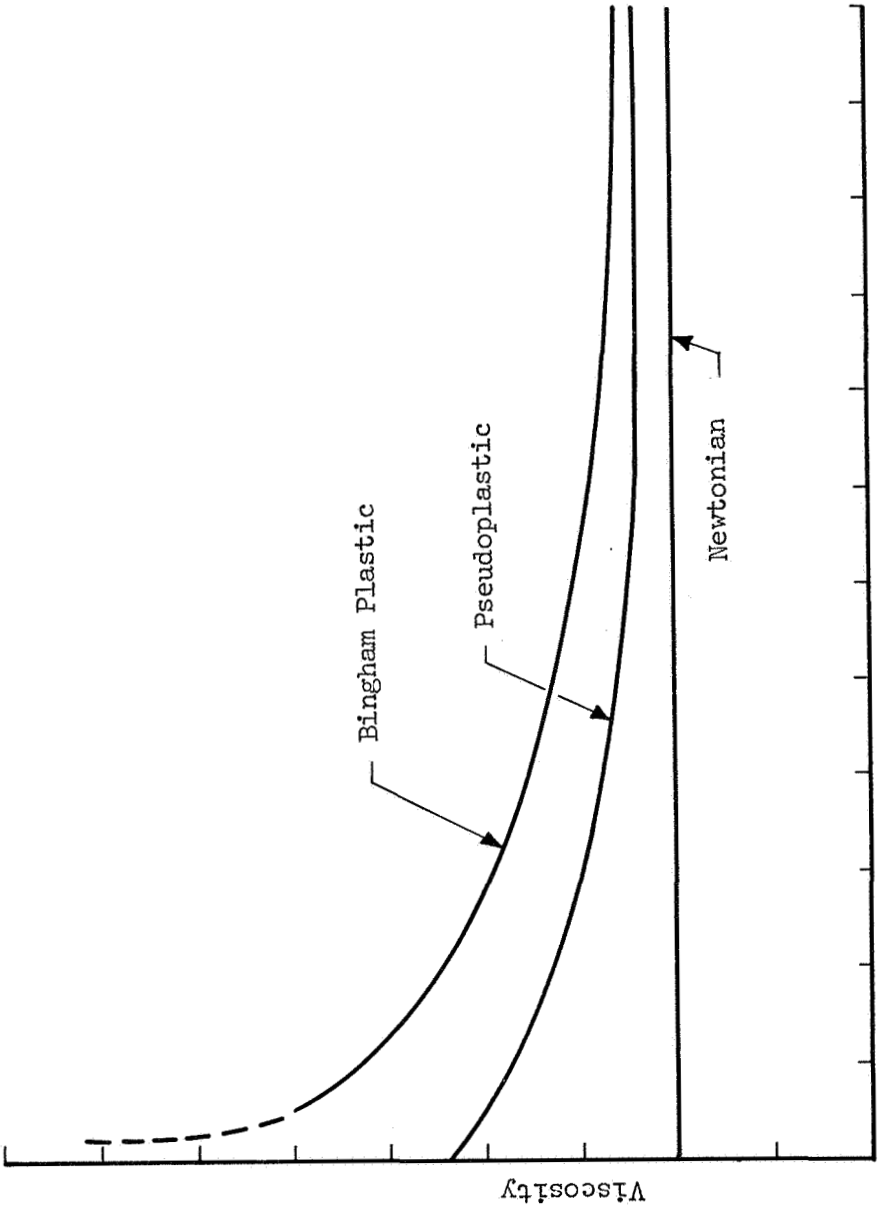
Mechanical property and burning rate (cured strand) tests on specimens from cured grains show variations dependent on orientation of the specimen in the grain. Such anisotropic behavior is common and has been observed in essentially all solid propellants. Improved batch sampling techniques that provide a true measure of motor grain properties are needed.

A new in-process acceptance test for the flow characteristics of propellant for use in 260-in. (6.6 m)-dia motors has been developed. This test, consisting of measurement of the rate-of-fall of a steel ball through the propellant, is simple, accurate, and reliable.

The 42-in.(107 cm)-dia subscale mold has been shown to be a valuable tool for assessment of propellant flow behavior in terms of the 260-in.(6.6 m)-dia motor bayonet cast process. The mechanism of defect formation was clearly revealed in these subscale castings, and subsequently reproduced in the full-scale mold, and the assessment of the adequacy of the flow behavior of the improved formulation was predicted successfully.

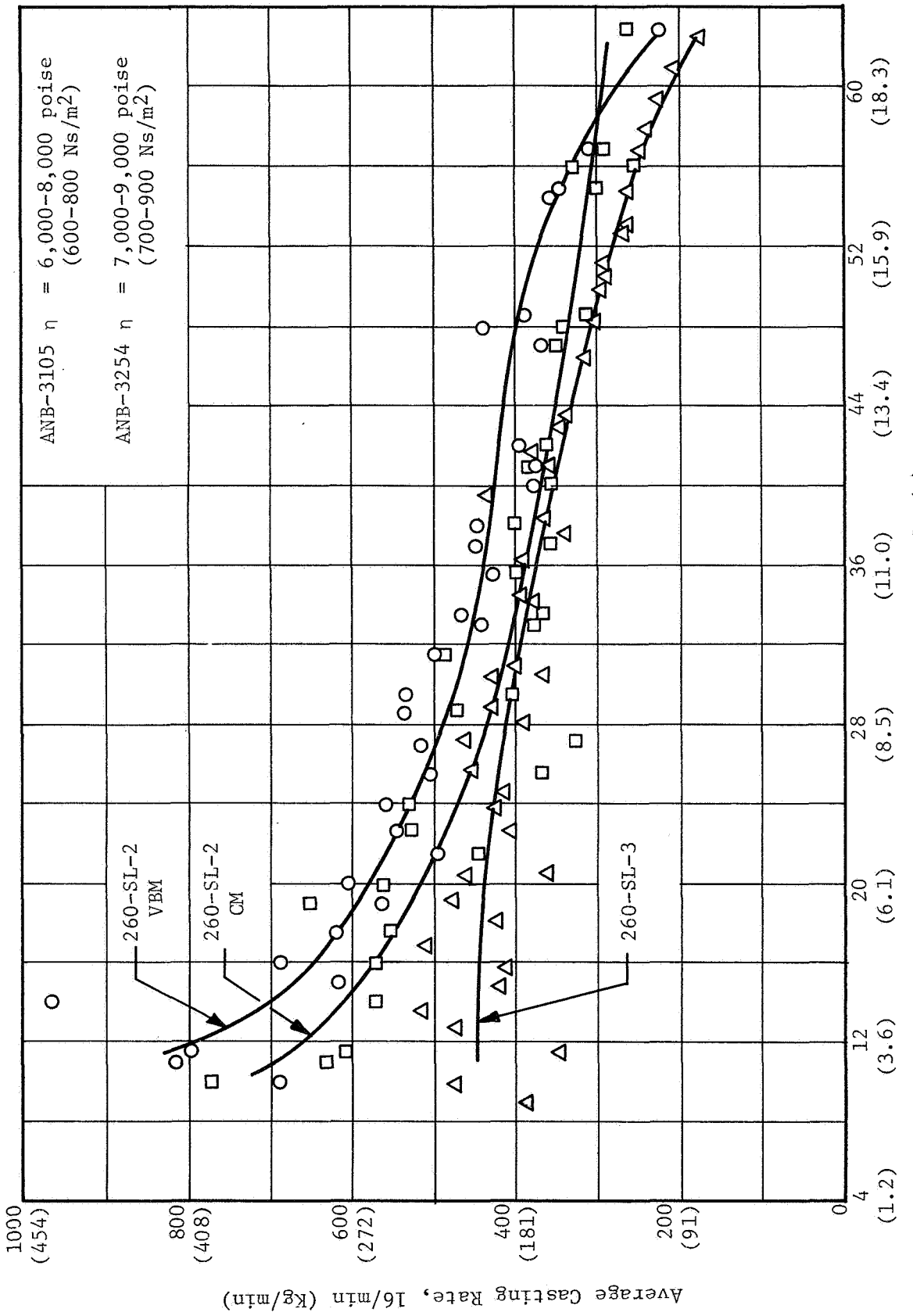
GLOSSARY

A-DD	Aerojet-Dade Department; at Dade County, Florida
AMPOT	American Potash Co.
AP	Ammonium perchlorate; NH_4ClO_4; oxidizer
BRA-101	Burning rate additive, Aerojet proprietary
CM	Continuous mixer
Cu0202	Copper Chromite; burning rate additive
DER-332	Diglycidal ether of Bisphenol A; diepoxide curing agent
DOA	Dioctyl adipate; plasticizer
DOT	U. S. Department of Transportation
E_o	Initial modulus of elasticity
FC-151	Cure catalyst; Aerojet proprietary
FC-167	Wetting agent, Aerojet proprietary
FeAA	Ferric acetylacetonate; curing catalyst
Gen-Gard V44	Silica and asbestos-filled butadiene acrylonitrile rubber motor internal insulation
L-45	Silicone fluid; polydimethyl siloxane
LSBR	Liquid strand burning rate
MA	Mikro Atomizer ground oxidizer
NOL	Naval Ordnance Laboratory
PBAN	Terpolymer of polybutadiene, acrylic acid, and acrylonitrile binder component
PBNA	Phenyl-B-Naphthyl-Amine; antioxidant
PEPCON	Pacific Engineering and Production Company of Nevada
Shore A	Shore durometer surface hardness measurement, Type A
Silon S	Colloidal silica
SRD	Solid Rocket Division at Sacramento, California
SSMP	Slow Speed Mikro Pulverizer ground oxidizer
TTIA	Tetrathio-bis-isoctyl acetate
VBM	Vertical batch mixer
ε_b	Elongation at break
ε_m	Elongation at maximum stress
σ_m	Maximum tensile stress



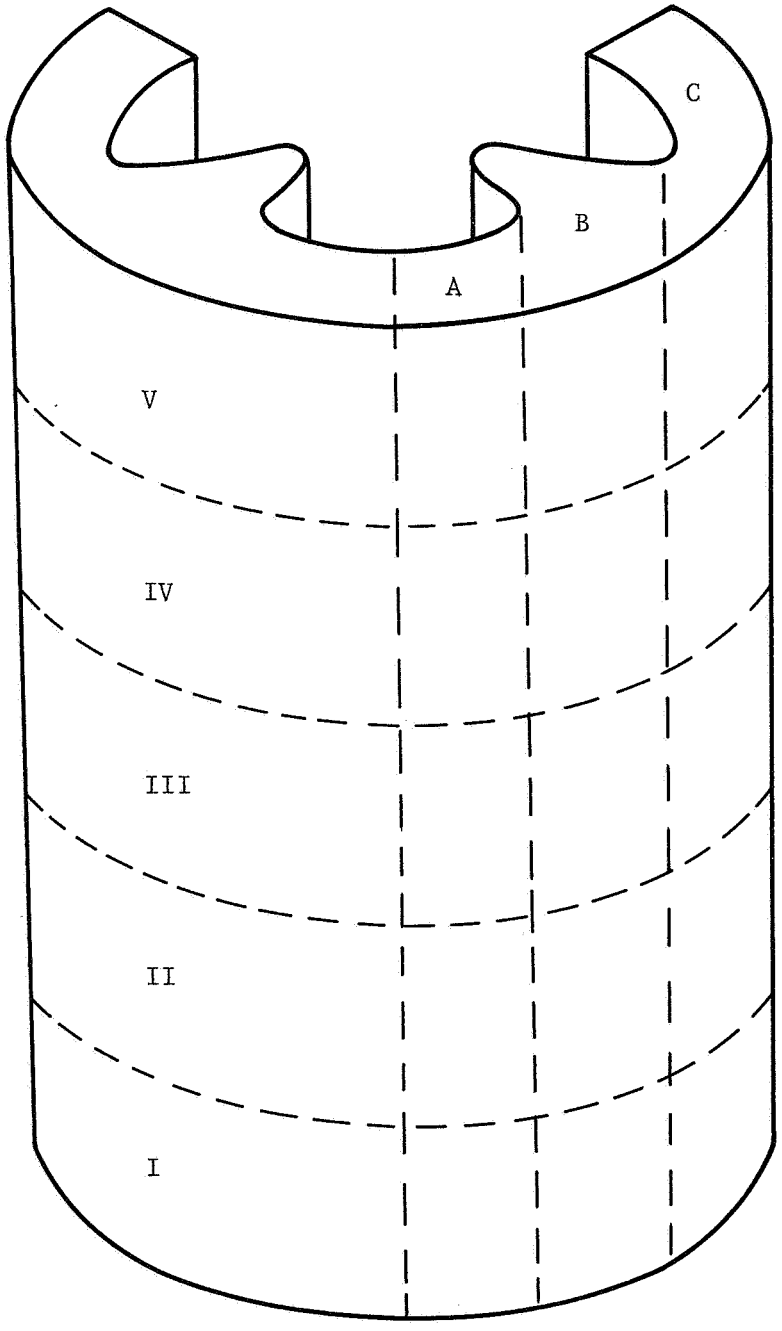
Effect of Applied Shear on the Viscosity of Different Fluids

Figure 1



Plot of Propellant Casting Rate as a Function of Bayonet Length for Motors 260-SL-2 and 260-SL-3

Figure 2



Schematic Diagram of Subscale Mold Showing Locations of Specimens Taken for Property Testing

Figure 3

Batch No.	Formulation Variable	Propellant Color	Casting				
			Bayonet Submergence in.	(cm)	Cast Rate lb/hr	(Kg/hr)	Time Between Batches, hrs
68-232	Iron Blue 0.60%/BRA-101 0.60%	Dark Blue	0-3	(0-8)	80	(36)	-
68-233	TiO_2 0.60%/BRA-101 0.60%	Gray	3-4	(8-10)	75	(34)	5
68-234	Benzidine Yellow 0.1%/BRA-101 0.60%	Green	4-12	(10-30)	90	(40)	4
68-235	Iron Blue 0.10%/BRA-101 0.60%	Light Blue	12-20	(30-51)	80	(36)	3
68-231A	Fe_2O_3 0.60%/BRA-101 0.60%	Red	20-28	(51-71)	85	(39)	3

1. Mold configuration was 240 degree (4.19 rad) cloverleaf
2. Propellant was mixed at a vacuum level of 29 in. (740 mm) Hg for 35 minutes

Summary of ANB-3254 Propellant Formulation Variables and Casting Parameters for Subscale Mold No. 1

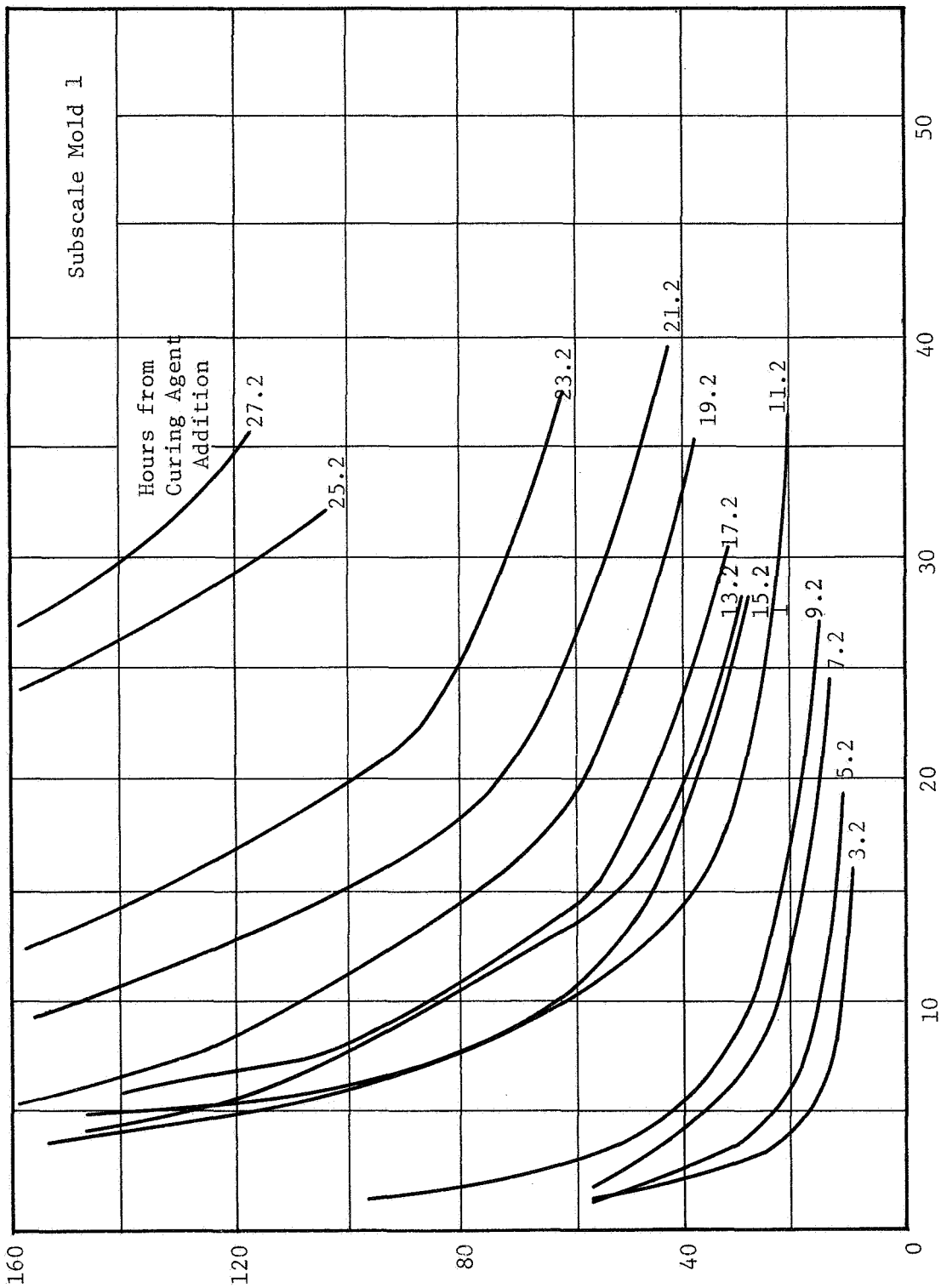
Figure 4

Batch No.	Submix				Premix		Uncured Propellant					
	Water Content, %	Acid Equivalents/ 100g	Liquid Density, g/cm^3	Refractive Index	Water Content, %	Liquid Density, g/cm^3	Liquid Density, g/cm^3	DER-332 Content, %	Liquid Strand Burning Rate at 600 psig, 80°F, in./sec	(at 414 N/cm^2, 27°C) (cm/S)	Viscosity*, poise (Ns/m^2) 6 hr	10 hr
68-232	0.042	0.0412	0.929	1.4910	0.119	1.426	1.744	1.32	0.671	(1.70)	29,000 (2,900)	83,000 (8,300)
68-233	0.063	0.0413	0.930	1.4915	0.098	1.436	1.748	1.39	0.533	(1.35)	22,000 (2,200)	50,000 (5,000)
68-234	0.050	0.0411	0.929	1.4915	0.113	1.404	1.736	1.35	0.531	(1.35)	34,000 (3,400)	72,000 (7,200)
68-235	0.055	0.0408	0.930	1.4910	0.113	1.407	1.735	1.39	0.588	(1.49)	20,000 (2,000)	44,000 (4,400)
68-231A	0.063	0.0411	0.929	1.4908	0.112	1.437	1.748	1.37	0.576	(1.46)	30,000 (3,000)	40,000 (4,000)

* Viscosity at 135°F (57°C), 5K dynes/cm^2 (500 N/m^2) shear stress, 6 and 10 hours after curing agent addition.

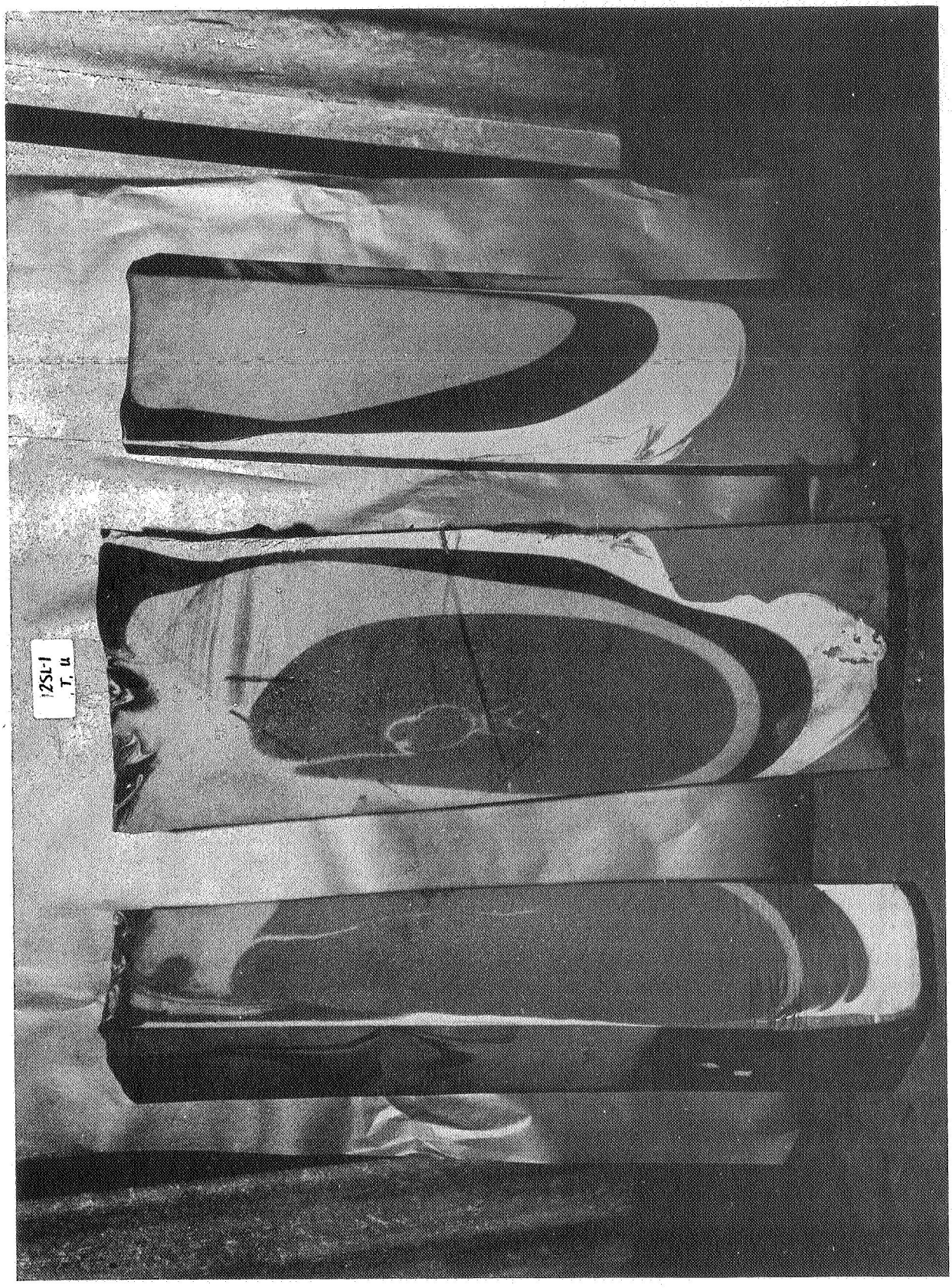
Figure 5

Summary of Uncured Propellant Data for ANB-3254 Propellant Cast into the First Subscale Mold



Viscosity Characteristics for Batch 68-232, Subscale Mold No. 1

Figure 6



Sections of First Subscale Mold

Figure 7

Batch No. 68-	Cure Time, Days	Shore A Hardness	Mechanical Properties at 77°F (25°C) σ_m, psi	(N/cm^2)	ε_m, %	ε_b, %	E_o, psi	(N/cm^2)
232	31	42	102	(70)	21	21	580	(400)
	36	42	101	(70)	20	20	590	(407)
233	31	52	119	(82)	17	17	789	(544)
	36	47	133	(92)	20	20	804	(554)
234	31	48	138	(95)	20	20	787	(543)
	36	47	118	(81)	19	19	708	(488)
235	31	48	128	(88)	18	18	815	(562)
	36	48	133	(92)	19	19	798	(550)
231A	31	46	127	(88)	23	23	677	(467)
	36	48	117	(81)	19	19	715	(493)

Figure 8

Mechanical Properties of Carton Samples from
Propellant Cast into Subscale Mold No. 1

Sample Location			Orientation	Mechanical Properties at 77°F (25°C) σ_m, psi	σ_m, (N/cm^2)	ε_m, %	ε_b, %	E_o, psi	E_o, (N/cm^2)	Solid Strand Burning Rate at 600 psig (414 N/cm^2) and 80°F (27°C) in./sec	(cm/s)
V	B	(green)	Vertical	124	(86)	22	23	843	(582)		
IV	B	(light blue)	Vertical	133	(92)	19	19	850	(586)		
			Horizontal	146	(101)	20	20	998	(688)		
III	B	(gray)	Vertical	119	(82)	20	22	909	(627)		
			Horizontal (Circum.)	117	(81)	20	22	926	(638)		
II	B	(red)	Vertical	120	(83)	18	18	837	(577)	0.657	(1.67)
			Horizontal	112	(77)	17	17	985	(679)	0.646	(1.64)
			Horizontal (Circum.)							0.657	(1.67)
I	B	(dark blue)	Vertical	106	(73)	22	25	723	(498)		
			Horizontal	92	(63)	23	25	560	(386)		
			Horizontal (Circum.)	100	(69)	21	24	715	(493)		
II/IV		(red/light blue)	Random	116	(80)	20	21	747	(515)		
V	C	(light blue)	Vertical	132	(91)	24	24	763	(526)	0.610	(1.55)
			Horizontal	142	(98)	24	25	990	(683)	0.602	(1.53)
IV	C	(green)	Vertical	122	(84)	22	23	804	(554)	0.548	(1.39)
			Horizontal	107	(74)	23	24	682	(470)	0.520	(1.32)
II & III	C	(gray)	Vertical	120	(83)	22	22	773	(533)	0.526	(1.34)
			Horizontal	119	(82)	22	23	848	(585)	0.544	(1.38)
I	C	(dark blue)	Vertical	92	(64)	21	22	610	(421)	0.644	(1.64)
			Horizontal	98	(68)	19	23	798	(550)	0.678	(1.72)
III/IV*		(gray/green)	Random	111	(77)	21	21	739	(510)		
I/II**		(dark blue/gray)	Random	86	(59)	13	13	850	(586)		

Location Code: See Figure 2

* Break in gray propellant

** Break in dark blue propellant

Properties of Propellant taken from First Subscale Mold

Figure 9

NASA CR 72621

Depth in Mold*	Position in Mold*	Bond Strength at 77°F (25°C)											
		A				B				C			
		Tensile psi	(N/cm^2)	Shear psi	(N/cm^2)	Tensile psi	(N/cm^2)	Shear psi	(N/cm^2)	Tensile psi	(N/cm^2)	Shear psi	(N/cm^2)
I		90	(62)	67	(46)	109	(75)	83	(57)	112	(77)	87	(60)
II		92	(63)	74	(51)	123	(85)	106	(73)	121	(83)	92	(63)
III		97	(67)	77	(53)	122	(84)	96	(66)	123	(85)	101	(70)
IV		93	(64)	70	(48)	116	(80)	100	(69)	119	(82)	105	(72)
V		98	(68)	78	(54)	113	(78)	104	(72)	126	(87)	96	(66)

Note: All sample failures occurred randomly within the propellant or at the propellant-to-plate bond line. No failures at liner-to-propellant of propellant-to-propellant interfaces were observed.

* See Figure 3 for Location Code

Bond Strength of Liner-Propellant Specimens from First Mold

Figure 10

Batch No.	Mixing			Casting*				
	Vacuum Level, in. Hg	(mm Hg)	Mix Time, min.	Bayonet Submergence, in.	(cm)	Cast Rate, lb/hr	(Kg/hr)	Time between Batches, hr
68-246	29	740	35	0-5	(0-13)	80	(36)	--
68-247	29	740	35	5-12	(13-30)	45	(20)	3
68-248	29 (pump off)	740	35	12	(30)	65	(29)	2.5
68-249	29	740	35	12	(30)	80	(36)	15
68-250	29 (pump off)	740	25	12	(30)	130	(59)	2.5

* NOTE: 1. All formulations contained 0.65 wt% Iron Blue and 0.65 wt% BRA-101. Batch 68-249 also contained 0.1 wt% Benzidine yellow dye.
2. Mold configuration was 240-degree (4.19 rad) clover.

Summary of ANB-3254 Propellant Formulation Variables and Casting Parameters for Subscale Mold No. 2

Figure 11

	Submix				Premix		Uncured Propellant					
Batch No.	Water Content, %	Acid Equivalents/ 100g	Liquid Density g/cm^3	Refractive Index	Water Content, %	Liquid Density g/cm^3	Liquid Density g/cm^3	DER-332 Content, %	Liquid Strand Burning Rate at 600 psig (414 N/cm^2) 80°F (27°C) in./sec	(cm/s)	Viscosity*, poise (NS/m^2) 6 hr	10 hr
68-246	0.058	0.0406	0.929	1.4910	0.197	1.429	1.747	1.18	0.672	(1.71)	53,000 (5,300)	64,000 (6,400)
68-247	0.057	0.0409	0.929	1.4905	0.126	1.422	1.746	1.26	0.682	(1.73)	46,000 (4,000)	86,000 (8,600)
68-248	0.076	0.0410	0.929	1.4905	0.174	1.427	1.747	1.24	0.678	(1.72)	42,000 (4,200)	84,000 (8,400)
68-249	0.075	0.0407	0.929	1.4908	0.178	1.427	1.747	1.32	0.672	(1.71)	69,000 (6,900)	150,000 (15,000)
68-250	0.043	0.0408	0.930	1.4907	0.194	1.426	1.746	1.24	0.658	(1.67)	33,000 (3,300)	- -

* Viscosity at 135°F(57°C), 5K dynes/cm^2 (500 N/m^2) shear stress, 6 and 10 hours after curing agent addition.

Summary of Uncured Propellant Data for ANB-3254 Propellant Cast into Subscale Mold 2

Figure 12

Batch No. 68-	Cure Time, Days	Shore A Hardness	Mechanical Properties at 77°F (25°C)					
			σ_m, psi	(N/cm^2)	ε_m, %	ε_b, %	E_o, psi	(N/cm^2)
246	17	33	96	(66)	25	27	493	(340)
	21	38	88	(61)	20	20	516	(356)
	25	38	91	(63)	19	19	538	(371)
247	17	34	85	(59)	20	21	481	(332)
	21	32	82	(57)	18	18	516	(356)
	25	36	84	(58)	17	18	538	(371)
248	17	24	62	(43)	26	27	285	(197)
	21	24	65	(45)	27	29	290	(200)
	25	27	67	(46)	24	25	330	(228)
249	17	36	88	(61)	22	23	470	(324)
	21	35	83	(57)	18	18	507	(350)
	25	35	75	(52)	19	20	433	(299)
250	17	28	67	(46)	22	22	363	(251)
	21	31	74	(51)	21	22	419	(289)
	25	31	71	(49)	21	22	387	(267)

Mechanical Properties of Carton Samples of Propellant Cast Into Mold No. 2

Figure 13

Sample Location (1)	Orientation	Mechanical Properties at 77°F (25°C)						Solid Strand Burning Rate at 600 psig (414 N/cm^2) 80°F (27°C), in./sec (cm/s)
		σ_m, psi	(N/cm^2)	ε_m, %	ε_b, %	E_o, psi	(N/cm^2)	
A-I	Vertical	130	(90)	20	22	900	(621)	0.689 (1.75)
	Horizontal (radial)	128	(88)	23	24	824	(568)	0.678 (1.72)
A-II	Vertical	131	(90)	20	22	931	(642)	0.692 (1.76)
	Horizontal (radial	124	(86)	22	24	824	(568)	0.663 (1.67)
A-III	Vertical	126	(87)	19	20	911	(628)	0.707 (1.80)
	Horizontal (radial)	130	(90)	21	23	933	(643)	0.670 (1.70)
A-IV	Vertical	129	(89)	19	20	994	(686)	0.683 (1.74)
	Horizontal (radial)	120	(83)	20	22	944	(652)	0.670 (1.70)
A-V	Vertical	117	(81)	19	21	911	(628)	0.669 (1.70)
	Horizontal (radial)	124	(86)	20	22	894	(617)	0.685 (1.74)

(1) See Figure 3

Properties of Specimens from Second Subscale Mold (Section A)

Sample Location	Orientation	Mechanical Properties at 77°F (25°C) σ_m, psi	(N/cm^2)	ε_m, %	ε_b, %	E_o, psi	(N/cm^2)	Solid Strand Burning Rate at 600 psig (414 N/cm^2) 80°F (27°C), in./sec (cm/s)
B-I	Vertical	96	(66)	20	23	671	(463)	0.690 (1.75)
	Horizontal (radial)	101	(70)	20	26	780	(538)	0.692 (1.76)
	Horizontal (circum.)	105	(72)	19	21	817	(563)	0.701 (1.78)
B-II	Vertical	102	(70)	22	22	588	(405)	0.662 (1.68)
	Horizontal (radial)	115	(79)	22	25	747	(515)	0.688 (1.75)
	Horizontal (circum.)	125	(86)	20	23	935	(645)	0.700 (1.78)
B-III	Vertical	89	(61)	22	24	584	(403)	0.620 (1.57)
	Horizontal (radial)	99	(68)	20	27	739	(509)	0.682 (1.73)
	Horizontal (circum.)	122	(84)	20	23	907	(625)	0.697 (1.77)
B-IV	Vertical	85	(59)	25	28	490	(338)	0.685 (1.74)
	Horizontal (radial)	90	(62)	23	27	562	(388)	0.658 (1.67)
	Horizontal (circum.)	85	(59)	20	25	636	(438)	0.674 (1.71)
B-V	Vertical	82	(57)	22	26	507	(350)	0.683 (1.74)
	Horizontal (radial)	88	(61)	17	22	730	(504)	0.689 (1.75)
	Horizontal (circum.)	92	(63)	18	23	771	(532)	0.694 (1.76)

Figure 15

Properties of Specimens from Second Subscale Mold (Section B)

Sample Location	Orientation	Mechanical Properties at 77°F (25°C)						Solid Strand Burning Rate at 600 psig (414 N/cm^2) 80°F (27°C), in./sec (cm/s)
		σ_m, psi	(N/cm^2)	ε_m, %	ε_b, %	E_o, psi	(N/cm^2)	
C-I	Vertical	118	(81)	19	20	852	(588)	0.706 (1.79)
	Horizontal (radial)	97	(67)	19	20	651	(449)	0.686 (1.74)
	Horizontal (circum.)	114	(79)	22	26	741	(511)	0.707 (1.80)
C-II	Vertical	121	(83)	21	25	832	(573)	0.697 (1.77)
	Horizontal (radial)	110	(76)	21	22	704	(485)	0.678 (1.72)
	Horizontal (circum.)	126	(87)	20	23	910	(628)	0.722 (1.83)
C-III	Vertical	85	(59)	20	23	621	(428)	0.709 (1.80)
	Horizontal (radial)	128	(88)	20	21	946	(653)	0.687 (1.75)
	Horizontal (circum.)	120	(83)	22	24	787	(543)	0.692 (1.76)
C-IV	Vertical	85	(59)	19	22	623	(430)	0.712 (1.81)
	Horizontal (radial)	130	(90)	20	22	977	(674)	0.718 (1.82)
	Horizontal (circum.)	119	(82)	22	24	789	(544)	0.699 (1.78)
C-V	Vertical	96	(66)	21	22	656	(452)	0.667 (1.69)
	Horizontal (radial)	99	(68)	21	23	708	(488)	0.695 (1.77)
	Horizontal (circum.)	87	(60)	20	23	640	(442)	0.715 (1.82)

Figure 16

Properties of Specimens from Second Subscale Mold (Section C)

Depth in Mold*	Position in Mold*	Bond Strength at 77°F (25°C)											
		A				B				C			
		Tensile psi	(N/cm^2)	Shear psi	(N/cm^2)	Tensile psi	(N/cm^2)	Shear psi	(N/cm^2)	Tensile Shear	(N/cm^2)	Shear psi	(N/cm^2)
I		104	(72)	95	(66)	111	(77)	122	(84)	105	(72)	97	(67)
II		112	(77)	92	(63)	112	(77)	101	(70)	109	(75)	98	(68)
III		109	(75)	76	(52)	116	(80)	107	(74)	147	(102)	100	(69)
IV		131	(90)	112	(77)	115	(79)	118	(81)	139	(96)	103	(71)
V		125	(86)	105	(72)	100	(69)	95	(66)	107	(74)	101	(70)

*Refer to Figure 3 for location.

Figure 17

Bond Strength of Liner-Propellant Specimens, Second Subscale Mold

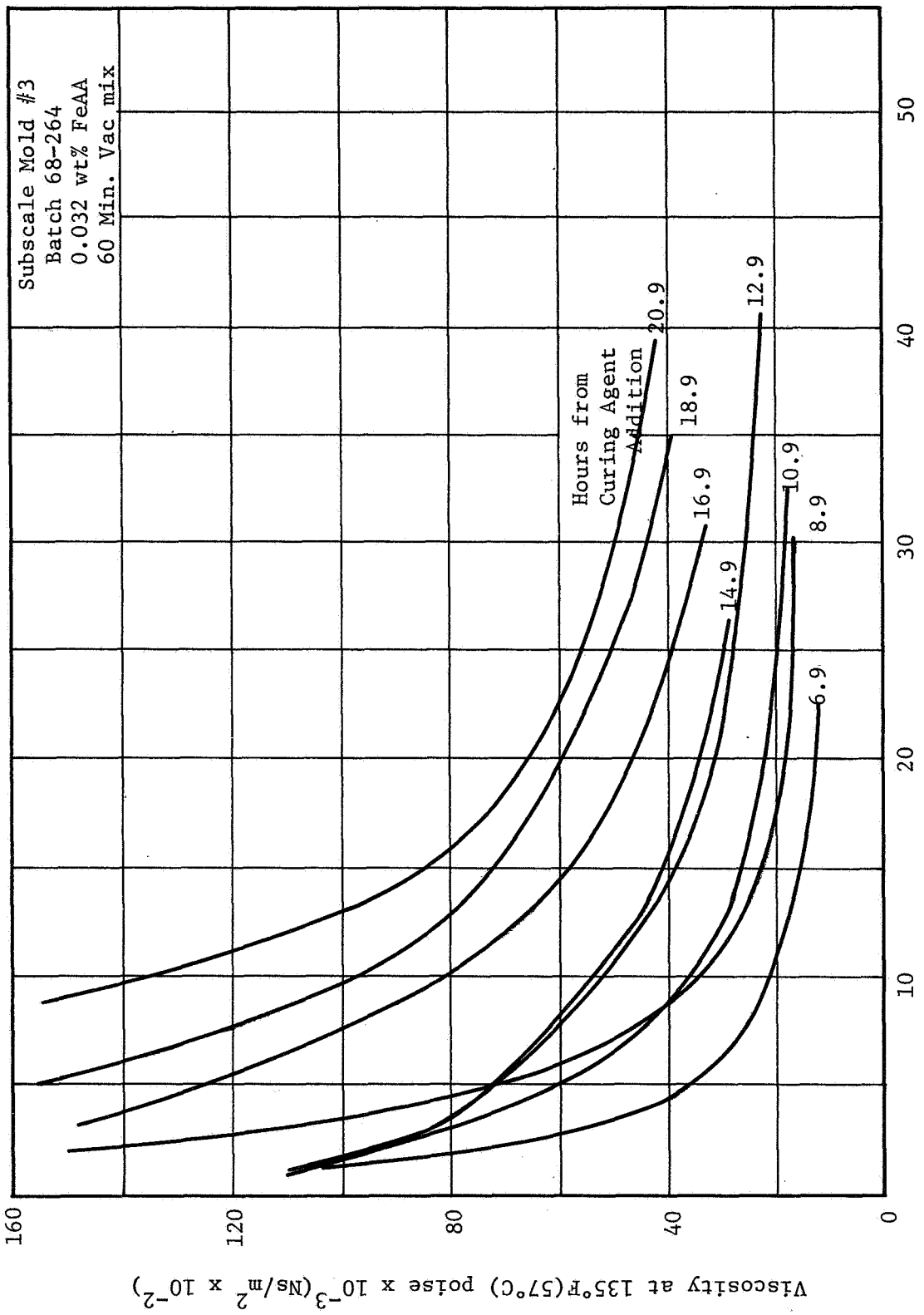
Batch No.	Final Vacuum Formulation FeAA Content Wt%	Mix Time, min	Casting Bayonet Submergence, in. (cm)	Cast Rate lb/hr	Cast Rate (Kg/hr)	Time Between Batches, hr
68-264	0.032	60	0-5 (0-13)	400	(180)	
68-265	0.032	60	5-13 (13-33)	300	(136)	5.3
68-266	0.032	60*	3 (8)	300	(136)	4.8
68-267	0.045	60	3 (8)	200	(90)	4.5
68-268	0.045	10	3 (8)	300	(136)	2.5

(1) Formulation contained 0.65 wt% Iron Blue and 0.65 wt% BRA-101.
(2) Propellant mixed at vacuum level of 29 in. (740 mm) Hg.
(3) Mold configuration was 240 degree (4.19 rad) cloverleaf.

*Final fuel added at 145°F (63°C)

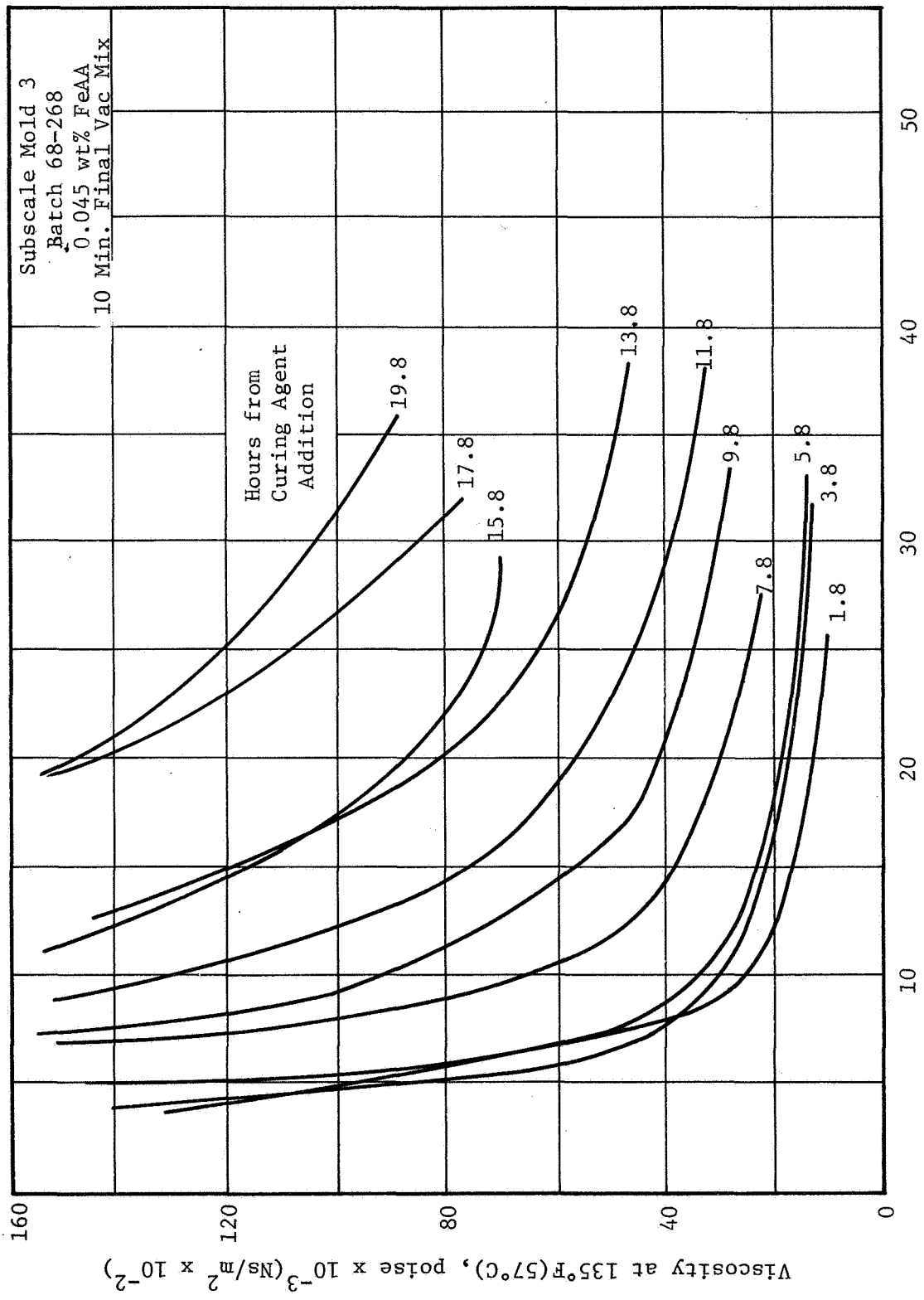
Summary of ANB-3254 Propellant Formulation and
Mixing Variables and Casting Parameters for Subscale Mold 3

Figure 18



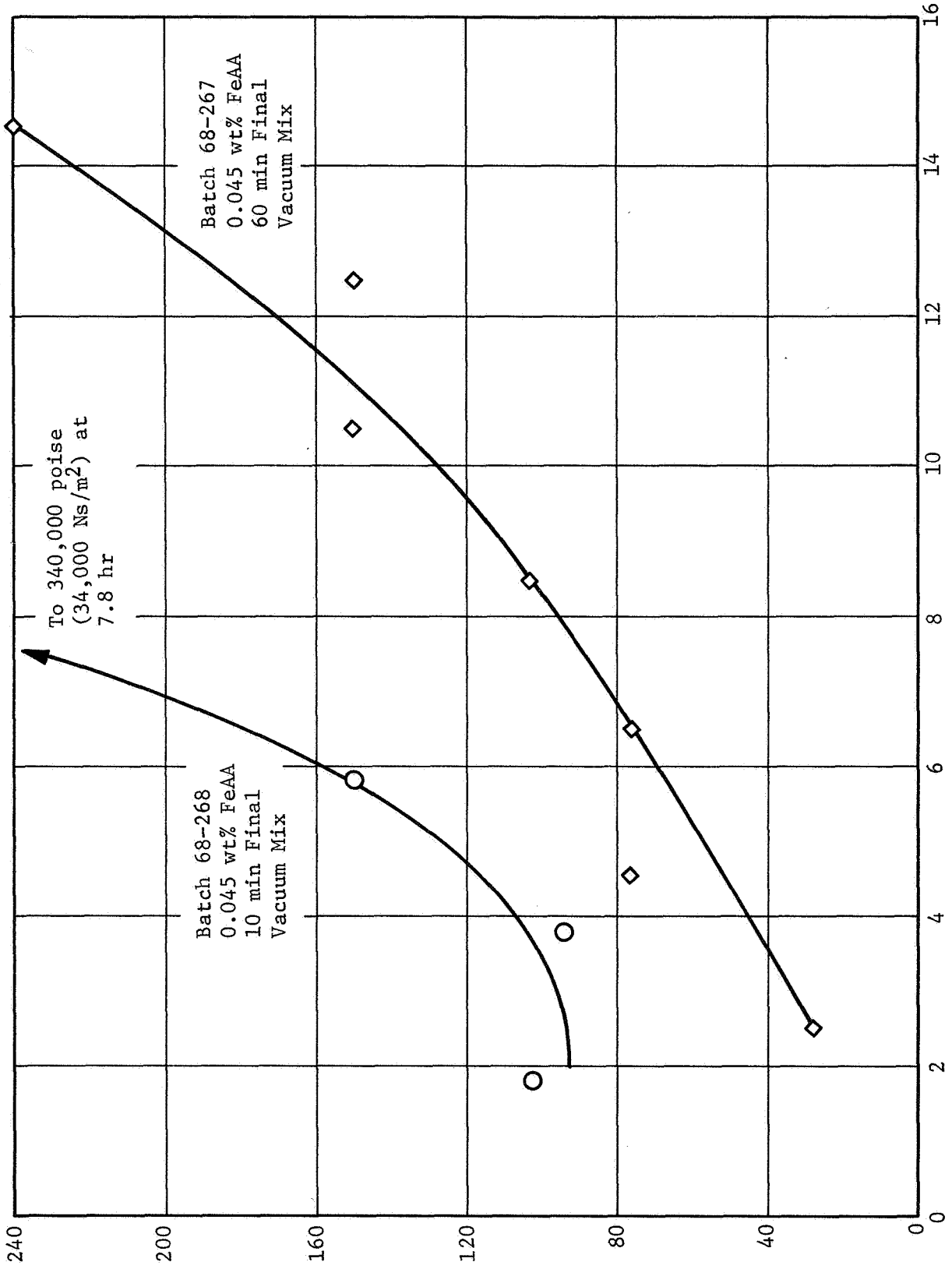
Viscosity Characteristics, Batch 68-264, Subscale Mold 3

Figure 19



Viscosity Characteristics, Batch 68-268, Subscale Mold 3

Figure 20



Comparison of the Viscosity Build-up Characteristics of Batches 68-267 and 68-268
(Subscale Mold No. 3)

Figure 21

Batch No.	Submix: Water Content, %	Submix: Acid Equivalents/ 100g	Submix: Liquid Density, g/cm^3	Submix: Refractive Index	Premix: Water Content, %	Premix: Liquid Density, g/cm^3	Uncured Propellant: Liquid Density, g/cm^3	Uncured Propellant: DER-332 Content, %	Uncured Propellant: Liquid Strand Burning Rate at 600 psig (414 N/cm^2) 80°F (27°C) in./sec	(cm/s)	Viscosity*, poise (NS/m^2) 6 hr	10 hr
68-264	0.047	0.0412	0.929	1.4910	0.148	1.426	1.748	1.21	0.688	(1.75)	30,000 (3,000)	58,000 (5,800)
68-265	0.049	0.0413	0.929	1.4920	0.139	1.423	1.746	1.23	0.686	(1.74)	40,000 (4,000)	75,000 (7,500)
68-266	0.044	0.0414	0.930	1.4916	0.148	1.428	1.747	1.30	0.692	(1.76)	50,000 (5,000)	62,000 (6,200)
68-267	0.066	0.0410	0.929	1.4918	0.149	1.429	1.748	1.26	0.704	(1.79)	75,000 (7,500)	150,000 (15,000)
68-268	0.056	0.0409	0.929	1.4916	0.147	1.429	1.747	1.28	0.686	(1.74)	130,000 (13,000)	off scale

* Viscosity at 135°F (57°C),
5 K dyne/cm^2 (500 N/m^2) shear stress,
6 and 10 hours after curing agent addition.

Summary of Uncured Propellant Data, Subscale Mold 3

Figure 22

Batch No. 68-	Cure Time, Days	Shore A Hardness	Mechanical Properties at 77°F (25°C)					
			σ_m, psi	(N/cm^2)	ε_m, %	ε_b, %	E_o, psi	(N/cm^2)
264	12	31	82	(57)	24	25	411	(283)
	16	35	80	(55)	19	19	466	(322)
	20	37	88	(61)	20	21	492	(339)
265	12	33	83	(57)	22	24	461	(318)
	16	35	94	(65)	23	25	498	(343)
	20	35	89	(61)	20	20	518	(357)
266	12	29	68	(47)	25	26	332	(229)
	16	28	74	(51)	23	25	378	(261)
	20	32	83	(57)	26	30	394	(272)
267	12	45	113	(78)	21	21	623	(430)
	16	46	126	(87)	21	21	725	(500)
	20	45	121	(84)	20	21	691	(477)
268	12	36	85	(59)	20	20	483	(333)
	16	39	89	(61)	20	21	551	(380)
	20	41	94	(65)	19	20	599	(413)

Figure 23

Mechanical Properties of Carton Samples from Propellant Cast Into Third Subscale Mold

Sample Location	Orientation	Mechanical Properties at 77°F (25°C)						Bond Strength at 77°F (25°C)			
		σ_m, psi	(N/cm^2)	ε_m, %	ε_b, %	E_o, psi	(N/cm^2)	Tensile, psi	Tensile, (N/cm^2)	Shear, psi	Shear, (N/cm^2)
B-I	Vertical	105	(72)	21	22	658	(453)				
	Horizontal (radial)	149	(103)	18	19	1150	(793)				
	Horizontal (circum.)	128	(88)	20	21	894	(616)	116	(80)	91	(63)
B-II	Vertical	157	(108)	18	20	1201	(828)				
	Horizontal (radial)	153	(106)	21	22	1079	(744)				
	Horizontal (circum.)	124	(86)	18	18	905	(624)	134	(92)	105	(72)
B-III	Vertical	117	(81)	17	17	887	(612)				
	Horizontal (radial)	129	(89)	18	19	944	(651)				
	Horizontal (circum.)	152	(105)	19	20	1162	(802)	113	(78)	94	(65)
B-IV	Vertical	107	(74)	20	21	656	(453)				
	Horizontal (radial)	125	(86)	19	19	896	(618)				
	Horizontal (circum.)	130	(90)	19	20	920	(635)	124	(85)	104	(72)
B-V	Vertical	117	(81)	20	20	717	(495)				
	Horizontal (radial)	125	(86)	18	18	878	(605)				
	Horizontal (circum.)	128	(88)	19	19	915	(631)	126	(86)	110	(76)

Figure 24

Mechanical and Bonding Properties, Third Subscale Mold

Mixing		Casting			
Batch No.	Mix Time, min	Bayonet Submergence, in. (cm)	Cast Rate lb/hr	(Kg/hr)	Time Between Batches, hr
68-281	10	0-4 (0-10)	300	(136)	-
68-282	10	1-7 (3-18)	300	(136)	24.0
68-283	10	3 (8)	250	(113)	4.5
22D-171	70	3 (8)	200	(90)	2.0
68-284	10	3 (8)	200	(90)	5.5

1. Formulation contained 0.65 wt% Iron Blue and 0.65 wt.% BRA-101.
2. Vacuum level during mixing was 29 in. (740 mm) Hg.
3. Mold configuration was 240 degree (4.19 rad) cylinder.

Summary of ANB-3254 Propellant Mixing Variables and Casting Parameter for Subscale Mold No. 4

Figure 25

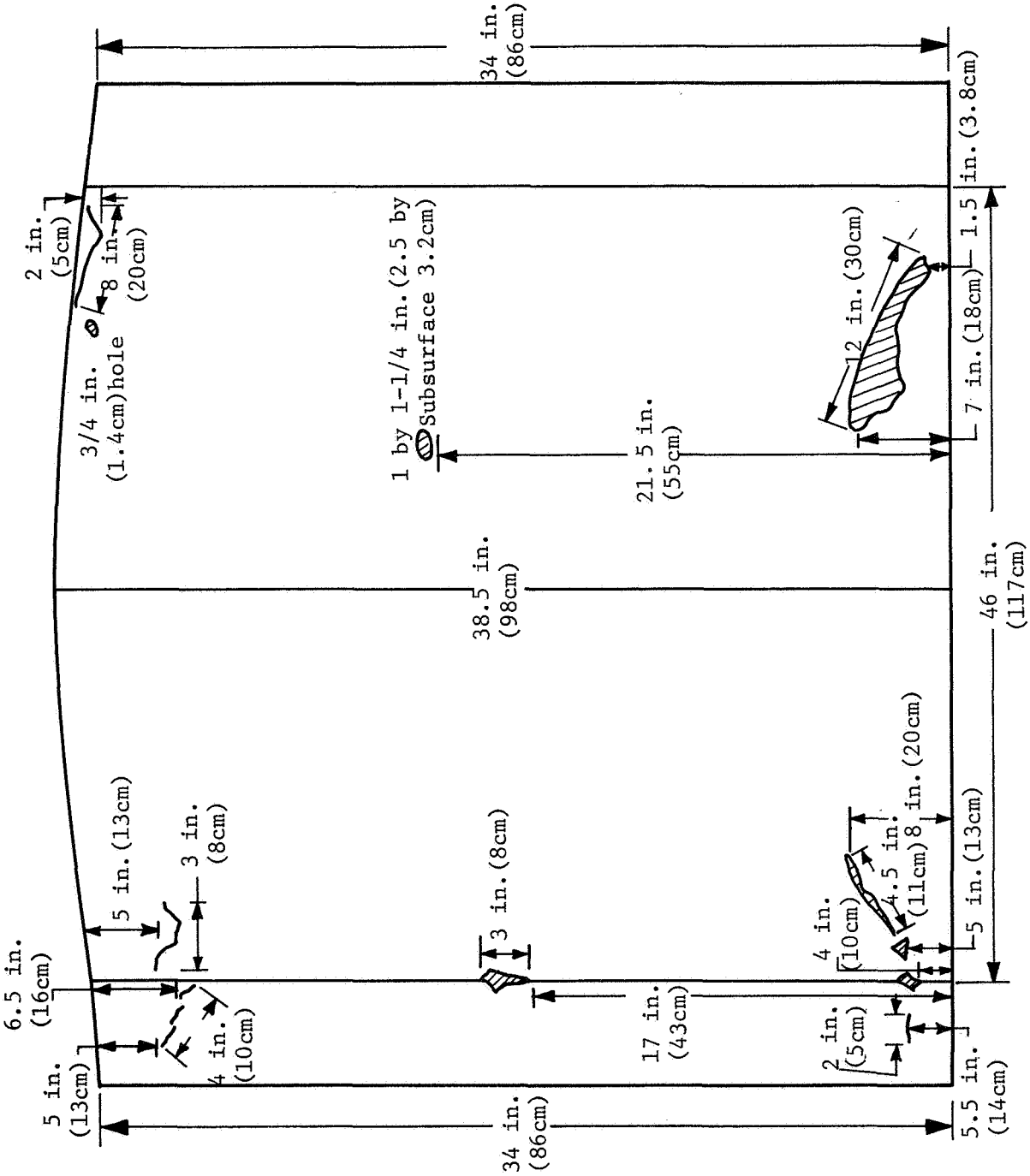
Batch No.	Submix: Water Content, %	Submix: Acid Equivalents/ 100g	Submix: Liquid Density, g/cm^3	Submix: Refractive Index	Premix: Water Content, %	Premix: Liquid Density, g/cm^3	Uncured Propellant: Liquid Density, g/cm^3	Uncured Propellant: DER-332 Content, %	Uncured Propellant: Liquid Strand Burning Rate at 600 psig (414 N/cm^2) 80°F (27°C) in./sec	Uncured Propellant: Liquid Strand Burning Rate at 600 psig (414 N/cm^2) 80°F (27°C) (cm/s)	Final Fuel FeAA Content %	Viscosity*, poise 6 hr	Viscosity*, poise (Ns/m^2) 6 hr	Viscosity*, poise 10 hr	Viscosity*, poise (Ns/m^2) 10 hr
68-281	0.066	0.0412	0.929	1.4910	0.174	1.427	1.746	1.24	0.696	(1.77)	2.42	83,000**	(8,300)	off scale**	
68-282	0.069	0.0414	0.929	1.4916	0.170	1.429	1.746	1.31	0.696	(1.77)	2.42	36,000**	(3,600)	off scale**	
68-283	0.052	0.0412	0.929	1.4918	0.201	1.428	1.742	1.20	0.694	(1.76)	2.57	120,000	(12,000)	off scale	
68-284	0.063	0.0413	0.930	1.4918	0.189	1.425	1.747	1.31	0.687	(1.75)	2.57	90,000**	(9,000)	140,000**	(14,000)
22D-171	0.079	0.0417	-	1.4915	0.170	1.428	1.747	1.31	0.711	(1.81)	2.61	80,000	(8,000)	115,000	(11,500)

* Viscosity at 135°F (57°C), 5K dynes/cm^2(500 N/m^2) shear stress, 6 and 10 hours after curing agent addition.

** Viscosity measurements changed from one cup for all readings to individual cups for each reading.

Summary of Uncured Propellant Data, Subscale Mold 4

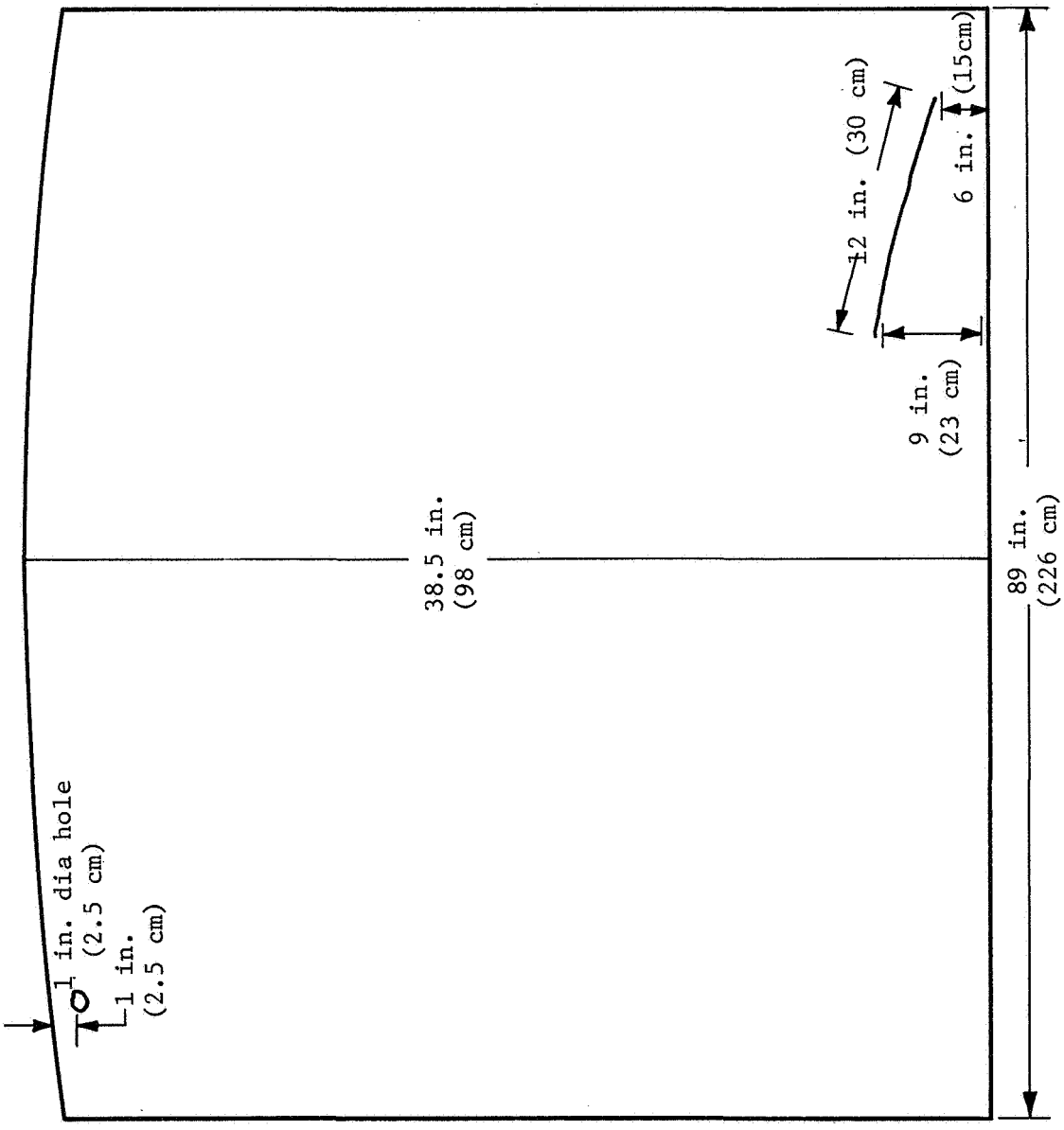
Figure 26



Core Configuration - 240 degree (4.19 rad) Cylinder

Grain Defect Map for the Fourth Subscale Mold
Interior View (ID)

Figure 27



Grain Defect Map for the Fourth Subscale Mold
Exterior View (OD)

Figure 28

Batch No. 68-	Cure Time, Days	Shore A Hardness	Mechanical Properties at 77°F (25°C)					
			σ_m, psi	(N/cm^2)	ε_m, %	ε_b, %	E_o, psi	(N/cm^2)
281	15	25	61	(42)	24	24	301	(208)
	20	28	60	(41)	25	25	272	(188)
	49	34	80	(55)	22	24	424	(293)
282	15	19	44	(30)	29	32	195	(135)
	20	17	48	(33)	32	34	192	(133)
	49	25	77	(53)	24	26	385	(265)
283	15	11	30	(21)	34	41	116	(80)
	20	11	33	(23)	34	39	125	(86)
	49	18	48	(33)	29	31	210	(145)
284	15	12	32	(22)	32	39	136	(94)
	20	12	33	(23)	32	41	138	(95)
	49	19	45	(31)	28	30	200	(138)
22D-171	15	18	41	(28)	38	53	151	(104)
	20	18	46	(32)	34	47	182	(126)
	49	30	65	(45)	29	34	295	(203)

Figure 29

Mechanical Properties of Carton Samples from Propellant Cast into Subscale Mold 4

Sample Location	Orientation	Mechanical Properties at 77°F (25°C)						Bond Strength at 77°F (25°C)				Burning Rate at 600 psig (414 N/cm²) 80°F (27°C)	
		σ_m, psi	(N/cm^2)	ϵ_m, %	ϵ_b, %	E_o, psi	(N/cm^2)	Tensile, psi	Tensile, (N/cm^2)	Shear, psi	Shear, (N/cm^2)	in./sec	(cm/s)
B-I	Vertical	111	(77)	21	23	743	(512)					0.726	(1.84)
	Horizontal	122	(84)	20	22	913	(630)	98	(68)	88	(61)	0.707	(1.79)
	Horizontal (circum.)	115	(79)	19	21	804	(554)					0.715	(1.82)
B-II	Vertical	79	(54)	21	22	503	(347)					0.664	(1.69)
	Horizontal	87	(60)	21	22	551	(380)	92	(63)	83	(57)	0.689	(1.75)
	Horizontal (circum.)	116	(80)	20	22	822	(567)					0.718	(1.82)
B-III	Vertical	79	(54)	21	21	494	(341)					0.701	(1.78)
	Horizontal	90	(62)	23	27	511	(352)	73	(50)	65	(45)	0.709	(1.80)
	Horizontal (circum.)	79	(54)	23	25	485	(334)					0.700	(1.78)
B-IV	Vertical	80	(55)	22	23	455	(314)					0.725	(1.84)
	Horizontal	91	(63)	23	26	560	(386)	70	(48)	59	(41)	0.702	(1.78)
	Horizontal (circum.)	85	(59)	24	30	479	(330)					0.716	(1.82)
B-V	Vertical	74	(51)	24	25	402	(277)					0.728	(1.85)
	Horizontal	89	(61)	23	27	522	(360)	65	(45)	55	(38)	0.696	(1.77)
	Horizontal (circum.)	87	(60)	23	27	520	(359)					0.742	(1.88)

Properties of Specimens from Fourth Subscale Mold

Figure 30

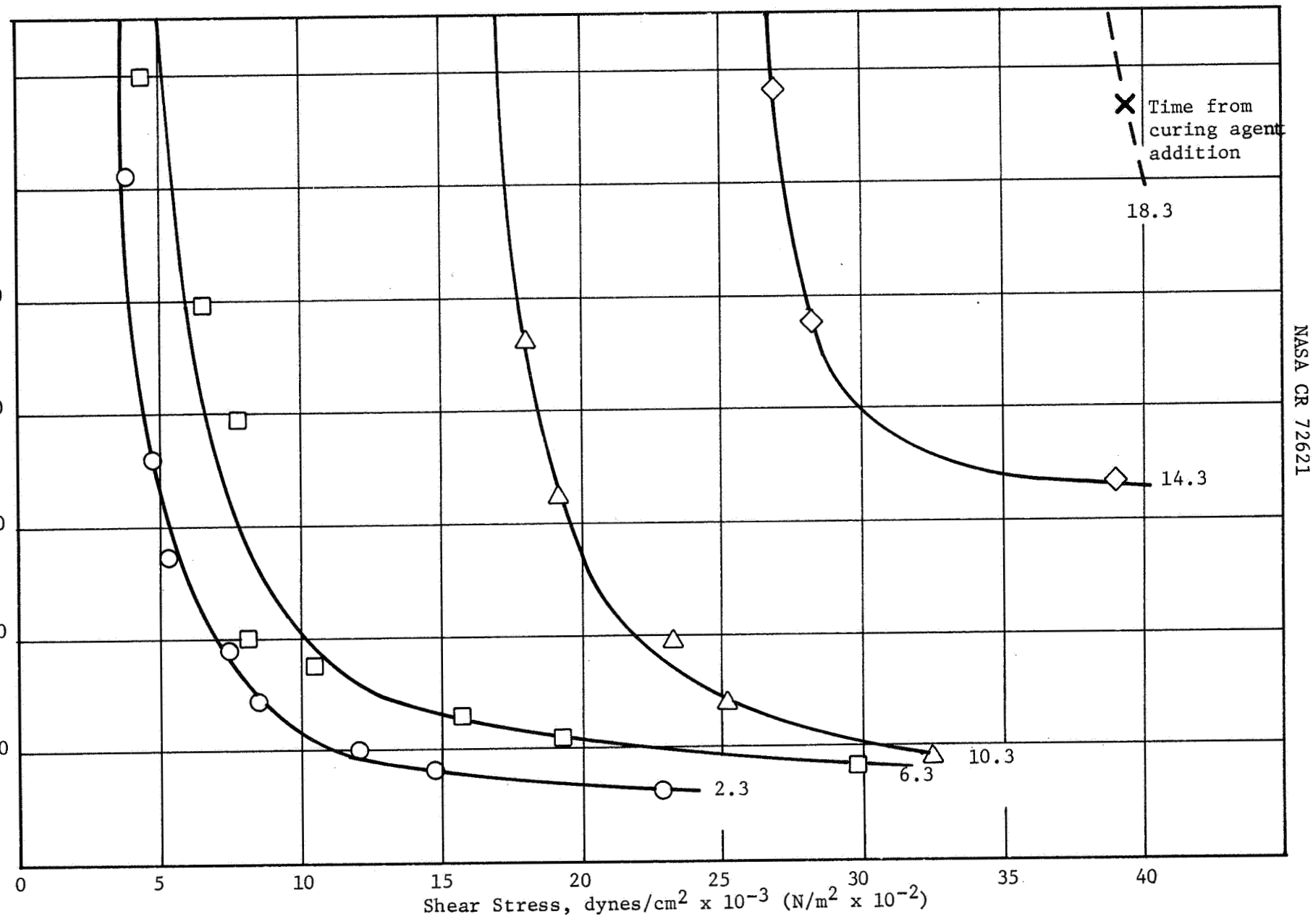


Figure 31

Viscosity as a Function of Shear Stress and Time from Curing Agent Addition for First Batch (68-290) Cast into Fifth Subscale Mold

Batch No.	Submix: Water Content, %	Submix: Acid Equivalents/ 100g	Submix: Liquid Density, g/cm^3	Submix: Refractive Index	Premix: Water Content, %	Premix: Liquid Density, g/cm^3	Uncured Propellant: Liquid Density, g/cm^3	Uncured Propellant: DER-332 Content, %	Uncured Propellant: Liquid Strand Burning Rate at 600 psig (414 N/cm^2) 80°F (27°C) in./sec	(cm/s)	Uncured Propellant: Viscosity*, poise (Ns/m^2) 6 hr	10 hr
68-290	0.058	0.0413	0.929	1.4915	0.147	1.427	1.744	1.20	0.691	(1.76)	150,000 (15,000)	off scale
68-291	0.078	0.0411	0.929	1.4915	0.163	1.426	1.747	1.11	0.693	(1.76)	60,000 (6,000)	off scale
68-292	0.075	0.0410	0.930	1.4914	0.178	1.427	1.746	1.25	0.667	(1.69)	70,000 (7,000)	off scale
68-293	0.067	0.0412	0.929	1.4913	0.170	1.424	1.742	1.30	0.693	(1.76)	120,000 (12,000)	off scale
68-294	0.073	0.0412	0.929	1.4913	0.159	1.424	1.748	1.18	0.685	(1.74)	95,000 (9,500)	off scale

* Viscosity at 135°F (57°C), 5K dynes/cm^2 (500 N/m^2) shear stress, 6 and 10 hr after curing agent addition.

Summary of Uncured Propellant Data, Fifth Subscale Mold

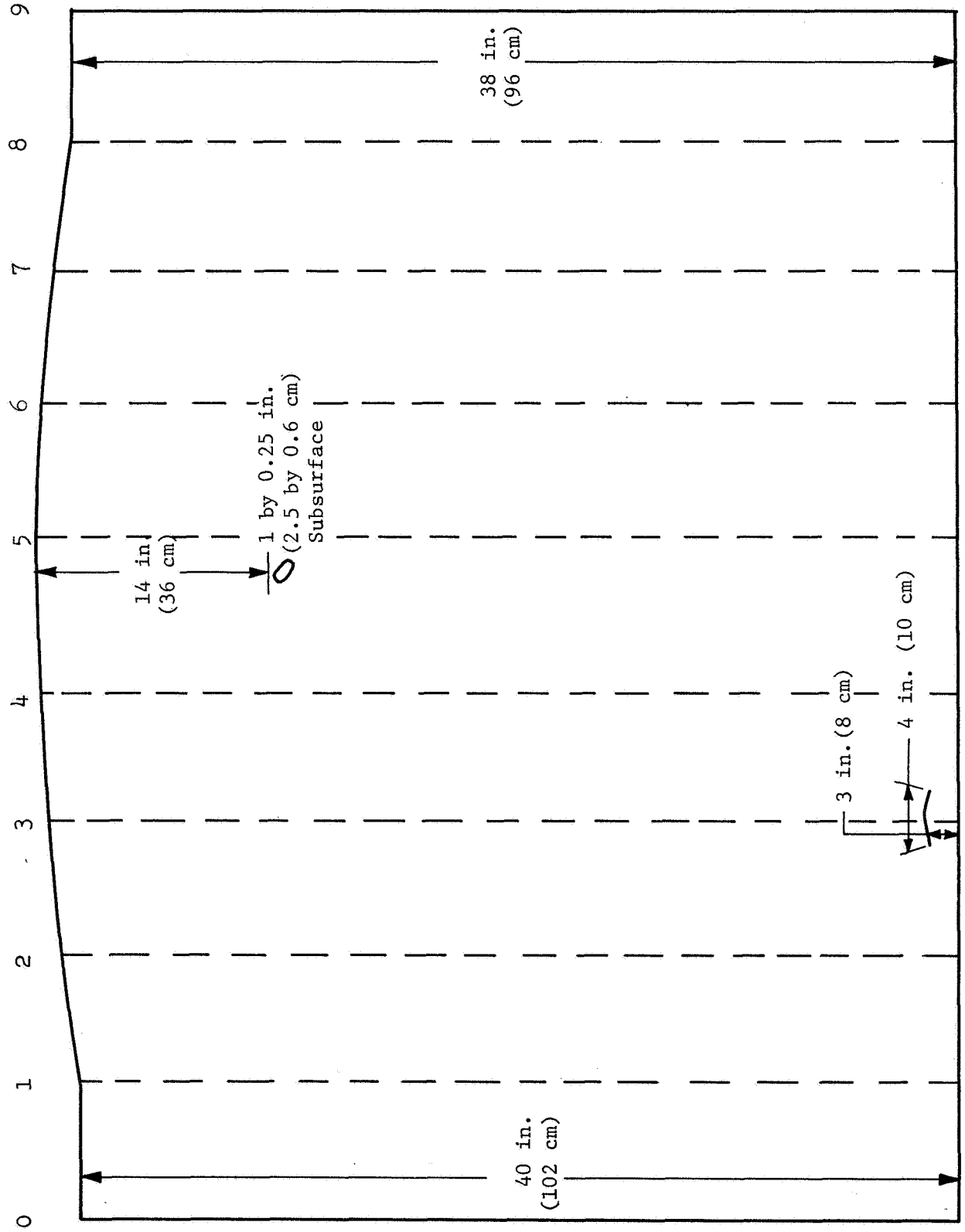
Figure 32

Mixing		Casting				
Batch No.	Mix Time, min	Bayonet Submergence, in. (cm)		Cast Rate lb/hr	Cast Rate (Kg/hr)	Time Between Batches, hr
68-290	10	0-5	(0-13)	400	(180)	
68-291	10	5-13	(13-33)	400	(180)	6
68-292	10	3	(8)	400	(180)	5
68-293	10	3	(8)	400	(180)	7
68-294	10	3	(8)	400	(180)	8

1. Formulation contained 0.65 wt % Iron Blue and 0.65 wt % BRA-101.
2. Propellant mixed at a vacuum level of 29 in. (740 min) Hg for 10 min.
3. Mold configuration was 240 degree (4.19 rad) cloverleaf.

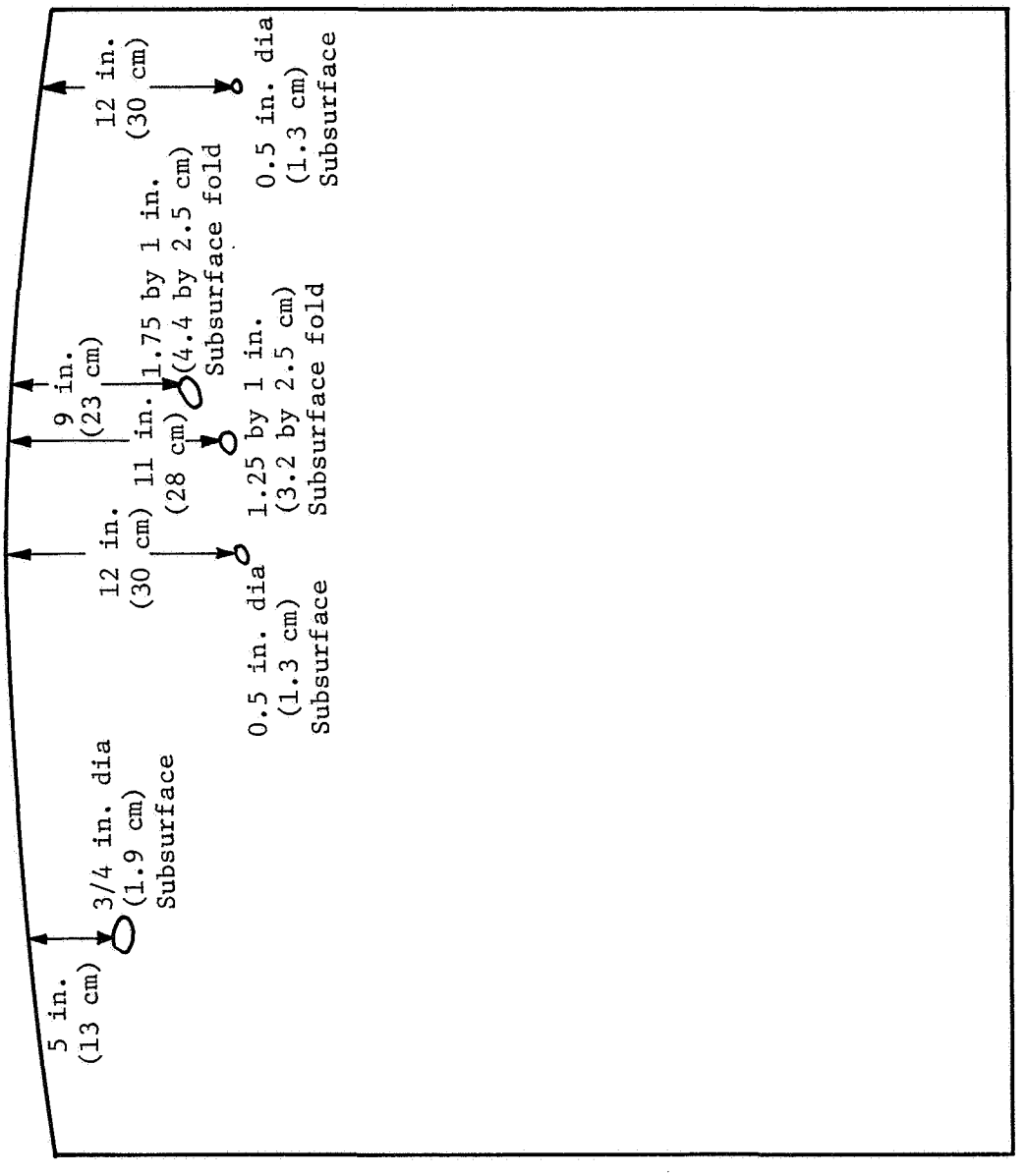
Summary of ANB-3254 Propellant Casting Parameters
for Subscale Mold No. 5

Figure 33



Core Configuration - 240 degree (4.19 rad) Clover
Grain Defect Map for the Fifth Subscale Mold
Interior View (ID)

Figure 34



Grain Defect Map for the Fifth Subscale Mold
Exterior View (OD)

Figure 35

Batch No. 68-	Cure Time, Days	Shore A Hardness	Mechanical Properties at 77°F (25°C)					
			σ_m, psi	(N/cm^2)	ε_m, %	ε_b, %	E_o, psi	(N/cm^2)
290	12	15	42	(29)	32	36	170	(117)
	15	20	48	(33)	32	34	189	(130)
	20	19	49	(34)	27	29	214	(148)
291	12	10	25	(17)	33	39	102	(70)
	15	12	32	(22)	30	34	145	(100)
	20	11	37	(26)	29	32	162	(112)
292	12	8	29	(20)	29	37	130	(90)
	15	12	33	(23)	30	34	140	(97)
	20	15	38	(26)	28	31	178	(123)
293	12	13-23	33	(23)	28	31	147	(101)
	15	16	42	(29)	29	30	184	(127)
	20	19	45	(31)	26	28	212	(146)
294	12	12	34	(23)	37	43	121	(83)
	15	16	42	(29)	31	33	171	(118)
	20	18	45	(31)	31	34	186	(128)

Mechanical Properties of Carton Samples from Propellant Cast into Fifth Subscale Mold

Sample Location	Orientation	Mechanical Properties at 77°F (25°C)						Bond Strength at 77°F (25°C)				Burning Rate at 600 psig (414 N/cm^2) 80°F (27°C)	
		σ_m,		ε_m,	ε_b,	E_o,		Tensile,		Shear,			
		psi	(N/cm^2)	%	%	psi	(N/cm^2)	psi	(N/cm^2)	psi	(N/cm^2)	in./sec	(cm/s)
B-I	Vertical	77	(53)	19	20	459	(317)					0.648	(1.65)
	Horizontal	89	(61)	21	23	551	(380)	73	(50)	70	(48)	0.686	(1.74)
B-II	Vertical	94	(65)	20	22	605	(417)					0.701	(1.78)
	Horizontal	84	(58)	22	23	481	(332)	70	(48)	59	(41)	0.706	(1.79)
B-III	Vertical	84	(58)	20	21	518	(357)					0.704	(1.79)
	Horizontal	84	(58)	21	21	481	(332)	80	(55)	66	(46)	0.678	(1.72)
B-IV	Vertical	95	(66)	24	24	494	(341)					0.658	(1.67)
	Horizontal	82	(57)	20	20	479	(331)	73	(50)	70	(48)	0.683	(1.73)
B-V	Vertical	88	(61)	25	27	477	(329)					0.697	(1.77)
	Horizontal	88	(61)	24	25	461	(318)	66	(46)	73	(50)	0.664	(1.69)

Properties of Specimens from Fifth Subscale Mold

Figure 37

Mixing		Casting				
Batch No.	Mix Time, min	Bayonet Submergence, in.	(cm)	Cast Rate lb/hr	(Kg/hr)	Time Between Batches, hr
68-327	10	0-3	(0-8)	700	(320)	-
68-328	10	2	(5)	620	(280)	4
68-329	10	2	(5)	840	(380)	4
68-330	10	2	(5)	530	(240)	14
68-331	10	2	(5)	470	(210)	3.8

1. Formulation contained 0.65 wt % Iron Blue and 0.65 wt % BRA-101.
2. Propellant mixed at a vacuum level of 29 in. (740 mm) Hg for 10 min.
3. Mold configuration was 360 degree (6.28 rad) cylinder.

Summary of ANB-3254 Propellant and Casting Parameters for Subscale Mold 6

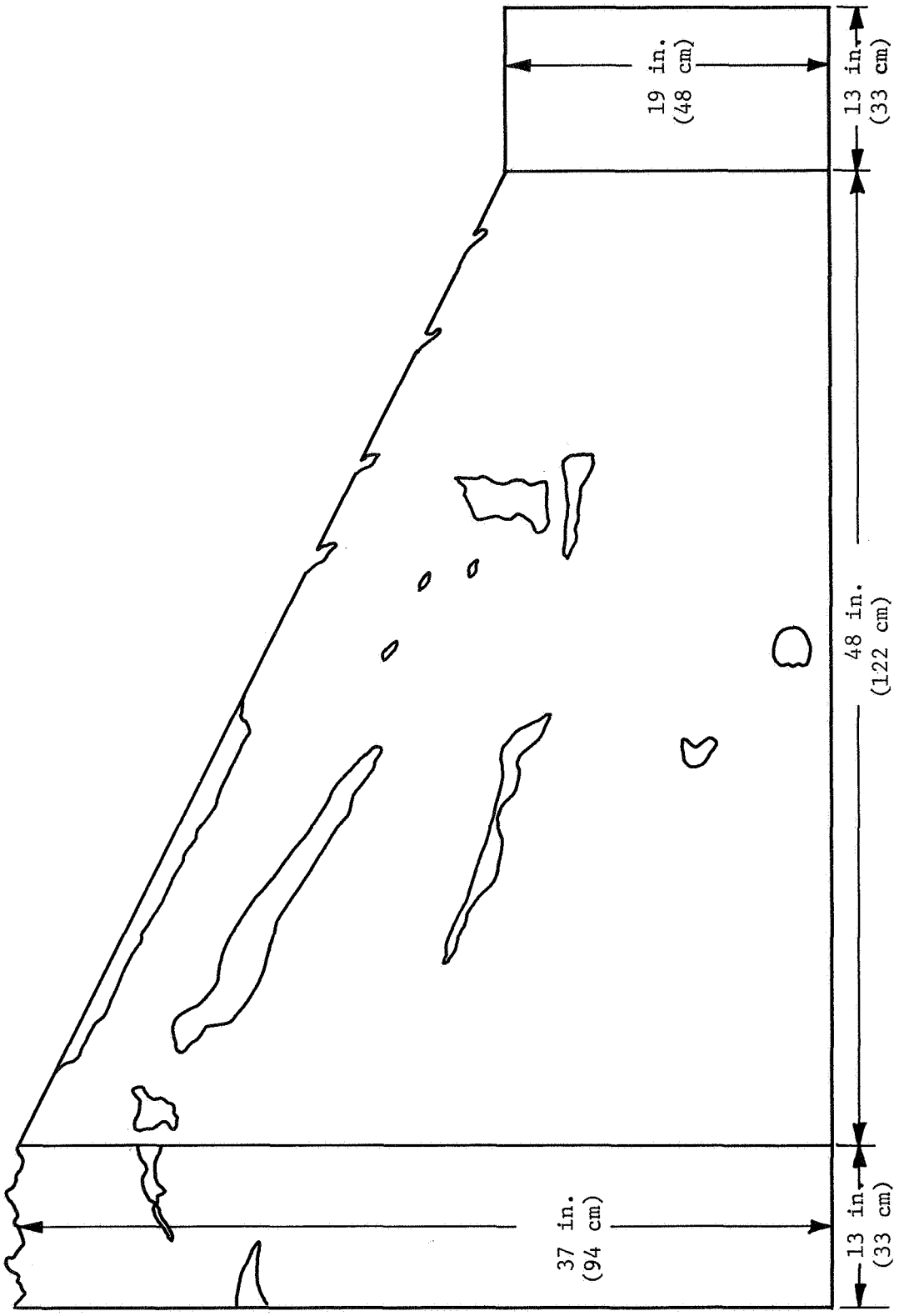
Figure 38

Batch No.	Submix				Premix		Uncured Propellant				
	Water Content, %	Acid Equivalents/ 100g	Liquid Density g/cm^3	Refractive Index	Water Content, %	Liquid Density g/cm^3	Liquid Density g/cm^3	DER-332 Content %	Liquid Strand Burning Rate at 600 psig (414 N/cm^2) 80°F (27°C)		Viscosity*, poise (NS/m^2)	
									in./sec	(cm/s)	6 hr	10 hr
68-327	0.065	0.0406	0.930	1.4911	0.164	1.422	1.749	1.24	0.691	(1.76)	100,000 (10,000)	Off scale
68-328	0.072	0.0406	0.929	1.4910	0.164	1.418	1.745	1.22	0.662	(1.68)	50,000 (5,000)	100,000 (10,000)
68-329	0.065	0.0409	0.929	1.4914	0.224	1.430	1.748	1.21	0.691	(1.76)	75,000 (7,500)	150,000 (15,000)
68-330	0.077	0.0409	0.929	1.4910	0.178	1.431	1.747	1.27	0.697	(1.77)	115,000 (11,500)	Off scale
68-331	0.077	0.0406	0.929	1.4910	0.137	1.429	1.747	1.20	0.678	(1.72)	Off scale	

* Viscosity at 135°F (57°C), 5 K dynes/cm^2 (500 N/m^2) shear stress, 6 and 10 hr after curing agent addition.

Summary of Uncured Propellant Data, Sixth Subscale Mold

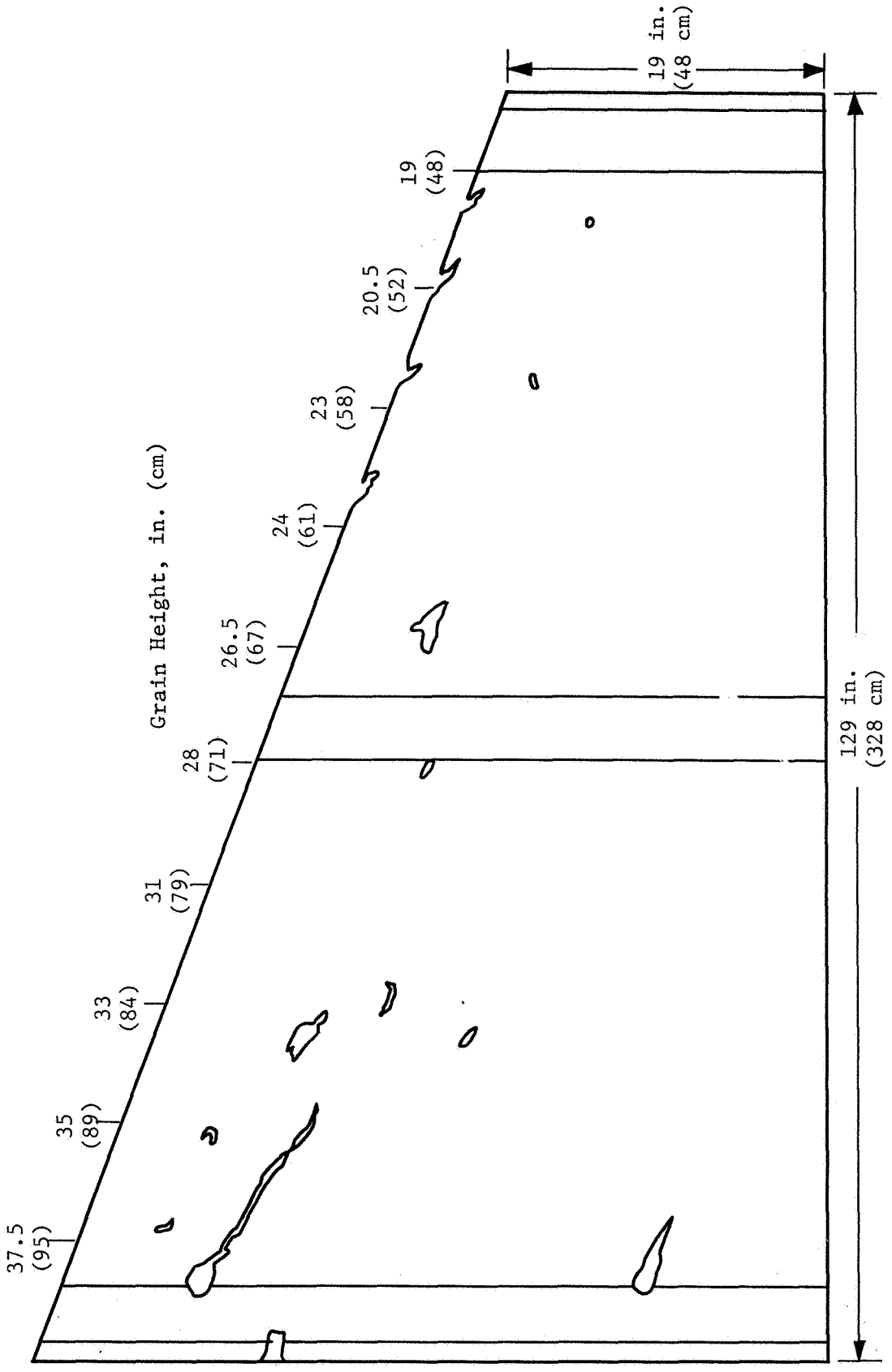
Figure 39



Core Configuration - 360-degree (6.28 rad) Cylinder

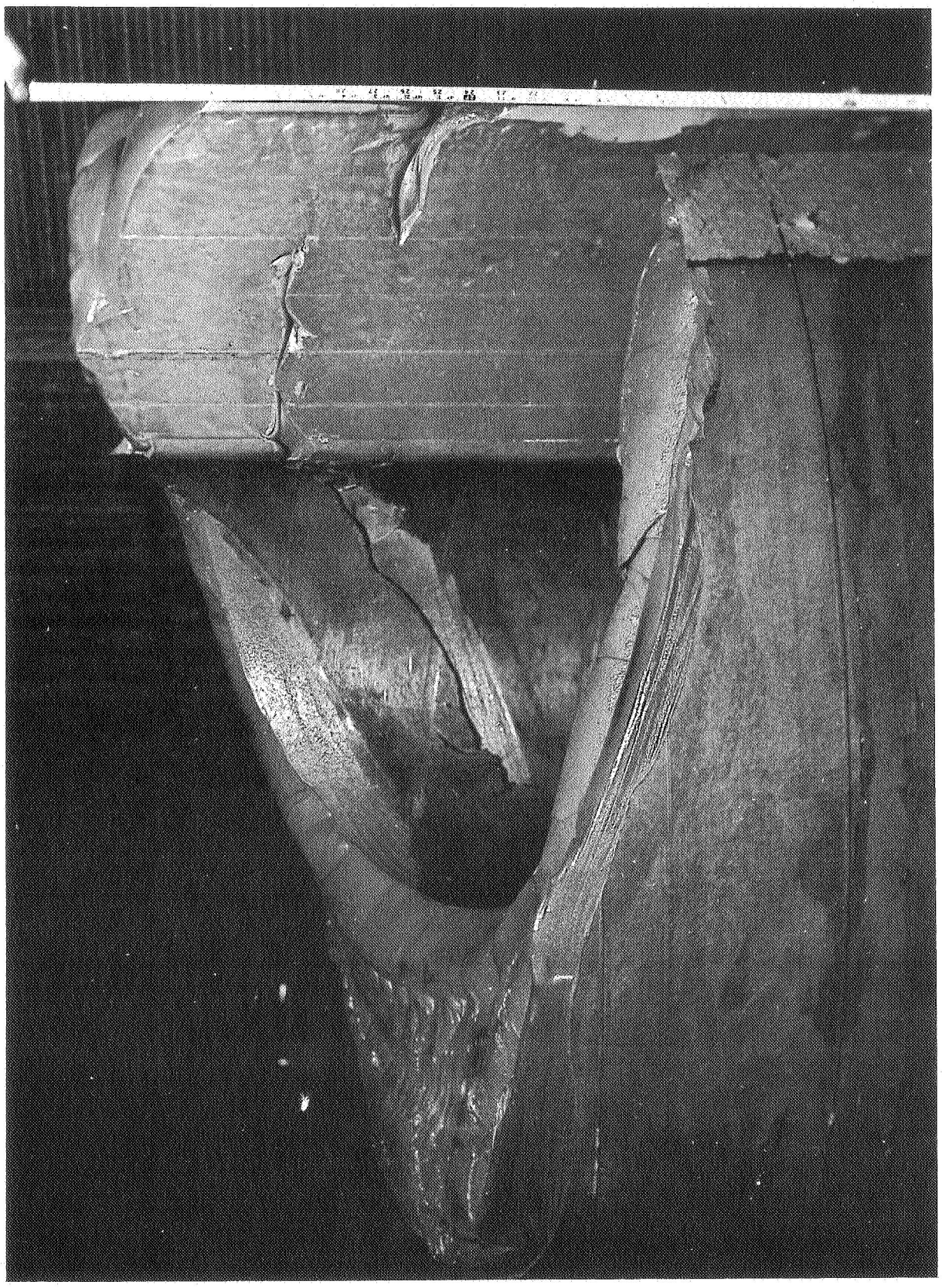
Grain Defect Map for the Sixth Subscale Mold
Interior View (ID)

Figure 40



Grain Defect Map for the Sixth Subscale Mold
Exterior View (OD)

Figure 41

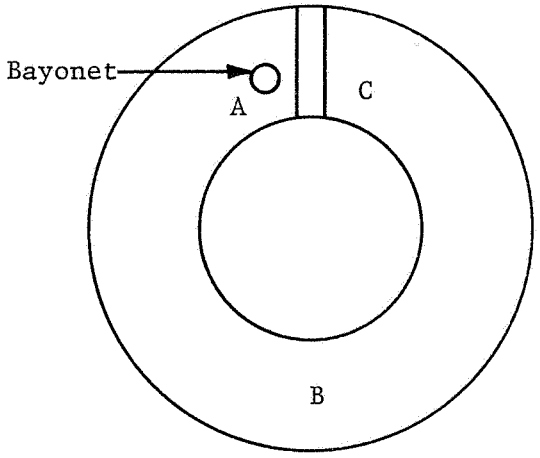


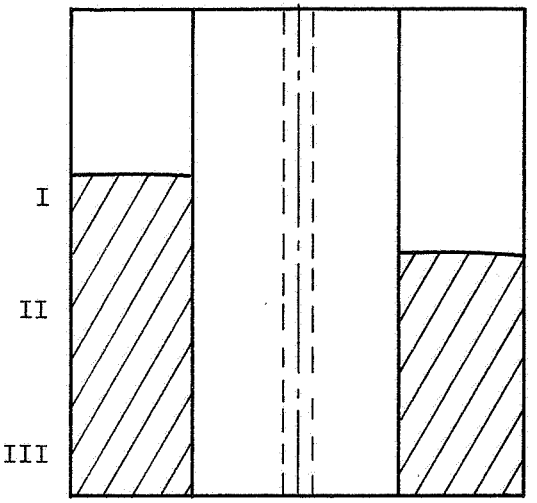
View of Sixth Subscale Mold

Figure 42

Sample Location*	Orientation	Mechanical Properties at 77°F(25°C) σ_m, psi(N/cm^2)	ε_m, %	ε_b, %	E_o, psi(N/cm^2)	Bond Strength at 77°F(25°C) Tensile$_2$ psi(N/cm^2)	Shear$_2$ psi(N/cm^2)	Solid Strand Burning Rate at 80°F(27°C) and 600 psig (414 N/cm^2), in./sec(cm/s)
I-B	Vertical	67 (46)	22	23	424 (292)			0.690 (1.75)
	Horizontal	79 (54)	19	21	588 (405)	83 (57)	77 (53)	0.699 (1.78)
I-C						95 (66)	87 (60)	
II-B	Vertical	83 (57)	21	22	531 (366)			0.711 (1.80)
	Horizontal	84 (58)	23	25	498 (343)	89 (61)	85 (59)	0.711 (1.80)
III-B	Vertical	90 (62)	20	22	601 (415)			0.701 (1.78)
	Horizontal	89 (61)	20	23	656 (453)	94 (65)	89 (61)	0.674 (1.71)
III-C						96 (66)	85 (59)	

* Three vertical locations (I, II, and III) and three circumferential locations (A, B, C) as shown in the sketch below:





Mechanical and Bond Properties and Solid Strand Burning Rate of Propellant Specimens Taken from the Sixth Subscale Mold

Figure 43

Batch No.	Formulation	Casting: Bayonet Submergence, in. (cm)		Cast Rate: lb/hr	Cast Rate: Kg/hr	Time Between Batches, hr
69-7	ANB-3354	0-3	(0-8)	740	(340)	-
69-8	ANB-3254	0-3	(0-8)	680	(310)	4.5
69-9	ANB-3254	0-3	(0-8)	680	(310)	6.5
69-10	ANB-3254	0-3	(0-8)	650	(290)	12.8
69-11	ANB-3350	0-3	(0-8)	575	(260)	8.0

1. Mold configuration was 360 degree (6.28 rad) cylinder
2. Propellant mixed at a vacuum level of 29 in. (740 mm) Hg for 55 minutes

Summary of Propellant Variables
Cast into Subscale Mold 7

Figure 44

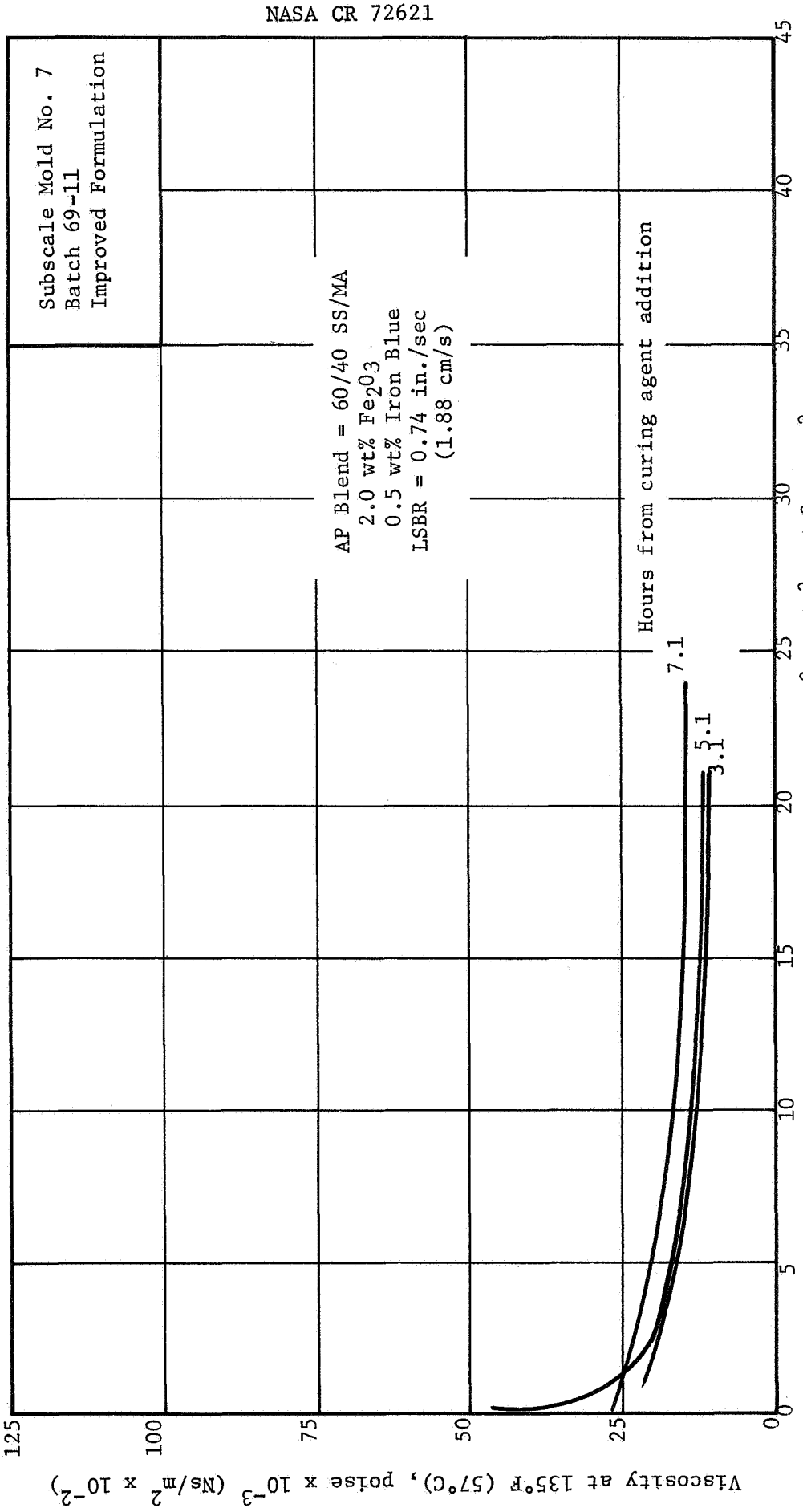


Figure 45

Propellant Viscosity as a Function of Shear Stress and Time from Curing Agent Addition

Batch No.	Submix				Premix		Uncured Propellant					
	Water Content, %	Acid Equivalents/ 100g	Liquid Density g/cm^3	Refractive Index	Water Content, %	Liquid Density g/cm^3	Liquid Density g/cm^3	DER-332 Content, %	Liquid Strand Burning Rate at 600 psig (414 N/cm^2) 80°F (27°C) in./sec	(cm/s)	Viscosity*, poise (Ns/m^2) 6 hr	10 hr
69-7	0.048	0.0412	0.929	1.4918	0.140	1.428	1.748	1.26	0.681	(1.73)	37,000 (3,700)	140,000 (14,000)
69-8	0.054	0.0414	0.929	1.4915	0.147	1.429	1.747	1.23	0.678	(1.72)	40,000 (4,000)	110,000 (11,000)
69-9	0.054	0.0414	0.929	1.4916	0.164	1.428	1.747	1.25	0.682	(1.73)	78,000 (7,800)	off scale
69-10	0.073	0.0414	0.929	1.4920	0.164	1.430	1.749	1.22	0.684	(1.74)	60,000 (6,000)	off scale
69-11	0.081	0.0430	0.929	1.4935	0.078	1.522	1.787	0.92	0.744	(1.89)	19,000 (1,900)	

* Viscosity at 135°F (57°C), 5K dynes/cm^2 (500 N/m^2) shear stress, 6 and 10 hours after curing agent addition.

Summary of Uncured Propellant Data, Seventh Subscale Mold

Figure 46

Batch No. 69-	Cure Time at 135°F (57°C), Days	Shore A Hardness	Mechanical Properties at 77°F (25°C)					
			σ_m, psi	(N/cm^2)	ε_m, %	ε_b, %	E_o, psi	(N/cm^2)
7	12	36	83	(57)	23	25	435	(300)
	17	38	99	(68)	25	26	509	(351)
	21	41	100	(69)	23	24	530	(365)
8	12	30	72	(50)	26	27	343	(237)
	17	36	76	(52)	20	20	418	(288)
	21	37	84	(58)	23	25	446	(308)
9	12	30	68	(47)	24	26	348	(240)
	17	33	82	(57)	26	30	377	(260)
	21	35	80	(55)	21	22	437	(301)
10	12	25	56	(39)	23	24	283	(195)
	17	31	67	(46)	22	23	341	(235)
	21	34	73	(50)	25	27	359	(248)
11	12	35	72	(50)	21	23	433	(299)
	17	36	78	(54)	21	23	470	(324)
	21	40	74	(51)	18	19	487	(336)
	25	40	77	(53)	19	20	483	(333)

Mechanical Properties of Carton Samples of Propellant Cast into the Seventh Subscale Mold

Figure 47

Sample Location	Orientation	Mechanical Properties at 77°F (25°C)						Bond Strength at 77°F (25°C)				Burning Rate at 600 psig (414 N/cm^2) 80°F (27°C)	
		σ_m,		ε_m,	ε_b,	E_o,		Tensile,		Shear			
		psi	(N/cm^2)	%	%	psi	(N/cm^2)	psi	(N/cm^2)	psi	(N/cm^2)	in./sec	(cm/s)
I-B	Vertical	94	(65)	23	28	568	(392)					0.680	(1.73)
	Horizontal	93	(64)	20	23	645	(445)	85	(59)	58	(40)	0.726	(1.84)
I-C								59	(41)	43	(30)		
II-B	Vertical	94	(65)	22	25	634	(437)					0.703	(1.79)
	Horizontal	89	(61)	22	25	590	(407)	92	(63)	63	(43)	0.725	(1.84)
II-C								89	(61)	47	(32)		
III-B	Vertical	83	(57)	19	20	601	(415)					0.674	(1.71)
	Horizontal	91	(63)	22	25	579	(399)	74	(51)	57	(39)	0.729	(1.85)
III-C								89	(61)	67	(46)		

Figure 48

Properties of Specimens from Seventh Subscale Mold

Subscale Mold	Formulation	Configuration	No. of Bayonets	Flow Behavior degree of pseudoplasticity	Propellant Viscosity,[1] poise x 10^{-3} (Ns/m^2 x 10^{-2})	No. of Defects	Size Range
1	ANB-3254	240 degree (4.19 rad) Cloverleaf	2	Normal	13 to 17	3	0.1 to 0.25-in.-dia (0.25 to 0.64 cm dia) to 3.0 in. (7.6 cm) long
2	ANB-3254	240 degree (4.19 rad) Cloverleaf	2	Normal	24 to 27[2]	0	-
3	ANB-3254	240 degree (4.19 rad) Cloverleaf	2	Normal	25 to 40[3]	0	-
4	ANB-3254	240 degree (4.19 rad) Cylinder	1	High	50 to >150[4]	13	1 in. (2.5 cm) dia to 3 by 12 in. (8 cm by 30 cm)
5	ANB-3254	240 degree (4.19 rad) Cloverleaf	2	High	65 to 120	7	0.5 in. (1.3 cm) dia to 0.25 by 4 in. (0.6 cm by 10 cm)
6	ANB-3254	360 degree (6.28 rad) Cylinder	1	High	47 to >150	28	1 in. (2.5 cm) dia to 4 by 20 in. (10 cm by 51 cm)
7	ANB-3254	360 degree (6.28 rad) Cylinder	1	Normal	27 to 37[5]	9	0.25 to 2.0 in.-dia (0.64 to 5.1 cm dia) to 7 in. (17.8 cm) long

(1) Viscosity at 135°F (57°C), 5 K dynes/cm^2 (500 N/m^2) shear stress, 3 hours after curing agent addition.
(2) Contained one batch with benzidine yellow that had a viscosity of 50,000 poise (5,000 Ns/m^2).
(3) Contained one batch mixed by the marginal mix cycle that had a viscosity of 90,000 poise (9,000 Ns/m^2).
(4) Contained an increment from the 5500-lb (2500 Kg) scale-up batch that had a viscosity of 30,000 poise (3,000 Ns/m^2).
(5) Contained one batch of the improved formulation that had a viscosity of 17,000 poise (1,700 Ns/m^2).

Summary of Results, Subscale Molds 1 through 7

Figure 49

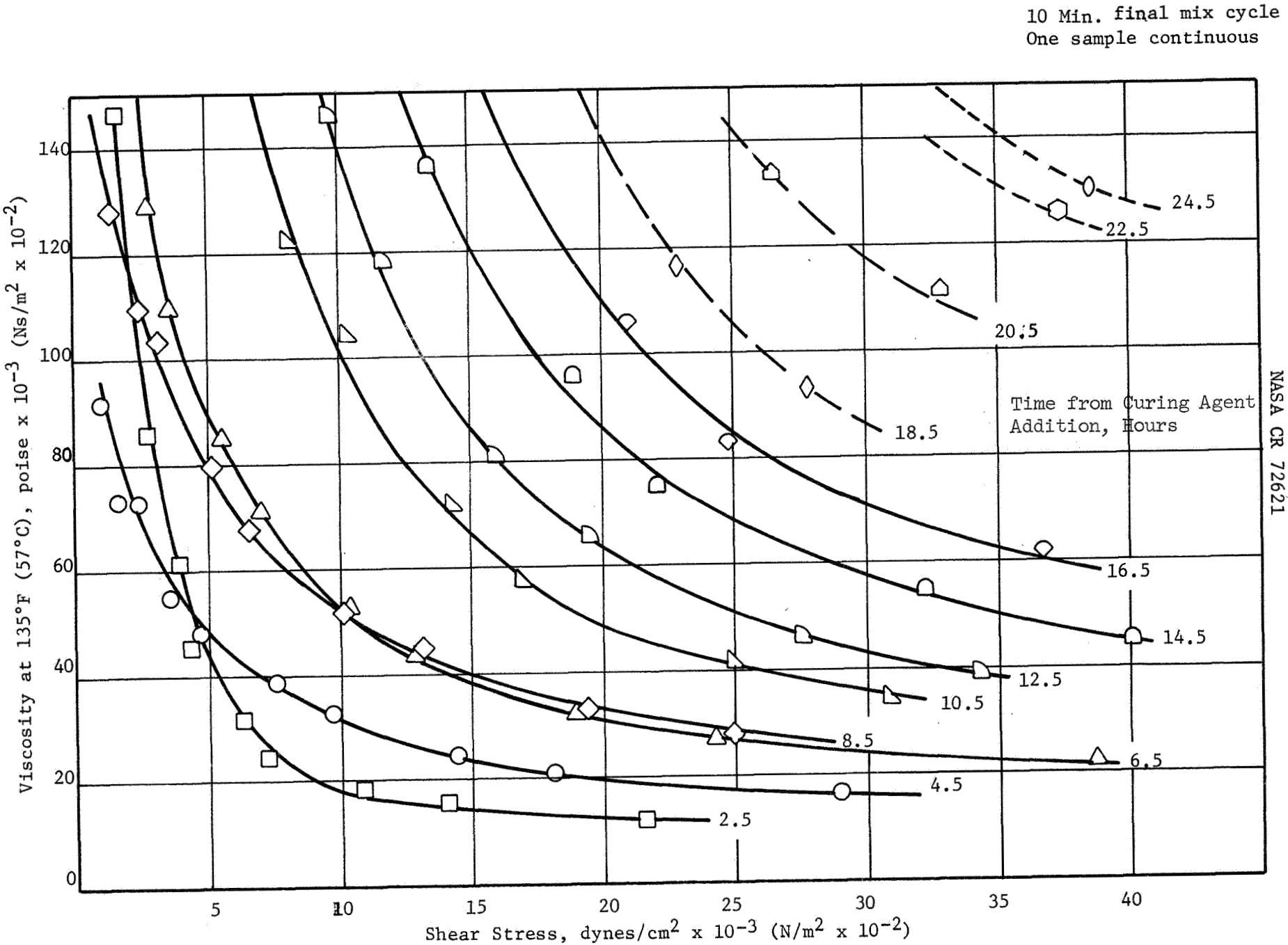
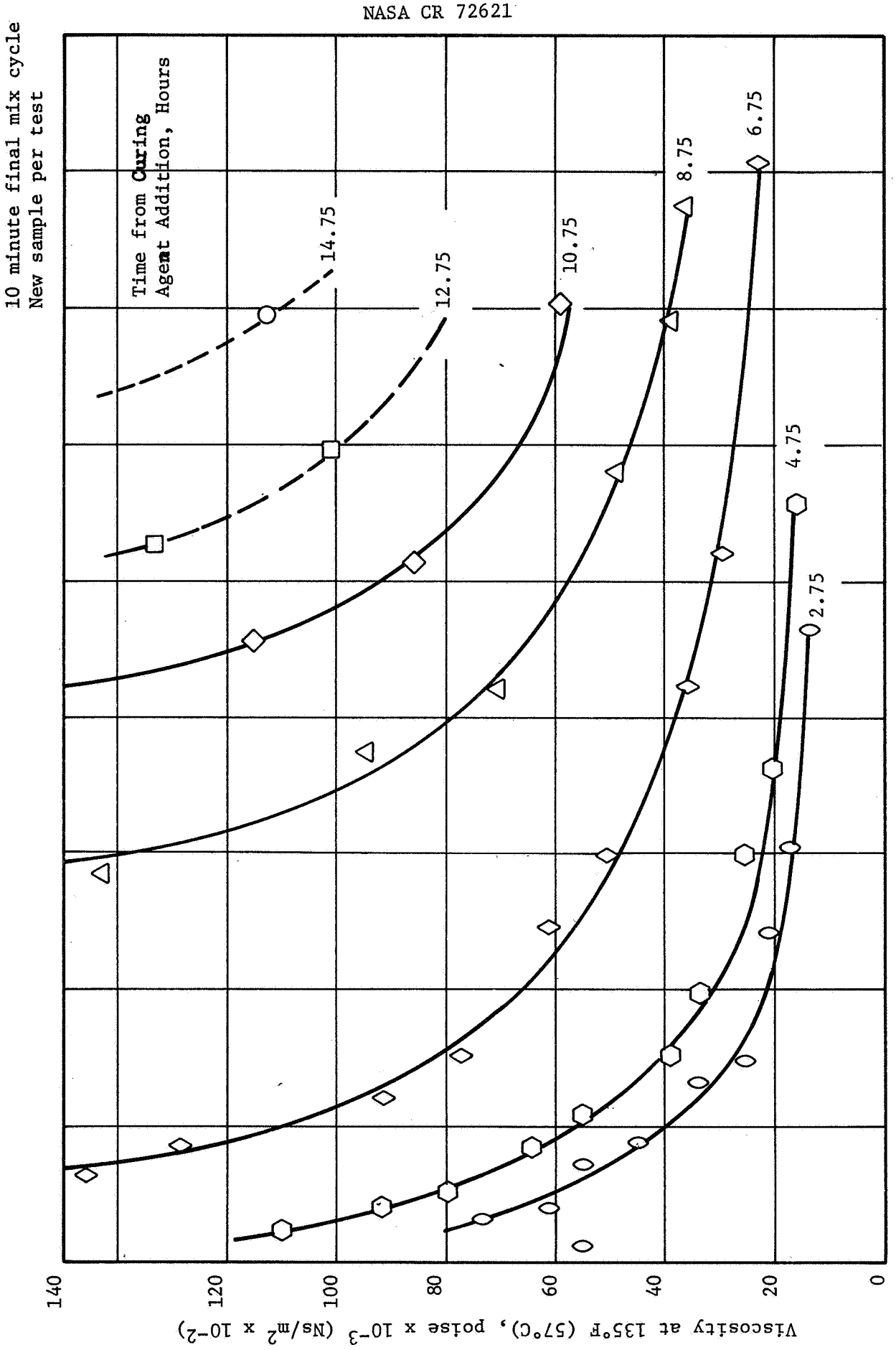


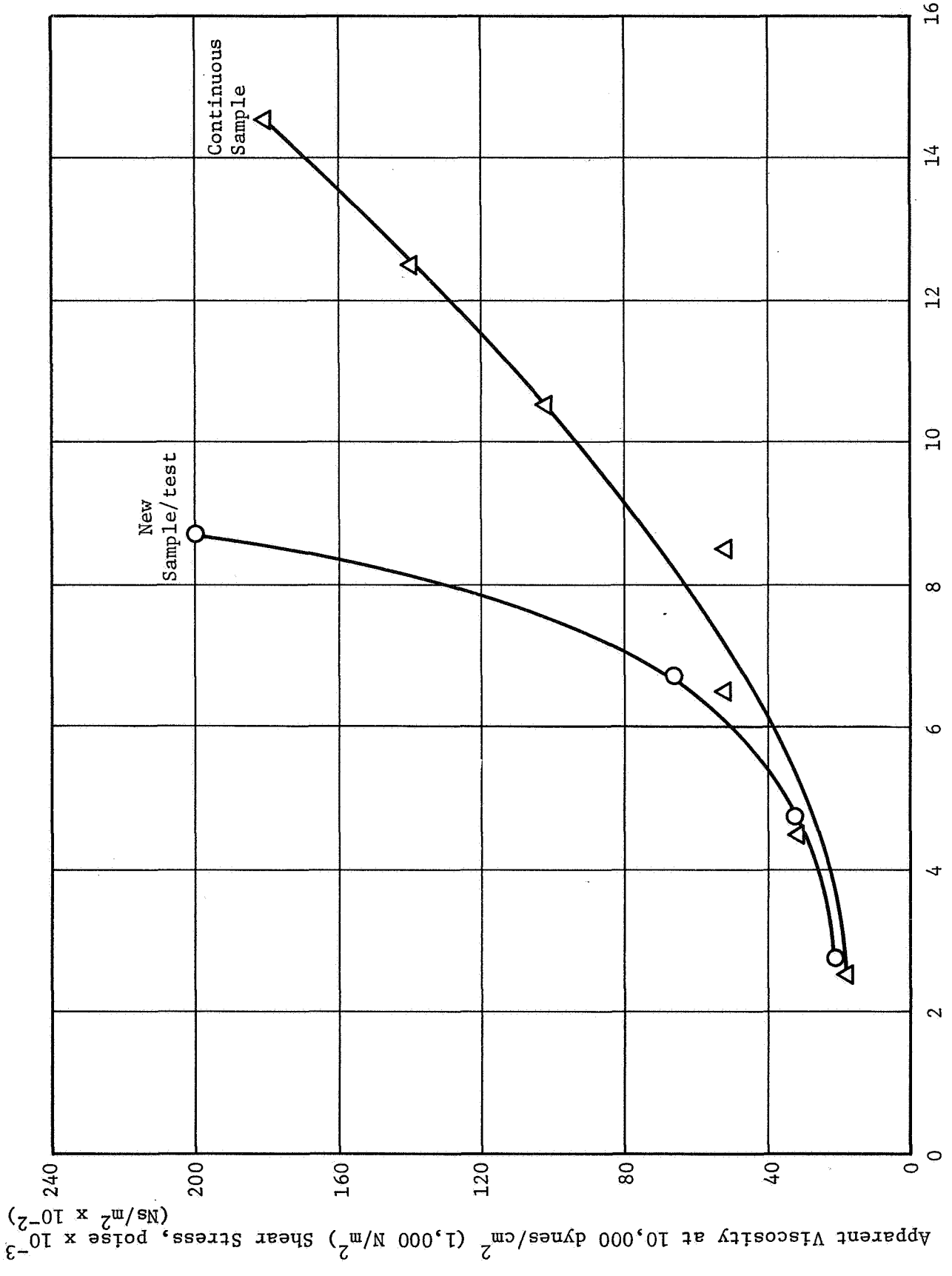
Figure 50

Viscosity Buildup Characteristics of ANB-3254 Propellant Prepared in a 5500-lb (2500 Kg) Vertical Batch Mix



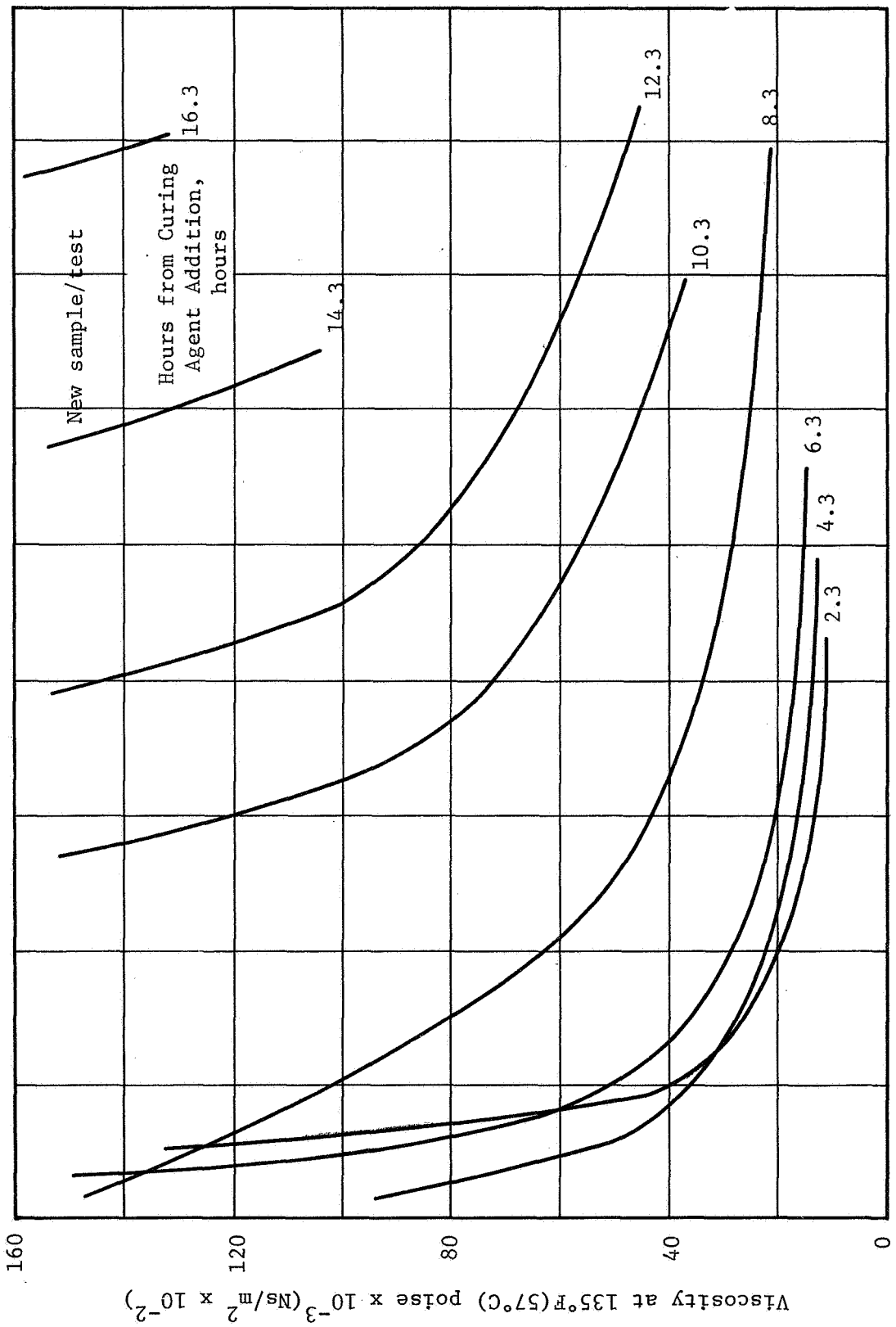
Viscosity Buildup Characteristics of ANB-3254 Propellant Prepared in a 5500-lb (2500 Kg) Vertical Batch Mix

Figure 51



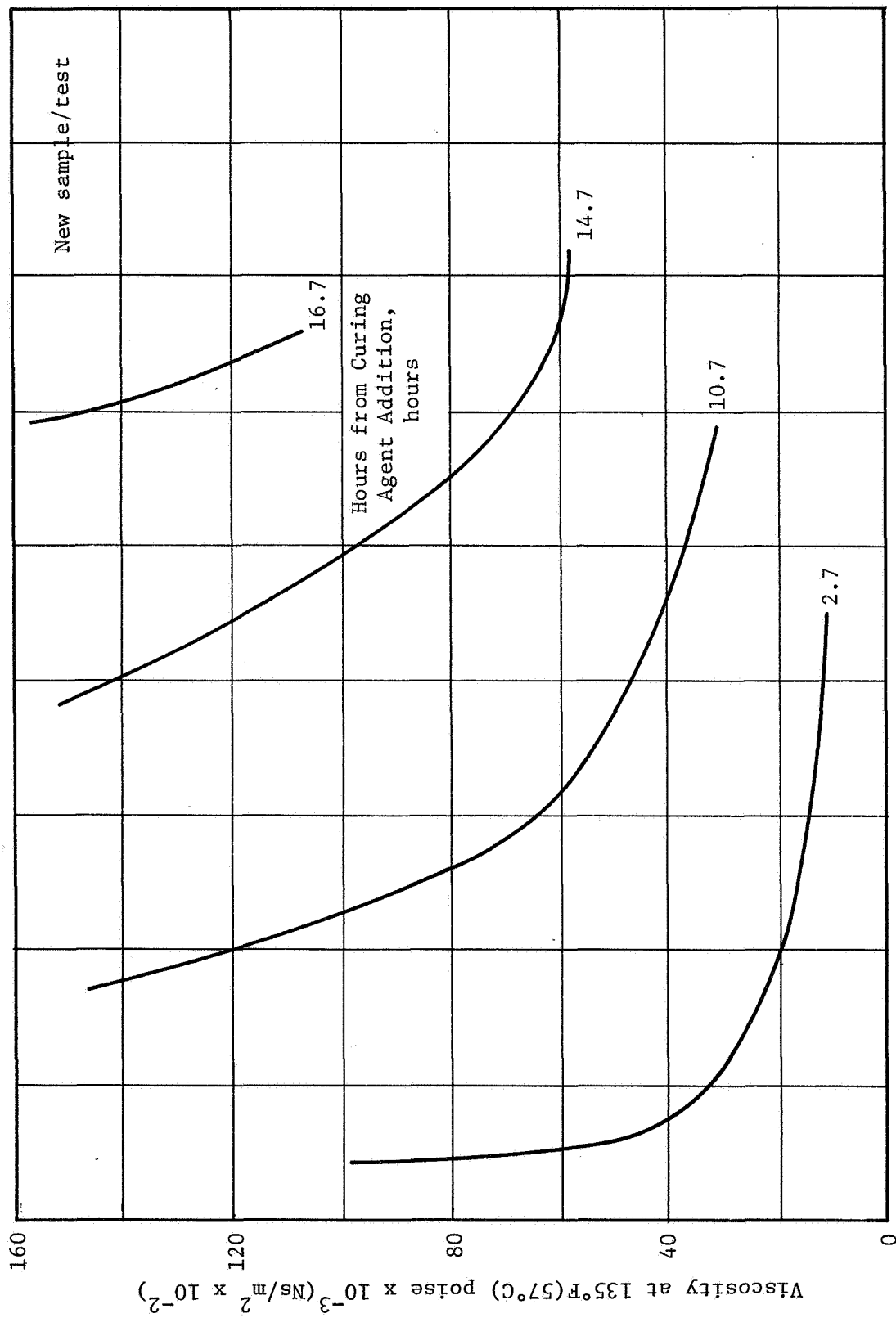
Comparison of Viscosity Build-up Measurements - Continuous Use of One Sample vs New Sample/Test

Figure 52



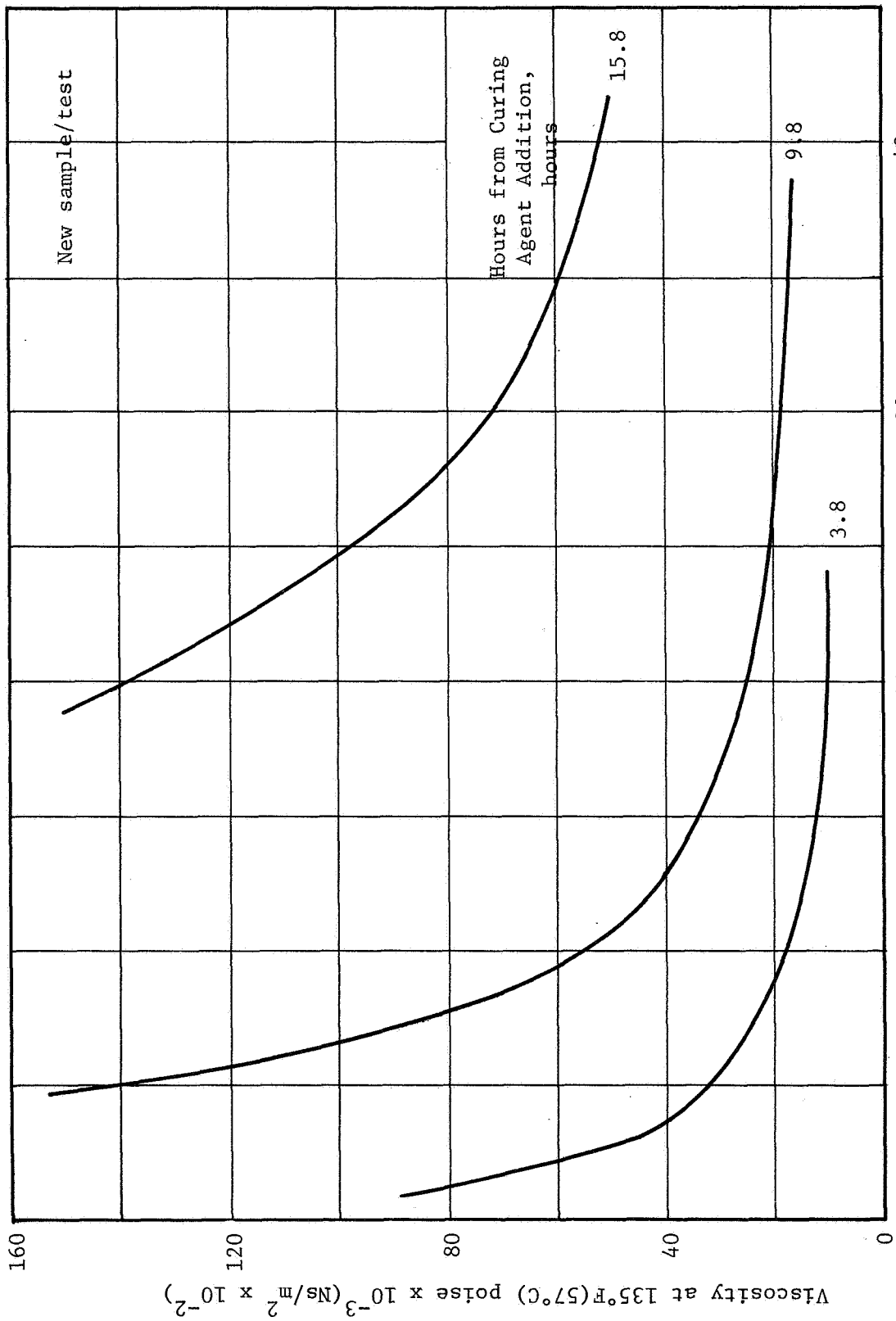
Viscosity Buildup Characteristics in a 5500-lb (2495 Kg) Batch
After 20 Minutes Final Mix

Figure 53



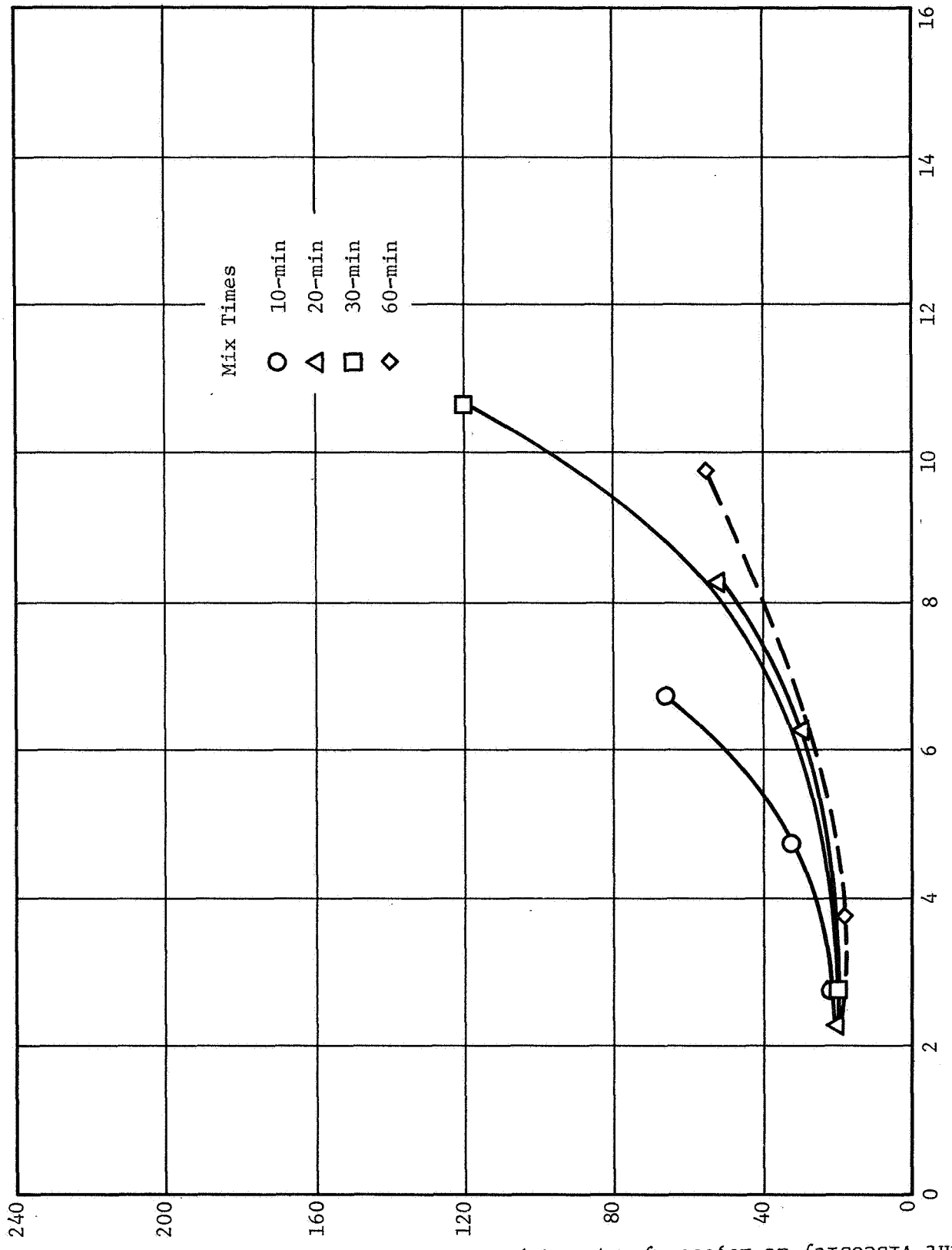
Viscosity Buildup Characteristics in a 5500-lb (2495 Kg) Batch After 30 Minutes Final Mix

Figure 54



Viscosity Buildup Characteristics in a 5500-lb (2500 Kg) Batch After 60 Minutes Final Mix

Figure 55



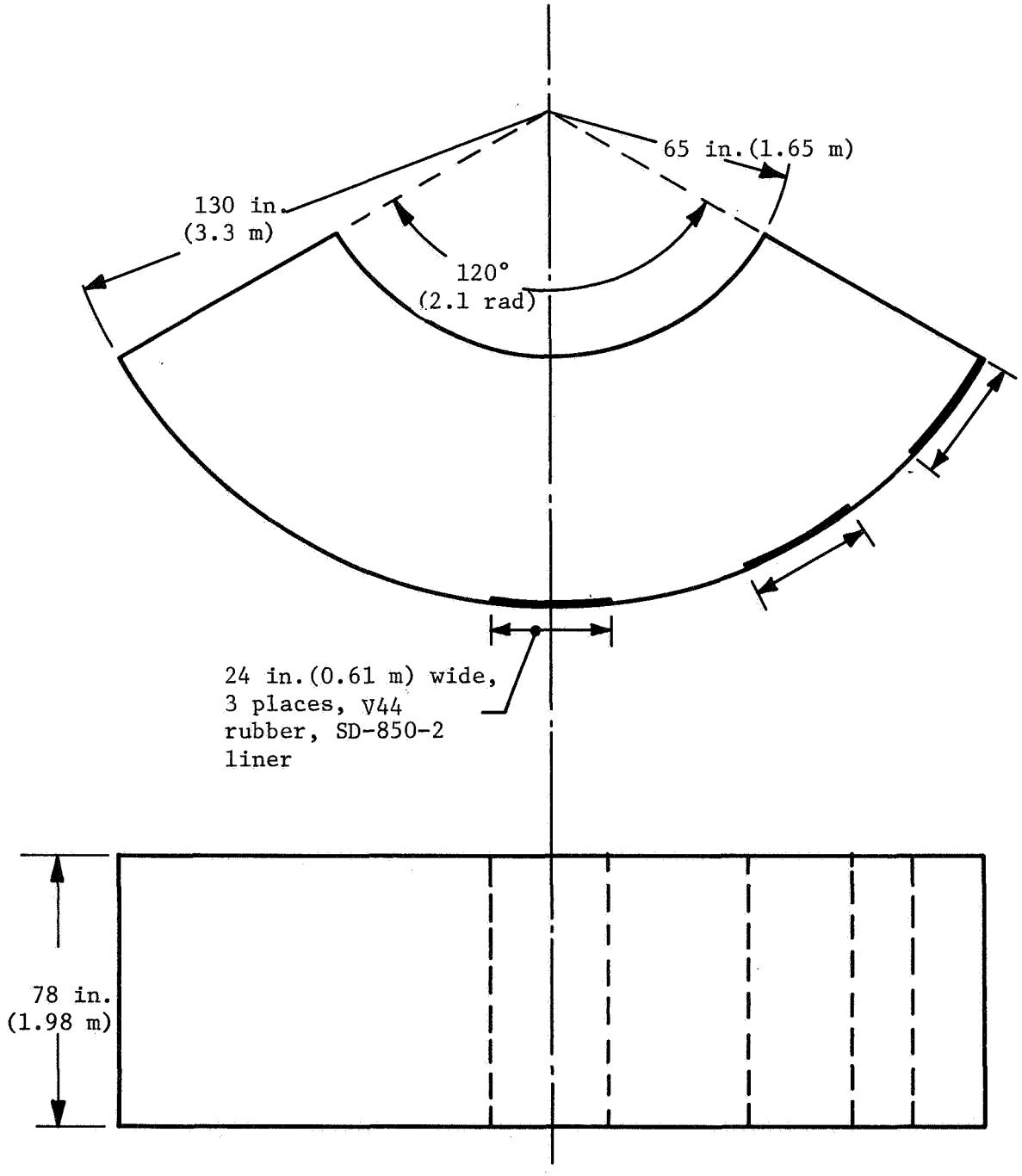
Effect of Final Vacuum Mix Time on Viscosity Buildup of ANB-3254 Propellant

Figure 56

Final Mix Time, min	Shore A Hardness	Mechanical Properties at 77°F (25°C)					
		σ_m psi	(N/cm^2)	ε_m %	ε_b %	E_o psi	(N/cm^2)
10	29	63	(43)	28	32	297	(205)
20	36	66	(46)	25	27	337	(233)
30	36	87	(60)	22	23	487	(336)
60	42	90	(62)	28	32	422	(291)

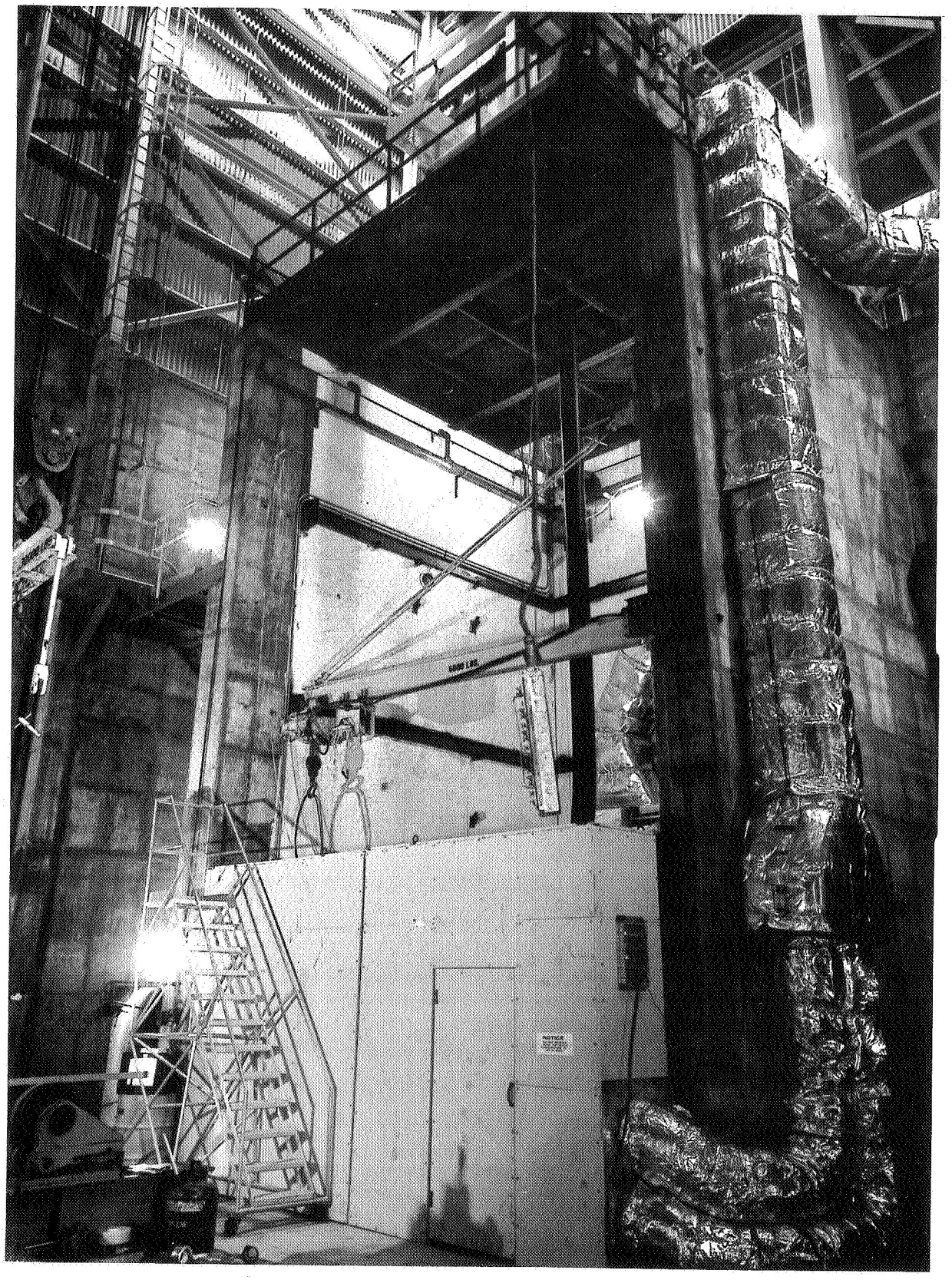
Figure 57

Effect of Vacuum Mix Time On The Mechanical Properties of ANB-3254 Propellant, 5500 lb (2500 Kg) Batch



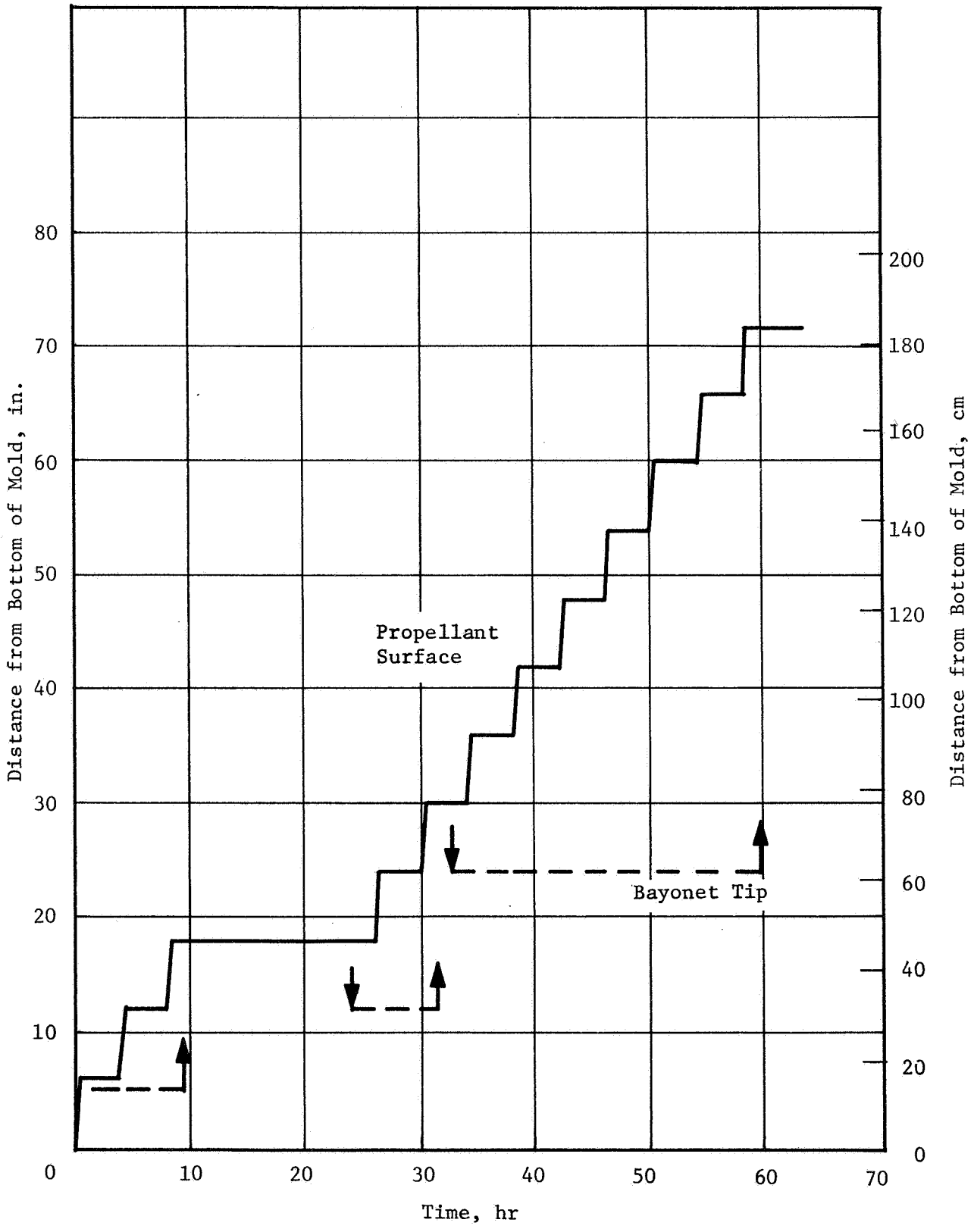
Full-Scale Casting Form

Figure 58



View of Casting Bay

Figure 59



Casting Sequence, First Full-Scale Mold

Figure 60

Batch No. 22D-172	Vacuum Level in Mixer, in. (cm) Hg	Propellant Surface Appearance in Mix Bowl	Rotovisko Viscosity*, poise x 10^{-3} (Ns/m^2 x 10^{-2}) 3 hr	6 hr	10 hr
A	29.5	Normal pseudoplastic	40	71	off-scale
B	24.5	Highly pseudoplastic	46	73	
C	29.5	Normal pseudoplastic	53	140	
D	25.3		123	130	
E	25.0		59	104	
F	24.8		46	off-scale	
G	25.0		off-scale	off-scale	
H	26.6		58	58	
I	26.5		142	off-scale	
J	26.5		off-scale	off-scale	
K	26.8		off-scale	120	
L	26.8		off-scale	off-scale	off-scale

*Viscosity at 135°F (57°C), 5,000 K dynes/cm^2 (500 N/m^2) shear stress, 3, 6, and 10 hr after curing agent addition.

Propellant Flow Characteristics First Full-Scale Mold

Figure 61

Component	Test	Premix Batch No. 22D-172MP-001	Premix Batch No. 22D-172MP-002	Theoretical
Submix	H_2O Content, %	0.065	0.069	0.20 max
	Acid Equivalent/100 g	0.0411	0.0410	0.410
	Refractive Index at 25°C	1.4914	1.4912	1.4911
	Ash Content, %	--	0.45	
Premix I	Liquid Density, g/cm^3	0.970	0.971	0.972
	Ash Content, %	5.69 5.35	5.52	5.37
Premix II	Liquid Density, g/cm^3	1.428	1.434*	1.430
	H_2O Content, %	0.157	0.179	0.25 max
Final Fuel	FeAA Content, %	2.61	2.61	2.62

*After 65.8 lb (29.8 Kg) Al added; original analysis 1.419

Figure 62

Submix and Premix Analyses for Propellant Cast into First Full-Scale Mold

Batch Designation 22D-172	Propellant Premix Batch	Density g/cm^3	DER-332 Content %	Liquid Strand Burning Rate at 600 psig (414 N/cm^2)(27°C) at 80°F	
				in./sec	(cm/s)
A	001	1.745	1.21	0.700	(1.78)
B	001	1.743	1.14	0.699	(1.78)
C	001	1.747	1.24	0.702	(1.78)
D	001	1.743	1.13	0.702	(1.78)
E	001	1.743	1.17	0.711	(1.81)
F	001	1.743	1.23	0.724	(1.84)
$\bar{X}$		1.744	1.19	0.706	(1.79)
S		0.0017	0.047	0.0095	(0.024)
G	002	1.716 Retest 1.745*	1.21	0.747**	(1.90)
H	002	1.746	1.23	0.706**	(1.79)
I	002	1.746*	1.23	0.712**	(1.81)
J***	002	1.747*	1.20	0.724**	(1.84)
K	002	1.747	1.20	0.711**	(1.81)
L	002	1.746	1.24	0.708	(1.80)
$\bar{X}$		1.746	1.22	0.718	(1.82)
S		0.00075	0.017	0.0152	(0.039)
$\bar{X}$		1.745	1.20	0.712	(1.81)
S		0.0017	0.038	0.0138	(0.035)

* Alternative procedure (high-speed centrifuging)
** Average of initial test and retest
***New lot of oxidizer

Uncured Propellant Data for First Full-Scale Mold

Figure 63

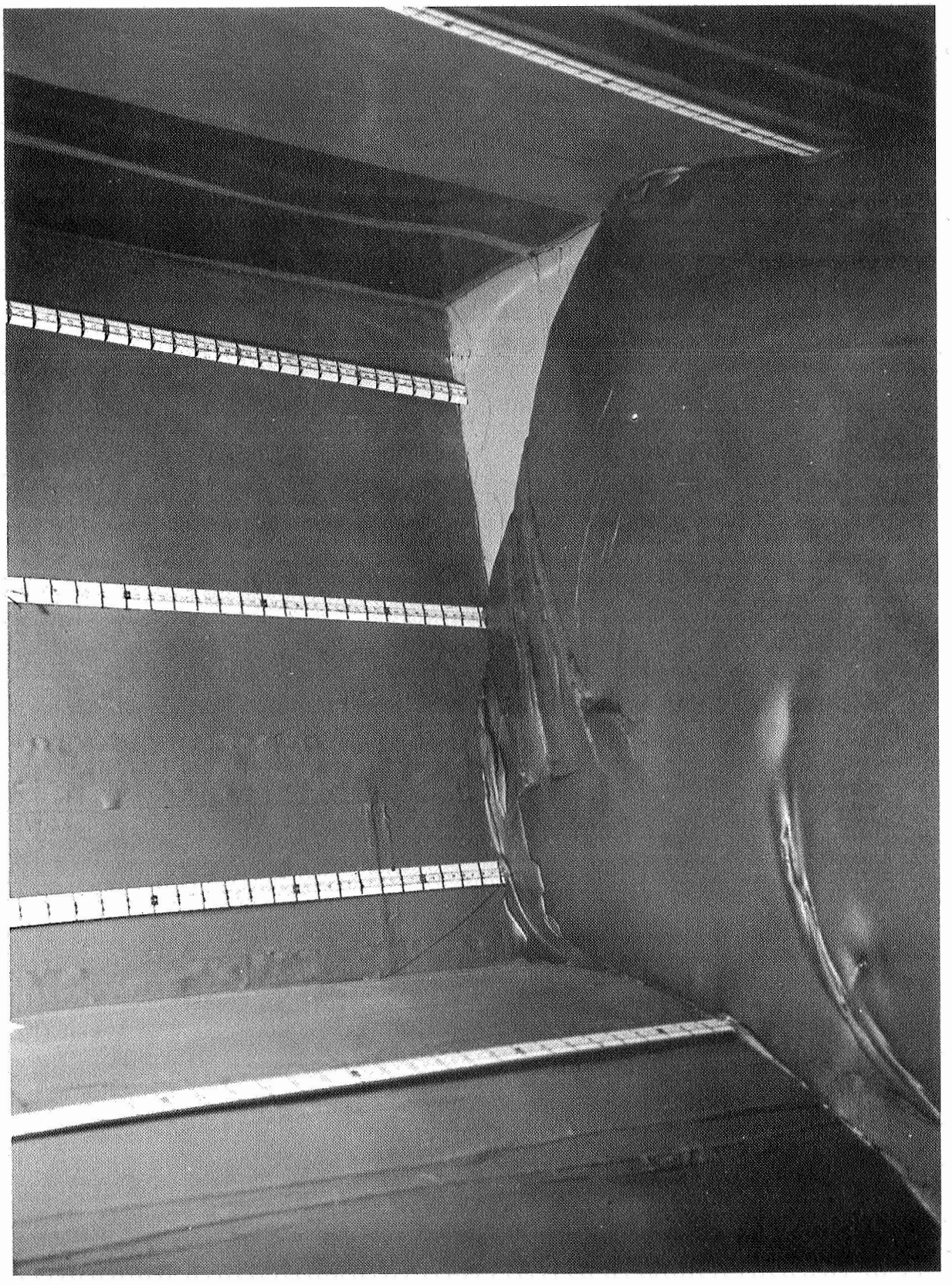
NASA CR 72621

Batch No. 22D-172	Time Between Batches, hr.(1)	Cast Time, min	Time from Curing Agent Addition to End of Cast, hr.
A		23	2.7
B	3.3	19(2)	2.5
C	5.2	29	2.5
D	16.7	23	2.5
E	3.6	28	2.9
F	3.0	21	2.4
G	3.0	26	2.5
H	4.8	25	2.6
I	4.0	31	2.7
J	4.8	34	2.6
K	4.9	34(3)	2.6
L	4.8	36	2.9

(1) Time from start-of-cast to start-of-cast.
(2) Cast terminated prematurely because of diaphragm leakage.
(3) Cast interrupted twice to avoid spillage from mold.

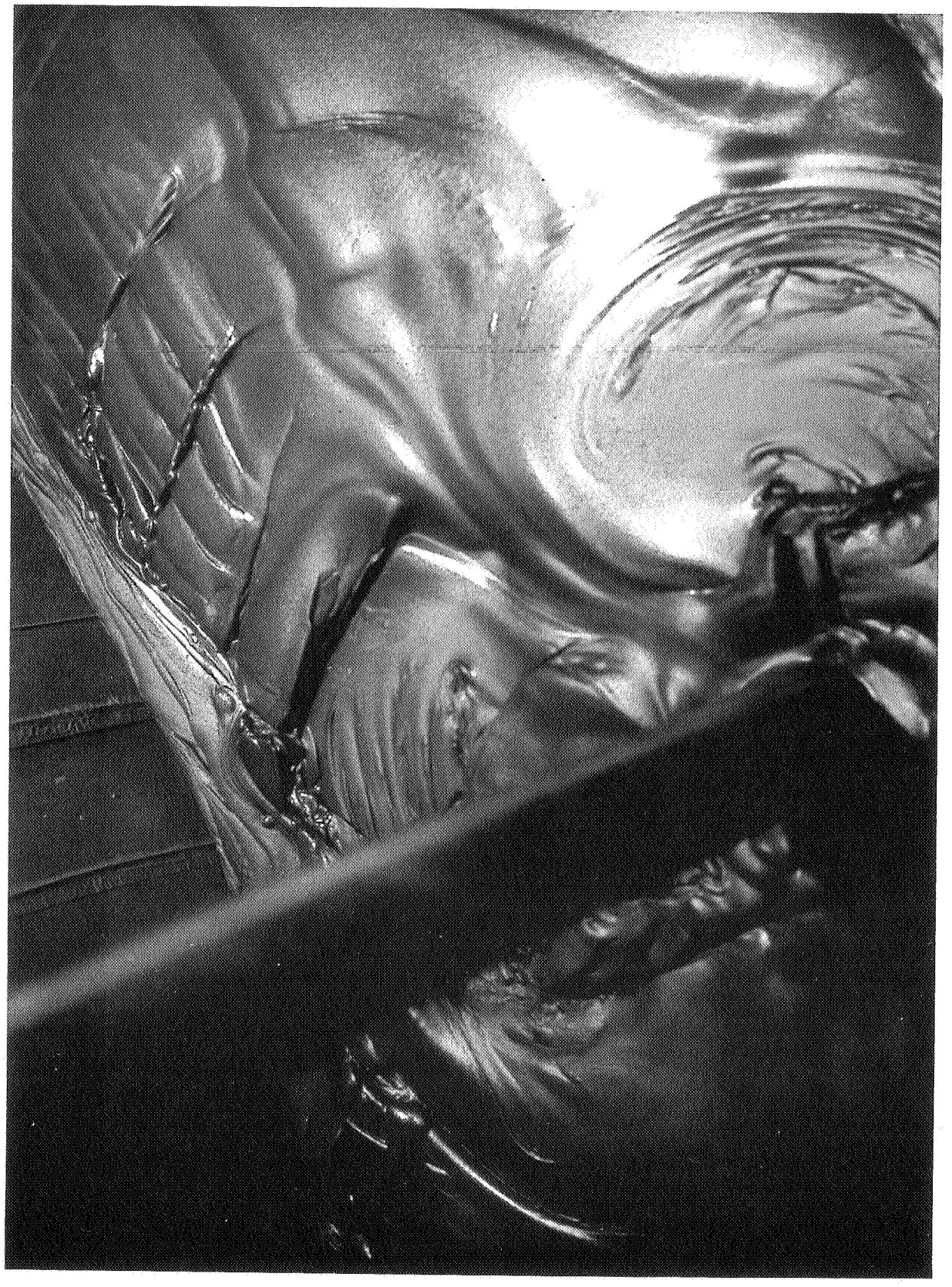
Summary of Process Times for First Full-Scale Mold Casting

Figure 64



Cast Propellant Surface, Batch 22D-172-A

Figure 65



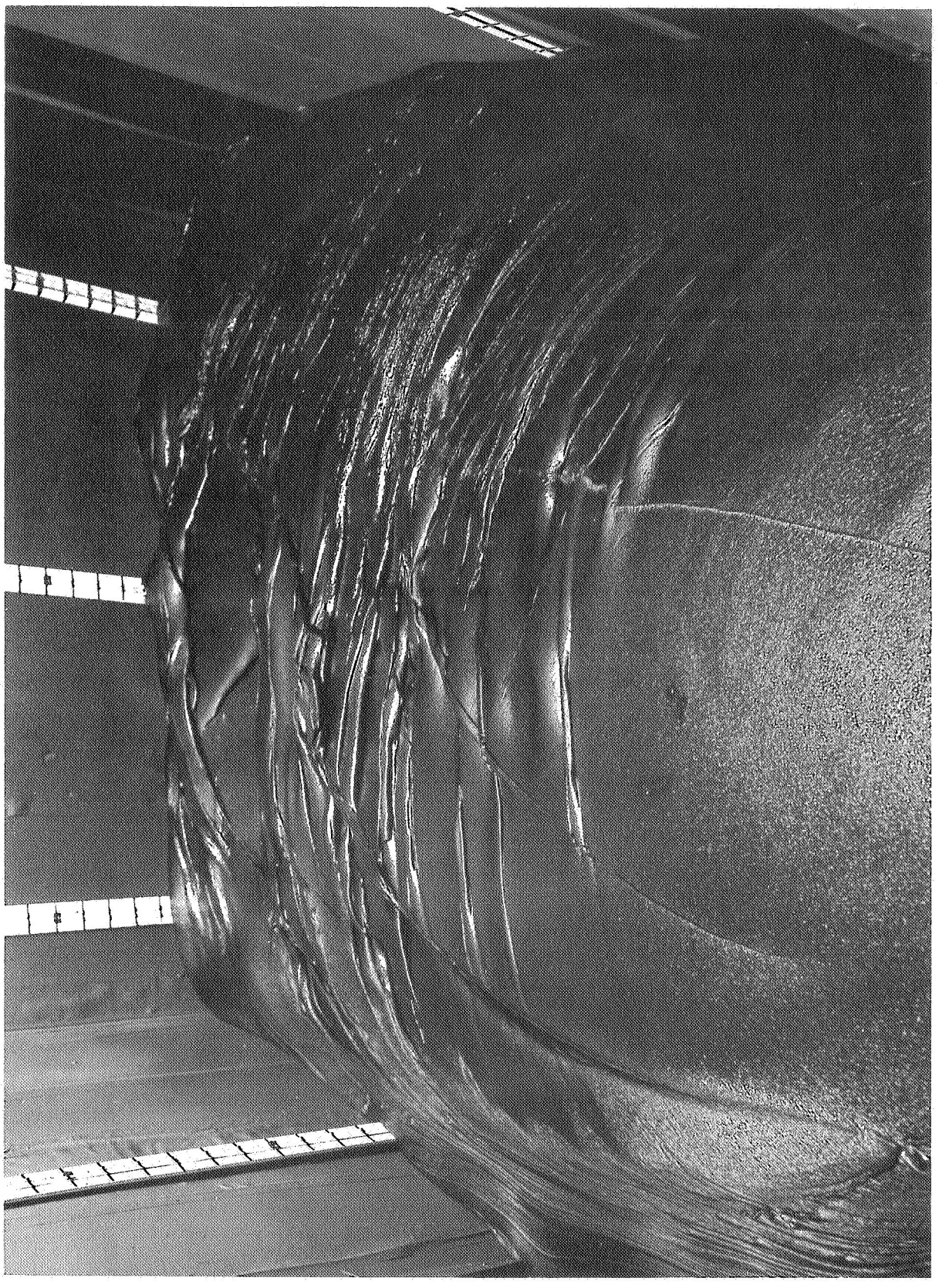
Cast Propellant Surface, Batch 22D-172-B

Figure 66



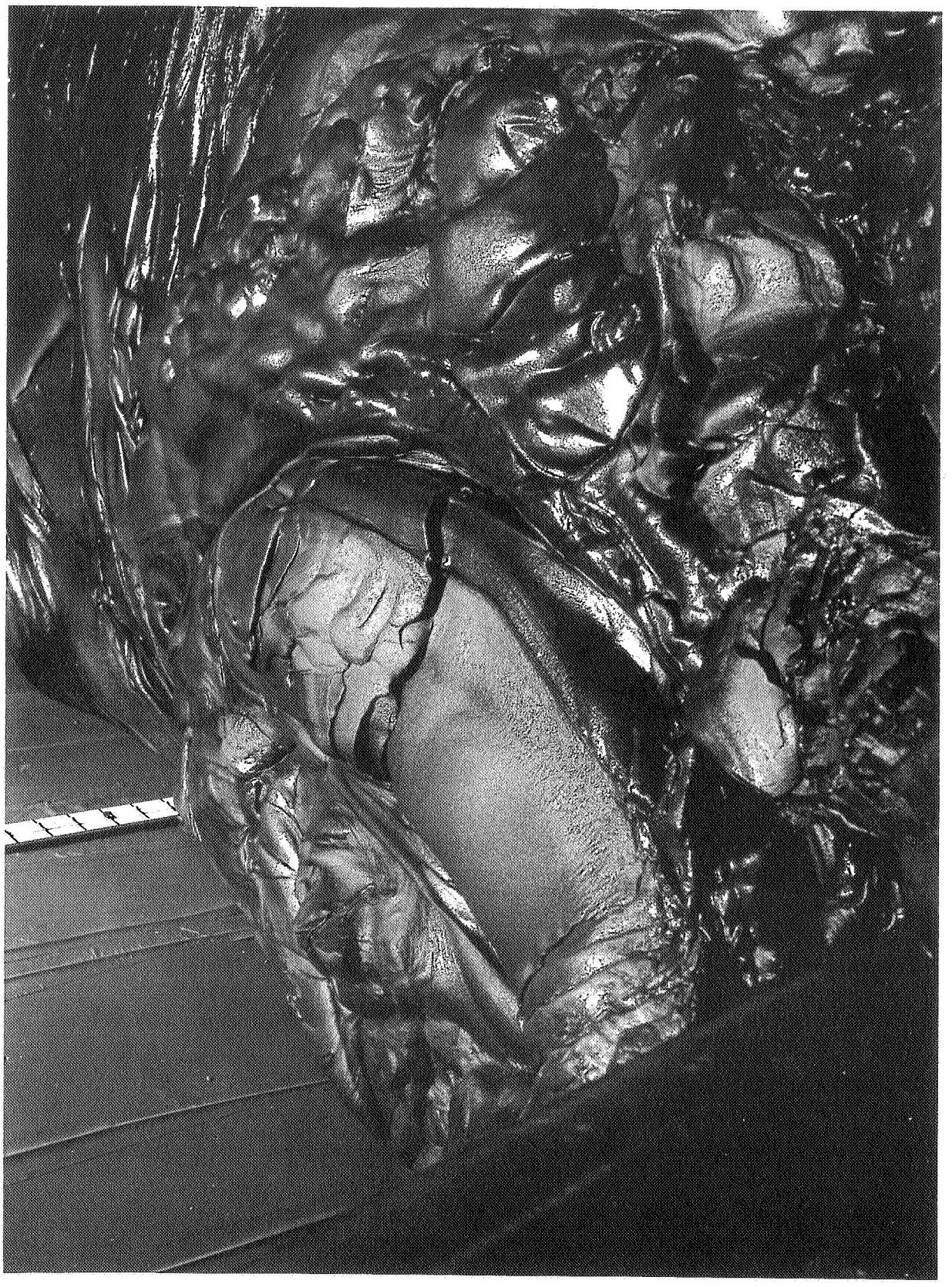
Cast Propellant Surface, Batch 22D-172-D

Figure 67



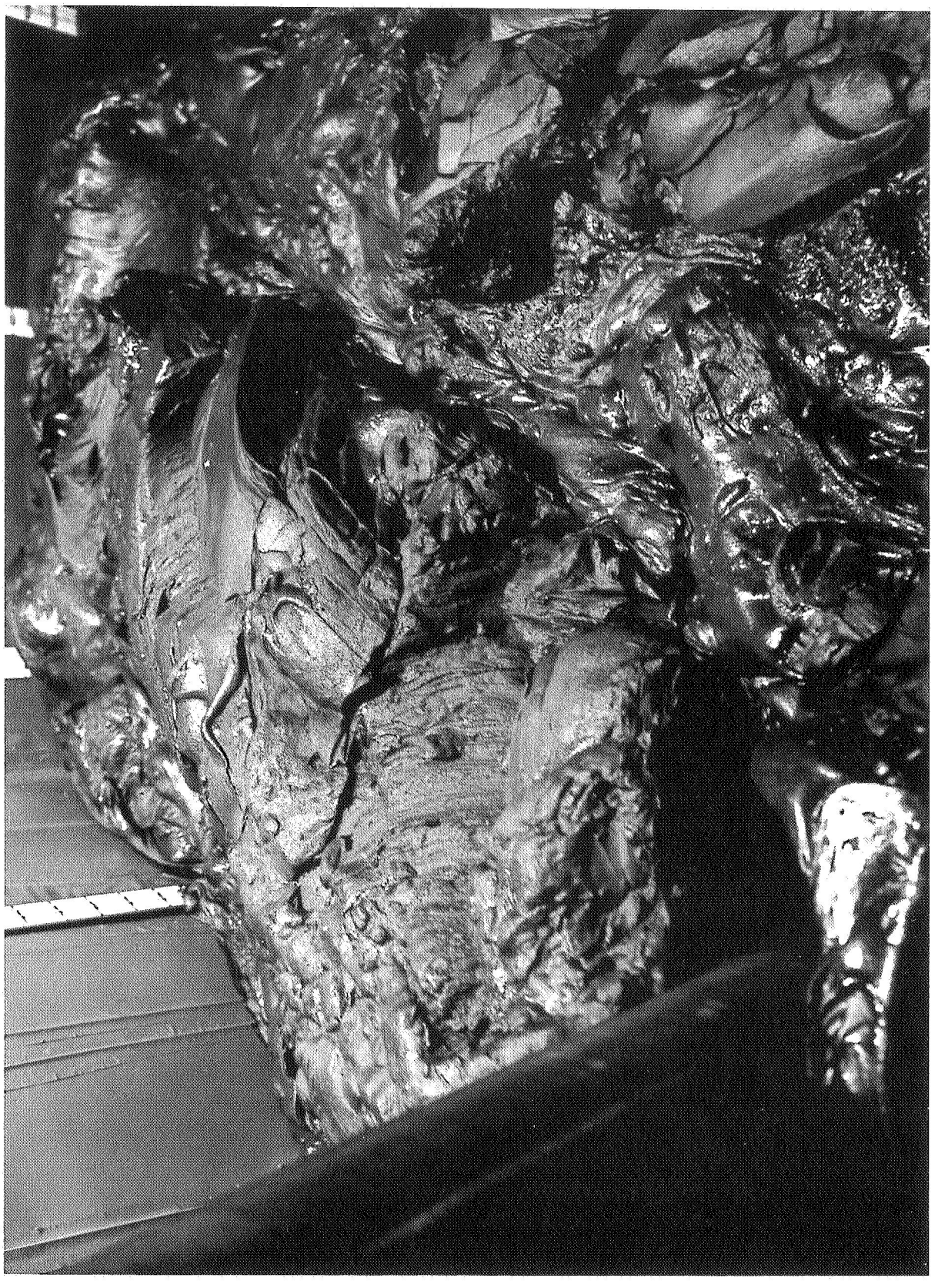
Cast Propellant Surface, Batch 22D-172-E

Figure 68



Cast Propellant Surface, Batch 22D-172-F

Figure 69



Cast Propellant Surface, Batch 22D-172-G

Figure 70



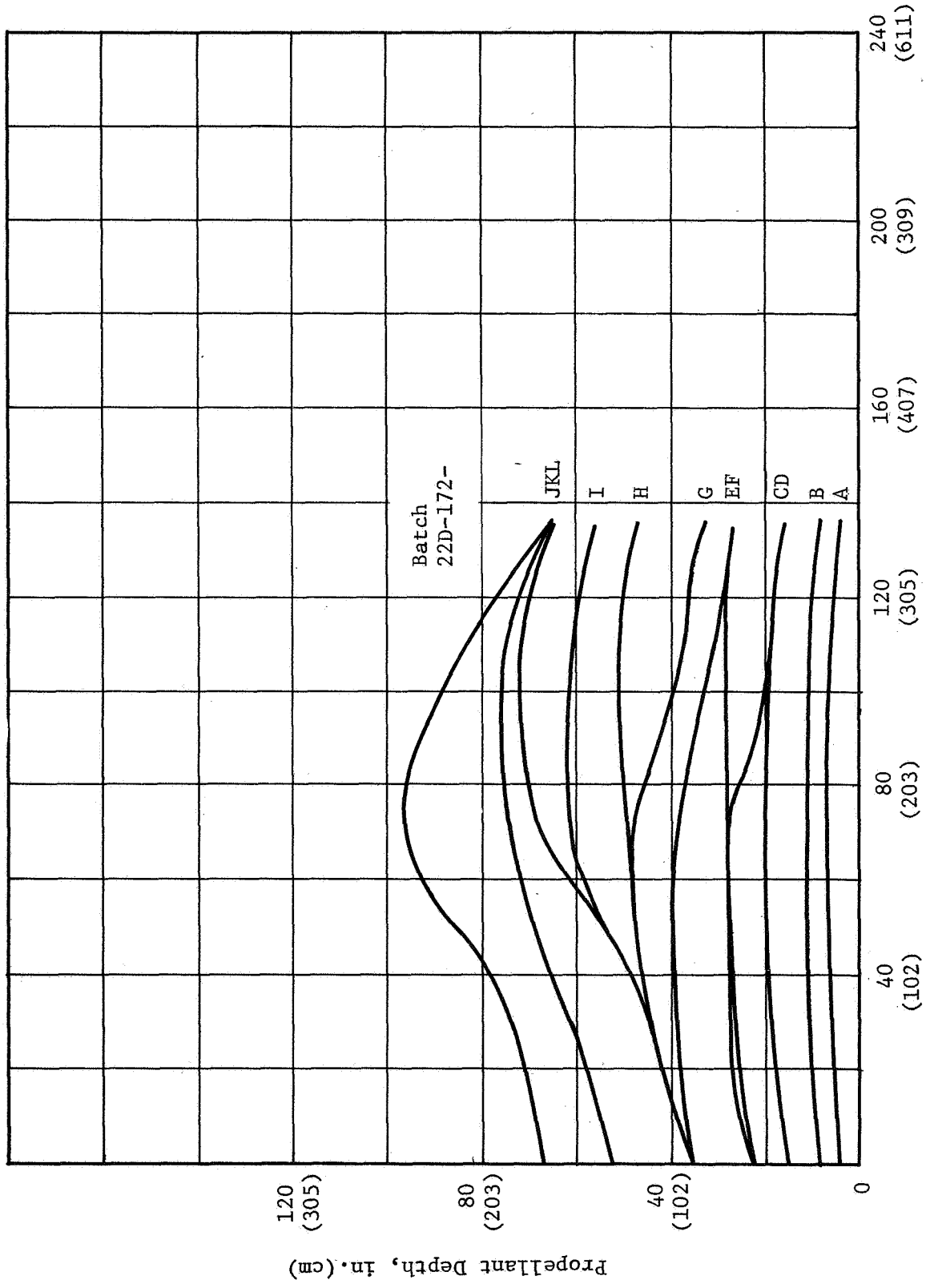
Cast Propellant Surface, Batch 22D-172-I

Figure 71



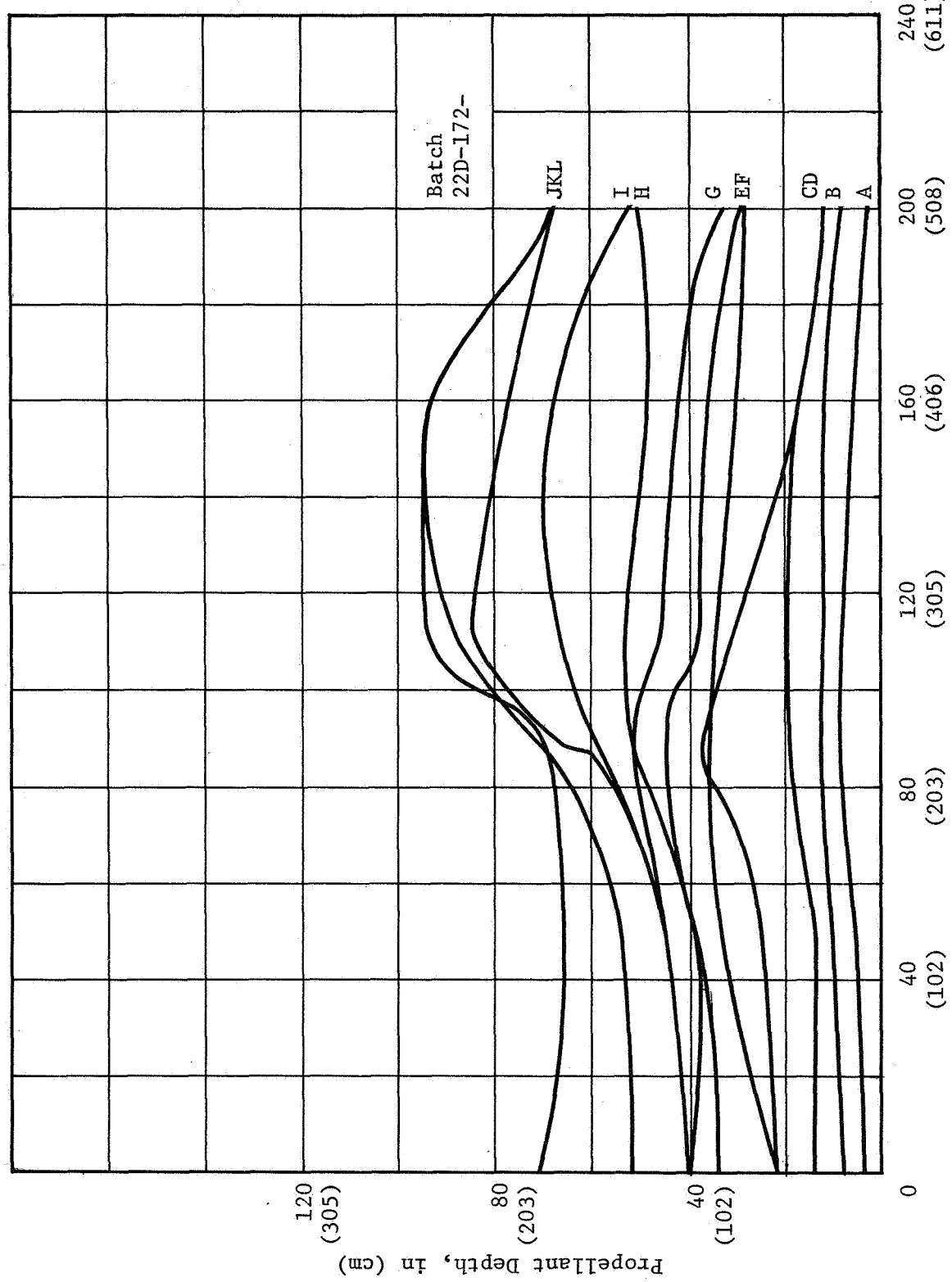
Cast Propellant Surface, Batch 22D-172-J

Figure 72



Batch-to-Batch Surface Contours, Inside Wall,
First Full-Scale Mold

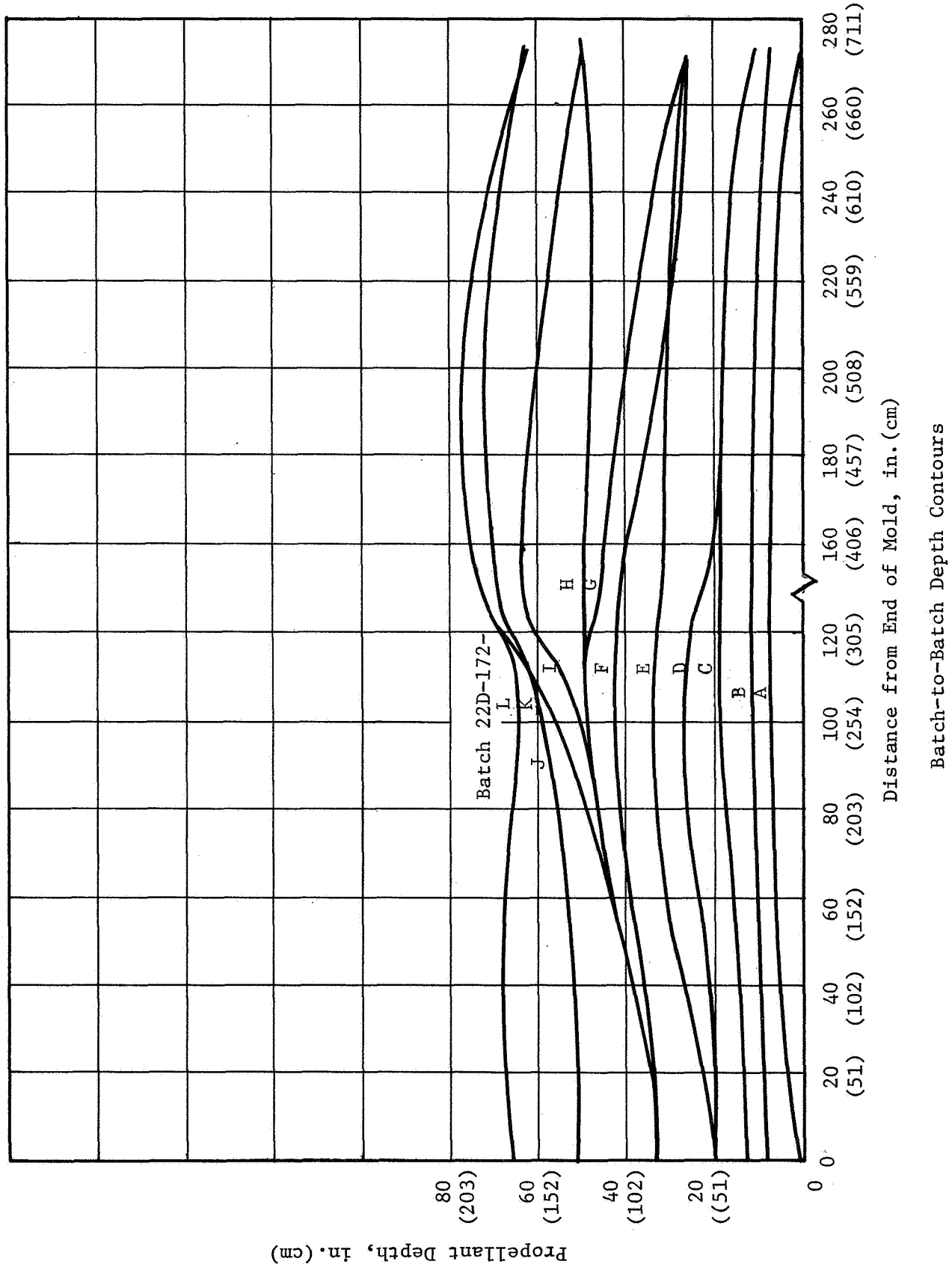
Figure 73



Batch-to-Batch Surface Contours, Midpoints, First Full-Scale Mold

Figure 70

Figure 74



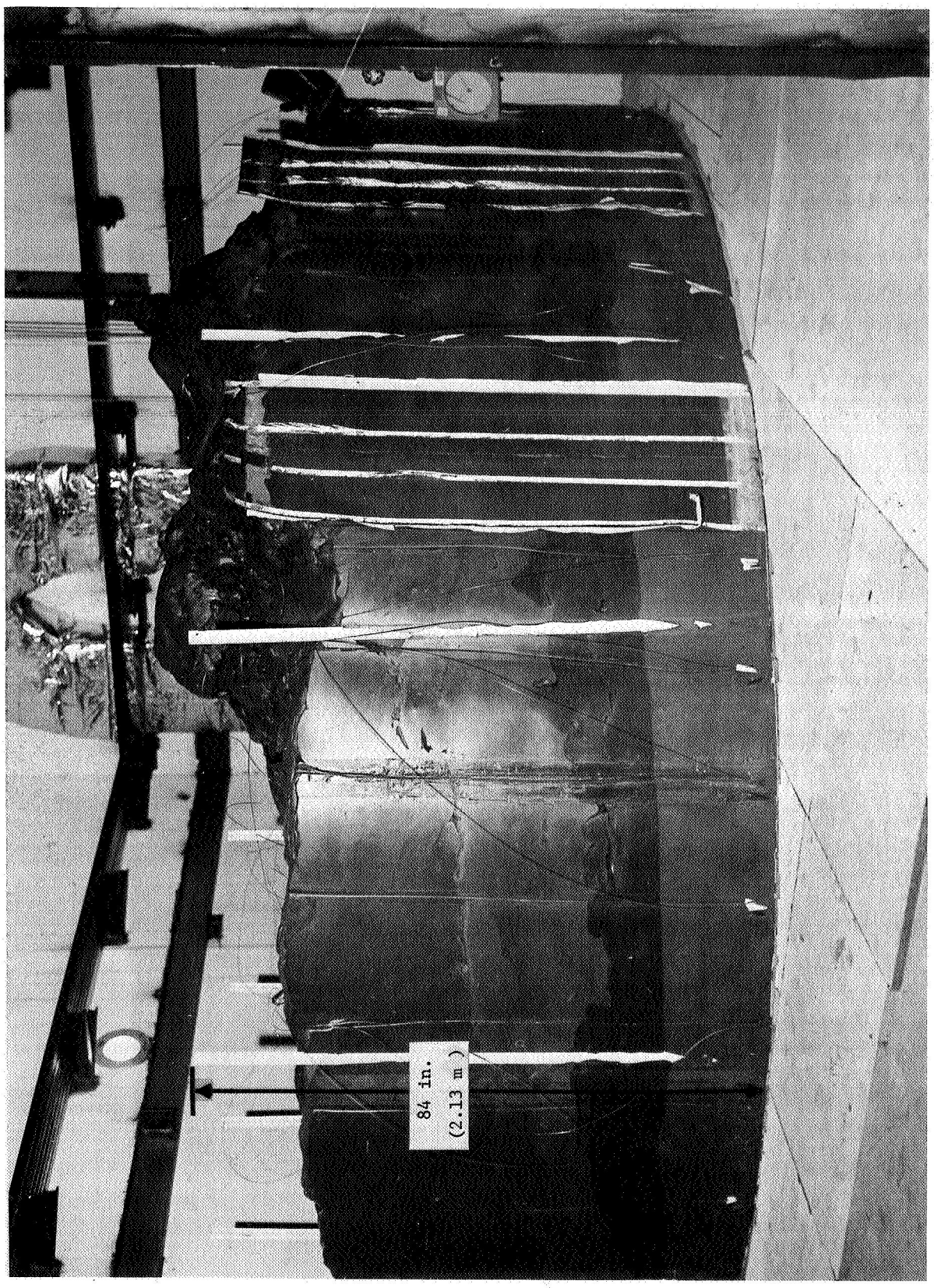
Batch-to-Batch Depth Contours

Figure 75



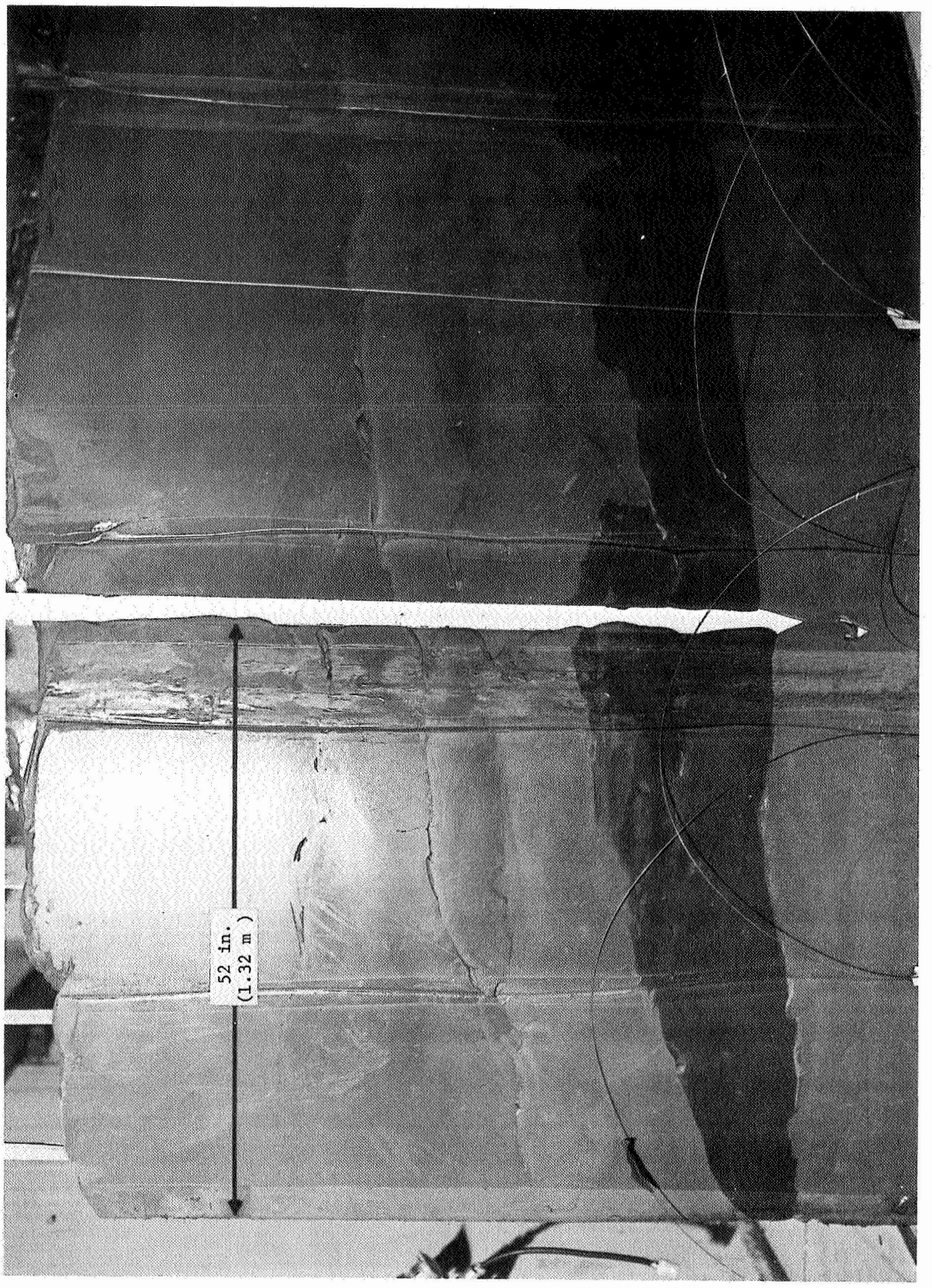
Overhead View, First Full-Scale Mold

Figure 76



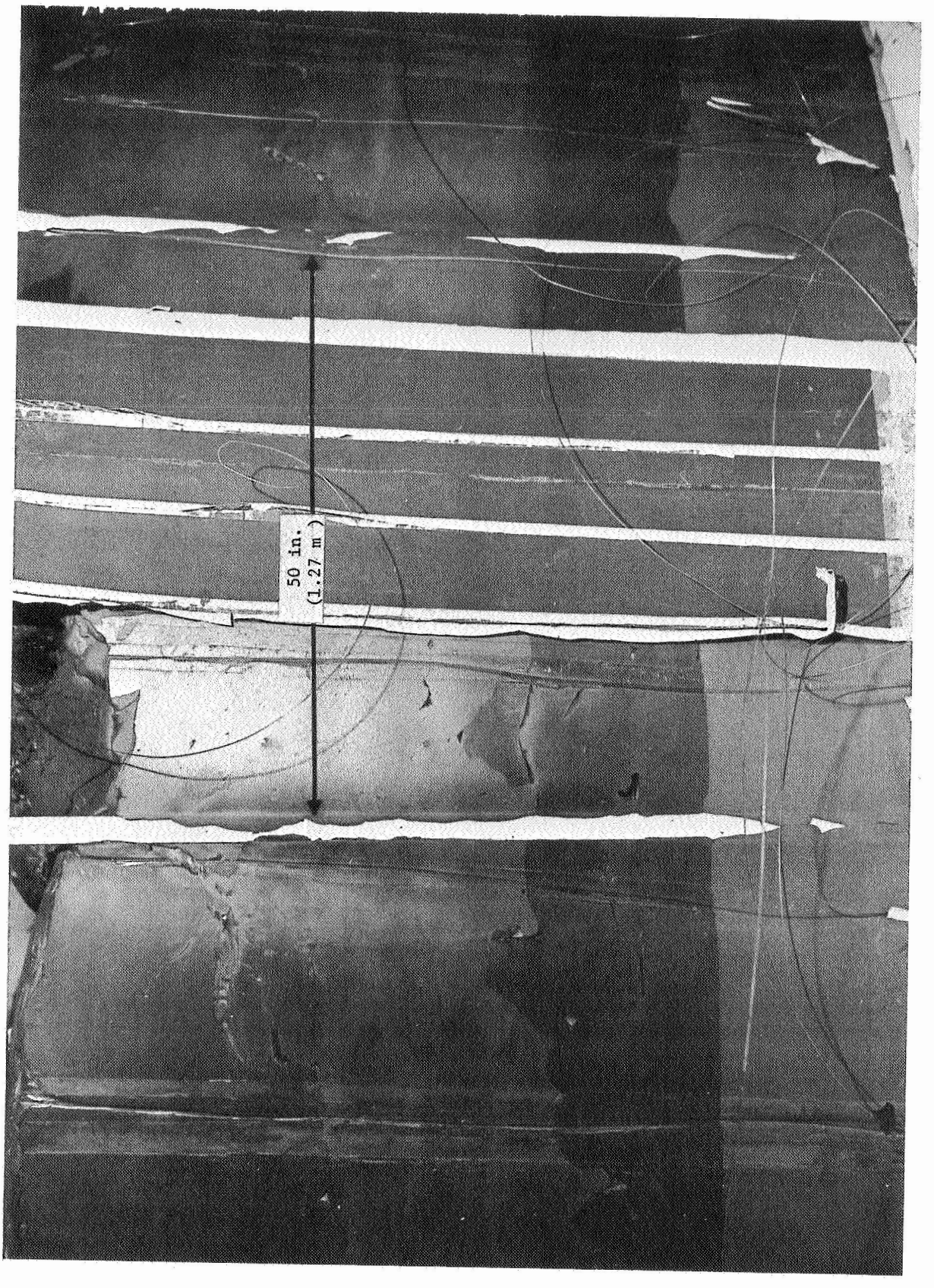
Outside Diameter of Cured Mold, Overall View

Figure 77



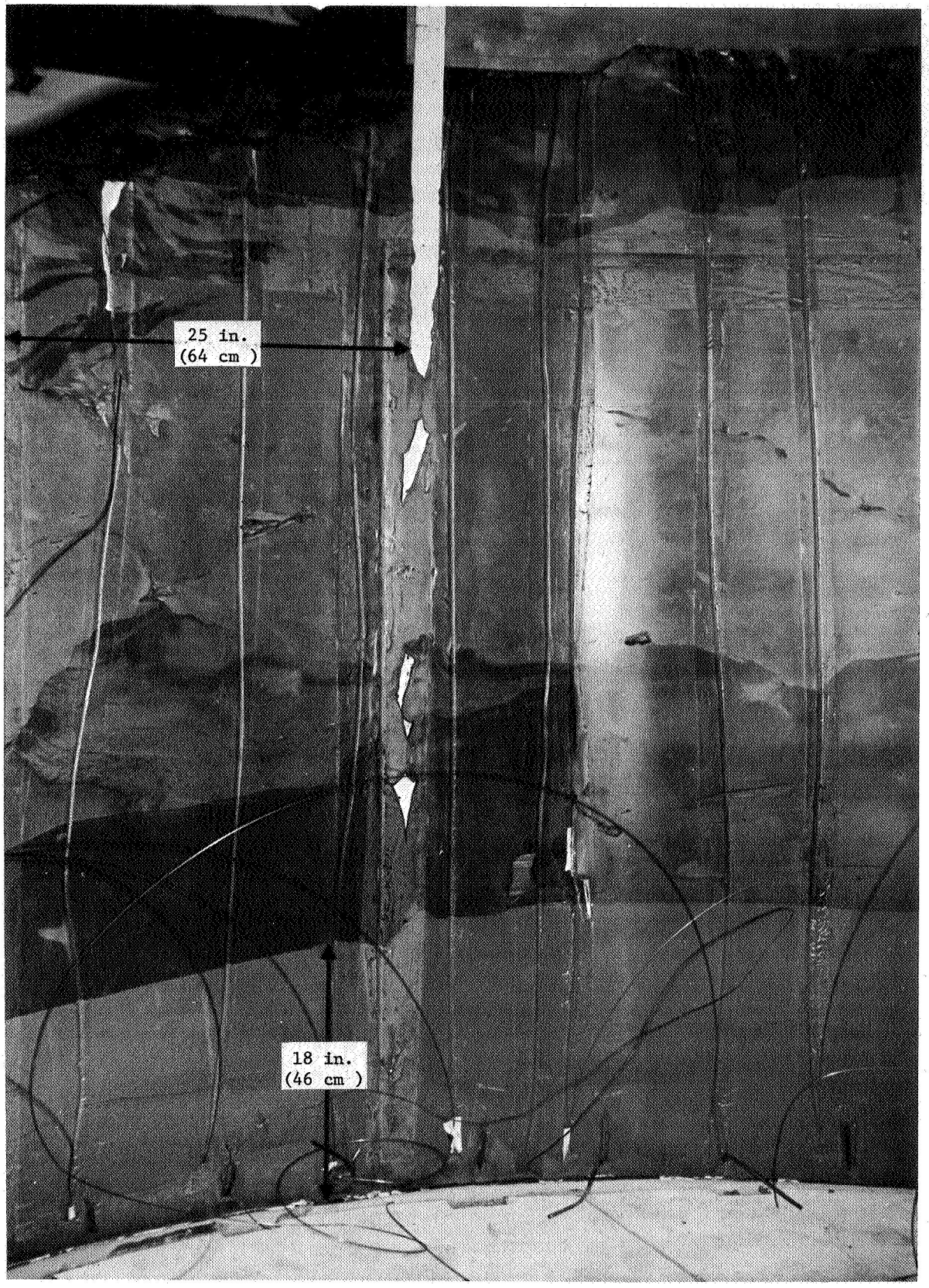
Outside Diameter of Cured Mold, Left Hand View

Figure 78



Outside Diameter of Cured Mold, Central View

Figure 79



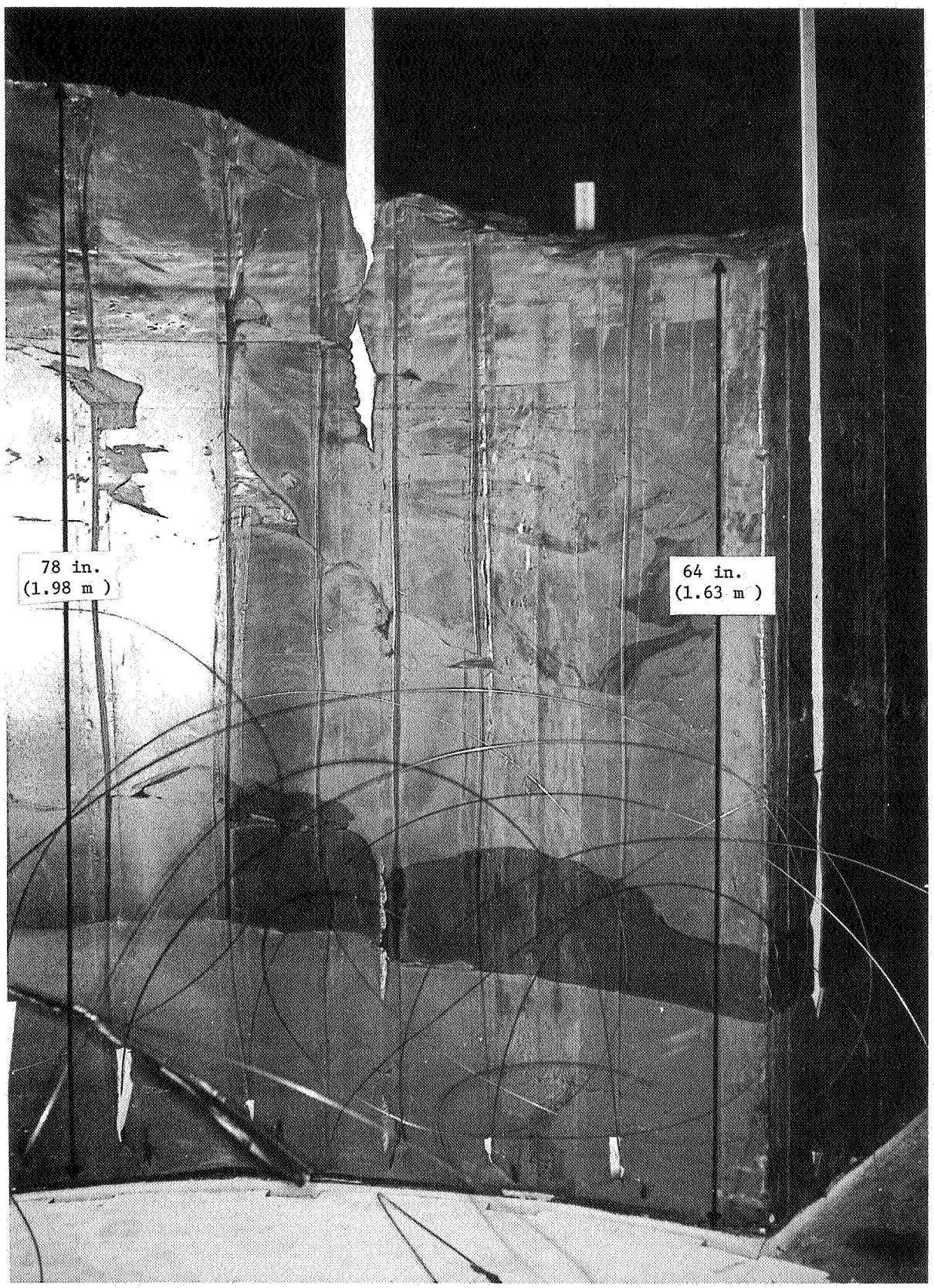
Inside Diameter of Cured Mold, Left Hand View

Figure 80



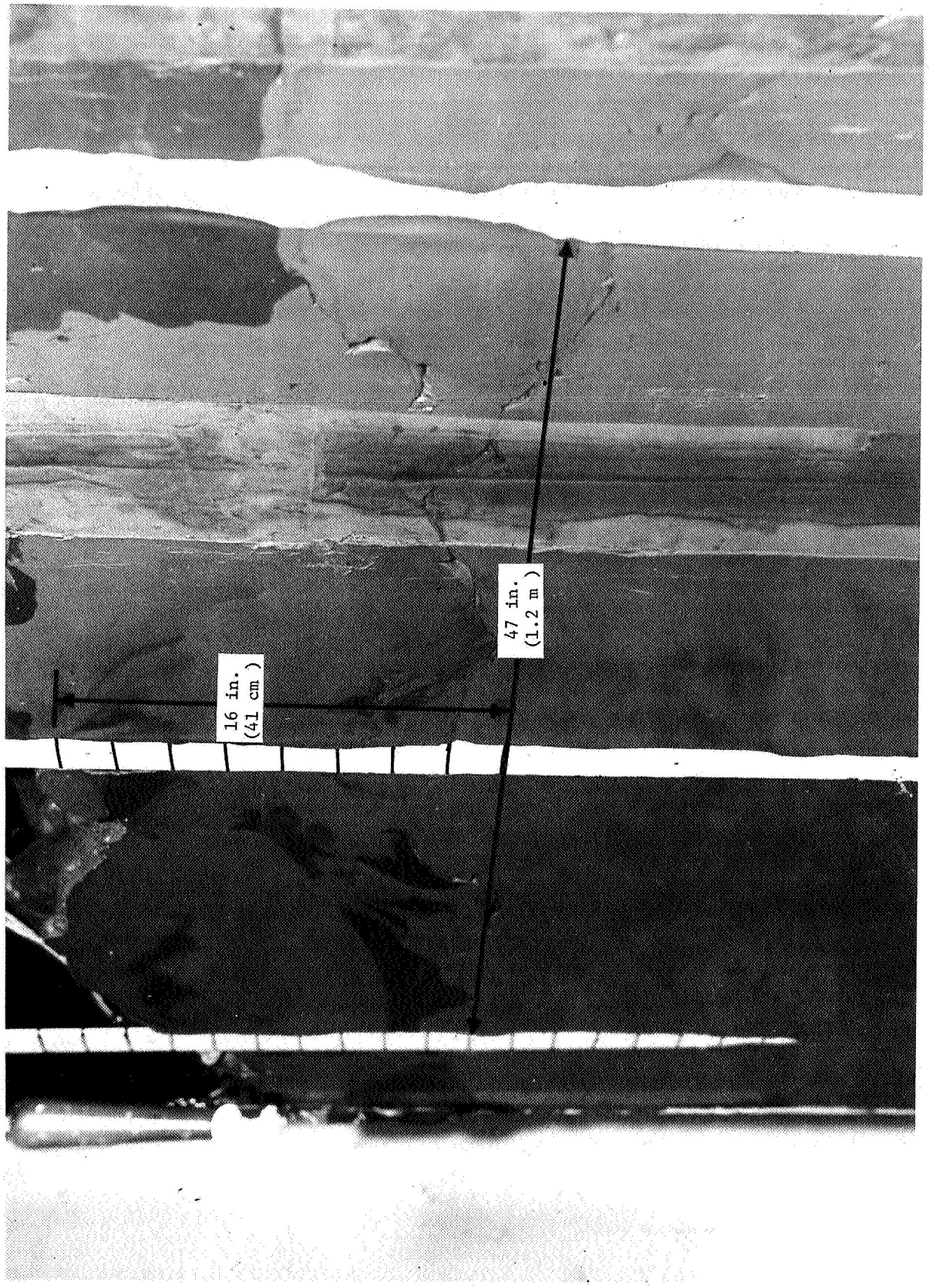
Inside Diameter of Cured Mold, Central View

Figure 81



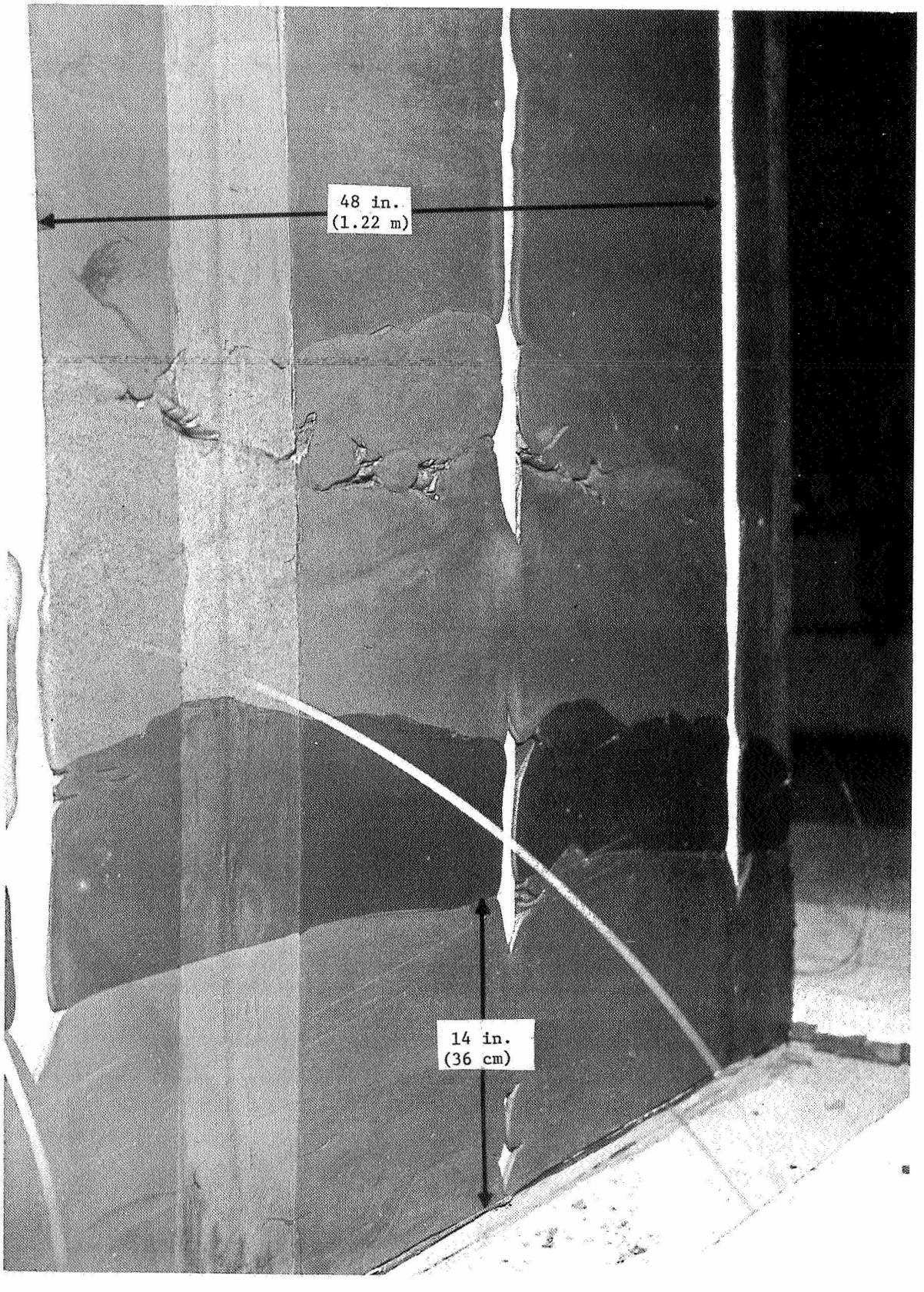
Inside Diameter of Cured Mold, Right Hand View

Figure 82



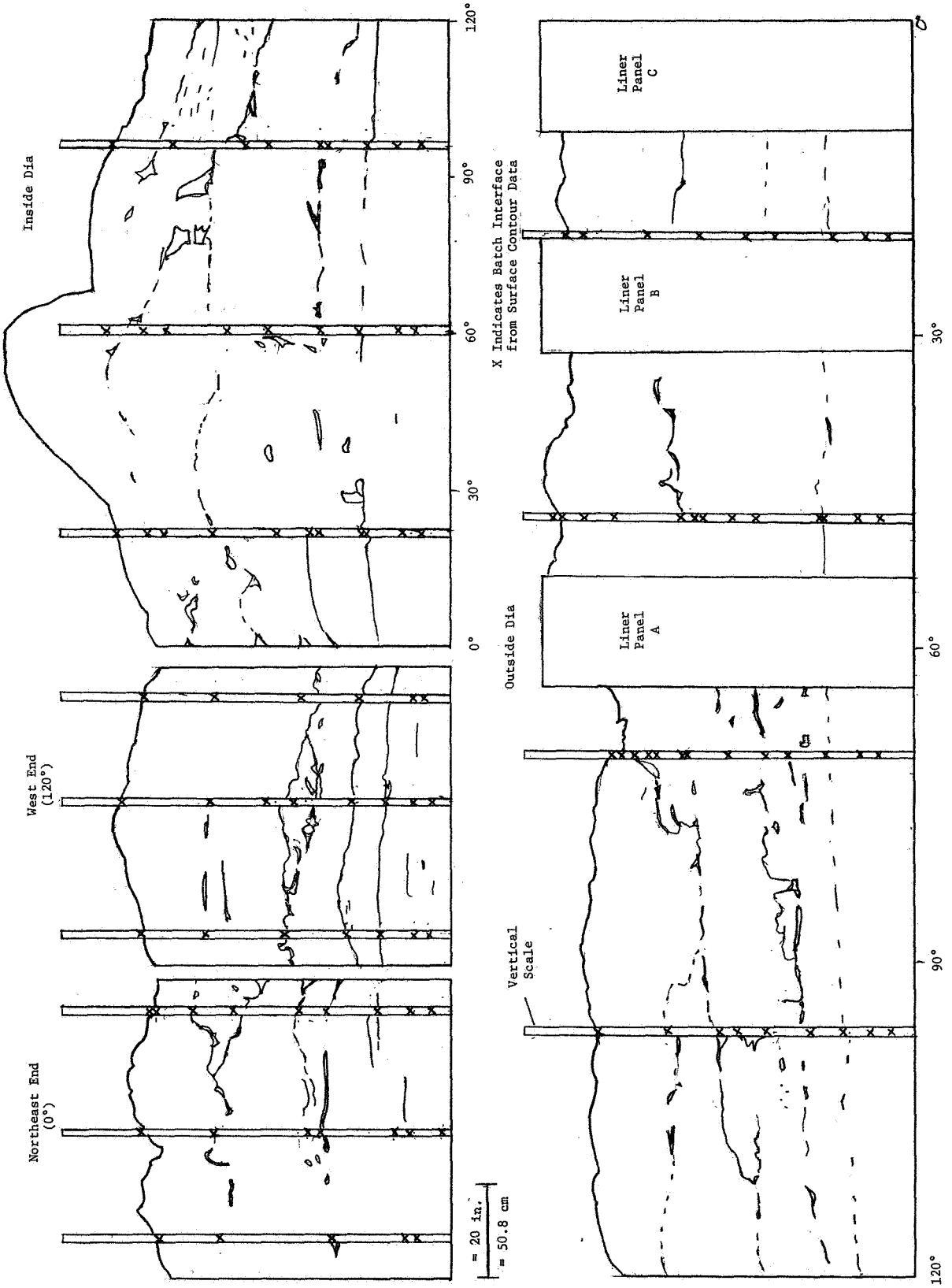
Northeast End of Cured Mold, Upper View

Figure 83



West End of Cured Mold, Lower View

Figure 84



Surface Defects Map, First Full-Scale Mold

Figure 85

Batch No. 22D-172-	Cure Time at 135°F (57°C), days	Mechanical Properties at 77°F (25°C)					
		σ_m, psi	(N/cm^2)	ε_m, %	ε_b, %	E_o, psi	(N/cm^2)
A	15	75	(59)	30	33	387	(267)
	20	85	(59)	29	32	407	(281)
	25	92	(63)	28	31	461	(318)
	40	93	(64)	28	29	437	(302)
B	15	59	(41)	24	26	343	(237)
	20	68	(47)	27	32	346	(239)
	25	79	(54)	21	24	553	(381)
	40	75	(52)	24	26	411	(283)
C	15	83	(57)	23	24	468	(323)
	20	84	(58)	22	22	439	(303)
	25	95	(66)	26	27	472	(326)
	40	103	(71)	24	25	575	(397)
D	15	62	(43)	30	31	270	(186)
	20	63	(43)	26	26	306	(211)
	25	75	(52)	24	25	391	(270)
	40	76	(52)	29	30	346	(239)
E	15	59	(41)	27	28	280	(193)
	20	66	(46)	26	29	321	(222)
	25	77	(53)	27	29	378	(261)
	40	78	(54)	25	26	402	(277)
F	15	64	(44)	26	28	332	(229)
	20	66	(46)	23	23	354	(244)
	25	77	(53)	24	25	418	(288)
	40	72	(50)	24	25	380	(262)
G	15	45	(31)	29	33	211	(146)
	20	52	(36)	27	30	260	(179)
	25	55	(38)	21	22	302	(208)
	40	57	(39)	22	23	313	(216)
H	15	37	(26)	26	28	192	(132)
	20	48	(33)	28	30	210	(145)
	25	47	(32)	21	22	267	(184)
	40	60	(41)	24	25	332	(229)

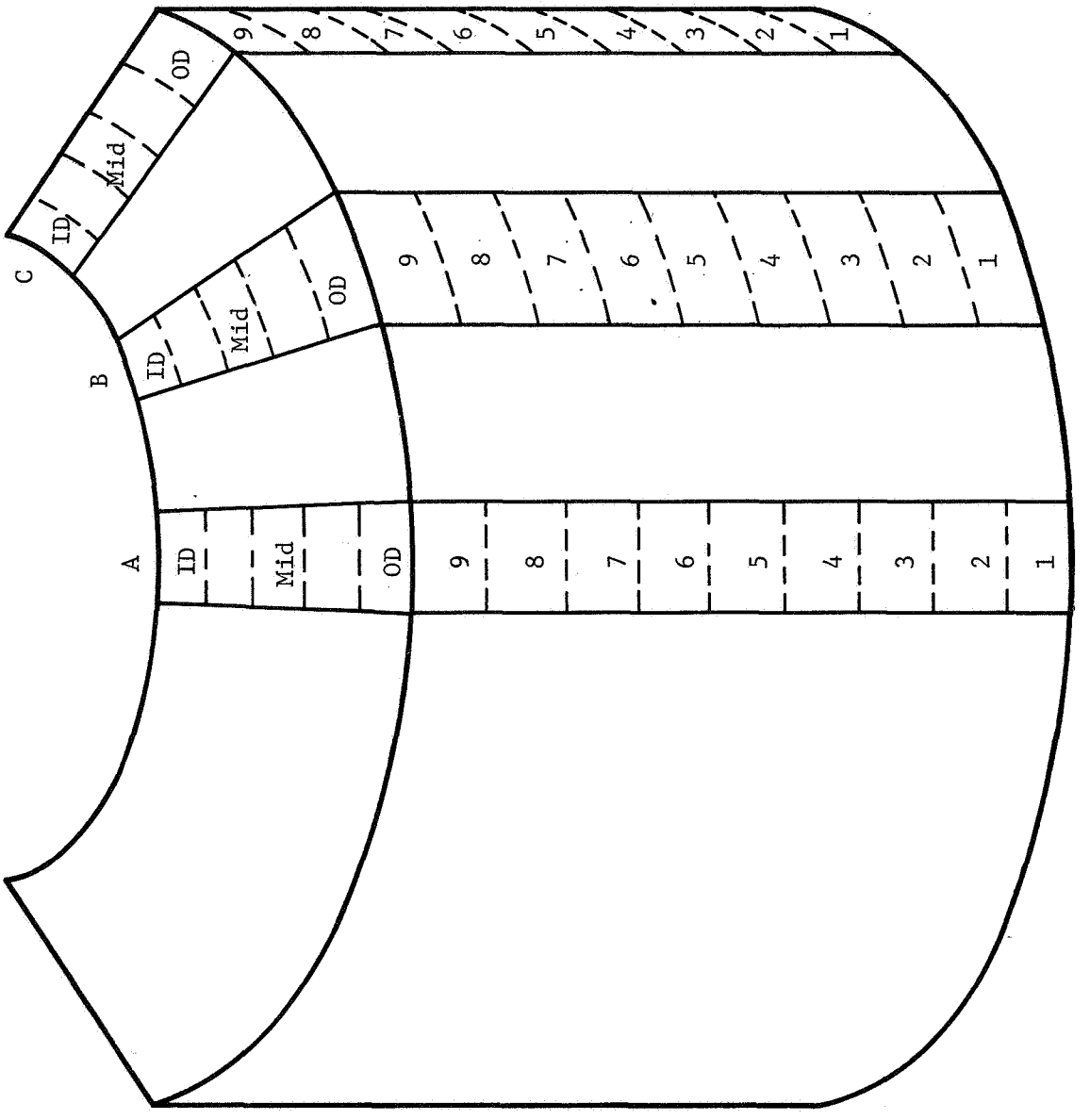
Mechanical Properties from Carton Samples of Propellant Cast into the First Full-Scale Mold

Figure 86, Sheet 1 of 2

Batch No. 22D-172-	Cure Time at 135°F (57°C), days	Mechanical Properties at 77°F (25°C)					
		σ_m, psi	(N/cm^2)	ε_m, %	ε_b, %	E_o, psi	(N/cm^2)
I	15	48	(33)	29	30	217	(150)
	20	52	(36)	28	30	247	(170)
	25	61	(42)	25	28	306	(211)
	40	64	(44)	29	32	301	(208)
J	15	63	(43)	22	25	372	(257)
	20	78	(54)	25	27	428	(295)
	25	89	(61)	25	28	483	(333)
	40	83	(57)	25	26	431	(297)
K	15	49	(34)	25	26	265	(183)
	20	52	(36)	25	25	254	(175)
	25	65	(45)	22	23	372	(257)
	40	65	(45)	26	26	332	(229)
L	15	49	(34)	26	30	271	(187)
	20	55	(38)	28	29	264	(182)
	25	59	(41)	20	20	346	(239)
	40	61	(42)	23	25	332	(229)

Mechanical Properties from Carton Samples of Propellant Cast into the First Full-Scale Mold

Figure 86, Sheet 2 of 2



Sample Locations for the First Full-Scale Mold

Figure 87

Sample Location	Orientation	Mechanical Properties at 77°F (25°C) σ_m, psi	(N/cm^2)	ε_m, %	ε_b, %	E_o, psi	(N/cm^2)	Bond Strength at 77°F (25°C) Tensile psi	(N/cm^2)	Shear psi	(N/cm^2)	Burning Rate at 80°F (27°C) and 600 psig (414 N/cm^2) in./sec	(cm/s)
OD-1	Vertical	114	(79)	22	26	782	(539)					0.696	(1.77)
	Horizontal	103	(71)	28	31	511	(352)	95*	(66)	88*	(61)	0.742	(1.88)
OD-2	Vertical	109	(75)	22	24	701	(484)					0.648	(1.65)
	Horizontal	98	(68)	19	20	763	(526)	96	(66)	76*	(52)	0.731	(1.86)
OD-3	Vertical	85	(59)	20	22	601	(415)					0.757	(1.92)
	Horizontal	83	(57)	22	24	551	(380)	88	(61)	74	(51)	0.708	(1.80)
OD-4	Vertical	64	(44)	13	13	656	(453)					0.713	(1.81)
	Horizontal	77	(53)	13	15	942	(650)	97	(67)	64*	(44)	0.743	(1.89)
OD-5	Vertical	66	(46)	16	19	704	(485)					0.738	(1.87)
	Horizontal	50	(34)	16	17	492	(339)	79	(55)	Bond Failure		0.728	(1.85)
OD-6	Vertical	61	(42)	17	18	564	(389)					0.702	(1.78)
	Horizontal	62	(43)	17	19	575	(397)	81	(56)	62*	(43)	0.713	(1.81)
OD-7	Vertical	60	(41)	20	25	468	(323)					0.705	(1.79)
	Horizontal	59	(41)	20	23	466	(322)	76	(52)	48*	(33)	0.688	(1.75)
OD-8	Vertical	70	(48)	17	20	686	(473)					0.719	(1.83)
	Horizontal	73	(50)	19	21	577	(398)	57*	(39)	35*	(24)	0.740	(1.88)
OD-9	Vertical	76	(52)	17	20	721	(497)					0.726	(1.84)
	Horizontal	63	(43)	21	23	463	(319)	Bond Failure				0.683	(1.73)

* Failure at liner-to-propellant interface of at least one sample

Properties of Specimens from First Full-Scale Mold

Sample Location	Orientation	Mechanical Properties at 77°F (25°C) σ_m, psi	(N/cm^2)	ε_m, %	ε_b, %	E_o, psi	(N/cm^2)	Burning Rate at 80°F (27°C) and 600 psig (414 N/cm^2) in./sec	(cm/s)
M-1	Vertical	95	(66)	16	17	662	(457)	0.734	(1.86)
	Horizontal	118	(81)	19	22	981	(677)	0.775	(1.97)
M-2	Vertical	65	(45)	16	21	693	(478)	0.730	(1.85)
	Horizontal	63	(43)	19	25	516	(356)	0.709	(1.80)
M-3	Vertical	100	(69)	18	20	874	(603)	0.744	(1.89)
	Horizontal	71	(49)	13	15	865	(597)	0.726	(1.84)
M-4	Vertical	75	(52)	20	23	535	(369)	0.701	(1.78)
	Horizontal	77	(53)	18	20	660	(455)	0.714	(1.81)
M-5	Vertical	65	(45)	15	18	653	(450)	0.715	(1.82)
	Horizontal	65	(45)	17	19	605	(417)	0.716	(1.82)
M-6	Vertical	72	(50)	19	21	588	(406)	0.726	(1.84)
	Horizontal	76	(52)	19	23	656	(453)	0.742	(1.88)
M-7	Vertical	68	(47)	21	25	472	(326)	0.730	(1.85)
	Horizontal	90	(62)	15	16	835	(576)	0.738	(1.87)
M-8	Vertical	72	(50)	19	26	601	(415)	0.718	(1.82)
	Horizontal	71	(49)	20	25	551	(380)	0.711	(1.81)
M-9	Vertical	70	(48)	20	23	542	(374)	0.720	(1.83)
	Horizontal	71	(49)	18	23	597	(412)	0.706	(1.79)

Mechanical Properties and Burning Rates of Propellant Specimens
Taken from the First Full-Scale Mold (Section A)

Sample Location	Orientation	Mechanical Properties at 77°F (25°C) σ_m, psi	(N/cm^2)	ε_m, %	ε_b, %	E_o, psi	(N/cm^2)	Burning Rate at 80°F (27°C) and 600 psig (414 N/cm^2) in./sec	(cm/s)
ID-1	Vertical	95	(66)	24	25	533	(368)	0.714	(1.81)
	Horizontal	81	(56)	21	22	549	(379)	0.709	(1.80)
ID-2	Vertical	106	(76)	20	22	756	(522)	0.702	(1.78)
	Horizontal	96	(66)	24	26	549	(379)	0.674	(1.71)
ID-3	Vertical	72	(50)	22	25	514	(355)	0.712	(1.81)
	Horizontal	74	(51)	23	28	487	(336)	0.715	(1.82)
ID-4	Vertical	78	(54)	20	23	608	(419)	0.732	(1.86)
	Horizontal	78	(54)	19	23	632	(436)	0.695	(1.76)
ID-5	Vertical	72	(50)	18	18	566	(391)	0.714	(1.81)
	Horizontal	67	(46)	18	19	520	(359)	0.692	(1.76)
ID-6	Vertical	57	(39)	17	18	564	(389)	0.711	(1.81)
	Horizontal	52	(36)	21	24	413	(285)	0.684	(1.74)
ID-7	Vertical	62	(43)	19	23	542	(374)	0.744	(1.89)
	Horizontal	60	(41)	21	25	479	(331)	0.704	(1.79)
ID-8	Vertical	69	(48)	15	15	687	(474)	0.736	(1.87)
	Horizontal	58	(40)	18	19	459	(317)	0.726	(1.84)
ID-9	Vertical	70	(48)	18	22	592	(408)	0.990	(2.52)
	Horizontal	66	(46)	19	23	522	(360)	0.951	(2.42)

Mechanical Properties and Burning Rates of Propellant Specimens
Taken from the First Full-Scale Mold (Section A)

Sample Location	Orientation	Mechanical Properties at 77°F (25°C)						Bond Strength at 77°F (25°C)				Burning Rate at 80°F (27°C) and 600 psig (414 N/cm²)	
		σ_m,		ε_m,	ε_b,	E_o,		Tensile		Shear			
		psi	(N/cm²)	%	%	psi	(N/cm²)	psi	(N/cm²)	psi	(N/cm²)	in./sec	(cm/s)
OD-1	Vertical	100	(69)	22	26	666	(460)					0.694	(1.76)
	Horizontal	96	(66)	24	26	560	(387)	105	(72)	85	(59)	0.693	(1.76)
OD-2	Vertical	87	(60)	18	18	728	(503)					0.714	(1.81)
	Horizontal	92	(64)	24	26	540	(373)	95	(66)	69*	(48)	0.675	(1.71)
OD-3	Vertical	80	(55)	23	27	529	(365)					0.678	(1.72)
	Horizontal	91	(63)	22	24	566	(391)	98	(68)	76*	(52)	0.676	(1.72)
OD-4	Vertical	85	(59)	20	23	618	(427)					0.700	(1.78)
	Horizontal	81	(56)	20	21	575	(397)	93	(64)	73*	(50)	0.692	(1.76)
OD-5	Vertical	59	(41)	12	13	623	(430)					0.697	(1.77)
	Horizontal	51	(35)	13	13	483	(333)	Bond Failure				0.714	(1.81)
OD-6	Vertical	65	(45)	17	18	560	(387)					0.726	(1.84)
	Horizontal	62	(43)	13	13	612	(422)	Bond Failure				0.733	(1.86)
OD-7	Vertical	61	(42)	20	23	466	(322)					0.712	(1.81)
	Horizontal	59	(41)	22	25	398	(275)	Bond Failure				0.712	(1.81)
OD-8	Vertical	63	(43)	18	23	555	(383)					0.716	(1.82)
	Horizontal	57	(39)	23	26	374	(258)	Bond Failure				0.701	(1.78)
OD-9	Vertical	64	(44)	17	20	610	(421)					0.725	(1.84)
	Horizontal	59	(41)	20	24	466	(322)	Bond Failure				0.718	(1.82)

* Failure at liner-to-propellant interface of at least one sample

Properties of Specimens from First Full-Scale Mold

Figure 91

Sample Location	Orientation	Mechanical Properties at 77°F (25°C) σ_m, psi	(N/cm^2)	ε_m, %	ε_b, %	E_o, psi	(N/cm^2)	Burning Rate at 80°F (27°C and 600 psig (414 N/cm^2) in./sec	(cm/s)
MID-1	Vertical	82	(57)	22	27	555	(383)	0.697	(1.77)
	Horizontal	91	(63)	23	27	590	(407)	0.690	(1.75)
MID-2	Vertical	81	(56)	19	19	533	(381)	0.685	(1.74)
	Horizontal	102	(70)	21	23	742	(512)	0.700	(1.78)
MID-3	Vertical	82	(57)	19	23	673	(464)	0.719	(1.83)
	Horizontal	72	(50)	21	22	496	(342)	0.668	(1.70)
MID-4	Vertical	54	(37)	21	27	409	(283)	0.708	(1.80)
	Horizontal	59	(41)	20	26	442	(305)	0.701	(1.78)
MID-5	Vertical	56	(39)	14	15	612	(422)	0.724	(1.84)
	Horizontal	51	(35)	18	19	448	(309)	0.714	(1.81)
MID-6	Vertical	62	(43)	14	16	699	(482)	0.730	(1.85)
	Horizontal	48	(33)	16	16	415	(286)	0.715	(1.82)
MID-7	Vertical	58	(40)	20	25	439	(303)	0.713	(1.81)
	Horizontal	55	(38)	21	24	365	(252)	0.710	(1.80)
MID-8	Vertical	60	(41)	20	24	424	(293)	0.702	(1.78)
	Horizontal	61	(42)	23	26	370	(255)	0.750	(1.90)
MID-9	Vertical	68	(47)	18	20	553	(381)	0.737	(1.87)
	Horizontal	61	(42)	22	25	389	(268)	0.675	(1.71)

Mechanical Properties and Burning Rates of Propellant Specimens
Taken from the First Full-Scale Mold (Section B)

Figure 92

Sample Location	Orientation	Mechanical Properties at 77°F (25°C)						Burning Rate at 80°F (27°C) and 600 psig (414 N/cm²)	
		σ_m, psi	(N/cm^2)	ε_m, %	ε_b, %	E_o, psi	(N/cm^2)	in./sec	(cm/s)
ID-1	Vertical	76	(52)	17	18	551	(380)	0.704	(1.79)
	Horizontal	73	(50)	23	28	494	(341)	0.655	(1.66)
ID-2	Vertical	78	(54)	22	25	503	(347)	0.665	(1.69)
	Horizontal	82	(57)	16	17	653	(450)	0.696	(1.77)
ID-3	Vertical	81	(56)	19	22	666	(460)	0.687	(1.74)
	Horizontal	87	(60)	17	21	832	(574)	0.730	(1.85)
ID-4	Vertical	66	(46)	16	18	638	(440)	0.691	(1.76)
	Horizontal	65	(45)	15	16	640	(442)	0.723	(1.84)
ID-5	Vertical	64	(44)	19	22	520	(359)	0.722	(1.83)
	Horizontal	66	(46)	18	20	549	(379)	0.711	(1.81)
ID-6	Vertical	59	(41)	19	22	496	(342)	0.700	(1.78)
	Horizontal	62	(43)	17	19	564	(389)	0.717	(1.82)
ID-7	Vertical	63	(43)	20	23	470	(324)	0.699	(1.78)
	Horizontal	69	(48)	18	23	629	(434)	0.738	(1.87)
ID-8	Vertical	88	(61)	18	19	662	(457)	0.737	(1.87)
	Horizontal	92	(64)	15	17	830	(573)	0.762	(1.94)
ID-9	Vertical	87	(60)	19	22	743	(513)	0.719	(1.83)
	Horizontal	96	(66)	18	20	798	(550)	0.776	(1.97)

Mechanical Properties and Burning Rates of Propellant Specimens
Taken from the First Full-Scale Mold (Section B)

Figure 93

Sample Location	Orientation	Mechanical Properties at 77°F (25°C) σ_m, psi	(N/cm^2)	ε_m, %	ε_b, %	E_o, psi	(N/cm^2)	Bond Strength at 77°F (25°C) Tensile psi	(N/cm^2)	Shear psi	(N/cm^2)	Burning Rate at 80°F (27°C) and 600 psig (414 N/cm^2) in./sec	(cm/s)
MID-1	Vertical	97	(67)	23	26	660	(455)					0.680	(1.73)
	Horizontal	104	(72)	19	23	839	(578)	75	(52)	71	(49)	0.739	(1.88)
MID-2	Vertical	78	(54)	16	16	588	(405)					0.695	(1.76)
	Horizontal	89	(61)	20	23	621	(428)	84	(58)	53	(37)	0.722	(1.83)
MID-3	Vertical	81	(56)	16	17	640	(441)					0.691	(1.76)
	Horizontal	89	(61)	19	24	675	(465)	84	(58)	58	(40)	0.734	(1.86)
MID-4	Vertical	83	(57)	21	22	584	(403)					0.699	(1.78)
	Horizontal	90	(62)	19	22	697	(480)	60	(41)	57**	(39)	0.723	(1.84)
MID-5	Vertical	75	(52)	17	17	621	(428)					0.726	(1.84)
	Horizontal	76	(52)	15	15	680	(469)	55	(38)	48	(33)	0.714	(1.81)
MID-6	Vertical	68	(47)	19	22	542	(374)					0.689	(1.75)
	Horizontal	69	(48)	18	22	599	(413)	69	(48)	53	(37)	0.703	(1.79)
MID-7	Vertical	63	(43)	18	21	557	(384)					0.702	(1.78)
	Horizontal	64	(44)	15	17	614	(423)	66**	(46)	44**	(30)	0.726	(1.84)
MID-8	Vertical	70	(48)	18	22	551	(380)					0.702	(1.78)
	Horizontal	72	(50)	18	19	627	(432)	No Bond				0.730	(1.85)
MID-9	Vertical	70	(48)	16	18	621	(428)					0.686	(1.74)
	Horizontal	70	(48)	19	22	568	(392)	No Bond				0.730	(1.85)

* Bond samples taken from OD position in mold. All breaks occurred within propellant except where indicated.

** Break occurred between propellant and liner.

Properties of Specimens from First Full-Scale Mold

Figure 94

Sample Location		Mechanical Properties at 77°F (25°C)						
Section	Area	σ_m, psi	(N/cm^2)	ε_m, %	ε_b, %	E_o, psi	(N/cm^2)	Failure Location
C	OD	68	(47)	17	19	608	(419)	Random
		58	(40)	15	16	511	(352)	Random
		94	(65)	15	15	752	(518)	Random
C	MID	90	(62)	19	20	673	(464)	Interface
B	MID	83	(57)	20	20	573	(395)	Interface

Mechanical Properties of Propellant Specimens from
First Full-Scale Mold Containing Bipropellant Interfaces

Figure 95

Vacuum Level, in. (mm) Hg	10	(254)	15	(381)	25	(635)	27 -29	(686-737)
Mix Temperature, °F (°C)	130	(54)	130	(54)	130	(54)	130	(54)
Final Mix Time, min.	20		20		20		20	
Mixer Speed, rpm	600		600		600		600	
Density, gm/cm^3	1.706		1.737		1.746		1.744	
Viscosity at 135°F (57°C), 5 $kdynes/cm^2$ ($500\ N/m^2$) shear stress, poise (Ns/m^2)								
6 hr	30,000	(3,000)	70,000	(7,000)	39,000	(3,900)	49,000	(4,900)
10 hr	100,000	(10,000)	86,000	(8,600)	63,000	(6,300)	56,000	(5,600)
LSBR at 600 psi ($414\ N/cm^2$), in./sec (cm/s)	0.663	(1.68)	0.700	(1.78)	0.681	(1.73)	0.666	(1.69)
Mechanical Properties at 77°F (25°C)								
σ_m, psi (N/cm^2)	83	(57)	88	(61)	77	(53)	99	(68)
ε_m, %	19		19		19		18	
ε_b, %	20		19		20		19	
E_o, psi (N/cm^2)	507	(350)	540	(373)	455	(314)	625	(431)

Figure 96

Effect of Final Mix Vacuum Level on Propellant Flow and Mechanical Properties In 10-lb (4.5 kg) Vertical Mixer Batches, Using a Large Vacuum Pump

Vacuum Level, in. (mm) Hg	25	(635)	25	(635)	25	(635)	20	(508)
Mix Temperature, °F (°C)	130	(54)	140	(60)	130	(54)	130	(54)
Final Mix Time, min.	60		60		20		5	
Mixer Speed, rpm	600		600		600		600	
Density, gm/cm^3	1.745		1.746		1.745		1.741	
Viscosity at 135°F (57°C), 5 $kdynes/cm^2$ (500 N/m^2) shear stress, poise (Ns/m^2)								
6 hr	22,000	(2,200)	18,000	(1,800)	19,000	(1,900)	32,000	(3,200)
10 hr	62,000	(6,200)	61,000	(6,100)	41,000	(4,100)	81,000	(8,100)
LSBR at 600 psi (414 N/cm^2), in./sec (cm/s)	0.695	(1.77)	0.660	(1.68)	0.654	(1.66)	0.646	(1.64)
Mechanical Properties at 77°F (25°C)								
σ_m, psi (N/cm^2)	73	(50)	62	(43)	63	(43)	69	(48)
ε_m, %	23		24		26		18	
ε_b, %	24		24		27		18	
E_o, psi (N/cm^2)	368	(254)	311	(215)	294	(203)	433	(299)

Effect of Final Vacuum Mix Level and Time on Propellant Flow and Mechanical Properties In 10-lb (4.5 kg) Vertical Mixer Batches Using a Small Vacuum Pump

Vacuum Level, in. (mm) Hg	29 (740)	29 (740)	29 (740)
Mix Temperature, °F (°C)	144 (62)	145 (63)	144 (62)
Final Mix Time, min	20	40	60
Mixer Speed, rpm	600	600	600
Density, gm/cm^3	1.746	1.746	1.746
Viscosity at 135°F (57°C), 5 Kdynes/cm^2 (500 N/m^2), shear stress, poise (Ns/m^2)			
6 hr	28,000 (2,800)	37,000 (3,700)	22,000 (2,200)
10 hr	60,000 (6,000)	62,000 (6,200)	69,000 (6,900)
LSBR at 600 psi (414 N/cm^2), in./sec (cms)	0.659 (1.67)	0.682 (1.73)	0.664 (1.69)
Mechanical Properties at 77°F (25°C)			
σ_m, psi (N/cm^2)	109 (75)	116 (80)	114 (79)
ε_m, %	22	23	24
ε_b, %	23	25	25
E_o, psi (N/cm^2)	612 (422)	612 (422)	621 (428)

Effect of Final Mix Time at High Temperature on Propellant Flow and Mechanical Properties

Vacuum Level, in. (mm) Hg	29	(740)	29	(740)	29	(740)	29	(740)
Mix Temperature, °F (°C)	138	(59)	130	(54)	130	(54)	130	(54)
Final Mix Time, min	5		20		40		60	
Mixer Speed, rpm	600		600		600		600	
Density, gm/cm^3	1.747		1.744		1.746		1.745	
Viscosity at 135°F (57°C), 5 $Kdynes/cm^2$ ($500\ N/m^2$), poise (Ns/m^2)								
6 hr	38,000	(3,800)	49,000	(4,900)	58,000	(5,800)	45,000	(4,500)
10 hr	>150,000	(>15,000)	57,000	(5,700)	108,000	(10,800)	58,000	(5,800)
LSBR at 600 psi ($414\ N/cm^2$), in./sec (cm/s)	0.685	(1.74)	0.666	(1.69)	0.677	(1.72)	0.690	(1.75)
Mechanical Properties at 77°F (25°C)								
σ_m, psi (N/cm^2)	101	(70)	99	(68)	113	(78)	118	(81)
ε_m, %	17		18		23		20	
ε_b, %	17		19		23		21	
E_o, psi (N/cm^2)	671	(463)	625	(431)	623	(429)	677	(467)

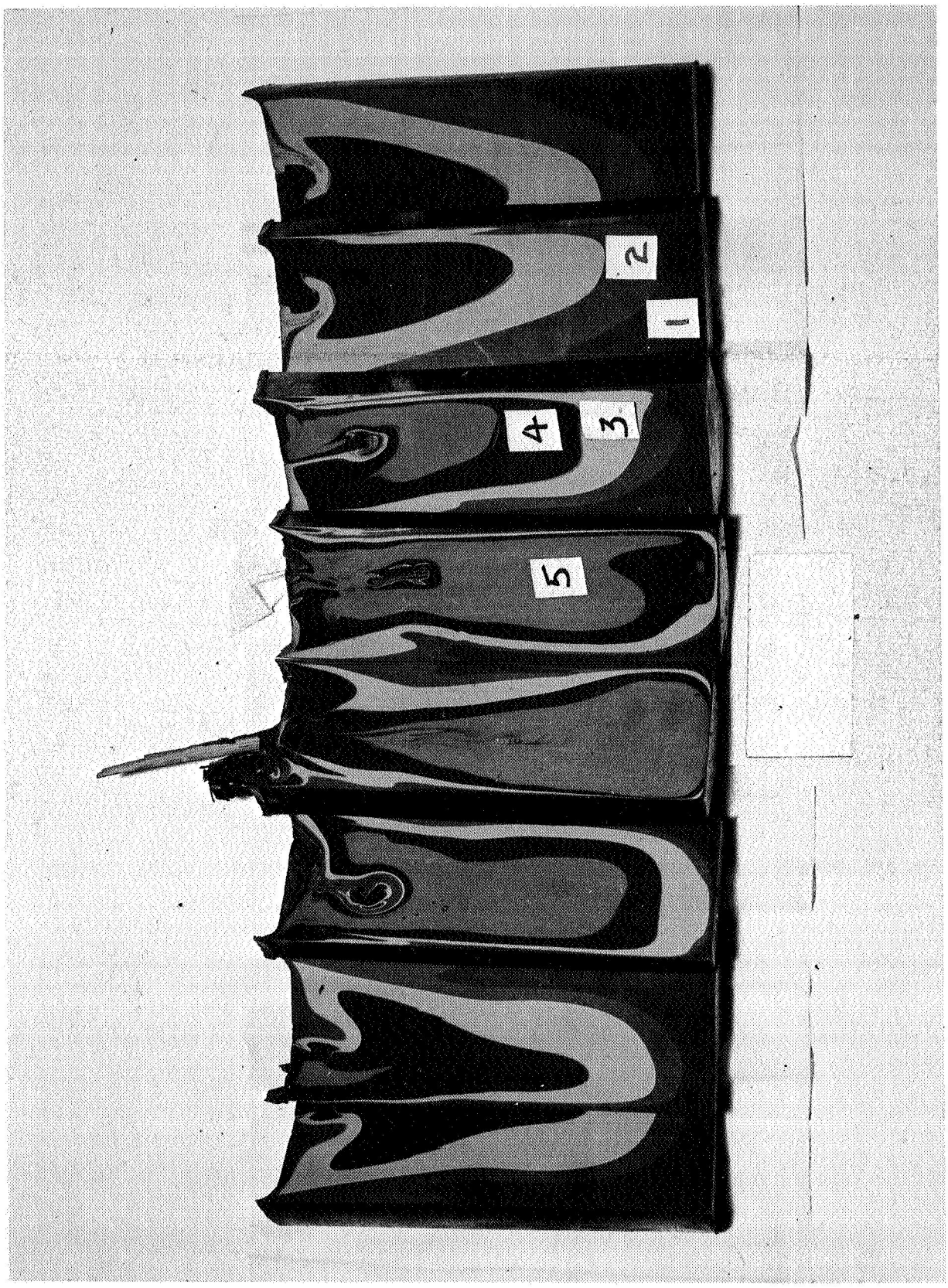
Figure 99

Effect of Final Mix Time at Low Temperature on
Propellant Flow and Mechanical Properties

Vacuum Level, in. (mm) Hg	29	(737)	29	(737)	29	(737)
Mix Temperature, °F (°C)	130	(54)	130	(54)	130	(54)
Final Mix Time, min.	20		20		20	
Mixer Blade Top Speed ft/min (cm/s)	31	(16)	67	(34)	104	(53)
Density, gm/cm^3	1.746		1.744		1.746	
Viscosity at 135°F (57°C), 5 $kdynes/cm^2$ (500 N/m^2) shear stress, poise (Ns/m^2)						
6 hr	38,000	(3,800)	49,000	(4,900)	17,000	(1,700)
10 hr	60,000	(6,000)	56,000	(5,600)	23,000	(2,300)
LSBR at 600 psi (414 N/cm^2), in./sec (cm/s)	0.685	(1.74)	0.666	(1.69)	0.650	(1.65)
Mechanical Properties at 77°F (25°C)						
σ_m, psi (N/cm^2)	115	(79)	99	(68)	78	(54)
ε_m, %	20		18		26	
ε_b, %	20		19		29	
E_o, psi (N/cm^2)	686	(473)	625	(431)	372	(257)

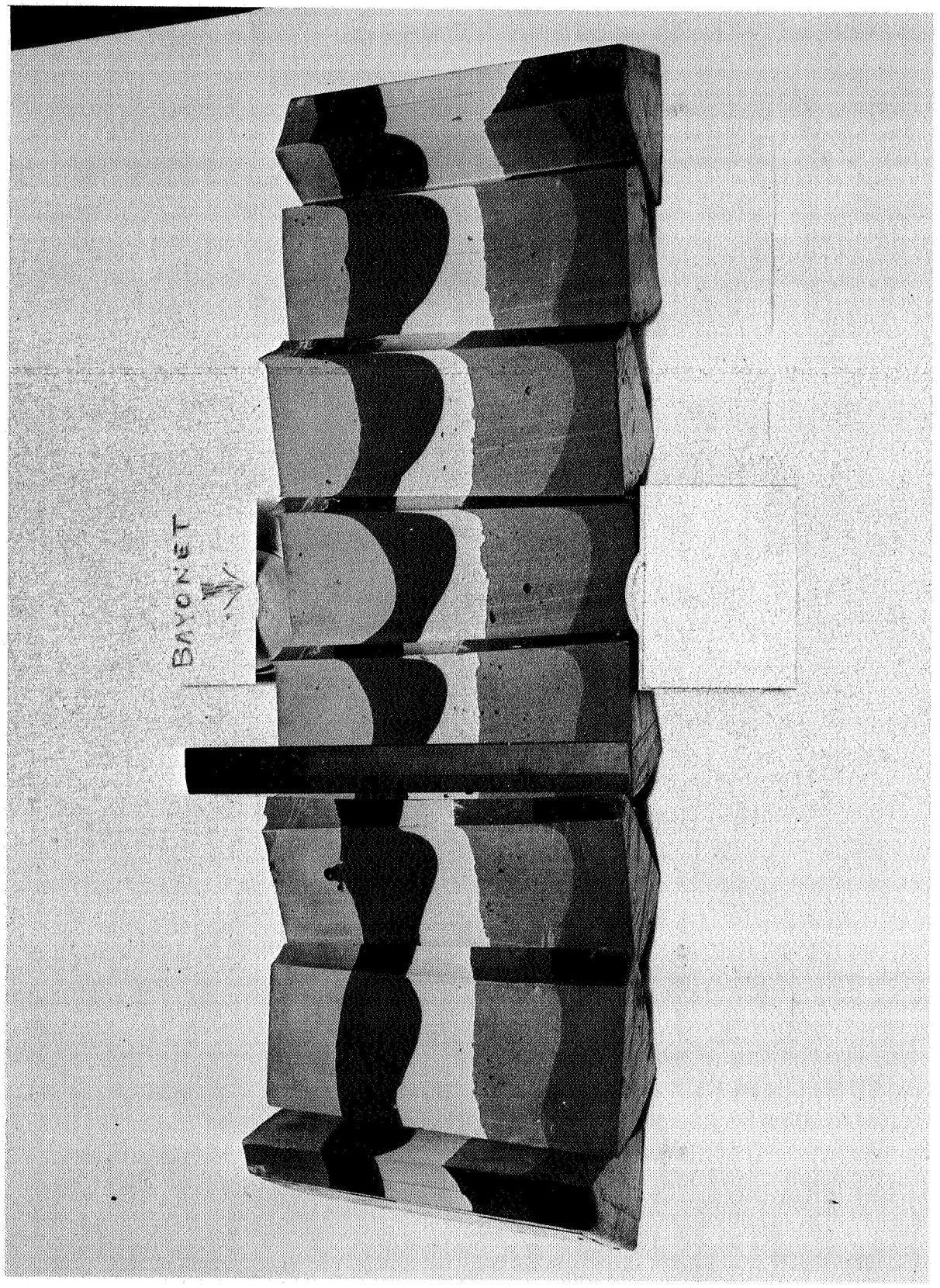
Effect of Mixer Speed on Propellant
Flow and Mechanical Properties

Figure 100



Sections of Laboratory Scale Casting

Figure 101



Sections of Laboratory Scale Casting

Figure 102

Batch No.	AP Blend SS/MA	Burning Rate Additive Type	Wt%	Liquid Density g/cm^3	Viscosity*, poise (NS/m^2) 6 Hr	10 Hr	LSBR at 600 psig (414 N/cm^2) in./sec (cm/S)	Mechanical Properties at 77°F σ_m psi	(N/cm^2)	ε_m %	ε_b %	E_o psi	(N/cm^2)
7200-17	60/40	IB/BRA-101	1.2	1.745	27,000 (2,700)	49,000 (4,900)	0.691 (1.76)	103	(71)	23	24	557	(384)
7200-4	65/35	IB/BRA-101	1.2	1.744	49,000 (4,900)	56,000 (5,600)	0.666 (1.69)	99	(68)	18	19	625	(431)
7200-19	70/30	IB/BRA-101	1.2	1.747	27,000 (2,700)	41,000 (4,100)	0.629 (1.60)	95	(66)	16	16	653	(450)
7245	65/35	IB	1.2	1.745	18,000 (1,800)	40,000 (4,000)	0.645 (1.64)	64	(44)	26	29	318	(219)
7246	65/35	BRA-101	1.2	1.745	off scale	off scale	0.526 (1.34)	40	(28)	26	30	229	(158)
7288	55/45	Fe_2O_3	1.5	1.762	17,000 (1,700)	28,000 (2,800)	0.595 (1.51)	127	(88)	21	22	730	(503)
7312	50/50	Fe_2O_3	2.0	1.779	40,000 (4,000)	46,000 (4,600)	0.663 (1.68)	141	(97)	18	19	909	(627)
7289	65/35	Cu 0202	1.2	1.780	53,000 (5,300)	120,000 (12,000)	0.660 (1.68)			No Cure			
7314	65/35	IB/Mod Silon S	1.2	1.748	10,000 (1,000)	17,000 (1,700)	0.610 (1.55)	95	(66)	23	26	540	(373)

* Viscosity at 135°F (57°C), 5 K dynes/cm^2 (500 N/m^2) shear stress, 6 and 10 hours after curing agent addition.

Figure 103

Effects of Oxidizer Blend and Burning Rate Additive on Properties of ANB-3254 Propellant

Batch No.	Plasticizer Type	BR Additive Type	BR Additive Wt%	Viscosity*, poise (NS/m^2) 6 Hr		Viscosity*, poise (NS/m^2) 10 Hr		LSBR at 600 psig (414 N/cm^2) in./sec (cm/s)	Mechanical Properties at 77°F σ_m psi	(N/cm^2)	ε_m %	ε_b %	E_o psi	(N/cm^2)
7290	Polybutene	BRA-101/IB	1.2	>120,000	(>12,000)	-	-	0.606 (1.54)	64	(44)	11	12	638	(440)
7334	TTIA	IB	1.2	35,000	(3,500)	60,000	(6,000)	0.643 (1.63)	No cure					
7289	TTIA	Cu 0202	1.2	50,000	(5,000)	120,000	(12,000)	0.660 (1.68)	No cure					
7476	Oleyl Nitrile	IB	1.2	19,000	(1,900)	35,000	(3,500)	0.638 (1.62)	No cure					
7605	Ricinoleic ester	IB	1.2	75,000	(7,500)	>120,000	(>12,000)	0.644 (1.64)	Not tested					
7395	DOA	IB	1.2	19,000	(1,900)	35,000	(3,500)	0.640 (1.63)	85	(59)	23	25	483	(333)

* Viscosity at 135°F (57°C), 5 K dynes/cm^2 (500 N/m^2) shear stress, 6 and 10 hr after curing agent addition

Effect of Plasticizer Type on Flow Behavior and Cure of ANB-3254 Type Propellant

Figure 104

Batch No.	Surface Active Agent Type	Wt%	Viscosity**, poise (Ns/m^2) 6 hr	10 hr	Mechanical Properties at 77°F (25°C) σ_m, psi	(N/cm^2)	ε_m, %	ε_b, %	E_o, psi	(N/cm^2)
7291	Sorbitan Oleate	0.2	30,000 (3,000)	100,000 (10,000)	104	(72)	24	26	568	(392)
7292	L-45	0.2	31,000 (3,100)	65,000 (6,500)	113	(78)	22	23	653	(450)
7293	FC-167	0.005	31,000 (3,100	50,000 (5,000)	98	(68)	18	18	599	(413)
7200-4	None	-	50,000 (5,000)	65,000 (6,500)	99	(68)	18	19	625	(431)

* Burning rate additive is 1.2 wt% IB/BRA-101

** Viscosity at 135°F (57°C), 5 K dynes/cm^2 (500 N/m^2) shear stress, 6 and 10 hr after curing agent addition.

Effect of Surface Active Agents on Flow Behavior and Cure of ANB-3254 Type* Propellants

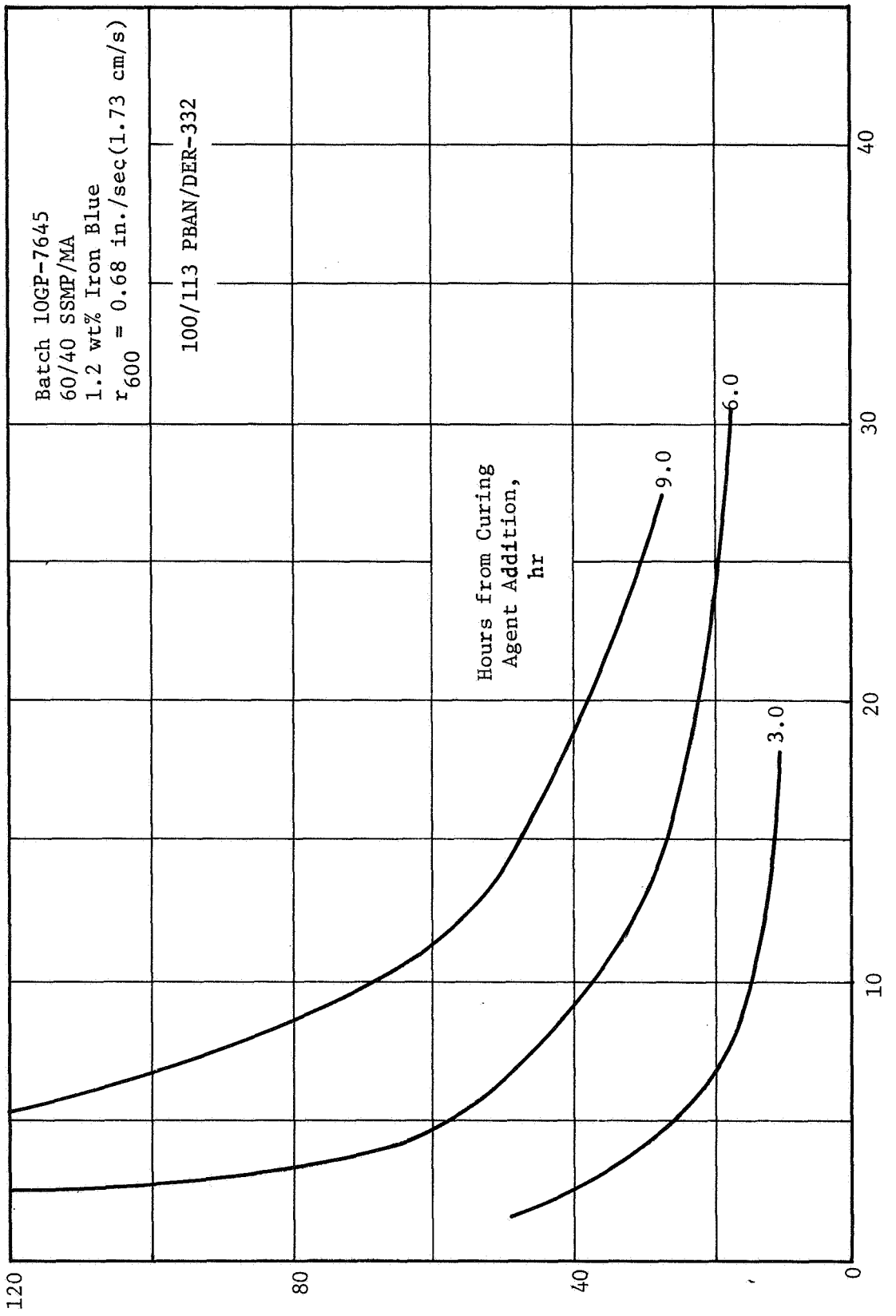
Figure 105

Batch No.	Equivalents DER-332	Wt% FeAA	Viscosity*, poise (Ns/m^2) 6 hr		10 hr		Mechanical Properties at 77°F (25°C) σ_m, psi	(N/cm^2)	ε_m, %	ε_b, %	E_o, psi	(N/cm^2)
7200-4	113	0.02	50,000	(5,000)	65,000	(6,500)	99	(68)	18	17	625	(431)
7372	130	0.035	110,000	(11,000)	>120,000	(>12,000)	152	(105)	14	14	1,230	(848)

*Viscosity at 135°F (57°C), 5 K dynes/cm^2 (500 N/m^2), 6 and 10 hr after curing agent addition.

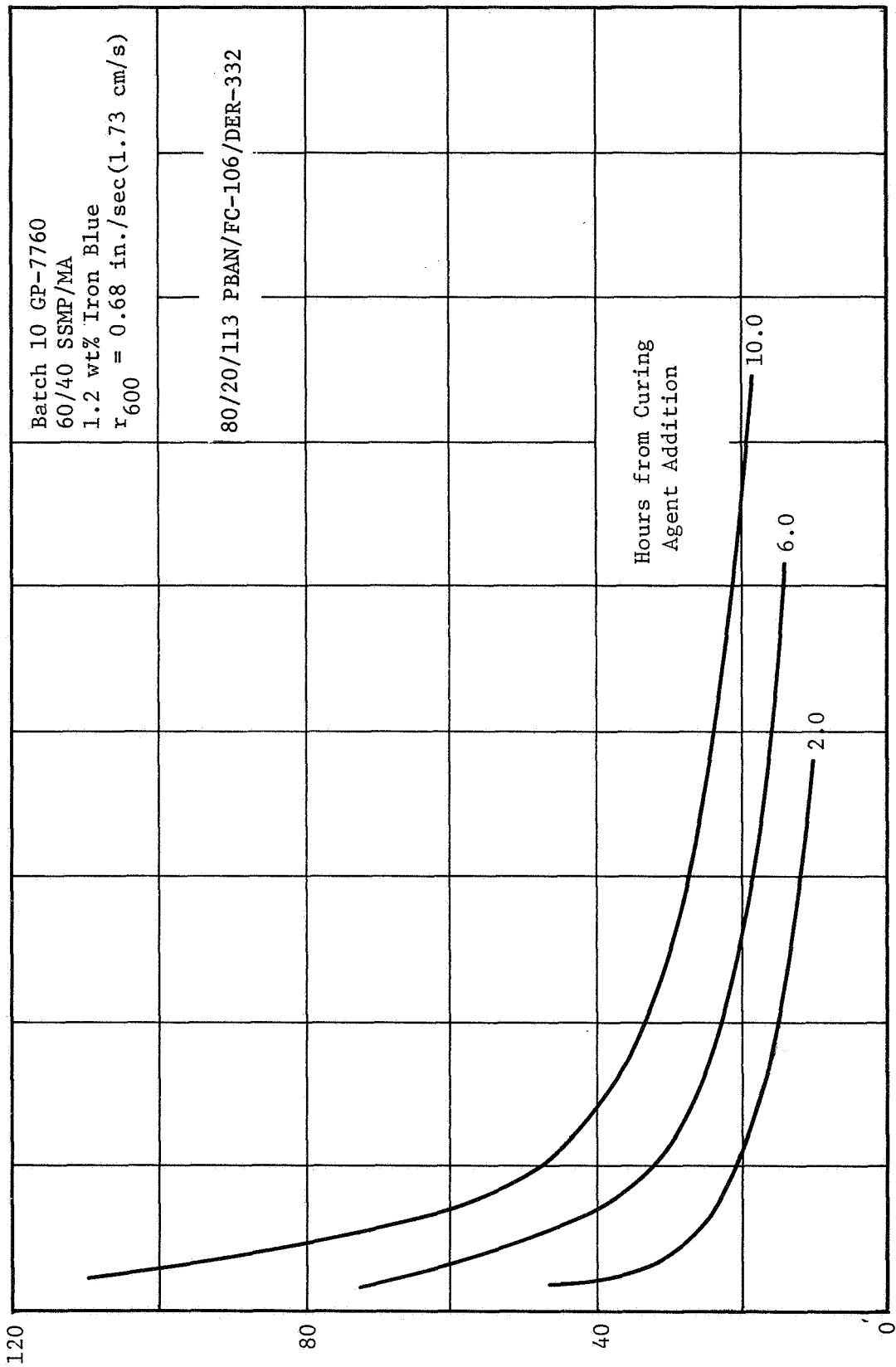
Figure 106

Effect of Curing Agent and Cure Catalyst Concentration on Flow Behavior of ANB-3254 Propellant



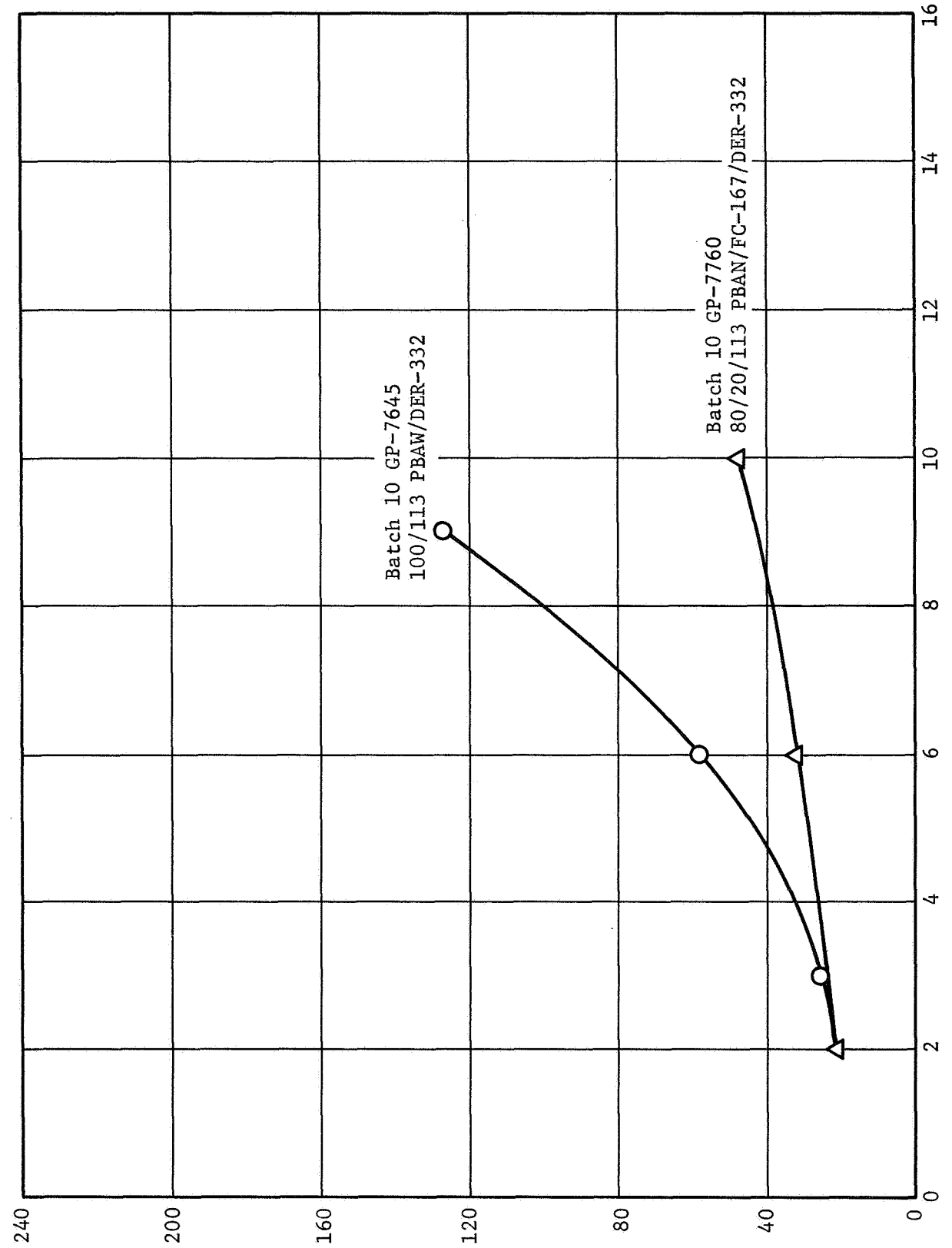
Viscosity as a Function of Shear Stress and Time from Curing Agent Addition

Figure 107



Viscosity as a Function of Shear Stress and Time from Curing Agent Addition

Figure 108



Effect of FC 167 Wetting Agent on Viscosity Build-up
(Oxidizer Blend: 60/40 SSMP/MA)
1.2 wt% Iron Blue

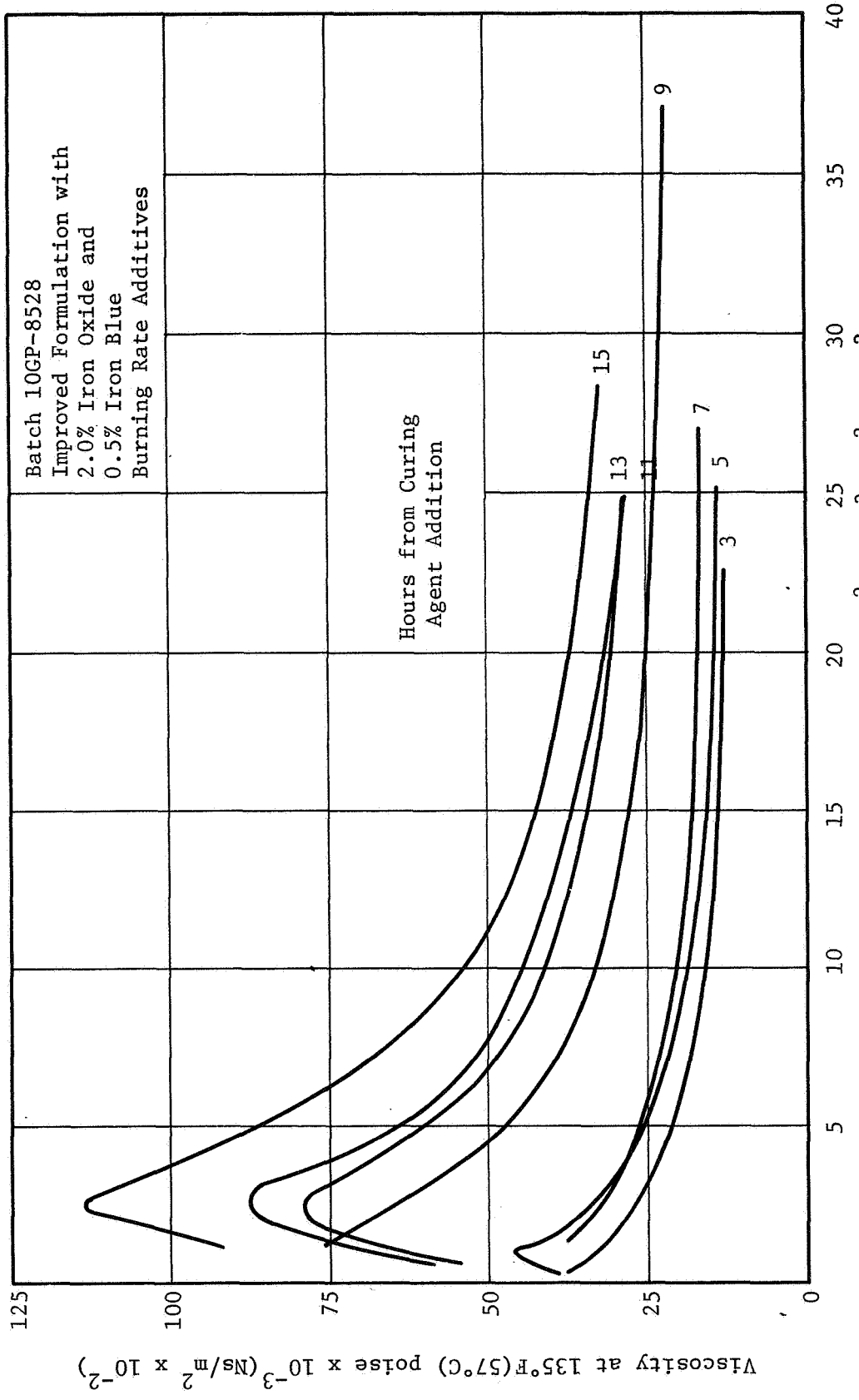
Figure 109

Storage Time at 180°F(82°C) Weeks	Test Specimen Type	Mechanical Properties at 77°F (25°C)											
		Batch 10GP-7410						Batch 10GP-7411					
		σ_m, psi	(N/cm^2)	ε_m, %	ε_b, %	E_o, psi	(N/cm^2)	σ_m, psi	(N/cm^2)	ε_m, %	ε_b, %	E_o, psi	(N/cm^2)
0	Instron bars	85	(59)	23	25	483	(333)	86	(59)	20	22	568	(392)
2	Instron bars	91	(63)	21	22	538	(371)	81	(56)	17	17	584	(403)
2	0.5 in. (1.3 cm) slabs	90	(62)	22	23	525	(362)	76	(52)	20	22	474	(327)

Binder:	PBAN/DER-332 100/130
BRA:	1.2 wt% Iron Blue
Cure Catalyst:	0.02 wt% FeAA (Batch 7410)
	0.05 wt% FeAA (Batch 7411)
Antioxidant:	0.20 wt% PBNA (phenyl β-naphthyl amine)

Storage Stability at 180°F (82°C) of PBAN Propellant Containing PBNA Antioxidant

Figure 110



Propellant Viscosity as a Function of Shear Stress and Time from Curing Agent Addition

Figure 111

Cure Catalyst Type	Wt%	Cured Propellant Mechanical Properties at 77°F (25°C) σ_m, psi	(N/cm^2)	ε_m, %	ε_b, %	E_o, psi	(N/cm^2)
FeAA	0.02	85	(59)	23	25	483	(333)
FeAA	0.05	86	(59)	20	22	568	(392)
FC-151	0.05	110	(76)	23	24	616	(425)

* Binder 100/130 PBAN/DER-332

BRA 1.2 wt% Iron Blue

Effect of Cure Catalyst Type and Concentration on Mechanical Properties of PBAN Propellant*

Oxidizer Blend	60/40 SSMP/MA
Burning Rate Additives	2.0 wt% Iron oxide 0 to 0.25 wt% Iron Blue
Wetting Agent	10 to 20 equiv FC-167
Cure Catalyst	0.025 to 0.05 wt% FC-151
Antioxidant	0.1 to 0.2 wt% PBNA
Plasticizer	25 to 30 wt% (of binder) DOA
Binder	PBAN 80-90 equiv DER-332 80 to 85 equiv

Improved Formulation ANB-3350

Figure 113

Batch No.	Storage Time, days	Viscosity* poise x 10^{-3} (Ns/m^2 x 10^{-2}) 6 hr	10 hr	Mechanical Properties at 77°F σ_m, psi	(N/cm^2)	ε_m, %	ε_b, %	E_o, psi	(N/cm^2)
8528	0	25	50	76	(52)	22	23	418	(288)
8529	1	27	35	65	(45)	23	24	350	(241)
8530	2	25	40	79	(54)	24	25	423	(292)
8531	3	30	45	65	(45)	24	24	331	(228)
8532	4	30	45	78	(54)	24	26	413	(285)
8533	11	-	-	70	(48)	24	26	365	(252)
8534	14	30	45	62	(43)	25	27	306	(211)

*Viscosity at 135°F (57°C), 5,000 dynes/cm^2 (500 N/m^2) shear stress, at 6 and 10 hr from curing agent addition.

Effect of Premix Storage on Mechanical Properties of ANB-3350 Propellant

Mold Designation	Batch No.	Formulation	Rotovisko Viscosity* poise (Ns/m^2)		Box Flow Test Size of Puddle, in. (cm)		Falling Ball, Time to Fall 3 in. (7.6 cm) sec
Full-Scale-1	22D-172 H	ANB-3254	55,000	(5,500)	~2 by 4	(5 by 10)	-
Sub-Scale-7	69-7	ANB-3254	30,000	(3,000)	6 by 7.5	(15 by 19)	-
	69-8		30,000	(3,000)	-		-
	69-9		32,000	(3,200)	-		-
	69-10	ANB-3254	32,000	(3,200)	3.5 by 5.5	(9 by 14)	-
	69-11	ANB-3350	17,000	(1,700)	6 by 11	(15 by 28)	-
Sub-Scale-8	69-21		20,000	(2,000)	8 by 12.5	(20 by 32)	34
	69-22		16,000	(1,600)	8 by 12	(20 by 30)	24
	69-23		17,000	(1,700)	7.5 by 10.5	(19 by 27)	28
	69-24		15,000	(1,500)	8.5 by 15	(20 by 38)	21
	69-25	ANB-3350	22,000	(2,200)	7.5 by 13.5	(19 by 34)	32
	10GP-3254	ANB-3254	60,000	(6,000)	-		1200 to fall 1 in. (2.5 cm)

* Viscosity at 135°F (57°C), 5,000 dynes/cm^2 (500 N/m^2) shear stress, 2 to 3 hr after curing agent addition.

Figure 115

Comparison of Viscosity Tests

Batch No.	Formulation Variables					Casting		
	Iron Blue, wt%	DER-332, Equiv.	DOA, %	FC-167, Equiv.	PBNA, %	Cast Rate, lb/hr	(Kg/hr)	Time between Batches, hr
69-21	0.5	85	30	20	0.10	425	(190)	--
69-22	0.25	85	30	20	0.20	395	(180)	5.5
69-23	0.25	85	30	10	0.10	560	(250)	16.0
69-24	0	82	30	20	0.10	550	(250)	4.5
69-25	0.10	82	25	20	0.10	420	(190)	5.8

NOTES:
1. All batches contain 2.0 wt% Iron Oxide and 0.05 wt% FC-151.
2. Mixer vacuum level was 29 in. (740 mm) Hg.
3. Mix time under vacuum was 55 min.
4. Mold design was 360-degree (6.28 rad) cylinder.
5. Bayonet submergence was 0 to 3 in. (0-8 cm) for all batches.

Summary of Propellant Formulation and Casting Parameters for Eighth Subscale Mold

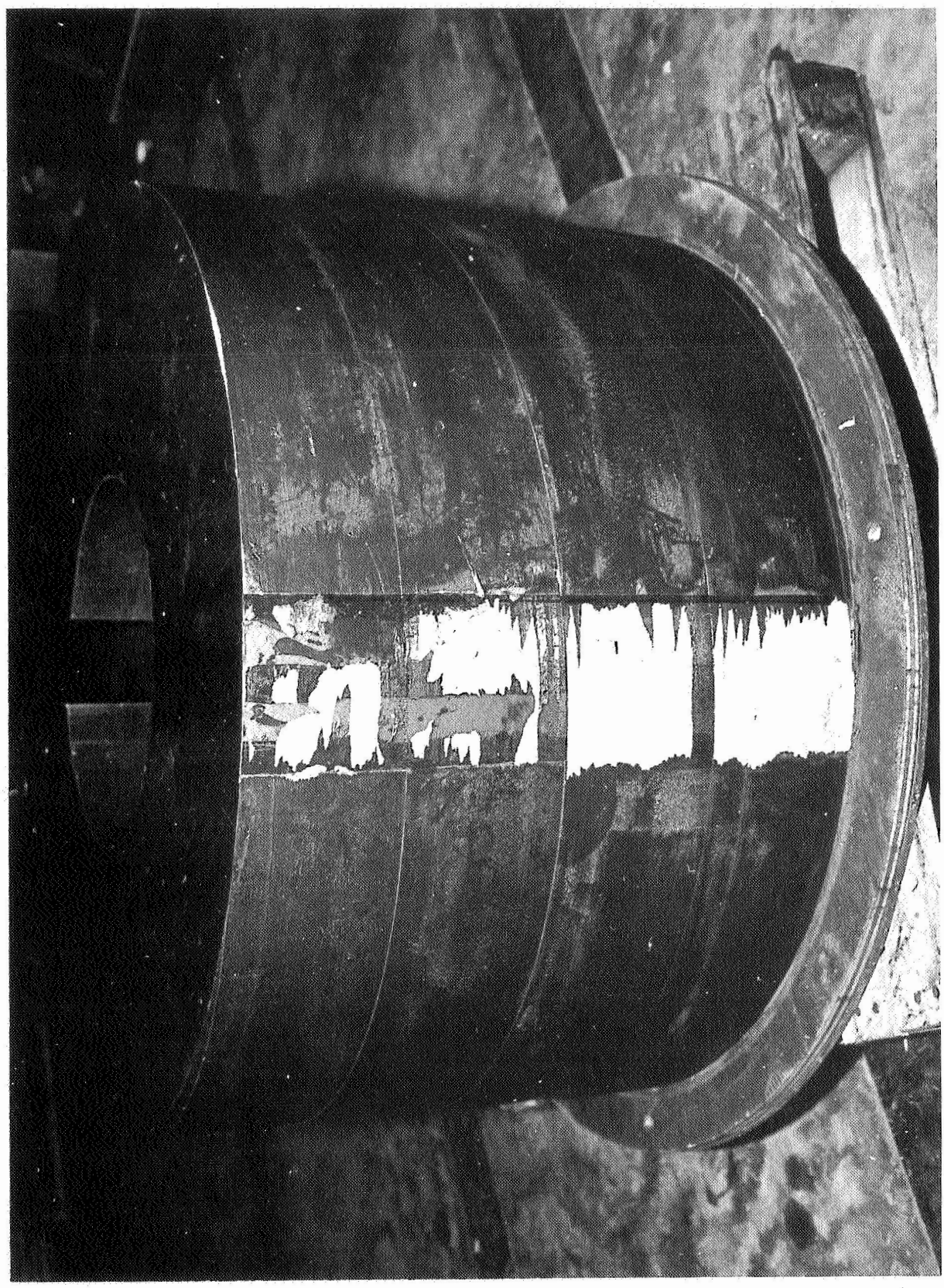
Figure 116

Batch No.*	Water Content, %	Acid Equiv., 100 g	Liquid Density, g/cm^3	Refractive Index	Water Content, %	Liquid Density, g/cm^3	Liquid Density, g/cm^3	DER-332 Content, %	Liquid Strand Burning Rate at 600 psig (414 N/cm^2) and 80°F (27°C), in./sec	(cm/s)	Viscosity, poise** (Ns/m^2) 6 hr	10 hr
69-21	0.050	0.0416	0.929	1.4295	0.084	1.521	1.788	0.97	0.728	(1.85)	30,000 (3,000)	43,000 (4,300)
69-22	0.052	0.0415	0.929	1.4294	0.071	1.520	1.788	1.02	0.707	(1.80)	23,000 (2,300)	33,000 (3,300)
69-23	0.050	0.0417	0.929	1.4921	0.066	1.516	1.788	0.93	0.708	(1.80)	22,000 (2,200)	28,000 (2,800)
69-24	0.060	0.0418	0.929	1.4925	0.057	1.515	1.788	0.95	0.653	(1.66)	16,000 (1,600)	21,000 (2,100)
69-25	0.070	0.0446	0.929	1.4955	0.063	1.519	1.790	0.99	0.668	(1.70)	30,000 (3,000)	38,000 (3,800)

* All batches made with ammonium perchlorate from lot 5343 (purchased for this program from AMPOT).
** Viscosity at 135°F (57°C), 5,000 dynes/cm^2) shear stress, 6 and 10 hr after curing agent addition.

Summary of Uncured Propellant Data, Eighth Subscale Mold

Figure 117



View of Eighth Subscale Mold

Figure 118

Batch No. 69-	Cure Time, days	Shore A Hardness	Mechanical Properties at 77°F (25°C) σ_m, psi	(N/cm^2)	ε_m, %	ε_b, %	E_o, psi	(N/cm^2)
21	12	36	72	(50)	21	22	442	(305)
	18	42	76	(52)	17	18	522	(360)
	22	40	87	(60)	19	20	564	(389)
22	12	41	82	(57)	18	18	551	(380)
	18	46	92	(63)	19	20	599	(413)
	22	41	87	(60)	19	20	651	(449)
23	12	32	57	(39)	21	24	348	(240)
	18	34	65	(45)	21	23	396	(273)
	22	32	65	(45)	19	20	424	(292)
24	12	38	66	(46)	22	24	407	(281)
	18	40	80	(55)	20	21	516	(356)
	22	41	87	(60)	21	22	568	(391)
25	12	45	92	(63)	21	23	581	(401)
	18	46	105	(72)	19	20	682	(470)
	22	48	108	(75)	20	21	708	(488)

Mechanical Properties of Carton Samples of Propellant Cast into Eighth Subscale Mold

Figure 119

Sample Location*	Orientation	Mechanical Properties at 77°F (25°C)						Bond Strength** at 77°F (25°C)				Solid Strand Burning Rate at 80°F (27°C) & 600 psig (414 N/cm²)	
		σ_m, psi	(N/cm²)	ε_m, %	ε_b, %	E_o, psi	(N/cm²)	Tensile psi	(N/cm²)	Shear psi	(N/cm²)	in./sec	(cm/s)
I-B	Vertical	90	(62)	19	20	647	(446)					0.674	(1.71)
	Horizontal	94	(65)	16	16	800	(552)	51	(35)	38	(26)	0.670	(1.70)
I-C								45	(31)	45	(31)		
II-B	Vertical	94	(65)	13	13	846	(583)					0.620	(1.57)
	Horizontal	89	(61)	17	18	699	(482)	51	(35)	56	(39)	0.662	(1.68)
II-C								42	(29)	54	(37)		
III-B	Vertical	89	(61)	19	21	684	(472)					0.647	(1.64)
	Horizontal	89	(61)	17	19	690	(476)	52	(36)	50	(34)	0.666	(1.69)
III-C								61	(42)	54	(37)		

* Refer to Figure 41 for sample location
** All failures occurred at the propellant to steel interface as a P-1 failure

Mechanical and Bond Properties and Solid Strand Burning Rate of Propellant Specimens taken from the Eighth Subscale Mold

Batch No.	Formulation Variables: Iron Blue, wt%	DER-332, Equiv.	FC-151, %	Mixing: Mix Time, min	Casting: Bayonet Height above Surface, in.	(cm)	Cast Rate, lb/hr	(Kg/hr)	Time between Batches, hr
69-32	0.10	85	0.05	55	0-1	(2.5)	840	(380)	--
69-33	0.25	85	0.03	55	3	(8)	850	(390)	3.7
60-34	0.25	85	0.03	55	6	(15)	670	(300)	18
69-35	0.25	85	0.05	55	9	(23)	680	(310)	4.5
69-36	0.25	85	0.05	10	6	(15)	570	(260)	3.2

NOTES:
1. All batches contain 2.0 wt% Iron Oxide, 85 equivalents DER-332, 30 wt% (of binder) DOA, 20 equivalents FC-167, and 0.10 wt% PBNA.
2. Mixer vacuum level was 29 in. (740 mm) Hg.
3. Mold design was 360-degree (6.28 rad) cylinder.

Summary of Propellant Formulation and Casting Parameters for Ninth Subscale Mold

Figure 121

Batch No.*	Submix				Premix		Uncured Propellant					
	Water Content, %	Acid Equiv., 100 g	Liquid Density, g/cm^3	Refractive Index	Water Content, %	Liquid Density, g/cm^3	Liquid Density, g/cm^3	DER-332 Content, %	Liquid Strand Burning Rate at 600 psig (414 N/cm^2) and 80°F (27°C), in./sec	(cm/s)	Viscosity, poise** (Ns/m^2) 6 hr	10 hr
69-32	0.057	0.0408	0.929	1.4919	0.051	1.506	1.781	1.11	0.645	(1.64)	14,000 (1,400)	18,000 (1,800)
69-33	0.062	0.0406	0.929	1.4918	0.054	1.506	1.783	1.10	0.685	(1.74)	14,000 (1,400)	18,000 (1,800)
69-34	0.061	0.0404	0.929	1.4918	0.065	1.509	1.782	1.08	0.722	(1.83)	15,000 (1,500)	20,000 (2,000)
69-35	0.062	0.0418	0.930	1.4910	0.062	1.507	1.783	1.02	0.686	(1.74)	17,000 (1,700)	19,000 (1,900)
69-36	0.055	0.0412	0.930	1.4910	0.061	1.507	1.782	1.03	0.677	(1.72)		

* All batches prepared with ammonium perchlorate from lot A-66042 (residual PEPCON material) except Batch 69-34 which used the new lot 5343.
** Viscosity at 135°F (57°C), 5,000 dynes/cm^2 (500 N/m^2) shear stress, 6 and 10 hr after curing agent addition.

Uncured Propellant Data, Ninth Subscale Mold

Figure 122

Batch No. 69-	Cure Time, days	Shore A Hardness	Mechanical Properties at 77°F (25°C) σ_m, psi	(N/cm^2)	ε_m, %	ε_b, %	E_o, psi	(N/cm^2)
32	12	30	62	(43)	20	21	380	(262)
	18	36	72	(50)	21	23	446	(308)
	22	37	72	(50)	21	22	444	(306)
33	12	25	49	(34)	23	26	265	(183)
	18	29	57	(39)	19	20	370	(255)
	22	31	58	(40)	22	23	324	(223)
34	12	33	68	(47)	22	23	415	(286)
	18	43	83	(57)	17	18	555	(383)
	22	44	77	(53)	18	18	496	(342)
35	12	30	60	(41)	24	25	331	(228)
	18	33	71	(49)	21	24	437	(302)
	22	36	69	(48)	21	22	424	(292)
36	12	29	56	(39)	23	24	320	(221)
	18	34	69	(48)	19	20	468	(323)
	22	35	60	(41)	22	23	346	(239)

Mechanical Properties Carton Samples of Propellant Cast into the Ninth Subscale Mold

Figure 123

Sample Location	Orientation	Mechanical Properties at 77°F (25°C)						Bond Strength* at 77°F (25°C)				Solid Strand Burning Rate at 80°F (27°C) & 600 psig (414 N/cm^2)	
		σ_m, psi	(N/cm^2)	ε_m, %	ε_b, %	E_o, psi	(N/cm^2)	Tensile psi	(N/cm^2)	Shear psi	(N/cm^2)	in./sec	(cm/s)
I-B	Vertical	74	(51)	23	25	459	(317)					0.828	(2.10)
	Horizontal	82	(57)	20	23	560	(386)	53	(37)	41	(28)	0.594-0.707	(1.51-1.79)
I-C								50	(34)	38	(26)		
II-B	Vertical	76	(52)	16	16	549	(379)					0.680	(1.73)
	Horizontal	106	(73)	20	20	723	(498)	51	(35)	53	(37)	0.679	(1.72)
II-C								47	(32)	42	(29)		
III-B	Vertical	78	(54)	19	20	529	(365)					0.668	(1.70)
	Horizontal	93	(64)	19	20	623	(430)	62	(43)	48	(33)	0.689	(1.75)
III-C								46	(32)	43	(30)		

* All failures occurred at the propellant to steel interface as a P-1 failure

Mechanical and Bond Properties and Solid Strand Burning Rate of Propellant Specimens Taken from the Ninth Subscale Mold

Figure 124

NASA CR 72621

Batch No.	Formulation Variables		Casting				
	DER-332, Equiv	FC-151, %	Bayonet Submergence, in.	(cm)	Cast Rate, lb/hr	(Kg/hr)	Time between Batches, hr
69-41	84	0.03	0-5	(0-10)	600	(270)	--
69-42	84	0.03	5-13	(10-33)	570	(260)	4.3
69-43	78	0.05	6-14	(15-36)	435	(200)	4.0
69-44	78	0.05	6-14	(15-36)	470	(210)	14.0
69-45	78	0.05	6-14	(15-36)	490	(220)	4.8

NOTES:

1. All batches contain 2.0 wt% Iron Oxide, 25 wt% (of binder) DOA, 20 equivalents FC-167, and 0.10 wt% PBNA.
2. Vacuum mixed at 29 in. (740 mm) Hg for 55 min.
3. Casting form was 240 degree (4.19 rad) cylinder; single bayonet, central location.

Summary of Propellant Formulation and Casting Parameters for Tenth Subscale Mold

		Submix				Premix		Uncured Propellant					
Batch No.	Oxidizer Lot*	Water Content, %	Acid Equiv., 100 g	Liquid Density, g/cm^3	Refractive Index	Water Content, %	Liquid Density, g/cm^3	Liquid Density, g/cm^3	DER-332 Content, %	Liquid Strand Burning Rate at 600 psig (414 N/cm^2) and 80°F (27°C), in./sec	(cm/s)	Viscosity, poise** (Ns/m^2) 6 hr	10 hr
69-41	5343/5343	0.054	0.0450	0.930	1.4950	0.057	1.510	1.782	1.19	0.680	(1.73)	18,000 (1,800)	22,000 (2,200)
69-42	5343/5343	0.072	0.0447	0.929	1.4947	0.067	1.507	1.782	1.09	0.694	(1.76)	20,000 (2,000)	24,000 (2,400)
69-43	5343/ A66042	0.047	0.0446	0.929	1.4955	0.058	1.508	1.783	0.97	0.680	(1.73)	22,000 (2,200)	30,000 (3,000)
69-44	5343/ A66042	0.076	0.0443	0.929	1.4945	0.066	1.509	1.783	0.98	0.669	(1.70)	22,000 (2,200)	28,000 (2,800)
69-45	5343/ A66042	0.052	0.0447	0.929	1.4949	0.051	1.509	1.783	1.02	0.663	(1.68)	19,000 (1,900)	26,000 (2,600)

* SSMP/MA Lot A66042 is residual PEPCON AP
Lot 5343 is residual AMPOT AP

** Viscosity at 135°F (57°C), 5,000 dynes/cm^2 (500 N/m^2) shear stress, 6 and 10 hr after curing agent addition

Uncured Propellant Data, Tenth Subscale Mold

Figure 126

NASA CR 72621

Batch No. 69-	Cure Time, days	Shore A Hardness	Mechanical Properties at 77°F (25°C) σ_m, psi	(N/cm^2)	ε_m, %	ε_b, %	E_o, psi	(N/cm^2)
41	12	45	92	(63)	18	18	633	(436)
	18	46	97	(67)	19	19	645	(445)
	22	46	98	(68)	18	19	677	(467)
42	12	44	88	(61)	22	23	529	(365)
	18	45	94	(65)	23	24	544	(375)
	22	48	100	(69)	22	23	634	(437)
43	12	28	57	(39)	21	22	325	(224)
	18	31	60	(41)	23	25	326	(225)
	22	30	57	(39)	26	28	278	(192)
44	12	27	55	(38)	24	26	291	(201)
	18	30	57	(39)	24	27	302	(208)
	22	30	58	(40)	25	27	311	(215)
45	12	25	51	(35)	26	28	247	(170)
	18	28	56	(39)	23	25	304	(210)
	22	29	54	(37)	26	27	270	(186)

Mechanical Properties Carton Samples of Propellant Cast into the Tenth Subscale Mold

Figure 127

Sample Location	Orientation	Mechanical Properties at 77°F (25°C)						Bond Strength at 77°F (25°C)				Solid Strand Burning Rate at 80°F (27°C) & 600 psig (414 N/cm^2)	
		σ_m, psi	(N/cm^2)	ε_m, %	ε_b, %	E_o, psi	(N/cm^2)	Tensile psi	(N/cm^2)	Shear psi	(N/cm^2)	in./sec	(cm/s)
I-B	Vertical	109	(75)	22	24	675	(465)					0.950/ 0.678*	(2.41/ 1.72)
	Horizontal	102	(70)	25	27	533	(367)	78	(54)	56	(39)	1.018/ 0.664*	(2.59/ 1.69)
I-C								93	(64)	70	(48)		
II-B	Vertical	64	(44)	25	29	335	(231)					0.667	(1.69)
	Horizontal	107	(74)	21	21	719	(496)	59	(41)	73	(50)	0.691	(1.75)
II-C								84	(58)	83	(57)		
III-B	Vertical	61	(42)	24	28	363	(250)					0.976	(2.48)
	Horizontal	64	(44)	23	25	367	(253)	57	(39)	45	(31)	0.689	(1.75)
III-C								60	(41)	55	(38)		

* Retest

Mechanical and Bond Properties and Solid Strand Burning Rate of Propellant Specimens Taken from the Tenth Subscale Mold

Figure 128

NASA CR 72621

Autoignition Temperature, Copper Block, °F (°C)	482 (250)
Impact Sensitivity, 50% point, cm/2Kg	38
Rotary Friction Sensitivity, 50% point, g load/RPM	4000/3250
NOL Card Gap, "0" Attenuation	Negative

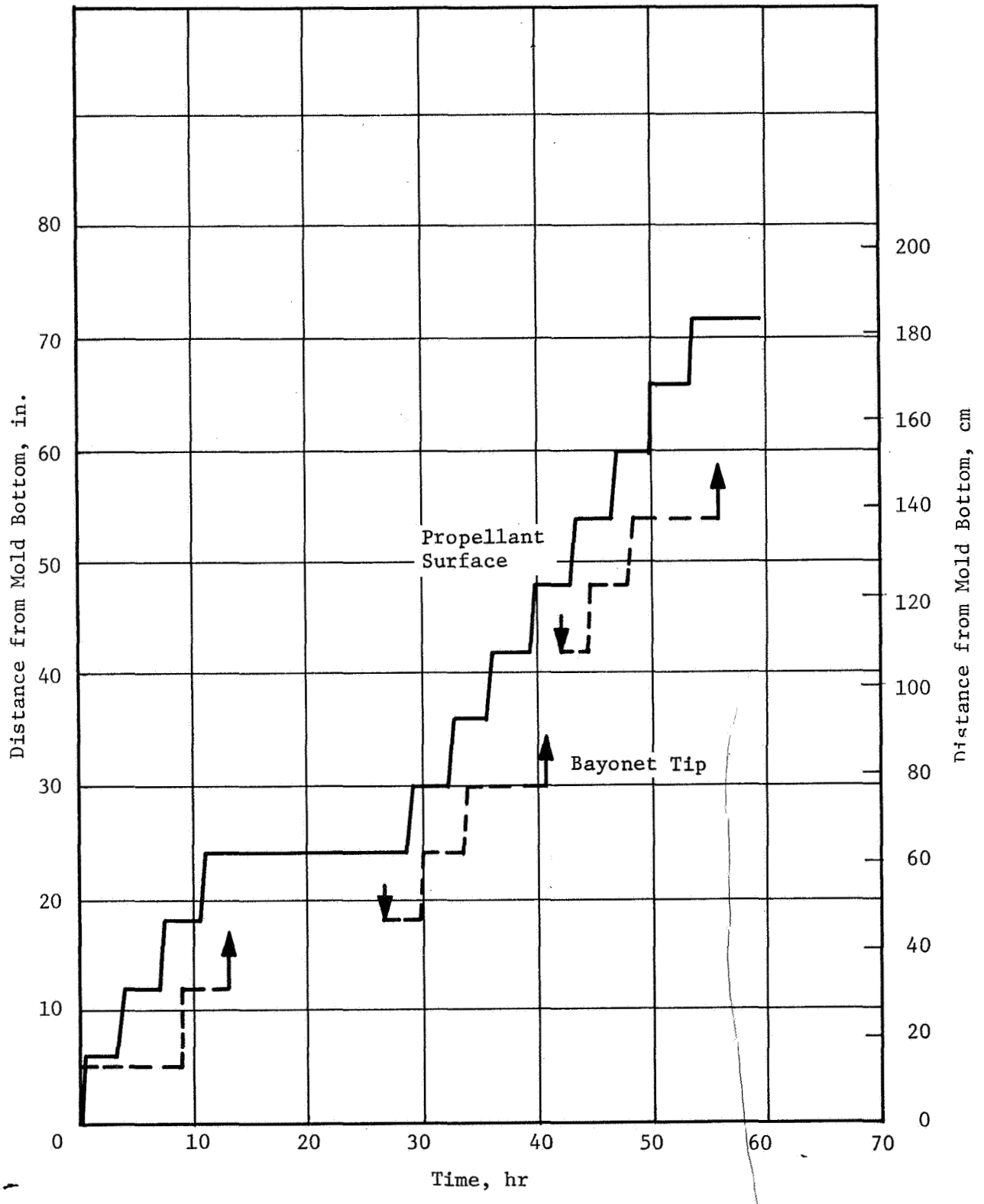
Safety Classification Testing for
ANB-3350 Type Propellant

Figure 129

Oxidizer Blend Ratio, SSMP/MA	60/40
Burning Rate Additives	
Iron Oxide, wt%	2.00
Iron Blue, wt%	0.10
FC-167 (wetting agent), equivalents	20
FC-151 (cure catalyst), wt%	0.05
PBNA (antioxidant), wt%	0.10
DOA (plasticizer), wt% of binder	30
Binder	
PBAN (terpolymer), equivalents	80
DER-332 (curing agent), equivalents	82

ANB-3350 Propellant Formulation Selection for Task III Process Demonstration

Figure 130



Planned Casting Sequence for Task III

Figure 131

Component	Test	Premix Batch 22D-181MP-001	Premix Batch 22D-181MP-002	Target Requirements
Submix	H_2O Content, %	0.029	0.045	0.20 max
	Acid Equivalents, 100 g	0.0407	0.0411	0.0403 ± 0.005
	Refractive Index at 25°C	1.4935	1.4933	Information
	Liquid Density, g/cm^3	0.933	0.935	0.931 ± 0.007
	FC-167 Content, %	0.597	*	0.60 ± 0.10
Premix I	Liquid Densit, g/cm^3	1.049	1.052	1.051 ± 0.007
	Ash Content, %	13.44	13.86	13.67 Information
Premix II	H_2O Content, %	0.066	0.054	0.25 max
	Liquid Density, g/cm^3	1.506	1.508	1.509 ± 0.007

* Test results invalid.

Submix and Premix Analyses for Propellant Cast into Second Full-Scale Mold

Figure 132

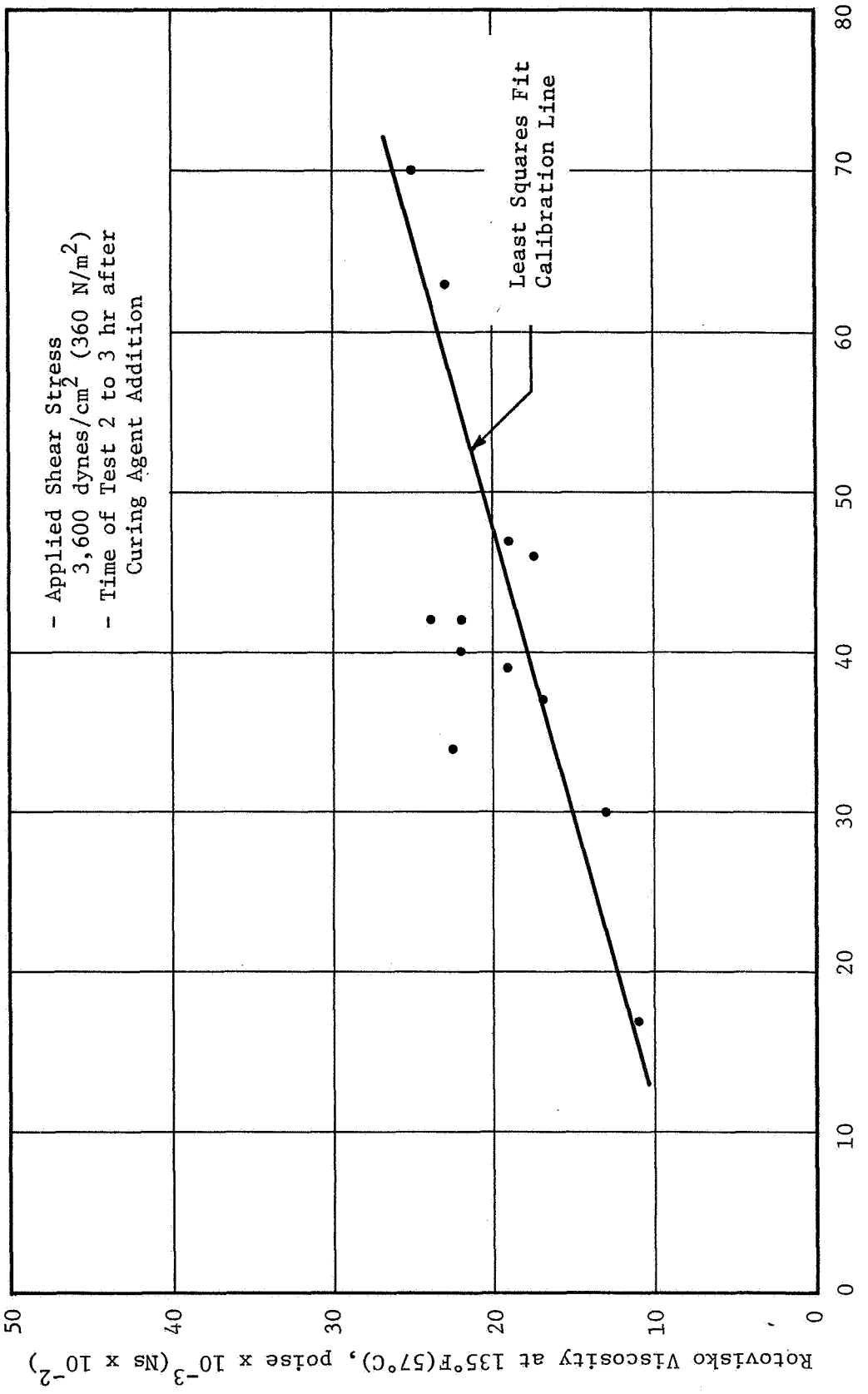
NASA CR 72621

Batch Designation 22D-181		Propellant Premix Batch	Oxidizer Ratio Blend SS/MA	Density, g/cm^3	DER-332 Content, %	LSBR 600 psig (414 N/cm^2) and 80°F (27°C)		Falling Ball Test			Rotovisko Viscosity,** poise x 10^{-3} (Ns/m^2 x 10^{-2})		
						in./sec	(cm/sec)	Drop Time, sec	Time from DER-332 Addition, hr	Draw-Off Temp, °F (°C)	3 hr	6 hr	10 hr
001		001	60/40	1.780	1.01	0.718	(1.82)	39	1.8	134 (57)	17	20	30
002		001	60/40	1.779	0.97	0.714	(1.81)	63	2.2	132 (56)	21	29	43
003		001	60/40	1.779	0.94	0.726	(1.84)	40	2.2	131 (55)	19	24	32
004		001	60/40	1.781	0.93	0.712	(1.81)	46	2.3	132 (56)	16	19	28
005		001	60/40	1.775	1.00	0.743	(1.89)	42	1.7	130 (54)	19	27	41
006		002	60/40	1.785	1.02	0.730	(1.85)	42	2.3	130 (54)	21	25	31
	$\bar{X}$			1.780	0.98	0.724	(1.84)						
	S			0.0033	0.038	0.012	(0.030)						
007		002	65/35	1.780	1.03	0.696	(1.77)	34	1.6	132 (56)	20	26	35
008		001	65/35	1.781	1.01	0.691	(1.76)	70	3.3	130 (54)	21	24	32
009		002	65/35	1.781	0.99	0.660	(1.68)	30	2.0	130 (54)	11	15	20
010*		002	65/35	1.775	1.02	0.627	(1.59)	17	1.9	132 (56)	10	12	18
011*		002	65/35	1.788	0.99	0.699	(1.78)	47	2.0	130 (54)	17	20	35
012		002	65/35	1.783	1.00	0.673	(1.71)	37	1.8	130 (54	15	19	26
	$\bar{X}$			1.781	1.01	0.680	(1.73)						
	S			0.0013	0.017	0.016	(0.041)						
$\bar{X}$				1.780	0.99	-	-	-					
S				0.0026	0.033	-	-	-					
Target Requirements				1.781 ± 0.007	0.93 ± 0.10	0.680 ± 0.030	(1.73) ± (0.08)						

* Not included in statistical analyses due to processing anomaly.
** Viscosity at 135°F (57°C), 5,000 dynes/cm^2 (500 N/m^2) shear stress, 3, 6, and 10 hr from curing agent addition.

Uncured Propellant Data, Second Full-Scale Mold

Figure 133



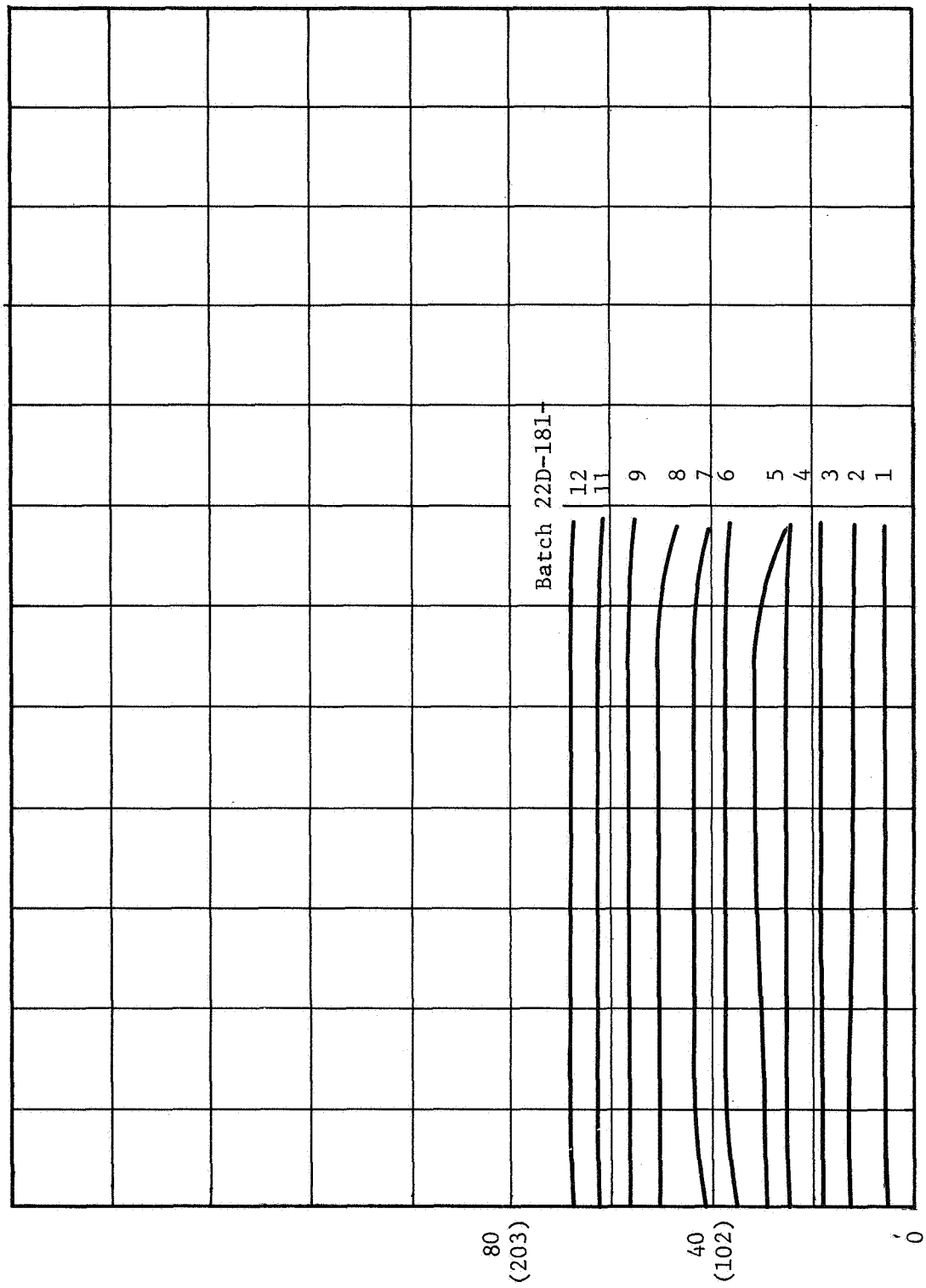
Correlation of Falling Ball Test with Rotovisko Data

Figure 134

Batch No. 22D-181-	Cast Sequence	Cast Time, min	Time between Batches, hr	Time from Curing Agent Addition to End of Cast, hr
001	1	24		3.6
002	2	30	4.8	4.0
003	3	28	4.8	3.6
004	4	25	4.2	3.6
005	5	29	18.6	3.4
006	6	31	3.9	3.7
008	7	34	6.1	5.1
007	8	26	4.4	3.5
009	9	24	3.7	3.3
011	10	32	7.2	3.7
012	11	28	5.0	3.6

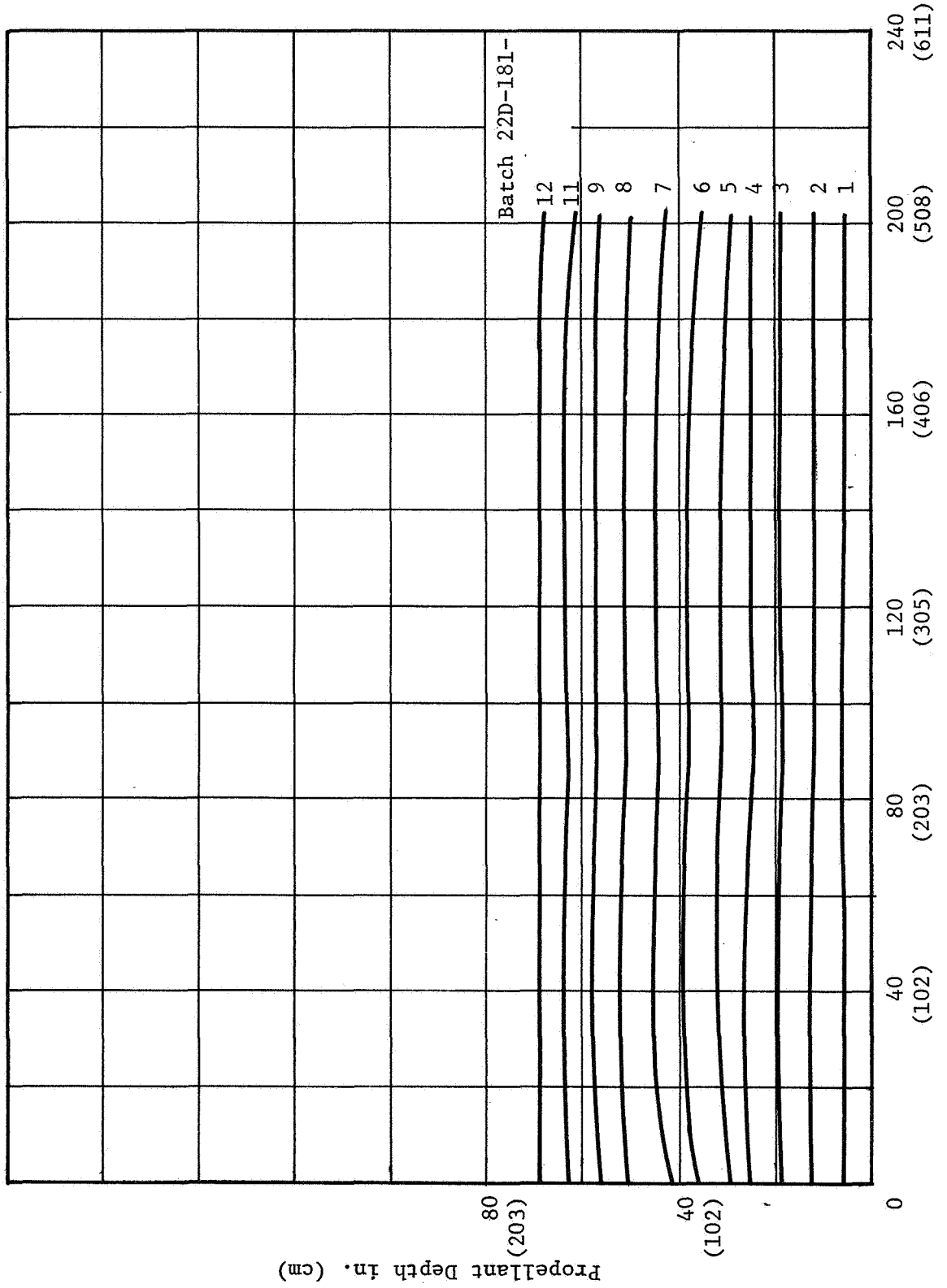
Process Times for Second Full-Scale Mold Casting

Figure 135



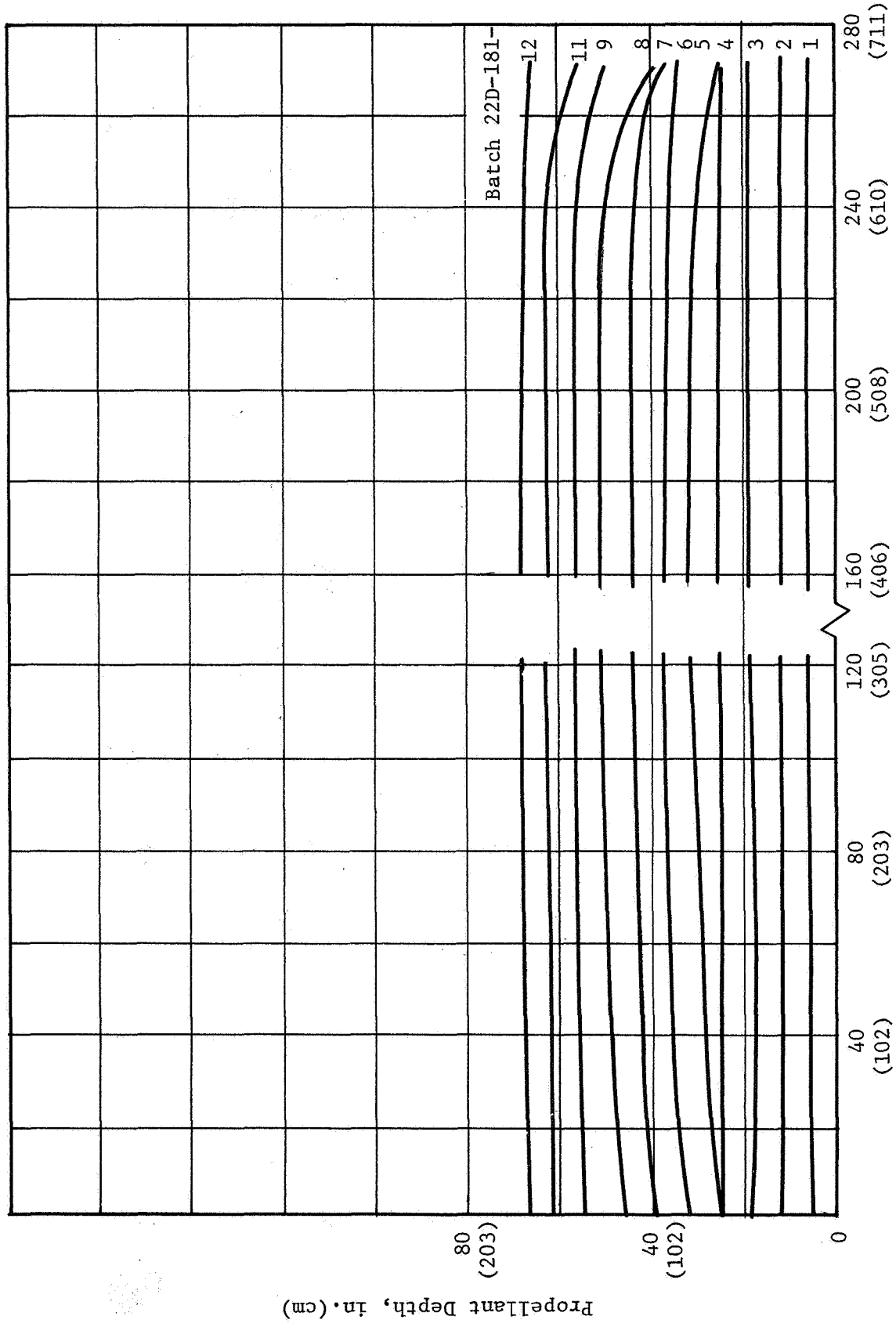
Batch-to-Batch Depth Contours for Inside Wall, Second Full-Scale Mold

Figure 136



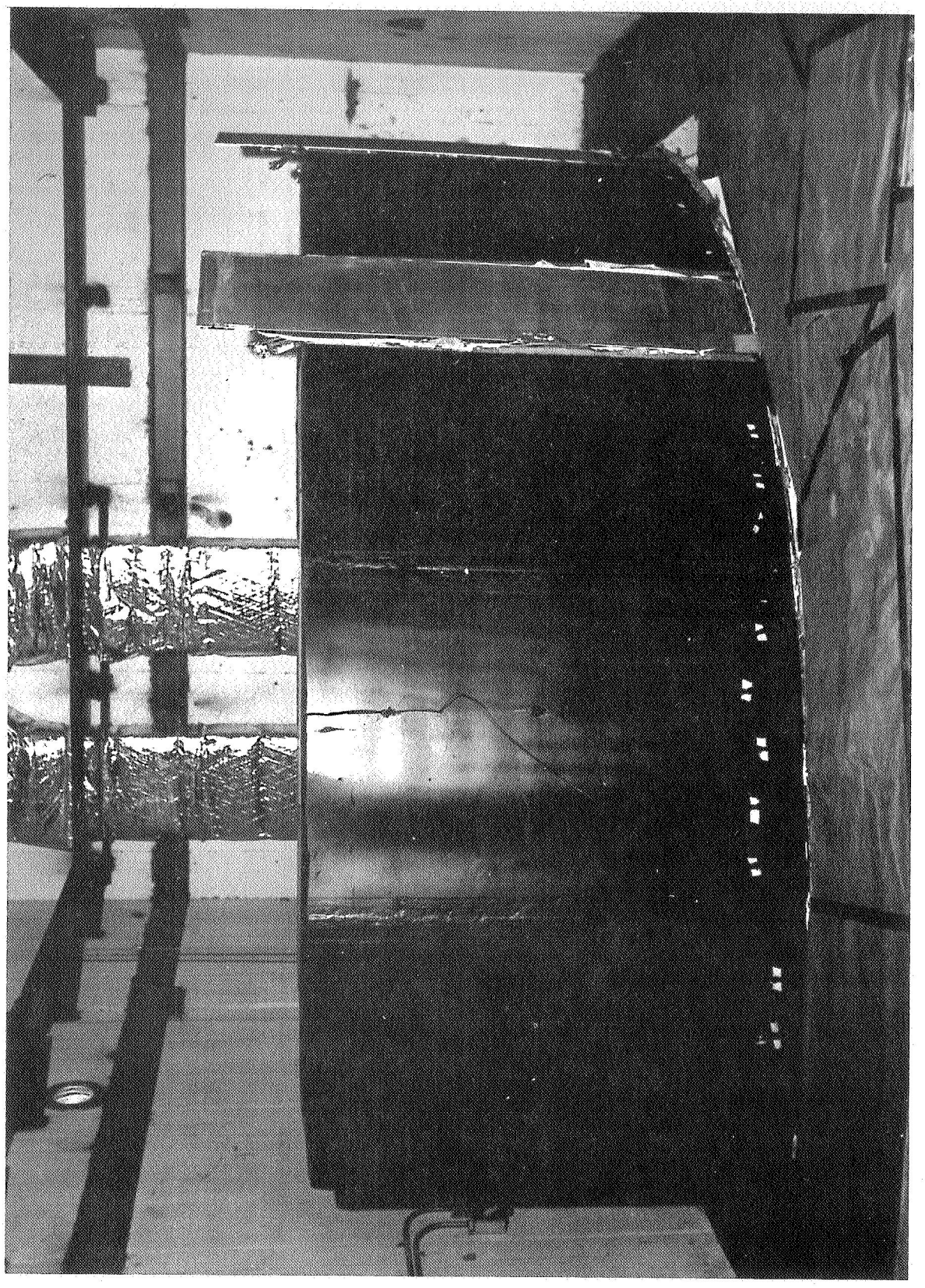
Batch-to-Batch Depth Contours for Mid-Points, Second Full-Scale Mold

Figure 137



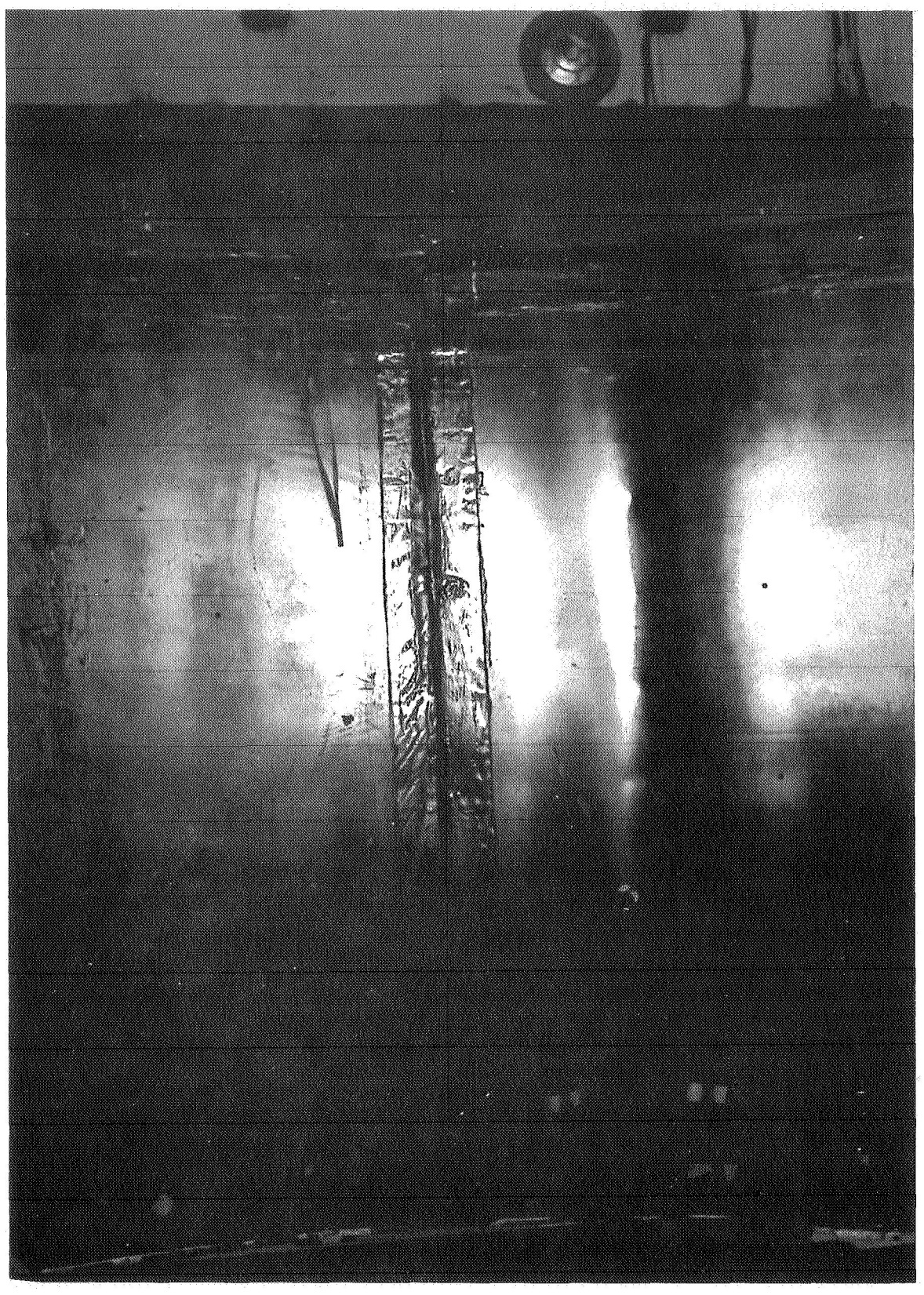
Batch-to-Batch Depth Contours for Outside Wall, Second Full-Scale Mold

Figure 138



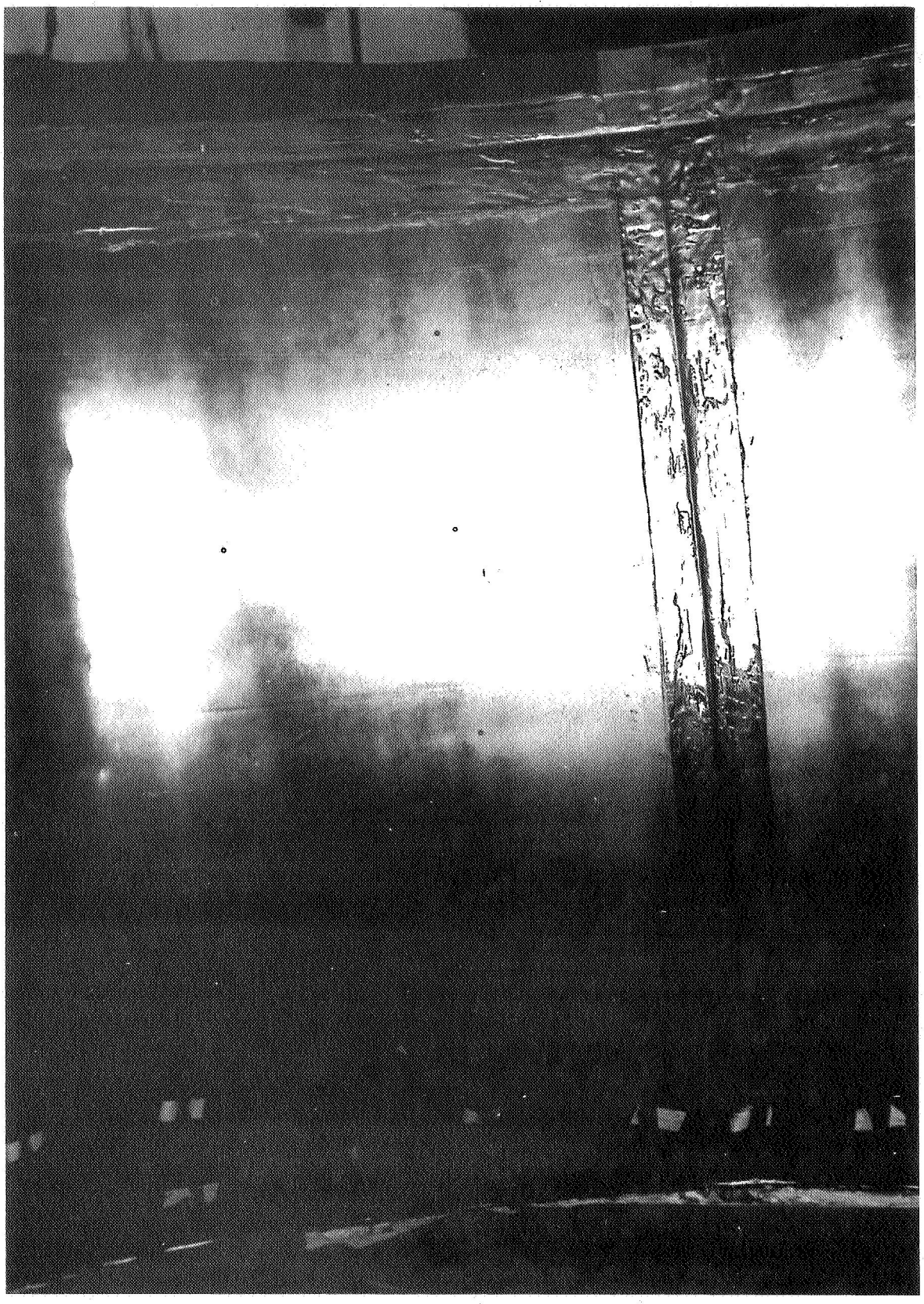
Outside Diameter of Cured Mold, Overall View

Figure 139



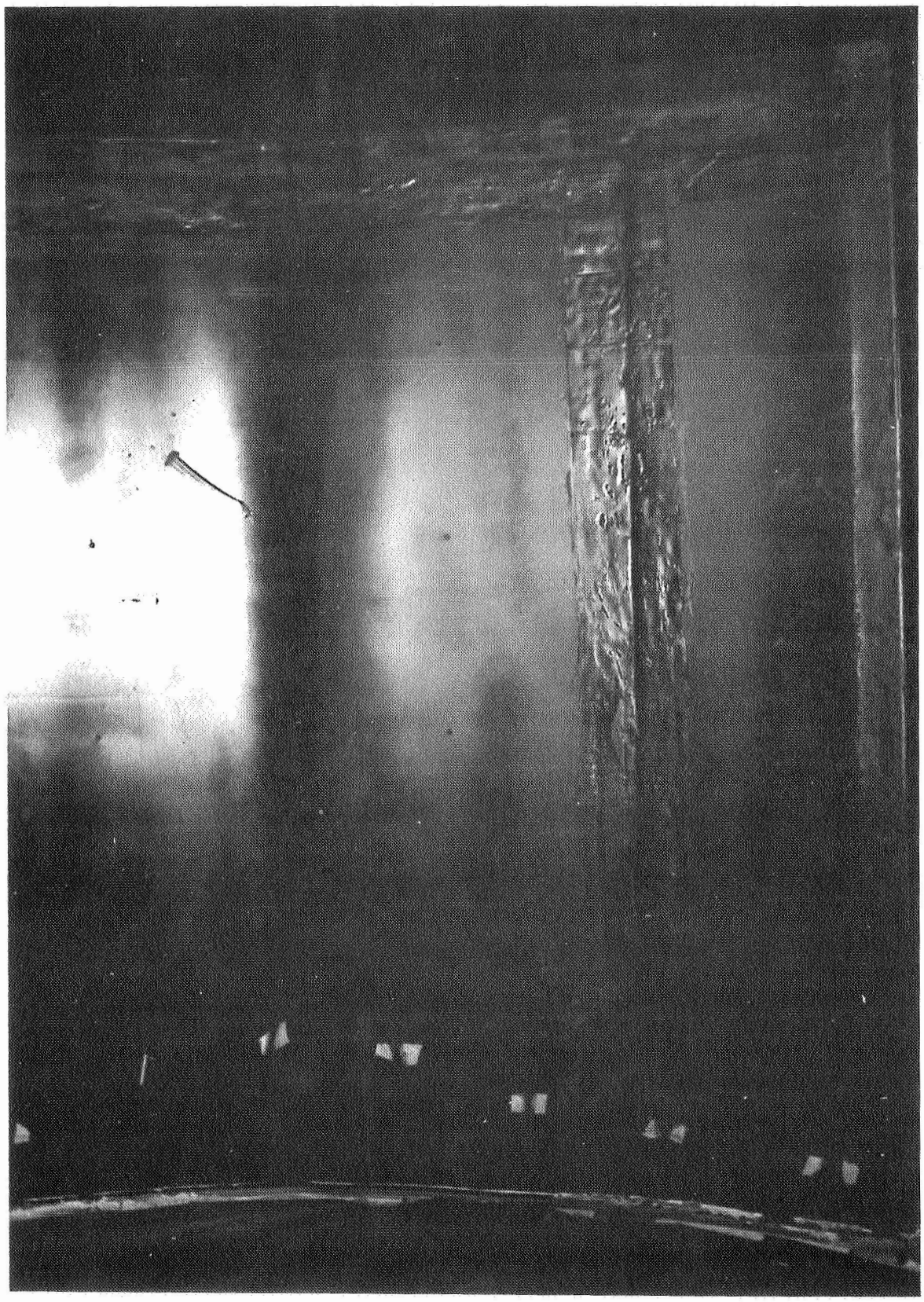
Inside Diameter of Cured Mold, Left Hand View

Figure 140



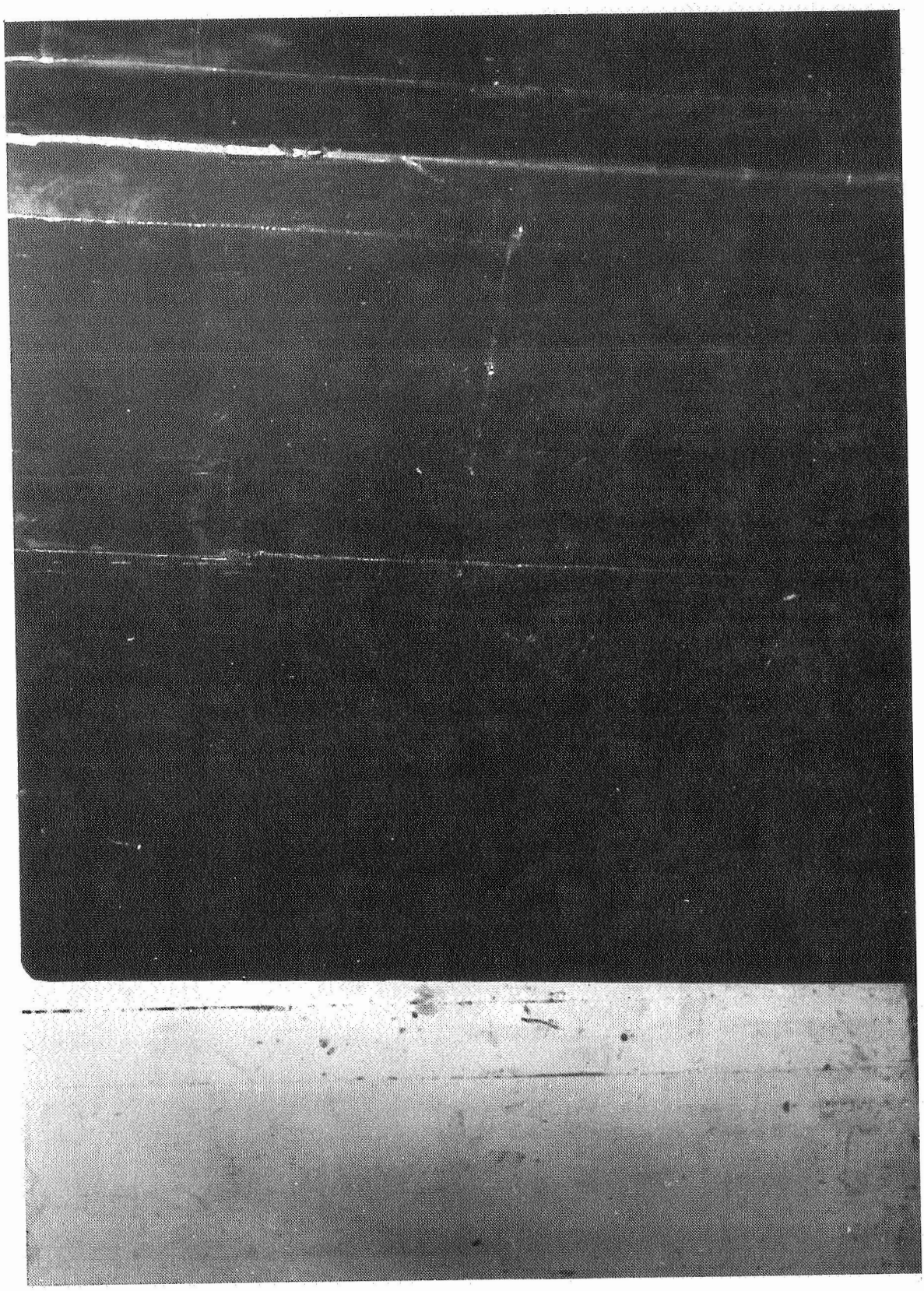
Inside Diameter of Cured Mold, Central View

Figure 141



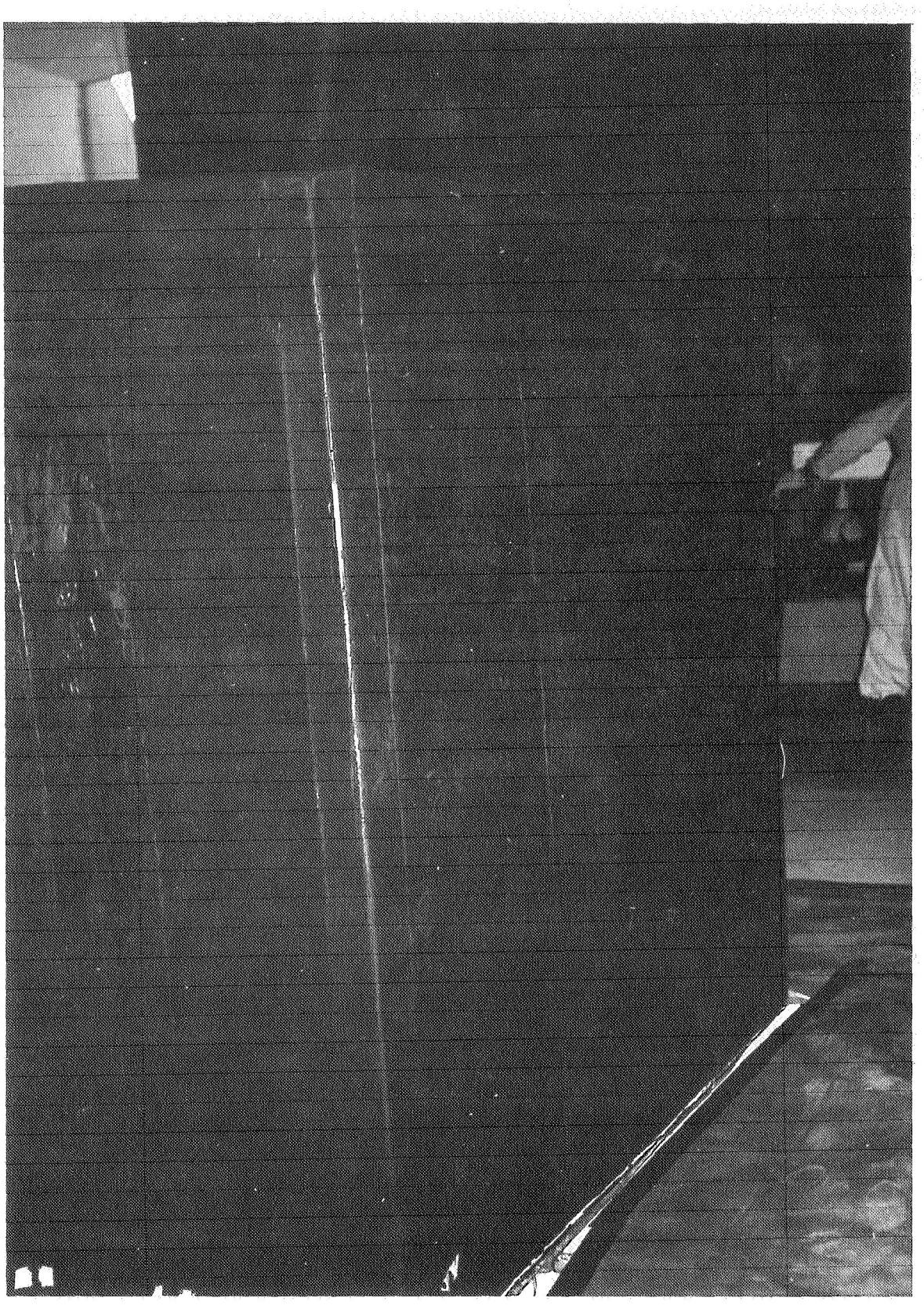
Inside Diameter of Cured Mold, Right Hand View

Figure 142



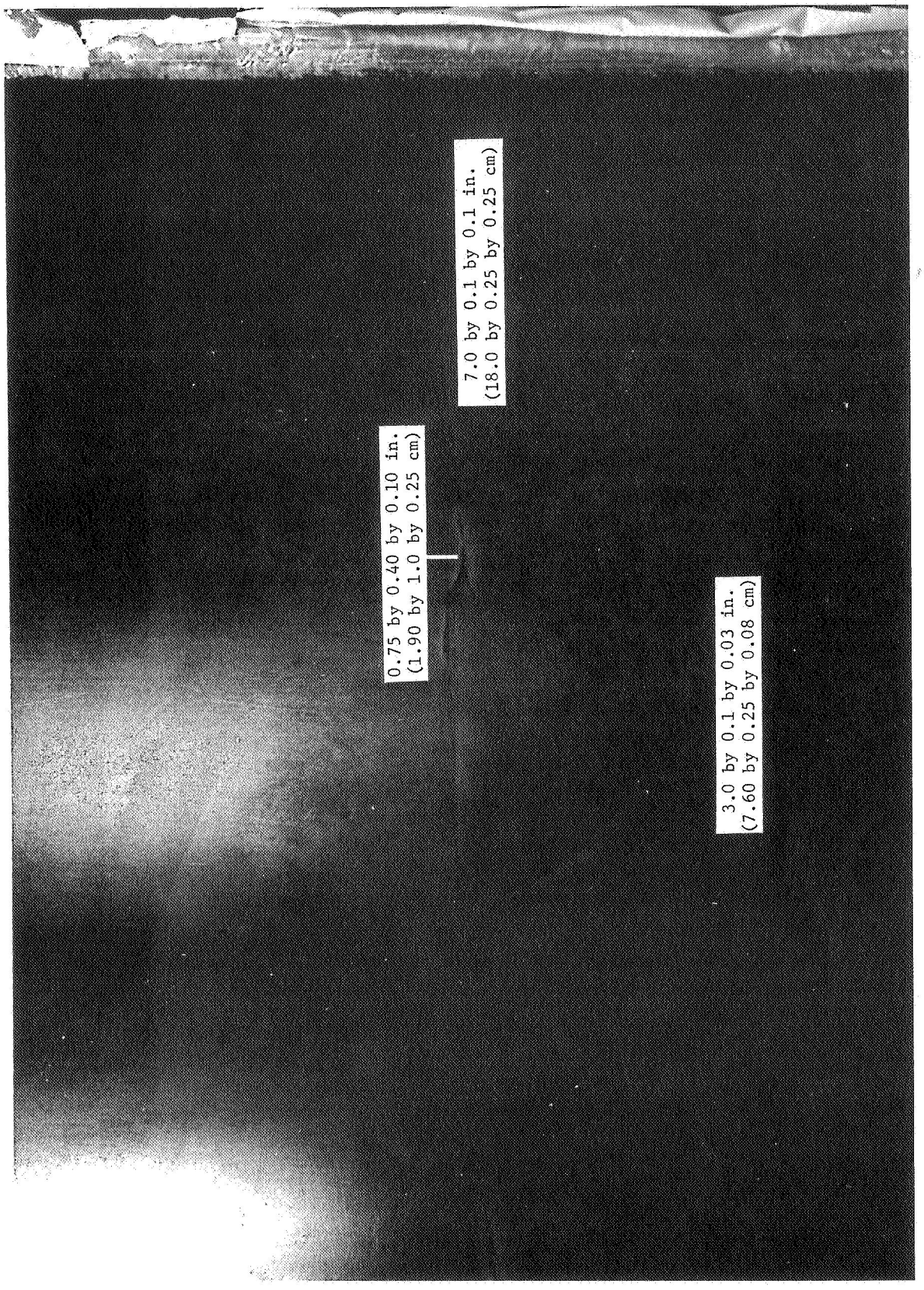
Northeast End of Cured Mold

Figure 143



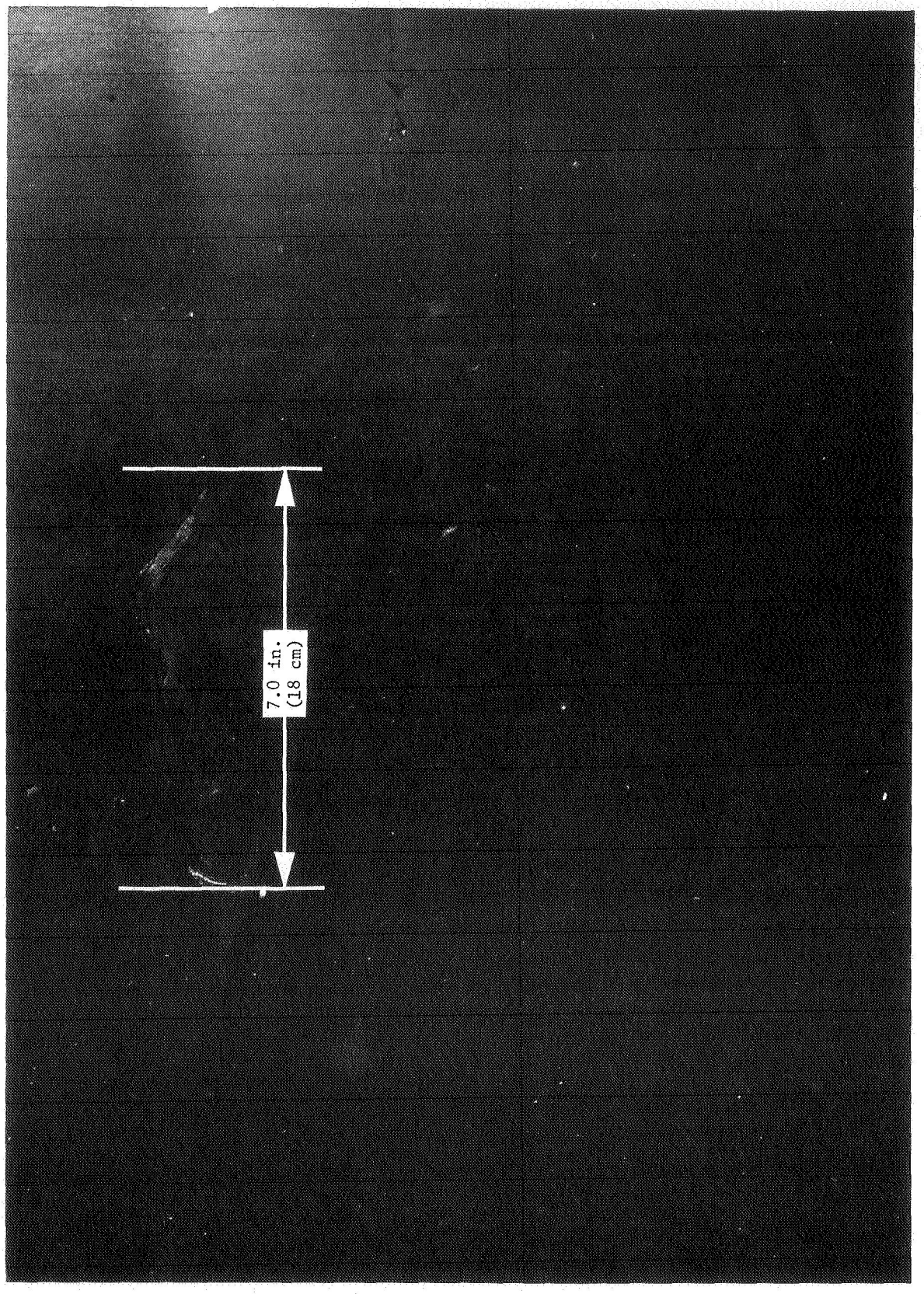
West End of Cured Mold

Figure 144



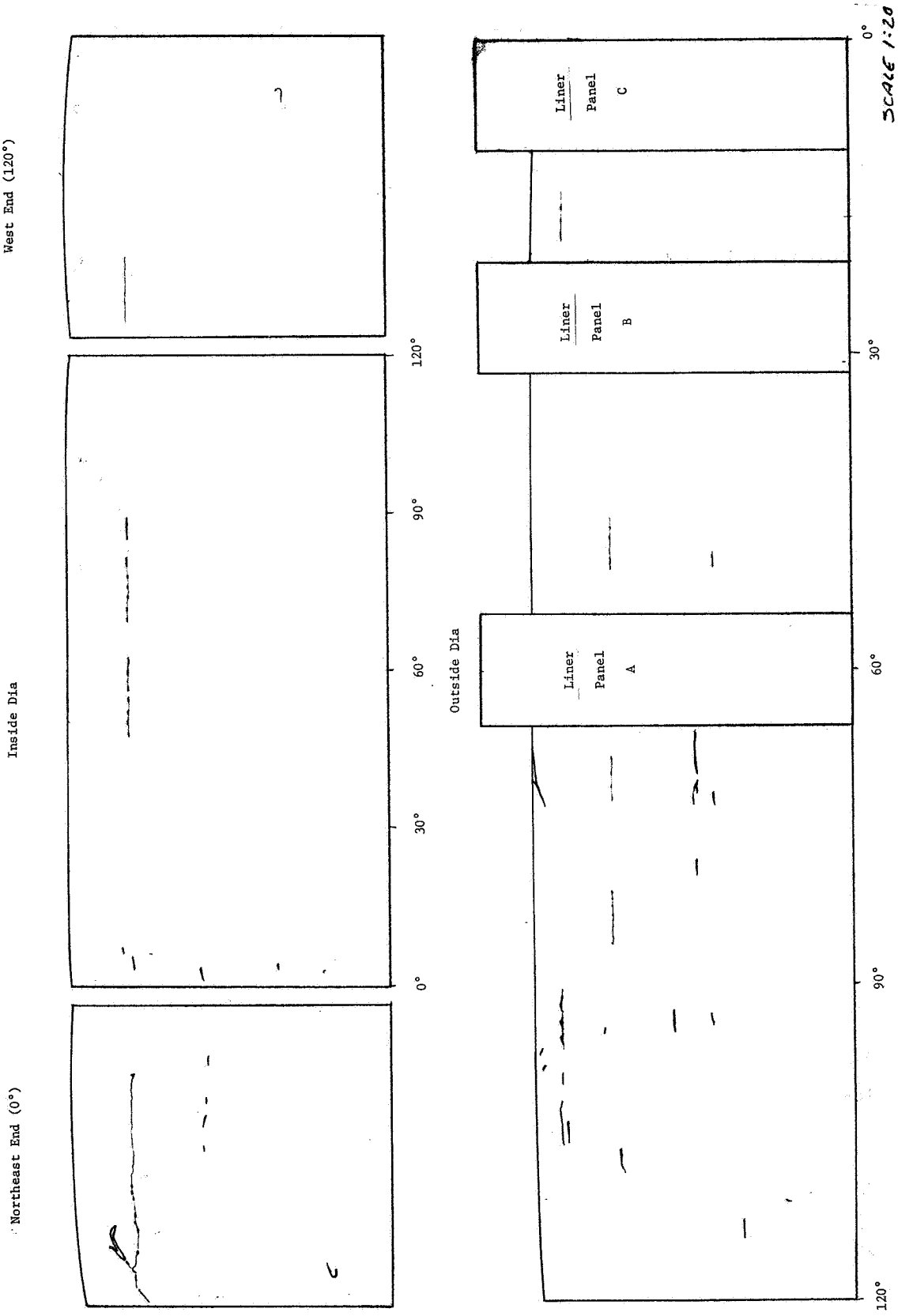
Surface Defects in Outside Diameter of Cured Mold

Figure 145



Surface Defects in Northeast End of Cured Mold

Figure 146



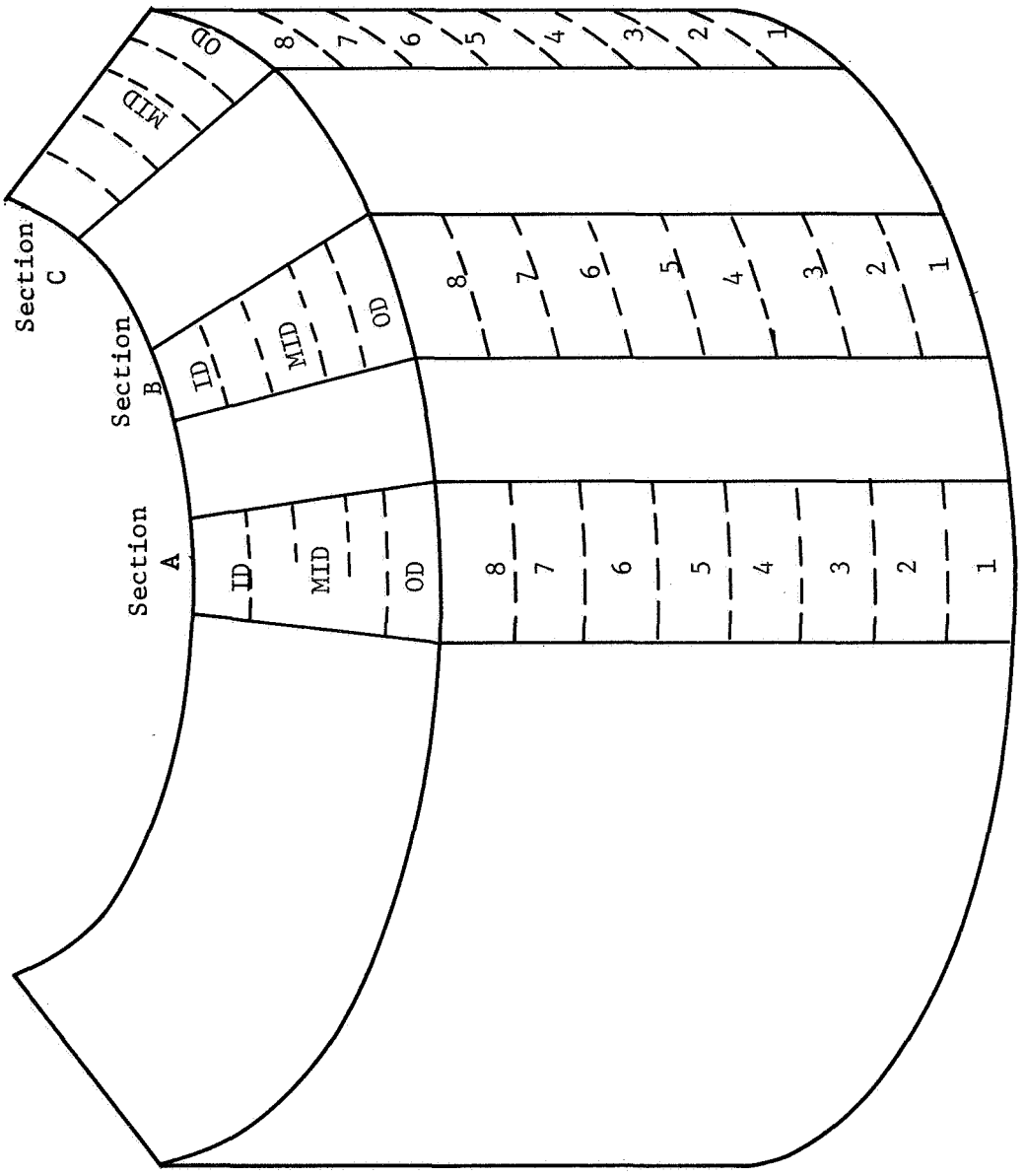
Map of Surface Defects in the Second Full-Scale Mold

Figure 147

Batch No. 22D-181-	Cure Time at 135°F (57°C) days	Shore A Hardness	Mechanical Properties at 77°F (25°C) σ_m, psi	(N/cm^2)	ε_m, %	ε_b, %	E_o, psi	(N/cm^2)
001	14	36	72	(50)	24	25	448	(309)
	17	39	75	(52)	24	25	404	(279)
	21	40	74	(51)	23	25	420	(290)
002	14	33	70	(48)	25	26	361	(249)
	17	36	68	(47)	26	28	341	(235)
	21	37	70	(48)	25	27	350	(242)
003	14	34	70	(48)	25	26	370	(255)
	17	36	70	(48)	24	26	372	(257)
	21	37	69	(48)	24	25	372	(257)
004	14	41	80	(55)	22	23	442	(305)
	17	39	70	(54)	23	24	431	(297)
	21	39	78	(54)	24	25	424	(293)
005	14	38	75	(52)	24	24	404	(279)
	17	40	76	(52)	25	26	380	(262)
	21							
006	14	42	79	(54)	21	22	485	(335)
	17	41	79	(54)	21	23	479	(331)
	21							
007	14	40	78	(54)	23	24	431	(297)
	17	41	80	(55)	24	25	422	(291)
	21							
008	14	39	74	(51)	27	29	361	(249)
	17	37	76	(52)	25	27	396	(273)
	21							
009	14	40	75	(52)	25	26	409	(282)
	17	42	79	(54)	25	26	431	(297)
	21	42	79	(54)	23	24	444	(306)
011	14	34	67	(46)	25	27	335	(231)
	17	36	69	(48)	22	23	404	(279)
	21	36	72	(50)	20	20	457	(315)
012	14	34	61	(42)	21	22	354	(244)
	17	33	66	(46)	26	27	341	(235)
	21	35	69	(48)	25	27	367	(253)

Mechanical Properties from Carton Samples of Propellant Cast into the Second Full-Scale Mold

Figure 148



Sample Locations for the Second Full-Scale Mold

Figure 149

Sample Location	Orientation	Mechanical Properties at 77°F (25°C) σ_m, psi	(N/cm^2)	ε_m, %	ε_b, %	E_o, psi	(N/cm^2)	Burning Rate at 80°F (27°C) and 600 psig (414 N/cm^2) in./sec	(cm/s)
ID-1	Vertical	83	(57)	20	21	542	(374)	0.678	(1.72)
	Horizontal	75	(52)	26	27	380	(262)	0.668	(1.70)
ID-2	Vertical	83	(57)	20	21	564	(389)	0.690	(1.75)
	Horizontal	89	(61)	24	25	492	(339)	0.699	(1.78)
ID-3	Vertical	93	(64)	18	19	664	(458)	0.672	(1.71)
	Horizontal	91	(63)	23	24	544	(375)	0.690	(1.75)
ID-4	Vertical	90	(62)	20	20	601	(415)	0.667	(1.69)
	Horizontal	90	(62)	19	20	651	(449)	0.730	(1.85)
ID-5	Vertical	94	(65)	17	18	739	(510)	0.724	(1.84)
	Horizontal	80	(55)	27	29	391	(270)	0.680	(1.73)
ID-6	Vertical	88	(61)	20	21	625	(431)	0.751	(1.91)
	Horizontal	88	(61)	19	20	653	(450)	0.738	(1.87)
ID-7	Vertical	87	(60)	15	15	745	(514)	0.730	(1.85)
	Horizontal	89	(61)	19	21	660	(455)	0.730	(1.85)
ID-8	Vertical	89	(61)	21	24	618	(426)	0.697	(1.77)
	Horizontal	94	(65)	19	20	649	(448)	0.758	(1.92)

Mechanical and Bonding Properties and Burning Rate of
Propellant Specimens Taken from the Second Full-Scale Mold (Section A)

Sample Location	Orientation	Mechanical Properties at 77°F (25°C)						Burning Rate at 80°F (27°C) and 600 psig (414 N/cm²)	
		σ_m, psi	(N/cm^2)	ε_m, %	ε_b, %	E_o, psi	(N/cm^2)	in./sec	(cm/s)
Mid-1	Vertical	76	(52)	23	25	448	(309)	0.653	(1.66)
	Horizontal	89	(61)	20	21	612	(422)	0.645	(1.64)
Mid-2	Vertical	83	(57)	22	22	503	(347)	0.645	(1.63)
	Horizontal	100	(69)	18	19	741	(511)	0.713	(1.81)
Mid-3	Vertical	83	(57)	22	24	507	(350)	0.950	(2.41)
	Horizontal	91	(63)	22	23	586	(404)	0.637	(1.62)
Mid-4	Vertical	86	(59)	19	23	647	(446)	0.644	(1.64)
	Horizontal	80	(55)	20	21	522	(360)	0.665	(1.69)
Mid-5	Vertical	89	(61)	20	22	618	(426)	0.627	(1.59)
	Horizontal	82	(57)	21	24	553	(381)	0.635	(1.61)
Mid-6	Vertical	92	(63)	18	19	651	(449)	0.675	(1.71)
	Horizontal	88	(61)	20	22	603	(416)	0.657	(1.67)
Mid-7	Vertical	86	(59)	21	23	562	(388)	0.663	(1.68)
	Horizontal	81	(56)	24	25	490	(338)	0.648	(1.65)
Mid-8	Vertical	74	(51)	21	22	466	(322)	0.663	(1.68)
	Horizontal	74	(51)	17	17	544	(375)	0.663	(1.68)

Mechanical and Bonding Properties and Burning Rate of
Propellant Specimens Taken from the Second Full-Scale Mold (Section A)

Sample Location	Orientation	Mechanical Properties at 77°F (25°C) σ_m, psi	(N/cm^2)	ε_m, %	ε_b, %	E_o, psi	(N/cm^2)	Bond Strength at 77°F (25°C) Tensile psi	(N/cm^2)	Shear psi	(N/cm^2)	Burning Rate at 80°F (27°C) and 600 psig (414 N/cm^2) in./sec	(cm/s)
OD-1	Vertical	92	(63)	19	20	656	(453)					0.690	(1.75)
	Horizontal	89	(61)	19	19	653	(451)	87	(60)	78	(54)	0.690	(1.75)
OD-2	Vertical	89	(61)	19	20	645	(445)					0.725	(1.84)
	Horizontal	88	(61)	19	20	632	(436)	92	(63)	77	(53)	0.726	(1.84)
OD-3	Vertical	90	(62)	18	18	708	(488)					0.772	(1.96)
	Horizontal	90	(62)	19	20	684	(472)	86	(59)	65	(45)	0.723	(1.84)
OD-4	Vertical	94	(65)	19	22	721	(498)					0.708	(1.80)
	Horizontal	92	(63)	18	20	715	(493)	84	(58)	74	(51)	0.733	(1.86)
OD-5	Vertical	90	(62)	19	23	736	(508)					0.702	(1.78)
	Horizontal	89	(61)	19	20	656	(453)	85	(59)	73	(50)	0.688	(1.75)
OD-6	Vertical	93	(64)	18	19	739	(510)					0.677	(1.72)
	Horizontal	91	(63)	18	19	732	(505)	87	(60)	79	(54)	0.693	(1.76)
OD-7	Vertical	89	(61)	18	19	712	(492)					0.723	(1.84)
	Horizontal	87	(60)	18	19	684	(472)	81	(56)	66	(46)	0.732	(1.86)
OD-8	Vertical	90	(62)	18	20	736	(508)					0.699	(1.78)
	Horizontal	90	(62)	18	20	723	(499)	84	(58)	70	(48)	0.742	(1.88)

Specimen Properties, Second Full-Scale Mold (Section A)

Figure 152

Sample Location	Orientation	Mechanical Properties at 77°F (25°C) σ_m, psi	(N/cm^2)	ε_m, %	ε_b, %	E_o, psi	(N/cm^2)	Burning Rate at 80°F (27°C) and 600 psig (414 N/cm^2) in./sec	(cm/s)
ID-1	Vertical	79	(54)	22	23	496	(342)	0.675	(1.71)
	Horizontal	82	(57)	21	22	509	(351)	0.670	(1.70)
ID-2	Vertical	77	(53)	19	21	531	(366)	0.710	(1.80)
	Horizontal	77	(53)	21	22	474	(327)	0.640	(1.63)
ID-3	Vertical	86	(59)	20	22	599	(413)	0.704	(1.79)
	Horizontal	76	(52)	23	23	457	(315)	0.657	(1.67)
ID-4	Vertical	87	(60)	19	20	612	(422)	0.715	(1.82)
	Horizontal	79	(54)	22	22	457	(315)	0.669	(1.70)
ID-5	Vertical	90	(62)	18	19	704	(485)	0.729	(1.85)
	Horizontal	79	(54)	23	24	455	(314)	0.667	(1.69)
ID-6	Vertical	90	(62)	18	20	664	(458)	0.689	(1.75)
	Horizontal	80	(55)	23	23	459	(317)	0.663	(1.68)
ID-7	Vertical	88	(61)	17	18	682	(470)	0.729	(1.85)
	Horizontal	79	(54)	23	24	463	(320)	0.617	(1.57)
ID-8	Vertical	90	(62)	17	18	701	(483)	0.611	(1.55)
	Horizontal	82	(57)	23	24	481	(332)	0.612	(1.55)

Figure 153

Mechanical and Bonding Properties and Burning Rate of
Propellant Specimens Taken from the Second Full-Scale Mold (Section B)

Sample Location	Orientation	Mechanical Properties at 77°F (25°C) σ_m, psi	σ_m, (N/cm^2)	ε_m, %	ε_b, %	E_o, psi	E_o, (N/cm^2)	Burning Rate at 80°F (27°C) and 600 Psig (414 N/cm^2) in./sec	(cm/s)
Mid-1	Vertical	88	(61)	19	19	594	(410)	0.658	(1.67)
	Horizontal	92	(63)	22	24	610	(421)	0.694	(1.76)
Mid-2	Vertical	91	(63)	20	21	660	(455)	0.691	(1.76)
	Horizontal	92	(63)	19	19	686	(473)	0.695	(1.76)
Mid-3	Vertical	94	(65)	18	19	688	(475)	0.896	(2.28)
	Horizontal	90	(62)	19	20	621	(428)	0.655	(1.66)
Mid-4	Vertical	79	(54)	20	20	468	(323)	0.627	(1.59)
	Horizontal	86	(59)	22	23	557	(384)	0.642	(1.63)
Mid-5	Vertical	81	(56)	22	23	496	(342)	0.664	(1.69)
	Horizontal	78	(54)	21	23	538	(371)	0.627	(1.59)
Mid-6	Vertical	79	(54)	19	20	560	(386)	0.658	(1.67)
	Horizontal	79	(54)	20	23	540	(373)	0.664	(1.69)
Mid-7	Vertical	78	(54)	22	24	503	(347)	0.657	(1.67)
	Horizontal	79	(54)	21	23	533	(368)	0.660	(1.68)
Mid-8	Vertical	75	(52)	25	27	413	(285)	0.612	(1.55)
	Horizontal	78	(54)	22	24	514	(354)	0.665	(1.69)

Mechanical and Bonding Properties and Burning Rate of
Propellant Specimens Taken from the Second Full-Scale Mold (Section B)

Sample Location	Orientation	Mechanical Properties at 77°F (25°C)						Bond Strength at 77°F (25°C)				Burning Rate at 80°F (27°C) and 600 psig (414 N/cm²)	
		σ_m, psi	(N/cm^2)	ε_m, %	ε_b, %	E_o, psi	(N/cm^2)	Tensile psi	(N/cm^2)	Shear psi	(N/cm^2)	in./sec	(cm/s)
OD-1	Vertical	86	(59)	20	22	597	(412)					0.697	(1.77)
	Horizontal	90	(62)	20	22	612	(422)	85	(59)	63	(43)	0.714	(1.81)
OD-2	Vertical	89	(61)	20	23	642	(443)					0.710	(1.80)
	Horizontal	88	(61)	20	22	614	(423)	81	(56)	74	(51)	0.715	(1.82)
OD-3	Vertical	82	(57)	19	21	629	(434)					0.727	(1.85)
	Horizontal	92	(63)	18	19	710	(490)	82	(57)	72	(50)	0.731	(1.86)
OD-4	Vertical	81	(56)	19	22	588	(406)					0.722	(1.83)
	Horizontal	84	(58)	17	19	730	(504)	77	(53)	84	(58)	0.725	(1.84)
OD-5	Vertical	87	(60)	19	21	662	(457)					0.737	(1.87)
	Horizontal	92	(63)	18	21	695	(480)	81	(56)	75	(52)	0.753	(1.91)
OD-6	Vertical	90	(62)	18	20	736	(508)					0.722	(1.83)
	Horizontal	92	(63)	17	18	760	(525)	68	(47)	65	(45)	0.740	(1.88)
OD-7	Vertical	90	(62)	18	19	719	(496)					0.725	(1.84)
	Horizontal	92	(63)	19	19	684	(472)	84	(58)	73	(50)	0.734	(1.86)
OD-8	Vertical	88	(61)	18	19	725	(500)					0.684	(1.74)
	Horizontal	83	(57)	22	23	501	(346)	72	(50)	76	(52)	0.640	(1.63)

Specimen Properties, Second Full-Scale Mold (Section B)

Figure 155

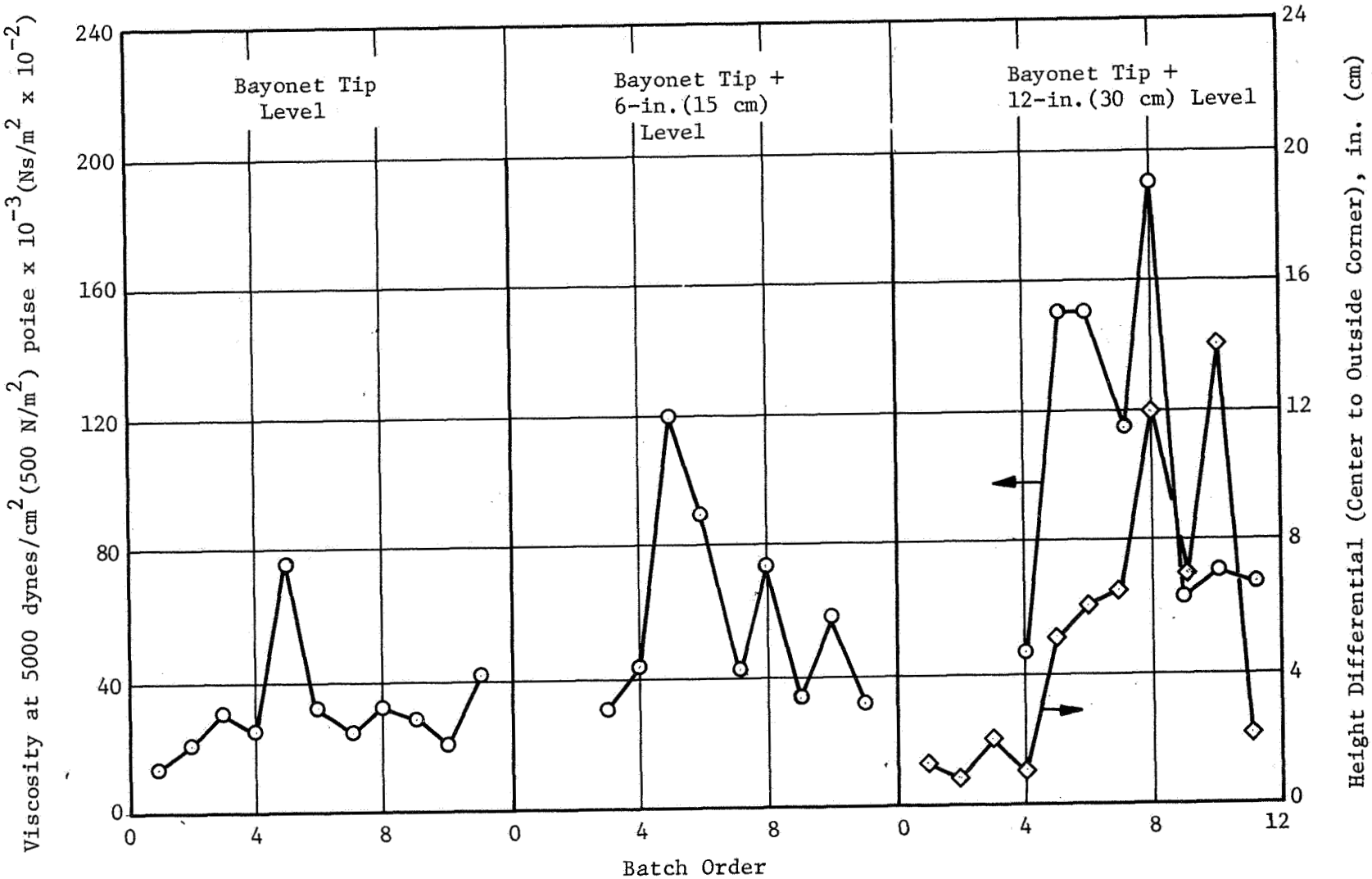
Sample Location	Orientation	Mechanical Properties at 77°F (25°C)						*Bond Strength at 77°F (25°C)				Burning Rate at 80°F (27°C) and 600 psig (414 N/cm²)	
		σ_m, psi	(N/cm²)	ε_m, %	ε_b, %	E_o, psi	(N/cm²)	Tensile psi	(N/cm²)	Shear psi	(N/cm²)	in./sec	(cm/s)
Mid-1	Vertical	86	(59)	20	22	570	(393)					0.679	(1.72)
	Horizontal	77	(54)	27	28	387	(267)	79	(54)	69	(48)	0.652	(1.66)
Mid-2	Vertical	83	(57)	18	19	682	(470)					0.637	(1.62)
	Horizontal	81	(56)	18	21	608	(419)	82	(57)	73	(50)	0.638	(1.62)
Mid-3	Vertical	91	(63)	21	23	603	(416)					0.715	(1.82)
	Horizontal	73	(50)	27	29	378	(268)	84	(58)	67	(46)	0.634	(1.61)
Mid-4	Vertical	79	(54)	19	20	546	(377)					0.716	(1.82)
	Horizontal	78	(54)	24	26	466	(321)	78	(54)	68	(47)	0.707	(1.80)
Mid-5	Vertical	81	(56)	20	21	623	(430)					0.693	(1.76)
	Horizontal	93	(64)	19	20	719	(496)	78	(54)	68	(47)	0.750	(1.90)
Mid-6	Vertical	90	(62)	20	21	636	(439)					0.669	(1.70)
	Horizontal	78	(54)	23	23	461	(318)	83	(57)	71	(49)	0.710	(1.80)
Mid-7	Vertical	76	(52)	17	17	540	(373)					0.697	(1.77)
	Horizontal	77	(53)	21	21	474	(327)	77	(53)	69	(48)	0.673	(1.71)
Mid-8	Vertical	91	(63)	19	21	656	(453)					0.655	(1.66)
	Horizontal	94	(65)	19	21	684	(472)	78	(54)	67	(46)	0.752	(1.91)

* Bond samples taken from OD location.

Specimen Properties, Second Full-Scale Mold (Section C)

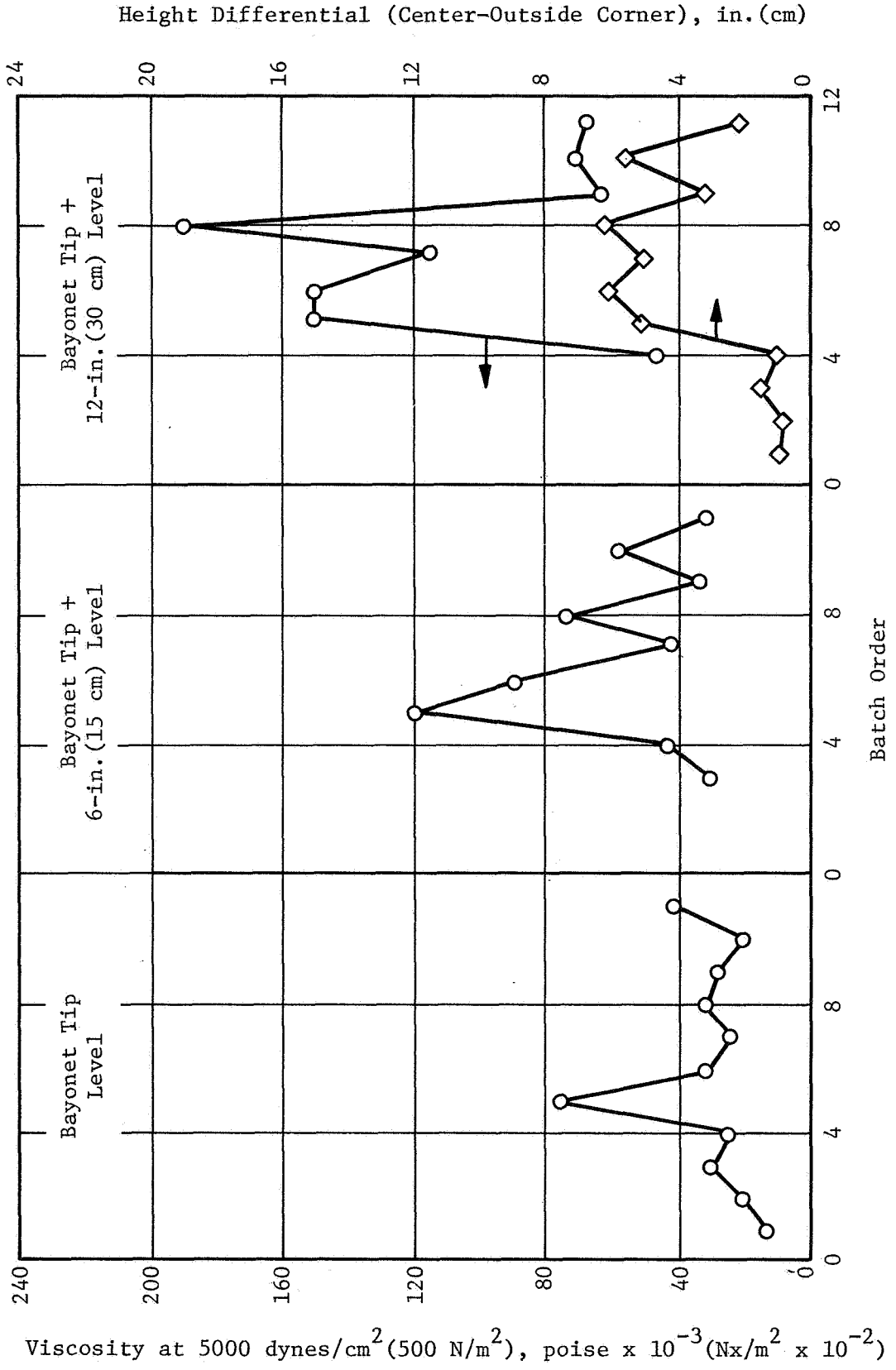
Figure 156

NASA CR 72621



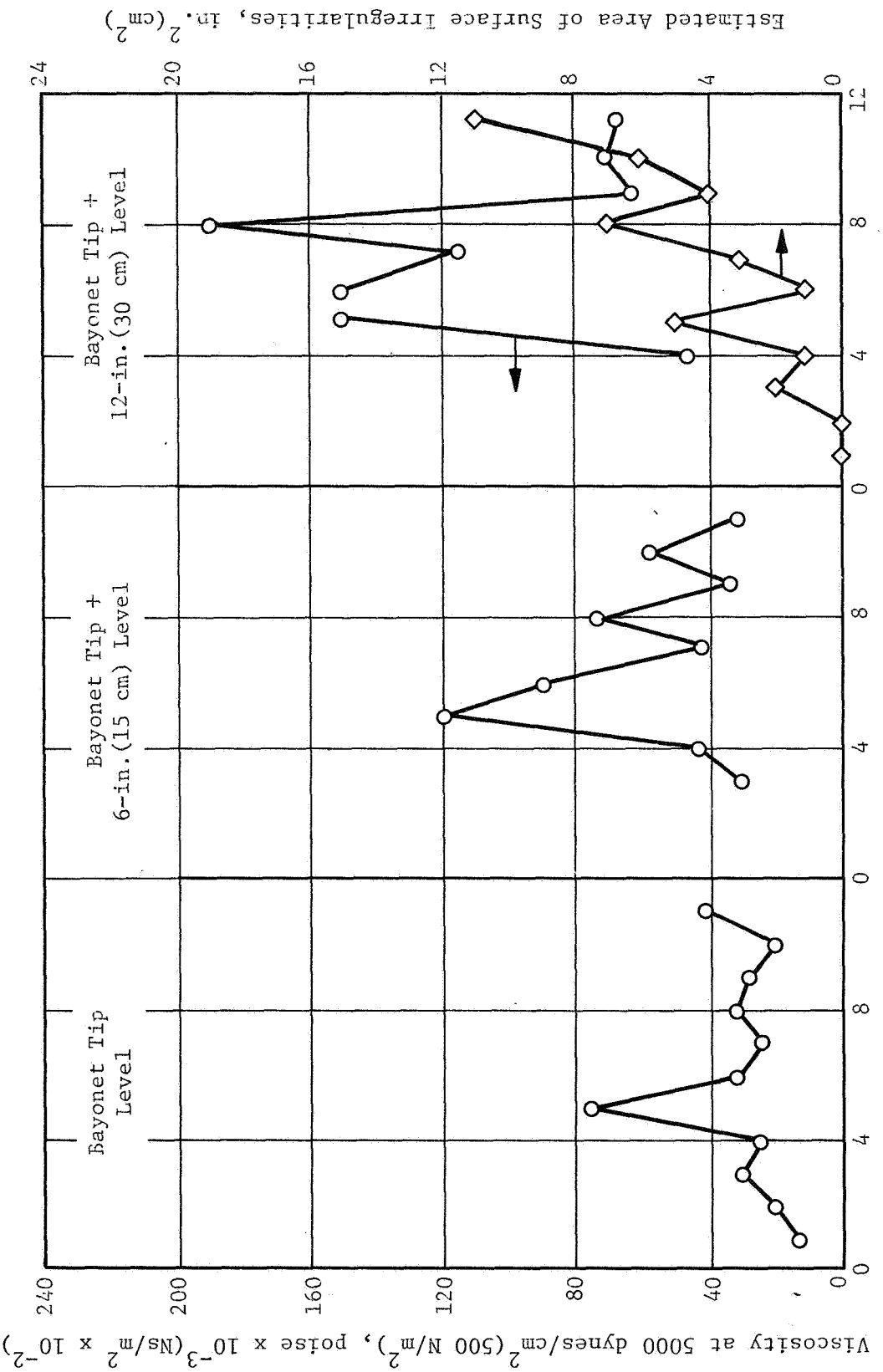
Comparison of Propellant Viscosities at Different Levels
With Surface Height in Second Full-Scale Mold
(Right Half of Mold)

Figure 157



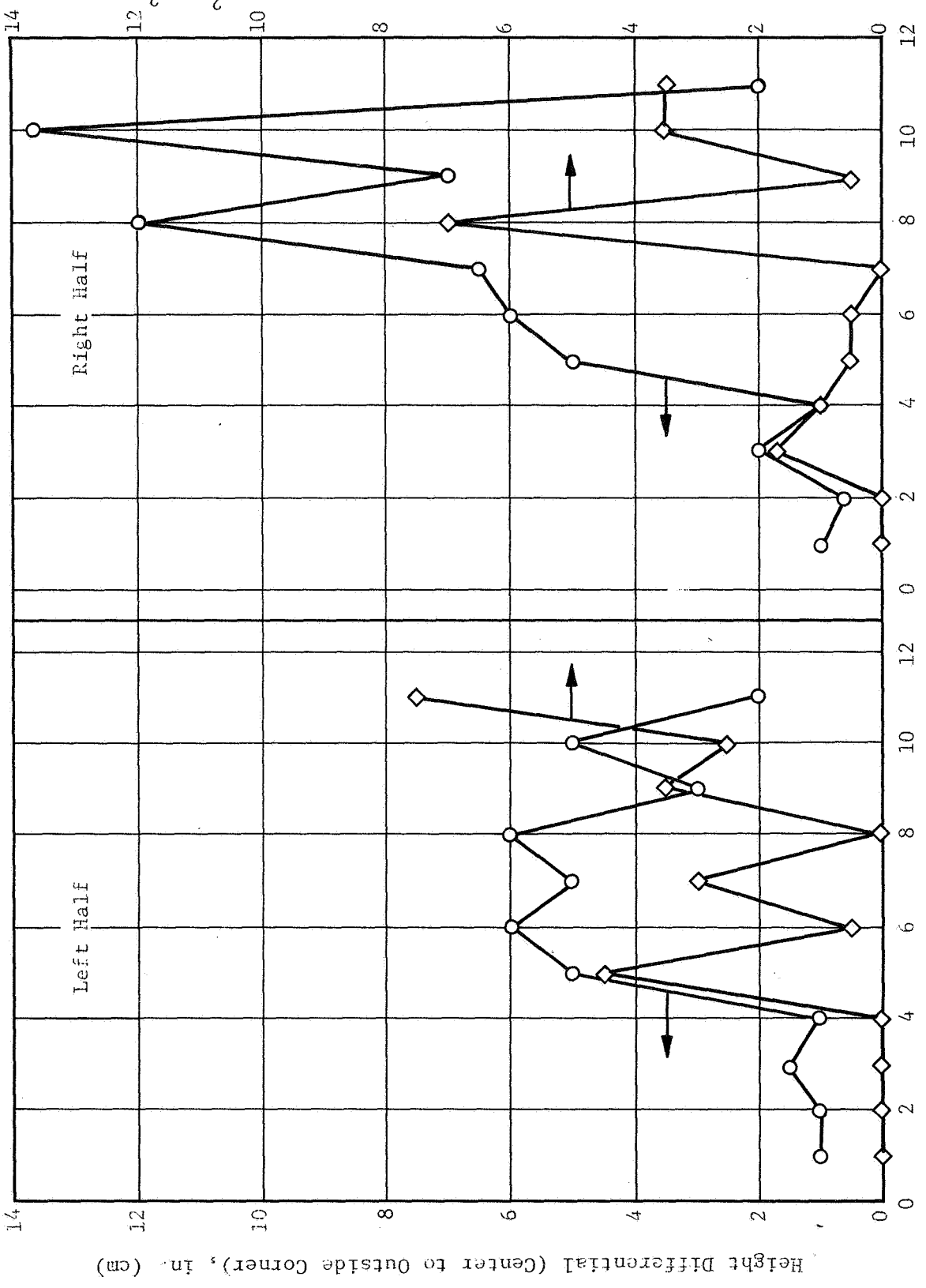
Comparison of Propellant Viscosities at Different Levels of Surface Height in Mold (Left Half of Mold)

Figure 158



Comparison of Propellant Viscosities at Different Levels with the Incidence of Surface Irregularities in Second Full-Scale Mold

Figure 159



Comparison of Height Differentials and Area of Surface Irregularities

Figure 160

APPENDIX

260-IN.-DIA MOTOR PROCESSING GUIDELINES

Appendix

On the basis of data obtained under Contract NAS3-12002 and in the processing of Motors 260-SL-1, -2 and -3, certain processing guidelines that provide increased assurance of propellant grain and bond integrity and motor reliability have been developed. These processing guidelines are to be used within the context of the facilities and equipment at the Aerojet-Dade facility, the procedures and materials used for processing Motor 260-SL-3, and the formulation improvements developed under Contract NAS3-12002.

1. Raw Materials

a. All propellant raw materials for a production run shall consist of a single homogeneous batch, or if multiple batches are required, a uniform blend. Particularly critical are the oxidizer, burning rate additives and the PBAN terpolymer. Triple cross-blending of the unground oxidizer is required. The process for blending the liquid PBAN terpolymer shall consist of mixing all batches used in the blend in an agitated tank.

b. A complete raw material lot qualification program using production mixing equipment must be accomplished to select the specific propellant formulation to be cast into the motor. Specific formulation components to be defined include: oxidizer blend ratio, burning rate additive, cure catalyst and curing agent level. The specific formulation shall be selected on the basis of cured propellant properties, burning rate, and flow properties, in accordance with the formulation guidelines (Paragraph 2.d.).

2. Formulation

a. Burning rate additive systems must be selected on the basis of minimum effect on propellant viscosity characteristics. BRA-101 in its present form is not considered suitable for a propellant to be cast by the 260-in.-dia motor bayonet casting process.

b. The propellant viscosity characteristics must be examined over a wide range of shear stresses as a function of time from curing agent addition. Propellant viscosities, at 5000 dynes/cm^2 (500 N/m^2) shear stress and 2 to 3 hr from curing agent addition, of more than 50,000 poise (5,000 Ns/m^2) are likely to produce grain defects. By contrast, propellant viscosities under the same conditions of less than 15,000 poise (1,500 Ns/m^2), may be expected to provide defect-free grains. For propellants in the middle range between these values, the probability of defect formation will depend on the exact processing conditions.

c. Iron Blue burning rate additive contains both a small amount of soluble iron and a relatively large amount of absorbed water. If Iron Blue is to be used in the propellant burning rate additive system, the propellant formulation must include a stabilizer to prevent catalysis of polymer degradation by the soluble iron and a polymerization catalyst which is hydrolytically stable. Phenyl-β-naphtyl amine is an acceptable degradation stabilizer. FC-151 is acceptable as a hydrolytically stable cure catalyst.

d. For the specific formulation to be cast into the motor, the cure catalyst level must be adjusted to achieve the optimum balance among viscosity buildup, zero flow time, and cure time for the propellant production rate anticipated for the motor. These parameters will be used in the determination of bayonet submergence, time between bayonet changes, and allowable propellant pot life.

3. Fuel Preparation

a. Submix and Premix

The submix and premix must be a uniform blend. Agitation is essential to prevent settling of solids. When relatively small amounts of

materials are added to the premix tank, it is necessary to pre-slurry the ingredients in a liquid binder state, such as plasticizer to preclude loss due to coating on tank walls or agitator. The 260-in.(6.6 m)-dia motor propellant process requires that the premix be stable for a period of up to 7 days. The acceptability of the premix for each propellant must be determined over this storage period. Uncured and cured propellant properties must be assessed in this determination.

4. Propellant Mixing

a. Batch Mix

(1) A vacuum mix cycle of 10 min minimum duration should be included in the batch mix process after oxidizer addition and before curing agent addition.

(2) The length of the final vacuum mix cycle should be 30 min minimum.

(3) The minimum acceptable vacuum level in the mixer bowl should be 28 in. (710 mm) Hg.

b. Continuous Mix

Qualification of a propellant for the continuous mix process must include verification of acceptable viscosity characteristics of propellant mixed by that process.

5. In-Process Control Tests

a. Definitive in-process tests that verify the presence and amount of submix and premix ingredients are required.

b. Uncured propellant visocsity acceptance limits are required. Rotovisko testing provides adequate data quality, but is not sufficiently rapid for an in-process test. The falling-ball test is the most suitable for this requirement. The acceptance limit for the falling-ball viscosity test is 90 sec maximum drop time for a 3-in. (7.6 cm) drop. Further testing to refine this limit is required. Correction factors are required for variations in propellant temperature and time after curing agent addition.

c. Carton samples for cured propellant properties may not be completely representative of the cast propellant. An improved sampling technique is required.

6. Propellant Casting

a. For the formulation ANB-3350, the time limit for casting of within 10 hr from curing agent addition established for the previous 260-in.-(6.6 m)-dia motor castings is adequate.

b. Propellant batch cast rate into the motor is not a critical processing variable, but a high motor cast rate is recommended. A minimum average motor cast rate of 120,000 lb (53,000 Kg) per day is required.

c. Bayonet submergence should be sufficiently shallow to prevent the movement of highly viscous propellant already in the motor. A submergence of 18 in. (46 cm) maximum is allowable for ANB-3350 propellant and a 260-in. (6.6 m)-dia motor cast rate of 5000-lb/hr (2300 Kg/hr) average.

d. With a multiple bayonet casting arrangement, the assignment of batches to be cast through each bayonet must be uniform so as to minimize flow path lengths.

e. Additional casting criteria are necessary for highly configurated core designs.

NASA CR 72621

FINAL REPORT DISTRIBUTION LIST

NASA Lewis Research Center
21000 Brookpark Road
Cleveland, Ohio 44135
Attn: Contracting Officer
Mail Stop 500-313 (1)
Solid Rocket Technology Branch
Mail Stop 500-205 (8)
Technical Library
Mail Stop 60-3 (2)
Tech. Report Control Office
Mail Stop 5-5 (1)
J. Kennard
Mail Stop 3-17 (1)
Tech. Utilization Office
Mail Stop 3-19 (1)
Patent Counsel
Mail Stop 500-311 (1)

National Aeronautics and Space Administration
Washington, D.C. 20546
Attn: RPM/William Cohen (3)
RPS/Robert W. Ziem (1)
ATSS-AL/Technical Library (2)

NASA Ames Research Center
Moffett Field, California, 94035
Attn: Technical Library (1)

NASA Langley Research Center
Langley Station
Hampton, Virginia, 23365
Attn: Robert L. Swain (1)
Technical Library (1)

NASA Goddard Space Flight Center
Greenbelt, Maryland, 20771
Attn: Technical Library (1)

NASA Manned Spacecraft Center
2101 Webster Seabrook Road
Houston, Texas, 77058
Attn: Technical Library (1)

NASA George C. Marshall Space Flight Center
Redstone Arsenal
Huntsville, Alabama, 35812
Attn: Technical Library (1)
R-P&VE-PA/K, Chandler (1)

Jet Propulsion Laboratory
Calif. Institute of Technology
4800 Oak Grove Drive
Pasadena, California, 91103
Attn: Richard Bailey (1)
Technical Library (1)

Scientific & Technical Information Facility
NASA Representative
P.O. Box 33
College Park, Maryland 20740
Attn: CRT (6)

GOVERNMENT INSTALLATIONS

AF Space Systems Division
Air Force Unit Post Office
Los Angeles, California, 90045
Attn: Col. E. Fink (1)

AF Research and Technology Division
Bolling AFB, D.C., 20332
Attn: Dr. Leon Green, Jr. (1)

AF Rocket Propulsion Laboratory
Edwards AFB, California, 93523
Attn: RPM/Mr. C. Cook (2)

AF Ballistic Missile Division
P.O. Box 262
San Bernardino, California
Attn: WDSOT (1)

Army Missile Command
Redstone Scientific Information Center
Redstone Arsenal, Alabama, 35809
Attn: Chief, Document Section (1)

Atlantic Research Corporation
Shirley Highway at Edsall Road
Alexandria, Virginia, 22314
Attn: Technical Library (1)

Boeing Company
P.O. Box 3999
Seattle, Washington, 98124
Attn: Technical Library (1)

Chrysler Corporation
Space Division
Michoud Operations
New Orleans, Louisiana
Attn: Technical Library (1)

Hercules, Inc.
Allegany Ballistics Laboratory
P.O. Box 210
Cumberland, Maryland, 21502
Attn: Technical Library (1)

Hercules Company
Bacchus Works
P.O. Box 98
Magna, Utah, 84044
Attn: Technical Library (1)

Lockheed Missiles & Space Company
P.O. Box 504
Sunnyvale, California
Attn: Technical Library (1)

Lockheed Propulsion Company
P.O. Box 111
Redlands, California, 93273
Attn: Bud White (1)

Martin Marietta Corporation
Baltimore Division
Baltimore, Maryland, 21203
Attn: Technical Library (1)

Mathematical Sciences Corporation
278 Renook Way
Arcadia, California, 91006
Attn: M. Fourney (1)

Philco Corporation
Aeronutronics Division
Ford Road
Newport Beach, California, 92660
Attn: Technical Library (1)

Rocketdyne
Solid Propulsion Operations
P.O. Box 548
McGregor, Texas
Attn: Technical Library (1)

Rocketdyne
6633 Canoga Avenue
Canoga Park, California, 91304
Attn: Technical Library (1)

Rohm and Haas
Redstone Arsenal Research Division
Huntsville, Alabama, 35807
Attn: Technical Library (1)

Thiokol Chemical Corporation
Wasatch Division
Brigham City, Utah, 94302
Attn: Dan Hess (1)
Technical Library (1)

Thiokol Chemical Corporation
Elkton Division
Elkton, Maryland, 21921
Attn: Technical Library (1)

Thiokol Chemical Corporation
Huntsville Division
Huntsville, Alabama, 35807
Attn: Technical Library (1)

TRW Systems
One Space Park
Redondo Beach, California, 90278
Attn: M. Lipow (1)

United Technology Genter
P.O. Box 358
Sunnyvale, California, 94088
Attn: Technical Library (1)

Ballistic Research Laboratory
Aberdeen Proving Ground,
Maryland, 21005
Attn: Technical Library (1)

Picatinny Arsenal
Dover, New Jersey, 07801
Attn: Technical Library (1)

Navy Special Projects Office
Washington, D.C., 20360
Attn: H. Bernstein (1)

Naval Air Systems Command
Washington, D.C., 20360
Attn: AIR-330/Dr. O. H. Johnson (1)

Naval Propellant Plant
Indian Head, Maryland, 20640
Attn: Technical Library (1)

Naval Ordnance Laboratory
White Oak
Silver Spring, Maryland, 20910
Attn: Technical Library (1)

Naval Ordnance Test Test Station
China Lake, California, 93557
Attn: Technical Library (1)
C. J. Thelen (1)

Naval Research Laboratory
Washington, D.C., 20390
Attn: Technical Library (1)

Chemical Propulsion Information
Agency
Applied Physics Laboratory
8621 Georgia Avenue
Silver Spring, Maryland, 20910 (1)

Defense Documentation Center
Cameron Station
5010 Duke Street
Alexandria, Virginia, 22314 (1)

Defense Materials Information Center
Battelle Memorial Institute
505 King Avenue
Columbus, Ohio, 43201 (1)

Materials Advisory Board
National Academy of Science
2101 Constitution Ave., N.W.
Washington, D.C., 20418
Attn: Capt. A. M. Blamphin (1)

Institute for Defense Analysis
1666 Connecticut Ave., N.W.
Washington, D.C.
Attn: Technical Library (1)

Advanced Research Projects Agency
Pentagon, Room 3D154
Washington, D.C., 20301
Attn: Tech. Information Office (1)

INDUSTRY CONTRACTORS

Aerojet-General Corporation
P.O. Box 1158
Solid Rocket Plant
Sacramento, California, 94086
Attn: Dr. B. Simmons (1)
Tech. Information Ctr. (1)
Space Booster Dept. (8)

Aerojet-General Corporation
P.O. Box 296
Azusa, California, 91702
Attn: Technical Library (1)

Aerospace Corporation
2400 East El Segundo Boulevard
El Segundo, California, 90245
Attn: Technical Library (1)
Solid Motor Dev. Office (1)

Aerospace Corporation
P.O. Box 95085
Los Angeles, California, 90045
Attn: Technical Library (1)